UNIVERSITY OF SOUTHAMPTON

ABSTRACT

FACULTY OF MEDICINE, HEALTH AND LIFE SCIENCES
SCHOOL OF BIOLOGICAL SCIENCES

Doctor of Philosophy

INVESTIGATION INTO THE MOLECULAR MECHANISMS OF AXONAL DEGENERATION AND CHARACTERISATION OF FOCAL ADHESION KINASE IN RESPONSE TO CNS INJURY

by Emma Louise Rankine

The molecular mechanisms of axonal degeneration following injury has been a largely neglected area of investigation. Axonal degeneration was thought to be a passive process, whereby the portion of axon distal to the injury simply withered away due to its loss of support from the cell body, the site of protein synthesis. This form of degeneration is termed Wallerian degeneration. The serendipitous discovery of the mutant mouse with delayed, or *slow* Wallerian degeneration (Wld^S) led to the conclusion that Wallerian degeneration is in fact an active process, akin to programmed cell death. These molecular mechanisms controlling axon degeneration are poorly understood, and the current methods of detecting axonal injury in the central nervous system (CNS) simply show us that an injury has occurred which has altered axonal integrity. The aim of this work is to unravel some of the mechanisms involved in axon degeneration.

We raised polyclonal antibodies against components of sciatic nerves undergoing Wallerian degeneration. The antibodies have been screened against a range of naive and injured tissues by immunohistochemistry and Western blotting. A proteomics approach has then been employed to deduce which antigen/s the antibodies recognise. Immunohistochemistry on injured CNS tissues, using these novel antibodies, revealed staining of damaged axons from as early as 6 hours, which intensifies through to 7 days in the spinal cord and 28 days in the brain, the longest timepoints studied. Western blot analysis indicates a number of bands that are either upregulated or down regulated in response to injury in CNS tissue when compared to the appropriate naive tissue. The bands identified by Western blot were subsequently analysed by matrix-assisted laser desorption/ionisation time-of-flight mass spectrometry (MALDI-TOF).

We identified changes in three proteins following CNS injury. Firstly, albumin appears to be taken up into damaged axons following injury prior to resealing. Secondly, kid-1, a transcription factor, was identified; Western blot and immunocytochemical analysis revealed no change in expression over the timecourse of injury investigated. And finally, focal adhesion kinase (FAK), a protein tyrosine kinase, was also identified.

Changes in FAK expression following injury were studied by Western blot and immuncytochemistry. Western blot analysis revealed a decrease in FAK expression following brain and spinal cord injury, however, immunocytochemistry revealed that there is a change in FAK distribution following the injury. Double immunofluorescence revealed that de novo FAK expression was present in oligodendrocytes as early as 6hrs post injury. This is possibly the earliest event occurring in the oligodendrocyte in response to Wallerian degeneration of their associated axons. At later times FAK expression was detected, to a lesser extent, in astrocytes and possibly microglial cells.

The work in this thesis demonstratesthat changes occur both in the axon and glia in the distal nerve stump following nerve transection. We have identified specific, novel changes in both the axon, using our own novel polyclonal antibody, and glia, using an antibody specific to FAK.

CONTENTS

FIGURE CONTENTS

CHAPTER 1 Introduction

CHAPTER 3 Antibody Production and Characterisation

Acknowledgements

I would like to start by thanking my supervisor whose belief in me kept me motivated throughout my time working on this arduous PhD, my supervisor Professor Perry, Hugh. His continuous support in my work kept me enthused and excited about my project (most of the time!). Without his help none of this work would have been possible.

Dr Paula Hughes, my mentor and inspiration to continue my scientific career and start the PhD in the first place, whether this was actually a good thing..... I'll tell you in a few years!! Paula taught me an unbelievable amount in the time we worked together, thank you for everything.

Dr Leigh Felton, what can I say, he has been a rock throughout my PhD, his continued support and encouragement has been greatly appreciated. Leigh, you are a fountain of knowledge and a true friend, we will always remain best of friends wherever our paths take us.

Bryony Gray, my fellow PhD student, we went through some mad times together! I shall always remember our random singing sessions, which, I think, got us through these fun years! (Although I'm sure they were not appreciated by all who heard us (John-Paul Jukes in particular springs to mind!)).

There are a great number of people I would like to thank, however, this in itself would form the contents of a thesis!! In summary, I would like to thank the following people: Dr Tracey Newman, you have been a constant support and friend throughout my time in the CNS Inflammation Group, you have always believed in me, for that I thank you wholeheartedly; Sara Waters, you know how special you are, you are the rock of the laboratory, thank you for everything you have done for me throughout my years with you. Katie Lunnon, you have been a fabulous support and help (especially in the final stages!), for that I thank you. I would also like to thank everybody else in the CNS inflammation Group past and present, too numerous to mention, but thank you all for your years of support and guidance.

Paul Skipp and Matt Cuttle, thank you to both of you for your technical help in the proteomics and COnfocal microscopy work which has formed an important part of my thesis.

Finally, none of the work described within this thesis would have been possible without the generous funding of the BBSRC and Nurin Ltd.

Abbreviations

ABC	Avidin-biotin-peroxidase complex
AP	Action Potential
APP	Amyloid precursor protein
ATP	Adenosine triphosphate
Bax	Bcl-2-associated X protein
BBB	Blood-brain barrier
BDNF	Brain derived neurotrophic factor
BNB	Blood-nerve barrier
Caspr	Contacin-associated protein
CNS	Central Nervous System
CON	Constricted axon segment
CSPGs	Chondroitin sulphate proteoglycans
Cyt c	Cytochrome c
DAB	3,3'-diaminobenzidine
DNA	Deoxyribose nucleic acid
DRG	Dorsal root ganglia
ECL	Enhanced Chemiluminescence
ECM	Extracellular matrix
ELR1 and 2	Emma Louise Rankine 1 and 2 (Antisera)
FAK	Focal adhesion kinase
FAT	Focal adhesion targeting sequence
FRNK	FAK related non-kinase
gad	Gracile axonal dystrophy
GAG	Glycosaminoglycans
GFAP	Glial fibrillary acidic protein
K+	Potassium
LHON	Leber's hereditary optic neuropathy
MAG	Myelin associated glycoprotein
MALDI-TOF MS	Matrix-assisted laser desorption/ionisation time-of-flight mass spectrometer
MS	Multiple sclerosis
Na+	Sodium
NAD	Nicotinamide adenine dinucleotide
NF	Neurofilament
NGF	Nerve growth factor
NgR	Nogo-66 receptor
Nmnat	Nicotinamide mononucleotide adenylyltransferease
NO	Nitric oxide
NT	Neurotrophin
OMgp	Oligodendrocytes-myelin glycoprotein
p.i	post injury
PAF	Paraformaldehyde
PAGE	Polyacrylamide gel electrophoresis
PARP	Poly(ADP-ribose) polymerase
PBS	Phosphate buffered saline
PLP	Periodate lysine paraformaldehyde
PN	Peripheral nerve
PNS	Peripheral Nervous System

RGC	Retinal ganglion cell
RNA	Ribose nucleic acid
SDS	Sodium dodecyl sulphate
Sir	Silent information regulators
SOD	Superoxide dismutase
TBS	Tris buffered saline
Ube4b	Ubiquitination factor E4B
UPP	Ubiquitin proteasome pathway
Wld^s	*slow* Wallerian degeneration

Chapter 1 Introduction

Historical background

One of the original theorists in the world of the nervous system was Santiago Ramon y Cajal. Ramon y Cajal is most famous for his studies on the fine structure of the central nervous system (CNS). Cajal used a staining method developed by his contemporary Camillo Golgi, the Golgi technique. This is a method used to visualise neurones by staining brain tissue with silver chromate solution. Staining methods will be discussed in greater detail later. By using his technique, Golgi concluded that the nervous system was a continuous reticulum (or web) of interconnected cells, like those in the circulatory system.

However, by using Golgis' technique, Ramon y Cajal reached a very different conclusion. He postulated that the nervous system was made up of billions of separate neurones that are polarised. Rather than the continuous web that Camillo Golgi has suggested, Cajal argued that the neurones communicate with each other via specialised junctions called 'synapses', a term that was coined by Charles Scott Sherrington in 1897. Electron microscopy later showed that the plasma membrane completely enclosed each neurone, completely supporting Ramon y Cajals theory, and weakening Camillo Gologi's theory. Although the discovery of electrical synapses, where neurones are in direct contact with each other, lead to the argument that Golgis theory was in part correct. Ramon y Cajal and Camillo Golgi shared the nobel prize in Physiology or Medicine in 1906.

Ramon y Cajals original ideas and data have been translated and published in "Cajal's Degeneration and Regeneration of the Nrvous System" Written by Santiago Ramon y Cajal, Edited by Javier DeFelipe and Edward G ones and translated by R. M. May.

General Introduction

The axon is the elongated fiber that extends from the cell body to the terminal endings and transmits the neural signal. The larger the axon the faster it transmits information. Some axons are covered by a fatty substance called myelin.

By transmitting impulses along their axons, neurones communicate with each other, or with target organs. In the peripheral nervous system (PNS), larger axons are myelinated by Schwann cells; in the central nervous system (CNS) axons are myelinated by oligodendrocytes. The main functions of myelin are to decrease the electrical capacitance of the axon and to insulate against any leakage of the bioelectrical nerve impulse. The lower the capacitance, resistance and the larger the diameter of the axon, the faster the nerve impulse will travel. A single Schwann cell myelinates only one neurone

whereas an oligodendrocyte can associate with a number of axons. The gaps between the segments of myelinated axon are known as Nodes of Ranvier.

Molecules and other intracellular components of the neurone move, both from the axon terminal towards the cell body (retrograde transport) and from the cell body towards the axon terminal (anterograde transport). In both the PNS and CNS, axon damage may disrupt both retrograde and anterograde transport; this may be followed by degeneration of the axon and possibly the cell body, depending upon location and severity of injury. Degeneration can originate at a number of different sites of the neuron and can be caused by a large variety of insults. Large axons degenerate much more slowly than medium sized axons, which in turn degenerate more slowly than small sized axons. In the 1970's Lubinska et al., estimated the velocity of proximo-distal degeneration in large fibres of the phrenic nerve to be 45.6mm/24hr, and in thin phrenic nerve fibres the rate of degeneration was reported to be 252mm/24hr; in both cases the whole nerve was reported to be involved by 48hrs (Lubinska 1977).

Axons within the CNS degenerate at a slower rate than axons within the PNS (Perry, Brown et al. 1991), and rates of degeneration can vary further between species, for example frog nerves degenerate much slower than that of mammals (Hasegawa, Rosenbluth et al. 1988).

The processes underlying axonal degeneration will form the focus of this introduction. The objective of the work described here is to produce novel reagents to help study axonal degeneration and to deduce mechanisms involved. If I can identify the molecular mechanisms involved in degeneration of axons I may be able to prevent the process and thus improve the outcome following nervous system injury.

1.1 ANATOMY OF THE NEURONE

A schematic diagram showing the general structure of a neurone is shown in Fig. 1.1. The axon hillock is the point at which the axon leaves the cell body. Each axon gives rise to varying numbers of collateral branches, each ending in synapses. The axons of neurones of the PNS vary in diameter, from 0.1μm to 20μm and can measure less than 1cm up to 1metre in length. Neurones of the PNS have larger surface to volume ratio. This means that these neurones have a large surface area compared to other cells in the body and are highly polarised; thus proteins do not simply diffuse throughout the cell, but undergo active transport which requires energy.

The neuronal cell body contains abundant rough endoplasmic reticulum, the machinery required for protein synthesis. Visible clusters of ribosomes, termed Nissl bodies, are present in the cell body but are almost totally absent in the axon. Hence, the majority of proteins required by the axon, although not all, must be synthesised in the cell

body and transported to the correct location by specific cellular machinery within the axon. Small amounts of particular proteins have been shown to be synthesised within axons in various species, for example, the giant squid axon contains the molecular components necessary for protein synthesis (Giuditta, Menichini et al. 1991; Galbraith and Gallant 2000). Protein synthesis within mammalian axons is discussed in more detail below.

1.2 STRUCTURE OF THE AXON

Both the PNS and CNS contain a mixture of myelinated and unmyelinated axons (see Fig. 1.2).

The axon leaves the cell body at the axon hillock (see Fig. 1.1), a specialised structure responsible for summating the graded inputs from the dendrites and producing action potentials if the threshold is exceeded. The axon has specialised cytoplasm, termed axoplasm, which is a gelatinous cytoplasm that is enclosed by the axolemma, the axon's plasma membrane. Within the axoplasm is the cytoskeleton, axoplasmic organelles (e.g. mitochondria) and the axoplasmic inclusions (e.g. granular material and lipid inclusions). The cytoskeleton is a very important structural component of the axon and consists of microtubules, neurofilaments and the microtrabecular matrix, which includes the microfilaments.

Compared to the cell body, the axon contains fewer organelles; for example, it does not contain Golgi apparatus or very much rough endoplasmic reticulum (Waxman, Stys et al. 1995). The axoplasm and the structural components, microtubules and neurofilaments, appear to be responsible for the tubular structure of the axon. Fig. 1.3 shows a cross section of a myelinated nerve fibre from a normal adult rat white matter in which neurofilaments and microtubules are clearly visable. The microtubules and neurofilaments are arranged parallel to the long axis of the axon.

Microtubules are made up of 13 protofilaments, each composed of heterodimers of α and β tubulin (Waxman, Stys et al. 1995). The orientation of the dimers results in positive/negative polarity of the microtubule (Susalka, Hancock et al. 2000). In the neurone, the cell body shows negative polarity compared to the synaptic end. Different motors within the axoplasm recognise the microtubule polarity and deliver cargo to either the positive or the negative end of the microtubule (Kasprzak and Hajdo 2002). These motors will be discussed in greater detail below.

Neurofilaments (NF) in vertebrates are composed of three related polymeric proteins. Their molecular weights are 68, 150 and 200 kDa and they are known as NF-L, NF-M and NF-H respectively. NF-H contains residues that can become phosphorylated: the extent of NF-H phosphorylation varies within different regions of the neuron. The

axonal NFs are more highly phosphorylated compared to those in the cell body and dendrites. The function of this phosphorylation is to maintain the calibre of the axon (Al-Chalabi and Miller 2003), via elevated charge-based repulsion of neighbouring filaments. Increasing the calibre of an axon increases the conduction velocity of that axon.

Myelination is an evolutionary strategy to increase the speed at which an action potential travels along an axon. Myelination insulates the axonal membrane, reducing the ability of current to "leak" out of the axon, and is formed by multiple layers of closely opposed glial membrane. Gaps in the myelin are known as nodes of Ranvier and are of utmost importance, since they allow the ions to move in and out of the axon, thereby generating an action potential (AP) (Waxman, Stys et al. 1995). As one node is depolarised, the AP generated elicits a current that flows passively within the myelinated segment until the next node is reached. This local current flow then generates another AP, which continues to the end of the axon. This type of conduction has been termed saltatory conduction, due to the fact that the APs 'jump' from one node to the next node.

The nodes of Ranvier allow efficient and rapid propagation of action potentials in myelinated axons. The nodal region is organised into several distinct domains, each of which contains a unique set of ion channels, cell adhesion molecules and cytoplasmic adaptor proteins. A schematic representation of a typical node of Ranvier along with an electron micrograph indicating all the major structures is shown in Fig. 1.4. The site at the centre of the node of Ranvier is called the constricted axon segment (CON). In this region the cross-sectional area is reduced by 75% to 90% when compared to the adjacent internode, the reduction in area being advantageous to conduction velocity (Waxman, Stys et al. 1995).

The nodal axolemma is highly specialised, with a high concentration of sodium (Na^+) channels, slow potassium (K^+) channels and Na-K-ATPases. The density of Na^+ channels at the nodes is 25 times that located at the internodes (Baba, Akita et al. 1999; Dupree, Girault et al. 1999). Nodes have a critical physiological role in conducting impulses along the neurone. The Na^+ channels, K^+ channels and the Na^+/K^+ ATPases are all important in regulating the resting membrane potential and generating action potentials. A rapid influx of Na^+ ions through the Na^+ channels at the nodes causes depolarisation of the axon, and hence an AP is initiated. The K^+ channels are located at the juxtaparanodal region where efflux of K^+ ions has a role in repolarising the section of axon after an AP (Baba, Akita et al. 1999).

The Na^+ and K^+ channels are clustered to the appropriate area at the node of Ranvier by interactions between the axon and the formation of the myelin sheath. During development of the nervous system it has been observed that clusters of Na^+ channels first

appear, on the axons, at the regions where myelinating cells first express myelin associated glycoprotein (MAG) (Rasband and Trimmer 2001). The molecular mechanisms involved are not yet fully understood, although a few candidate proteins have been investigated, such as ankyrin and tenascin (Rasband and Trimmer 2001). Specialised junctions form between the axolemma and myelin loops at the paranodal regions to anchor the myelin to the axon (Rios, Melendez-Vasquez et al. 2000). Contactin-associated protein (Caspr) and contactin are two important proteins involved in this anchoring. Caspr can be visualised by immunofluorescence between voltage-gated Na^+ channels and K^+ channels, which are concentrated at the nodes, and are clustered at the juxtaparanodal region (Fig. 1.5).

1.3 AXON HOMEOSTASIS

Axonal transport

The majority of proteins located within the axon must be synthesised in the cell body and then transported to where they are required, in the axon this is carried out by anterograde transport. Axonal transport has been investigated and the rates of transport has been determined using tracers. There are two forms of anterograde and retrograde axonal transport, fast and slow. Fast axonal transport primarily transports membranous organelles at a rate of 100-400mm per day, whereas slow axonal transport moves cytoskeletal proteins and soluble enzymes at a rate of 0.1-3mm per day (Hirokawa 1993). In man, an axon may be as long as one metre, and it is therefore important to consider how cell organelles and proteins that are required throughout the axon and in the synapses are transported.

Proteins and organelles are transported along the axon by transport proteins with 'motors' called kinesins and dyneins, these are specialised proteins that hydrolyse ATP in order to transport their cargo along the microtubules (Hirokawa 1993). In order to ensure the correct direction of movement, these microtubules are oriented in a specific orientation, as mentioned above it is the orientation of the microtubule dimers that results in positive/negative polarity of the microtubule (Susalka, Hancock et al. 2000) . Kinesins generally transport cargo towards the positive end of the axon (anterograde transport), whereas dyneins transport their cargo towards the negative end (retrograde transport). In anterograde transport, kinesins drive fast transport of vesicles and mitochondria and slow transport of tubulin, neurofilaments and actin, from the cell body in the direction of the synapse (Mandelkow and Mandelkow 2002). In retrograde transport, carried out by the dyneins, cargo such as endosomes, mitochondria, neurotrophic signals and viruses are moved from the synaptic end towards the cell body.

Kinesins are divided into 10 major subfamilies, together forming a total of greater than 30 different family members (Kull 2000). Kinesins are heterodimers, made up of two heavy chains and two light chains. The heavy chains of the kinesins consist of a globular motor domain, an α-helical coiled-coil tail domain and a carboxyl (C)-terminal tail domain. It is the C-terminal tail domain that is believed to interact with the amino (N)-terminal domain of the light chain, regulating motor activity and perhaps binding some of the cargo. Cargo is mainly attached via the C-terminal of the light chain, which contains specific peptide sequences that participate in protein-protein interactions. How the cargo is specifically determined remains unclear, although the diversity of the light chain tail is thought to be important.

Dyneins are divided into two groups, flagellar and cytoplasmic. They are formed from complexes of between 1 and 3 heavy chains and a varying number of intermediate and light chains. It is the heavy chain in both kinesins and dyneins that contains the motor machinery (Hirokawa 1993) and these are the regions that hydrolyse ATP in order to move along the microtubule. In the case of kinesins, the heavy chain also binds the microtubule directly. By contrast, the dyneins bind cargo through another side arm linked onto the heavy chains (microtubule binding protein). The kinesins and dyneins both have a hinge in the two heavy chains, it is via this hinge that they move along the microtubule in a hand-over-hand like motion (Hancock and Howard 1999) (Fig. 1.6).

Axonal protein synthesis versus axonal transport

It was the general consensus for many years that the axon was devoid of ribosomes and hence could not synthesise its own proteins. Axonal and synaptic proteins were therefore thought to all originate from the cell body and undergo transport to their appropriate locations (see below). Proteins within the axon degrade at rates comparable to proteins throughout the body: they are not, as once thought, uniquely stable (Alvarez, Giuditta et al. 2000). The half-life of proteins undergoing slow axonal transport in axons ranges from 10-100, days whereas proteins transported via fast axonal transport have reported half lives of less than one day (Nixon 1980). One model system used to analyse axonal protein degradation is the visual system. Tritiated amino acids are injected intravitreally, binocularly. At different timepoints post injection the optic nerves are removed, homogenised, centrifuged (to separate free amino acids from those in proteins) and the radioactivity is measured (Nixon 1980). A similar protocol can be utilised to investigate protein transport; the optic nerves are removed, sectioned and the radioactivity measured at different distances from the eye. Slow transport ranges from 0.1-4mm per day and therefore proteins may undergo degradation before reaching their target.

The idea that axons are devoid of ribosomes arose from the inability to detect them by conventional electron microscopy (Peters, Palay et al. 1970). Furthermore, early RNA analysis of axoplasm from squid giant fibers demonstrated no evidence of ribosomal RNA (rRNA) (Lasek, Dabrowski et al. 1973). However, there is now an abundance of evidence demonstrating that ribosomes are present within axons. For example, it was shown in the 1980s that amino acids from radiolabelled neurofilaments are released into the extracellular space, and that amino acids released during degradation are re-utilised locally (Nixon 1980). Recent evidence now suggests that there is ongoing synthesis of proteins within axons.

Following axonal injury in mammals regeneration in the periphery starts after a delay of about 1-2 days (Bisby and Keen 1985). By applying a protease inhibitor distal to a nerve crush injury Tapia and colleagues were able to reduce this delay, demonstrating that regeneration occurs before signals would have time to reach the cell body, and indicating that the axon itself has an intrinsic capacity to develop growth cones and elongate independent of the cell body (Tapia, Inestrosa et al. 1995; Gaete, Kameid et al. 1998). However, this does not provide conclusive evidence that mRNA is present in the axon.

Fluorescent staining with either rRNA-specific or ribosomal P protein antibodies in presynaptic terminals in Mauthner (M-) cell axons (from teleost fish, a model used to study RNA content of axons) indicates that the necessary equipment for protein synthesis is present in this axon terminal subcompartment (Alvarez, Giuditta et al. 2000). Ribosomes and polyribosomes have also been identified by immunocytochemistry in the giant squid axon (and small axons) using specific antibodies (Sotelo, Kun et al. 1999). It has been shown in both squid axons and in cultures of sympathetic neurones from newborn rats that axons contain between 100 and 200 different polyadenylated mRNAs, which represents less than 1 percent of the total mRNAs expressed in the cell bodies (Eng, Lund et al. 1999; Kaplan, Lavina et al. 2004). This thus indicates that protein synthesis does occur within the axon, but that the majority of total protein synthesis still occurs within the cell body. However, the presence of the machinery for protein synthesis is not the same as 'synthesis'. However, some major proteins have been found to be synthesised within the axon to date, and these include actin and β-tubulin (Eng, Lund et al. 1999).

Local protein synthesis has also been shown to be important in navigation of the growth cone, axon regeneration (Zheng, Kelly et al. 2001) and synthesis of membrane receptors used as axon guidance molecules (Brittis, Lu et al. 2002). Protein synthesis within axons under normal physiological conditions is postulated to be involved in the maintenance of axonal structure and general health of the axon (Kaplan, Lavina et al.

2004). A model for maintaining axoplasm has been devised by Alvarez et al. (2000), which takes into account the need for axons to maintain a steady state and their ability to change and to become dynamic when required, e.g. following injury or during plasticity. This model hypothesises that amino acids are taken up across the axolemma into the axoplasm where they can freely diffuse, leak back out, or be utilised for protein synthesis; degradation of proteins, via the ubiquitin-proteasome system, occurs locally to also supply amino acids for protein synthesis (Alvarez, Giuditta et al. 2000).

1.4 AXONAL DEGENERATION

Apoptosis versus Necrosis

Apoptosis was adopted from the Greek word for the process of leaves falling from trees or petals falling from flowers; necrosis was taken from the Greek word for death of a bodily tissue.

In order to maintain tissue homeostasis, in almost every tissue except the CNS, dying cells must be in balance with proliferating cells. Cell death is essential in many processes, both during development and in the mature organism. For example, during human development a tail is formed from the base of the spine, which subsequently disintegrates in utero, and in a mature female mammals endometrial cells die and are removed during menstruation. The signals which lead to cell death and the mechanisms involved vary but there are two main types: apoptosis and necrosis.

The major morphological changes that occur during apoptosis are shown in Fig. 1.7. A major feature often associated with apoptotic cells is pyknosis; this is the name for the nuclear fragmentation observed at the light microscope level. Apoptosis is a regulated process in which energy is required, and in which cells participate in their own regulated death. Apoptosis is typically characterised by cell shrinkage, nuclear and cytoplasmic condensation, chromatin fragmentation and removal of the dead cell by a phagocyte. Clearance of the apoptotic cells is rapid in order to prevent the release of intracellular debris, which may lead to an inflammatory response. A cell undergoing apoptosis exposes phosphotidylserine (PS) on the outer leaflet of the plasma membrane. PS is normally restricted to the inner leaflet of the plasma membrane. Exposed PS is normally recognised by a PS receptor (PSR) (Fadok, Bratton et al. 2000). Without this PS-PSR interaction the apoptotic cell is not phagocytosed (Hoffmann, deCathelineau et al. 2001). Initiation of apoptosis begins with an external trigger, such as binding of tumour necrosis factor-α (TNF-α) to its' receptor leading to cellular signalling. The trigger event is followed by permeablisation of the outer mitochondrial membrane by intermembrane space proteins, leading to release of cytochrome c. Once released, cytochrome c activates caspases, which

are a group of intracellular proteolytic enzymes (Kumar and Vaux 2002). ATP levels are maintained due to the continued integrity of the mitochondria, but when cysteine proteases of the caspase family become activated, mitochondrial membranes become depolarised, the cell becomes overloaded with calcium and factors are released from the mitochondria that can induce nuclear chromatin condensation and DNA fragmentation (Mattson and Duan 1999).

In contrast to apoptosis, necrosis is a random, uncontrolled process often bought about by an injurious stimulus to the tissue. When a cell dies by necrosis, the cells' contents are released and an inflammatory response is initiated which can lead to bystander damage (Pettmann and Henderson 1998). The morphological events that occur when a cell undergoes necrosis are shown in Fig. 1.8. The major morphological change in necrosis is cellular swelling due to an imbalance of the ion homeostasis that normally keeps the cell healthy (Syntichaki and Tavernarakis 2003). There is a limited array of biochemical events in necrosis, unlike in apoptosis.

During development of the nervous system many more neurones grow and make connections with their target organ than are needed or than can be supported by their target. Many neurones degenerate and are lost or 'pruned' due to competition for trophic resources, this will be discussed further later (Raff, Whitmore et al. 2002). Typically the cell body, of the neurones that do not survive, degenerates in a non-inflammatory, apoptotic fashion. However, following injury, neurones can die by either apoptosis or necrosis depending on type, severity or location of injury; thus both apoptosis and necrosis are important mechanisms in the nervous system (Pettmann and Henderson 1998). The mechanisms by which the axon degenerates are not fully understood and will be discussed later.

1.5 NEURONAL DEATH

Death of the cell body of the neurone has been a focus of research for some time, but death of the axon has been largely neglected. Neurons may die during development as a normal physiological process or as a consequence of pathological conditions and is discussed below.

Neurotrophic theory and neuronal survival

In the 1940s Rita Levi-Montalcini discovered the first neurotrophic factor, nerve growth factor (NGF) (Aloe 2004). Rita Levi-Montalcini began her studies investigating the relationship between the developing neurones and their peripheral targets. She noted a failure of neurones to thrive in the absence of their peripheral targets, and concluded degeneration was occurring (Aloe 2004). Rita Levi-Montalcini was awarded the Nobel

Prize for the development of the neurotrophic theory, which states that neurones require trophic (nourishing) interactions to survive; this is particularly true during development (Henderson 1996). These neurotrophic factors are generally secreted from the target cell/tissue. NGF was found to be one member of a gene family called neurotrophins. Other mammalian neurotrophic factors (NF), or neurotrophins, include brain-derived neurotrophic factor (BDNF), neurotrophin-3 (NT-3) and neurotrophin-4 (NT-4) (Henderson 1996). The mature mammalian neurotrophins have greater than 80% identity at the amino acid level. The neurotrophin(s) required by a neurone for survival may change over time (Henderson 1996). The physiological role of neurotrophins in many systems is to promote neuronal survival by acting through one of the Trk receptor tyrosine kinases, A, B or C, in association with the low affinity neurotrophin receptor, $p75^{NTR}$ (Pettmann and Henderson 1998). The most frequently proposed theory to explain why such a great number of neurones die during development concerns competition for neurotrophins. Many more neurones develop than are needed or that can be supported by the levels of neurotrophins produced. Therefore a large number of these will not form viable connections with target cells and degenerate. It is unclear why there is an over production of neurones leading to competition for trophic resources. The axon that the neuronal cell body sends out may also produce exuberant projections with only the strongest and most robust projection making the correct connection with the target cell and thus surviving, the other projections degenerate (Luo and O'Leary 2005).

Neurones can gain the neurotrophins they need in a number of different ways (Fig. 1.9): a) from a target tissue (retrograde support); b) from an afferent input (anterograde support); or c) from local interactions between closely opposed neurones and/or glia (paracrine support). Some cells show autocrine support by expressing neurotrophins to which they themselves respond (Henderson 1996).

1.6 AXON DEATH

Development of the nervous system is extremely complex, one way in which the nervous system is sculpted is by neuronal cell death (Cowan, Fawcett et al. 1984). The mechanisms involved in the regulation of this 'fine-tuning' is an area still in need of investigation. Excess projections/connections are removed to ensure correct connections pre- and postsynaptically, i.e. fine tuning (Cowan, Fawcett et al. 1984). Neurones may die prematurely during adult life following acute or chronic insults to the PNS/CNS, or due to disease or genetic disorders. Levels of **some** neurotrophins are high during development and rapidly decrease post-natally; this is thought to be a signal for some of the axons/axonal sprouts to degenerate (Henderson 1996). However, there are some

neurotrophins that increase postnatally, for example Neuregulin-2 (Longart, Y et al. 2004). The processes involved in axonal and cell body death are illustrated in Fig. 1.10. The molecular mechanisms involved in degeneration of the axon are still not well understood, but it is speculated that the same mechanisms are involved in elimination of axons during development and following injury (Raff, Whitmore et al. 2002). In order to study axonal degeneration it is important to be able to visualise the process histologically. The methods used to date are discussed below.

Methods for studying axons/axon damage

Silver staining has been used since the early 1900s to study axons and their degeneration; silver binds to neurofilaments with a greater affinity than to other tissue elements (Loewy 1969). This method is difficult, capricious and very time consuming with each tissue specimen requiring individual adjustments to obtain optimal staining. Alterations in the staining protocol by Nauta lead to specific staining of axons undergoing Wallerian degeneration (Grant, Hollander et al. 2004). This method was again, capricious and also suppressed some degenerating fibre staining as well as suppressing the normal fibre staining. Silver staining methods were used a great deal in the 1950s and 1960s, despite their capricious nature and proved useful in studying specific anatomical pathways following damage to a known areas of the CNS. Another method used to study axonal integrity is electron microscopy. The morphology of a dying axon by electron microscopy is extremely different to a healthy axon (see Fig. 1.11).

Other techniques employed to investigate axons and axonal degeneration utilise the axonal transport systems, described earlier. Tritiated amino acids can be injected at the level of the cell body and these amino acids become incorporated into proteins that are transported via anterograde transport to the axon and synapse. The movement of these tritiated proteins can be tracked and has been particularly useful for studying protein transport, see above for more detail. A similar method used to study axons and their projections takes advantage of retrograde transport. Horseradish peroxidase (HRP) is injected at the level of the synapse or target organ. HRP injected into the developing hind limb buds of Xenopus laevis tadpoles was found to be retrogradely transported to the cell bodies of motoneurones in the ventral horn (Lamb 1977). In a similar study, HRP and related compounds have been injected in a variety of areas to study projections in other species (Enevoldson, Gordon et al. 1984).

Antibodies against neurofilaments (NFs), in particular the heavy chain (NF-H), can also be used to study axonal integrity: healthy intact axons show continuous staining, whereas damaged axons have a 'blebbed' appearance, indicating disintegration of NFs, and therefore disintegration of the axon (Al-Chalabi and Miller 2003).

Another method widely used in to investigate axonal damage approaches the problem from a different angle. Amyloid precursor protein (APP), a protein constitutively expressed throughout the nervous system, can be visualised by immunocytochemistry. In normal tissues, APP levels are undetectable in axons by standard immunocytochemistry, for example in formalin-fixed tissue, due to its very low concentration. However, following axonal injury, APP accumulates in 'end-bulb' structures, where it is easy to visualise (Gentleman, Nash et al. 1993). However, standard immunocytochemistry for APP does not reveal whether or not an axon is permanently injured, or whether axonal transport has simply halted. Thus, such an approach tells us very little about the state of degeneration of the axon. However, confocal microscopy can be utilised to identify axonal transection (Trapp, Peterson et al. 1998). By using an axonal maker, such as NF-H as well as APP the two together can be used to visualise whether an axon is transected or not.

More recently, fluorescence has been used to study axonal transport and damage *in vivo* (Lu, Ashwell et al. 2001). This method employs the use of the axonal tracer dye, fluororuby (a fluorescent rhodamine-conjugated dextran) and is highly sensitive and simple to use. To study axonal damage, the dye is injected at the site of injury. Fluoruby is then taken up and transported along the axon; undamaged axons are characterised by a band of even-thickness with continuous fluorescence, whereas damaged axons are characterised by disrupted profiles, irregular thickness of axons and swollen-discontinuous fragments (Lu, Ashwell et al. 2001).

Although all of these methods may indicate that the axon has been damaged, they do not help in the understanding of the mechanisms involved in axonal degeneration.

Wallerian degeneration

When an axon is transected, the distal portion undergoes a sequence of axonal and myelin degeneration termed Wallerian degeneration after the Scientist that first described Wallerian degeneration, Augustus Volney Waller (Waller 1850). Waller trained early in physical sciences followed by Medicine in Paris, where he received his M.D. degree in 1840. During his student years, between 1834 and 1840, Waller became involved in microscopy. This was around the time when microscopy was advancing and resolution improving dramatically. Waller wrote a paper in 1850 detailing his findings from studying glosso-pharyngeal and hyperglossal nerves of the frog in which he showed that the distal segment cut off from the cells underwent degeneration, whilst the proximal segment remained intact for a long period of time. He concluded that nerve fibres were simply prolongations from the cells which they derived their nourishment and from this arose the term Wallerian degeneration (Waller 1850). The mechanisms that initiate Wallerian degeneration are not known, however one hypothesis is that degeneration may be due to

the loss of connection with the proximal axon and cell body (Ochs 1975). In the 19th century, Waller anticipated a role for trophic factors from the cell body stating that following loss of connection with the cell body, axons would lose their trophic or nutritional support and degenerate (Waller 1850). Another hypothesis states that the axon degenerates due to an influx of calcium through the transected end of the axon, which then activates calcium dependent proteases, such as calpain (Schlaepfer and Hasler 1979). Wallerian degeneration has been associated with many neurodegenerative disorders and can be triggered by a diverse range of stimuli including neurotoxins, defects in myelin, defects in axonal transport and compromised oxygen delivery. How these multitude of insults lead to the same process of degeneration is unclear.

In the distal portion of a transacted axon, within hours following injury, organelles and mitochondria of the axon accumulate in paranodal regions near the site of injury, the effects then spread distally throughout the axon (Hasegawa, Rosenbluth et al. 1988; Griffin, George et al. 1996). At this initial stage, axonal transport is unaffected (Miledi and Slater 1970). Furthermore, if the distal stump of the axon is stimulated, electrical conduction and synaptic transmission remain intact (Miledi and Slater 1970; Ribchester, Tsao et al. 1995). Following organelle accumulation, approximately 24 hours following injury, the endoplasmic reticulum loses its structure and neurofilaments begin to degrade; this is associated with an influx of calcium and activation of calpain. At this point axons become fragmented and can no longer conduct action potentials (Hasegawa, Rosenbluth et al. 1988) (Fig. 1.12).

Wallerian degeneration in the periphery differs considerably from that in the CNS. In the periphery, the ability of a nerve to conduct an action potential is lost by approximately 24 hours, whereas in the CNS, a transected nerve has the ability to conduct action potentials for up to three days (Ludwin 1990; George and Griffin 1994). In addition to the variation between peripheral and central nerves, the responses of the surrounding cells, the Schwann cells and oligodendroctyes, also differ. In the periphery there is a decreased expression of myelin basic protein (MBP) and P_0 producing genes (Trapp, Hauer et al. 1988), and proliferation of Schwann cells as early as two days post-injury. By contrast in the CNS, it can take up to 40 days for the myelin protein producing genes (PLP and MBP) to become downregulated and for the oligodendrocytes to resemble resting or quiescent oligodendrocytes (Ludwin 1990). There is also a marked difference between the reaction of the peripheral blood-nerve barrier (BNB) and CNS blood-brain barrier (BBB). When a peripheral nerve undergoes a crush injury the blood-nerve barrier breaks down 2-3 days post injury. However, following an optic nerve crush, the blood-brain barrier remains intact distal to the site of injury (George and Griffin 1994). In the PNS, macrophages are

recruited to the injury site by day three (Perry, Brown et al. 1987), whereas, in the CNS there is a relative delay with macrophage proliferation at around 5-7 days post injury (Lawson, Frost et al. 1994). Other differences noted between Wallerian degeneration in the PNS and CNS concern clearance of both axonal and myelin debris. In the periphery, axonal debris is cleared away by 10-12 days p.i and myelin debris 12-21 days p.i. (Stoll, Griffin et al. 1989). In the CNS, however, neither axonal nor myelin debris are cleared away until at least 90 days p.i. and can persist for up to 22 months p.i. (Bignami, Dahl et al. 1981; Ludwin 1990). The reason for this delay is unclear, but Lawson and colleagues (1994) hypothesised that Schwann cells in degenerating peripheral nerves promptly modify their myelin sheaths so that they can be recognised and phagocytosed by macrophages, whilst in the CNS oligodendrocytes do not (Lawson, Frost et al. 1994). However, in 1995 Perry and colleagues used radiation to deplete macrophages from mice. This was carried out to investigate whether the rate of myelin clearance from the distal stump following sciatic nerve crush or transection was altered (Perry, Tsao et al. 1995). From this work they concluded that there are two stages of myelin breakdown in peripheral nerves undergoing Wallerian degeneration. Initially, myelin removal is dependent on the Schwann cells alone, but later removal is dependent on both Schwann cells and macrophages (Perry, Tsao et al. 1995).

Delayed Wallerian degeneration

In mice, the ability of a peripheral distal segment of an injured axon to conduct an action potential is lost within 24 hours after transection. This process of degeneration was originally hypothesised to be passive, the axon distal to the injury site withering away, due to loss of connection with the cell body (Waller 1850; Ochs 1975). The discovery of a mutant mouse with slow Wallerian degeneration (Wld^S) changed this concept. In the Wld^S mouse, the distal segment of a peripheral transected axon is able to conduct action potentials for more than two weeks following a transection injury (Lunn, Perry et al. 1989; Ribchester, Tsao et al. 1995). This lead Perry and colleagues to the hypothesis that Wallerian degeneration does not simply occur due to the loss of connection with the cell body: it is more likely that one or more factors are signalling/initiating the degenerative process to occur (Perry, Brown et al. 1990). It was also noted that older Wld^S mice showed a rate of synapse degeneration similar to that of wild-type mice (Ribchester, Tsao et al. 1995), indicating that degeneration that is occurring in the synapse is a separate process to that occurring in the axon. Therefore, Wallerian degeneration is not as once thought a passive process but is in fact an active process requiring activation of as yet unknown processes to initiate/facilitate degeneration, akin to programmed cell death.

Wallerian degeneration and programmed cell death

Wallerian degeneration, like programmed cell death, can be triggered by a wide variety of insults for example, physical damage, chemical injury and a wide number of disease processes. Unlike apoptosis, however, Wallerian degeneration does not involve activation of caspase-3, and degeneration is not slowed or halted by caspase inhibitors (Finn, Weil et al. 2000). It seems that when the cell body of the dying axon subsequently degenerates, caspase-3 becomes involved and 'typical' apoptosis occurs (Raff, Whitmore et al. 2002). There are other controlled mechanisms of cell death that do not involve caspases, one of the most studied caspase-independent processes being autophagy. The cytoplasm in cells undergoing autophagic cell death is destroyed by lysosomal or proteasomal proteases, and this process has been described as apoptosis-like cell death (Lockshin and Zakeri 2002). In autophagic cell death, the cytoplasm is actively destroyed long before nuclear changes become apparent. Autophagy is often confused with necrosis due to the similar pattern of cell destruction. During autophagy, a preautophagosome forms in the cytosol. This engulfs cytosolic components, including organelles. The organelle, for example, will become enclosed by this phagosome to form what is termed an autophagosome. Fusion with a lysosome then leads to degradation of the contents of the autophagosome (Tanida, Ueno et al. 2004). The identification of these autophagosomes by electron microscopy tells us that the cell is undergoing autophagy. There are many proteins involved in autophagy, one such protein, LC3-II, is localised to preautophagosomes and autophagosomes and is therefore known as an autophagosomal marker (Tanida, Ueno et al. 2004).

Bcl-2 family in apoptosis and Wallerian degeneration

The Bcl-2 family of proteins plays a pivotal role in regulating apoptosis by influencing the permeability of the outer mitochondrial membrane (Chao and Korsmeyer 1998). Bcl-2, Bcl-xL, Bcl-w and Mcl-1 are all anti-apoptotic, whilst Bax, Bak and Bok are pro-apoptotic (Chao and Korsmeyer 1998). The important question to ask when comparing apoptosis to active axonal degeneration is whether these proteins are also involved in axonal degeneration. Two important members of the Bcl-2 family, Bcl-2 and Bax will be discussed in more detail below and their actions are schematically summarised in Fig. 1.13.

Bcl-2 protects the cell body but not the axon following neuronal injury

Bcl-2 is a 25kDa integral membrane protein that localises to the membranes of mitochondria, the endoplasmic reticulum and the nucleus (Merry and Korsmeyer 1997). It has been known for some time that Bcl-2 is a suppressor of apoptotic cell death (Korsmeyer 1992). Bcl-2 is expressed at its highest levels in the nervous system during

development and neurogenesis (Sorenson 2004). In the adult, Bcl-2 is expressed at low levels throughout the CNS and at high levels throughout the PNS. Transgenic mice that overexpress Bcl-2 have been used to study its role *in vivo* (Sagot, Dubois-Dauphin et al. 1995; Burne, Staple et al. 1996). These mice have increased numbers of various types of neurones due to the suppression of programmed cell death. This increased number of neurones appears to have little effect on normal life span (Dubois-Dauphin, Frankowski et al. 1994; Burne, Staple et al. 1996). Overexpression of Bcl-2 in a mouse model of motorneurone disease, a genetic mouse model with neuromuscular dysfunction, has shown that while the cell bodies of the neurones are protected from apoptosis, there is no effect on the rate of degeneration of the axons (Sagot, Dubois-Dauphin et al. 1995). It has also been shown in axotomy-induced injury of retinal ganglion cells (RGCs) that overexpression of Bcl-2 protects the cell body but not the axon (Burne, Staple et al. 1996). Thus it appears that although Bcl-2 is of great importance in programmed cell death (apoptosis) of the neuronal cell soma Bcl-2 has little, if any role in Wallerian degeneration.

Bax is important in apoptosis but does Bax have a role in Wallerian degeneration?

Bax (Bcl-associated X protein) is a relative of Bcl-2, but has pro-apoptotic actions. Bax interacts with Bcl-2 to form heterodimers, and its overexpression antagonises the protective effect of Bcl-2 (Merry and Korsmeyer 1997). Bax has an important role in neuronal death (Deckwerth, Elliott et al. 1996), and this is highlighted by the consequences of Bax deficiency: in Bax knockout (Bax -/-) mice, developmental cell death is virtually eliminated in many populations of neurones (White, Keller-Peck et al. 1998). Despite this, Bax-/- mice show no other overt changes in the nervous system. In the adult nervous system Bax is expressed in neurones of both the CNS and PNS (Merry and Korsmeyer 1997) and it has been found to be important in CNS injury. For example, upregulated expression of Bax is reported following cerebral ischemia (Krajewski, Mai et al. 1995), and in striatal dopaminergic neurones of the substantia nigra pars compacta in a mouse model of Parkinson's disease (Vila, Jackson-Lewis et al. 2001). Furthermore, Bax-ablation attenuates neurological symptoms in a mouse model of Multiple Sclerosis (Lev, Barhum et al. 2004).

Whitmore and colleagues (2003) used a double knockout mouse, Bax-/-Bak-/- to investigate their role in Wallerian degeneration. Bak is another member of the Bcl-2 family, and like Bax is pro-apoptotic. Homo-oligomerisation of Bak forms pores in the mitochondrial membrane that allow cytochrome c release. These mice were used to investigate the effects of Bax and Bak on Wallerian degeneration in sciatic and optic nerve explants. Their findings indicate that Bax and Bak are not involved. However, their work was performed *in vitro* due to the early lethality of the double knockout mouse (Whitmore,

Lindsten et al. 2003). In a recent paper, Dong *et al.* (2003) observed enhanced oligodendrocyte survival following spinal cord injury in Bax-/- and Wld^s mice (Dong, Fazzaro et al. 2003). At 8 days following spinal cord hemisection there was a reduction in oligodendrocyte death in both Wld^s and Bax-/- mice. The protective effect is lost in Wld^s mice by 30 days post-injury; however, in Bax-/- mice the oligodendrocytes are still protected at this late timepoint. The protection provided in the Wld^s mice may be due to the axon-derived factors thought to be important to oligodendrocyte viability (Barres, Schmid et al. 1993). The protection of oligodendrocytes in the Bax-/- mice is thought to be due to inhibition of apoptosis (Dong, Fazzaro et al. 2003). Axonal integrity was also investigated both by light and electron microscopy, and axons were found to be present in the Bax-/- mice at the 8 day and absent by day 30 post injury, intervals between these two timepoints was not investigated (McDonald, personal communication). This is an area that deserves further investigation.

Wld^s mutation

The molecular basis of the protection offered by the Wld^s mutation has been studied. Investigations of the mutant mouse have revealed that all PNS and CNS neurones studied show delayed Wallerian degeneration following axonal injury. These include both PNS motor and sensory neurones (Lunn, Perry et al. 1989) and CNS retinal ganglion cells (Perry, Brown et al. 1991) and others (Steward 1992; Lyon, Ogunkolade et al. 1993). Conventional genetic approaches demonstrated that the mutation has an autosomal dominant phenotype. An 85kb tandem triplication was identified that encodes for a novel chimeric gene. This is translated into an in-frame fusion protein of the N-terminus of ubiquitination factor E4B (Ube4b), and the entire coding region of the nicotinamide adenine dinucleotide (NAD) synthesising enzyme, nicotinamide mononucleotide adenylyltransferase (Nmnat). The later of these fusion genes also includes a sequence encoding 18 amino acids not normally translated – termed W18 (Coleman, Conforti et al. 1998; Conforti, Tarlton et al. 2000; Fernando, Conforti et al. 2002).

It is now known that the Wld^s protein is located solely in the nucleus and has been excluded from being present in the axon (Fang, Bernardes-Silva et al. 2005). Whether the protein is simply at undetectable levels in the axon, or that is it not transported from the cell body down the axon has been a highly debated area. However, it has now been concluded that the Wld^s protein is absent from the axon (Fang, Bernardes-Silva et al. 2005). If the protein is indeed absent from the axon then it must act in the nucleus to exert its effect indirectly. Identifying these other downstream factors would thus help to unravel the mechanisms involved in Wallerian degeneration.

As well as having protective affects on axons undergoing Wallerian degeneration, the Wld^S gene is neuroprotective following a number of injuries and diseases, for example, the Wld^S gene is protective following transient cerebral ischemia (Gillingwater, Haley et al. 2004) and in a mouse model of Parkinson's disease (Sajadi, Schneider et al. 2004). It may therefore follow that this gene may be protective in an array of neurodegenerative diseases along with those mentioned above. Although Nmnat is encoded for in the parent Wld^S protein, it has not until recently been considered as having a role in the delay observed in Wallerian degeneration in the mutant mouse (Mack, Reiner et al. 2001; Coleman and Perry 2002). The ubiquitination factor E4B (Ube4b) was hypothesised to be the key factor. The reasons for which Ube4b received most attention in delayed Wallerian degeneration came from a number of observations: (1) an unpublished finding by Coleman and Perry demonstrating that a shorter Ube4b sequence fused to Nmnat does not delay Wallerian degeneration (Coleman and Perry 2002), (2) the basal levels of NAD are unaltered in the unlesioned Wld^S nervous system (Mack, Reiner et al. 2001), and (3) axonal degeneration is affected by mutations in other ubiquitin related proteins (Mukoyama, Yamazaki et al. 1989). It therefore follows that the ubiquitin proteasome pathway (UPP) may be important in degeneration. New evidence has recently emerged that indicates increased expression of Nmnat also has a role in axonal protection (Araki, Sasaki et al. 2004). The role of both the UPP and Nmnat will be discussed in greater detail below.

Ubiquitin proteasome pathway (UPP)

The UPP is one of the pathways involved in protein turnover within cells. Since Ube4b is encoded by the Wld^S mutant gene, it is possible that the UPP may be involved in axonal degeneration. Repeated ubiquitination of proteins is a signal to factors/proteins involved in the UPP for degradation. The role of Ube4b in this process is to regulate multi-ubiquitination of the proteins to be degraded; it does this in conjunction with other proteins of the UPP such as E1-activating enzyme, E2-conjugation factors and E3 ligase. In support of the idea of involvement of UPP proteins in degeneration, mutations in these other proteins can also affect axonal degeneration (Fig. 1.14). For example, mutation in Uch-L1 (a ubiquitin hydrolase), leads to spontaneous axon degeneration in the gracile axonal dystrophy (gad) mouse (Mukoyama, Yamazaki et al. 1989). The UPP is also important in a chronic disease, Familial Parkinson disease, caused by a mutation in the E3 ligase, parkin (Shimura, Hattori et al. 2000), although there are several familial forms of Parkinson disease.

In a study by Laser et al (2003), inhibition of the UPP by a proteasome inhibitor (lactacystin) 2 hours prior to transecting Wld^S neurones in vitro did not influence degeneration (Laser, Mack et al. 2003). However, it was observed that the proteasome

inhibitor did affect the uninjured axons: immediate arrest of neurite outgrowth was noted followed within 24hours by retrograde degeneration, however, a lower dose of lactacystin in PC12 cells leads to neurite outgrowth (Laser, Mack et al. 2003). By contrast, Zhai et al (2003) have demonstrated both *in vitro* and *in vivo* that inhibition of the ubiquitin proteasome system by both pharmacological and genetic means does delay axon degeneration (Zhai, Wang et al. 2003). They demonstrated that when applied in advance of injury (1-3hours in culture, 1 hour prior to optic nerve injury), protease inhibitors could delay axonal degeneration (Zhai, Wang et al. 2003). The need for the pre-treatment may indicate that the ubiquitin proteasome pathway is important in the early stages of Wallerian degeneration.

NAD/Nmnat

NAD, the molecule synthesised by Nmnat, has been described as the universal energy- and signal-carrying molecule that is essential for all organisms (Berger, Ramirez-Hernandez et al. 2004). NAD is involved in electron-transport in the mitochondria and also has a role in DNA repair and transcription at the nuclear level. The role of NAD in Wallerian degeneration has been investigated using an *in vitro* model of degeneration, initiated by either a transection injury or a toxic insult (Araki, Sasaki et al. 2004). Araki and colleagues studied cultures of primary dorsal root ganglion explant neurones infected with lentivirus expressing the entire Wld^S protein, or the Ube4b or Nmnat portions of the Wld^S protein alone, linked to enhanced green fluorescent protein (EGFP). Neurones expressing Nmnat showed comparable delayed axonal degeneration to those neurones expressing the entire chimeric Wld^S protein. However, neurones expressing the 70 amino acid Ube4b coding region, showed no delay of axonal degeneration. Thus, Araki concluded that it is the Nmnat portion of the Wld^S protein that was responsible for the delay in degeneration observed in the *Wld^S* mice (Araki, Sasaki et al. 2004). It has been shown that there is a four-fold increase in Nmnat activity but no increase in NAD levels in *Wld^S* tissues (Mack, Reiner et al. 2001). Araki and colleagues showed that exogenous NAD, added to neuronal culture medium at the time of axon injury, or for up to 8 hours before injury, had no protective effect. However, when preincubated with NAD for a longer time, at least 24 hours, there was a delay in axonal degeneration, suggesting that the protective effect of Nmnat possibly comes from transcriptional/translational events in the nucleus (Araki, Sasaki et al. 2004).

A family of NAD dependent deacetylases, the silent information regulators, or Sir family, along with poly(ADP-ribose) polymerase (PARP), are involved in major NAD-dependent nuclear enzymatic activities and may be involved in the mechanisms involved in axonal protection. The logic that has driven this thinking is that NAD and Sir have been

shown to be involved in changes in metabolism implicated in age-associated diseases. For example, neurodegenerative diseases, diabetes and cancers (Lin and Guarente 2003). Araki and colleagues investigated whether inhibitors of Sir and PARP would affect the axonal protection afforded by preincubation with NAD following axonal transection. DRG cells were preincubated with NAD alone, or NAD in the presence of either Sirtinol, an inhibitor of Sir, or 3AB, an inhibitor of PARP. Those DRG cells incubated with both NAD and Sirtinol together showed a significant inhibition of axonal protection, whereas inhibition of PARP had no effect. These results indicate a role for Sir in axonal protection. This is particularly interesting because of the relationship between Bax and Sir in apoptosis. In a healthy cell Bax is bound to Ku70 in the cytoplasm (Cohen, Lavu et al. 2004). This interaction prevents Bax from forming pores in the mitochondria, which leads to cytochrome c release. When Ku70 becomes acetylated, by CBP and/or PCAF (Cohen, Lavu et al. 2004), Bax is released and is able to associate with the mitochondrial membrane. SIRT1 is one of seven molecules (SIRT1-7) in humans and rodents that share the Sir conserved domain (Sirtuin, SIRT). SIRT1, like Sir, is a histone deacetylase and can remove the acetyl group from Ku70, allowing it to bind with Bax and prevent programmed cell death (Araki, Sasaki et al. 2004; Cohen, Miller et al. 2004). Therefore, NAD may be acting via SIRT1 at the level of the nucleus to regulate a specific genetic programme to prevent axonal degeneration in the *Wld*^{S} axons.

1.7 REGENERATION

It has been widely accepted that unlike those in the PNS, neurones of the CNS of mammals do not regenerate following injury (Jackowski 1995). As discussed earlier, following transection of CNS axons, the cell body undergoes chromatolysis, which eventually leads to apoptosis. This section will review some of the mechanisms that influence this lack of regeneration.

Following axonal transection in the PNS it is important for the axon distal to the injury to be cleared away, allowing the remaining proximal axon to regenerate (Brown, Perry et al. 1991; Brown, Lunn et al. 1992). If, following injury the distal axons of sensory fibres do not degenerate, or are slow to degenerate, such as in the Wld^{S} mouse, regeneration is halted until degeneration has completed (Brown, Perry et al. 1991; Brown, Lunn et al. 1992). However, certain axons have a different reaction to this. For example motor axons have been shown to be capable of regrowth even in the absence of degeneration of the distal axon (Lunn, Perry et al. 1989).

Even though CNS neurones do not regenerate, a number of studies, in adult rodents have shown that the axons of certain CNS neurones are intrinsically capable of

regeneration (David and Aguayo 1981). This means that the axons themselves have the ability to regenerate, and therefore there must be other factors preventing regeneration in the CNS. One obvious difference between the CNS and PNS are the cell types that surround the axons, i.e. the oligodendrocytes and astrocytes in the CNS and Schwann cells in the PNS. A widely used system for studying CNS degeneration and regeneration is optic nerve injury. It has been observed that retinal ganglion cells (RGCs) of rats and hamsters have the capacity to regenerate following injury in the appropriate environment. When one end of a peripheral nerve (PN) segment is inserted into the retina or attached/placed near to the optic nerve stump of a transected optic nerve, it has been observed that the axons of the RGCs do indeed grow along the PN graft. The Schwann cell has been determined to be the most important factor in the graft (Aguayo, Bray et al. 1990; Aguayo, Bray et al. 1990).

There are two main obstacles that must be overcome if an axon is to regenerate within the CNS. Firstly, intrinsic inhibitors may act to prevent regeneration when damage occurs, and secondly, formation of a glial scar following injury act as a physical barrier to regeneration:

(1) Schwab and Caroni (1988) demonstrated *in vitro* that neurites can grow over astrocytes and immature oligodendrocytes, but that they cannot grow over differentiated oligodendrocytes (Schwab and Caroni 1988). CNS white matter, oligodendrocytes and CNS myelin are all strong inhibitors of neurite outgrowth in culture. *In vivo* experiments have shown that antibodies raised against myelin-associated neurite growth inhibitors promote regeneration of damaged axons in the CNS (Schnell and Schwab 1990).

(2) The glial scar formed following injury acts as a physical barrier to regeneration (David and Aguayo 1981) and contains inhibitory factors, which when removed or neutralised allow axon growth to occur (Bradbury, Moon et al. 2002).

Three classes of CNS associated inhibitors have been identified: i) Nogo, ii) myelin-associated glycoprotein (MAG) and oligodendrocyte-myelin glycoprotein (OMgp) and iii) chondroitin sulphate proteoglycans (CSPGs).

NOGO

Nogo is a myelin-derived axon outgrowth inhibitor. It is expressed in CNS white matter and by cultured oligodendrocytes. Nogo induces growth cone collapse and inhibition of axon growth *in vitro*. Three isoforms of Nogo exist – A, B and C; neutralising antibodies directed against Nogo-A counteract much of the inhibitory activity of CNS myelin *in vitro* (Fournier and Strittmatter 2001) . Within Nogo there are two separate inhibitory domains: the amino-Nogo domain and the Nogo-66 domain. When

tested in soluble recombinant forms, both amino-Nogo and Nogo-66 have independent inhibitory activities (Fournier, GrandPre et al. 2001). Amino-Nogo is the fragment of Nogo from the amino-terminal to the first hydrophobic domain, and is only found in Nogo-A. Nogo-66 is a short residue region that is located between 2 hydrophobic domains; Nogo-66 is found in all three isoforms of Nogo.

A Nogo-66 receptor (NgR) has been identified that is expressed predominantly in the brain. This receptor also has high affinity for MAG and OMgp. NgR is G-protein linked to the cell surface and does not have an intracellular signalling domain. As a result it must act as a complex in order to function. It has been suggested that $p75^{NTR}$, a transmembrane receptor for neurotrophins, may act as a co-receptor for NgR, driving intracellular signalling through a Rho signalling pathway. Myelin and MAG both inhibit axonal growth by Rho-dependent mechanisms (Lehmann, Fournier et al. 1999); inactivation of the Rho signalling pathway promotes axonal regeneration (Lehmann, Fournier et al. 1999). Recently, a third protein has been identified that is proposed to be essential for NgR function. This is a CNS specific protein known as LINGO-1 of previously unknown function (LRR and Ig domain-containing, Nogo Receptor-interacting protein) (Mi, Lee et al. 2004). In non-neuronal cells, NgR and $p75^{NTR}$ are unable to form functional receptors, indicating that additional component(s) are required. Mi and colleagues (2004) identified LINGO-1 as the essential protein

Myelin-associated glycoprotein (MAG) and Oligodendrocyte-myelin glycoprotein (OMpg)

It has been known for some time that myelin-associated glycoprotein (MAG), a glycoprotein associated with the myelin sheath that surrounds the axon, inhibits neurite extension *in vitro* (Mukhopadhyay, Doherty et al. 1994). Whether MAG acts as an inhibitor or is simply nonpermissive for axon growth was not clear until recently. MAG-coated beads induce the collapse of growth cones (Li, Shibata et al. 1996), and soluble MAG released from myelin inhibits axonal growth (Tang, Woodhall et al. 1997). This may indicate that MAG is an inhibitory molecule. However, it is interesting to note that MAG also has a positive effect on neurone growth during development (Mukhopadhyay, Doherty et al. 1994). This is in contrast to its negative effect on neurite growth *in vitro*.

Oligodendrocyte-myelin glycoprotein (OMgp), purified from myelin, was previously called arrestin due to its potent neurone growth inhibition *in vitro* (Kottis, Thibault et al. 2002). Arrestin consists predominantly of OMgp, which once purified was identified as the neurone growth inhibitor component of arrestin (Kottis, Thibault et al. 2002). This protein is a relatively minor component of CNS myelin, so it is likely that inhibition of regeneration is not its only physiological role.

Chondroitin sulphate proteoglycans (CSPGs)

Glial scars, a barrier to regeneration formed following CNS injury, contain astrocytes, oligodendrocyte precursor cells and extracellular matrix molecules, such as CSPGs. CSPGs are up-regulated in the CNS following injury, specifically around the lesion site where the glial scar forms. CSPGs consist of a protein core and long, unbranched polysaccharides (glycosaminoglycans [GAGs]), comprising chondroitin sulphates (CS) disaccharide unit repeats (Properzi, Asher et al. 2003). It has been shown that glial scar-associated proteoglycans are potent inhibitors of axon growth *in vitro* (McKeon, Schreiber et al. 1991), and i*n vivo,* removal of the GAG chains of CSPG can restore neurite growth following axonal damage (Bradbury, Moon et al. 2002).

1.8 GLIA RESPONSE TO INJURY

The brain contains glial cells as well as neurones, which, following injury react accordingly. These cells include microglia, astoroctes and oligodendrocytes. Below if a brief description of these glial cells.

Microglia

All tissues of the body contain a population of resident macrophages. These cells form the first line of defence against tissue injury or infection, and respond rapidly to changes in tissue homeostasis. The microglia are the resident macrophages of the CNS parenchyma and are the smallest of the glial cells. In the healthy CNS these microglia are quiescent, i.e. they have a down regulated phenotype, however, they are highly responsive cells that, when activated alter their morphology, antigen expression and hey also proliferate (Perry, Bell et al. 1995).

Astrocytes

Astrocytes are star shaped glial cells that perform a variety of functions in the CNS. Astrocytes provide physical support to neurones and clean up debris, via phagocytosis, within the brain. They also provide neurones with some of the chemicals needed for proper functioning and help control the chemical composition of fluid surrounding neurones.

Astrocytes, like microglia, are highly responsive cells, following injury astrocytes change their morphology and proliferate. Staining for an intermiediate filament, glial fibrillary acidic protein (GFAP), is often used to observe changes in astrocytes.

Oligodendrocytes

The principle function of oligodendrocytes is to provide support to axons and to produce the Myelin sheath, which insulates the axons. Oligodendrocytes are capable of

myelinating numerous axons, this is in contrast to Scwann cells in the periphery, which myelinate only one axon.

Little is known about the response of the oligodendrocytes following injury (Bartholdi and Schwab 1998). The Oligodendrocytes precursors are known to proliferate following an injury such as a cortical stab injury, close to the site of injury (Hampton, Rhodes et al. 2004).

1.9 SUMMARY

Until recently, the molecular mechanisms of axonal degeneration following injury has been a largely neglected area of investigation. Axonal degeneration was thought to be a passive process, whereby the portion of axon distal to the injury, and disconnected from the cell body, simply withered away due to its loss of nutritional support and loss of connection with the cell body, i.e. the site of protein synthesis. This form of degeneration was termed Wallerian degeneration. The serendipitous discovery of the mutant mouse with delayed, or *slow* Wallerian degeneration (*Wld^s*) lead to the conclusion that Wallerian degeneration is in fact an active process, akin to programmed cell death.

The molecular mechanisms of axon degeneration are poorly understood, and the current methods of detecting axonal injury in the central nervous system (CNS) do little but simply show us that an injury has occurred which has altered axonal integrity.

To further our understanding of axonal degeneration it is imperitive to develop new tools and approaches to study this area of neuroscience.

1.10 OBJECTIVES

Our overall objective of this work was to investigate the molecular mechanisms of axonal degeneration. The rationale for this has been detailed above, however, in summary the reasons why the work in this thesis has been carried out is as follows: Wallerian degeneration is an active process akin to programmed cell death, if we can identify the mechanisms involved in Wallerian degeneration it may be possible in the future to limit damage caused by axonal loss in diseases such as multiple sclerosis, and to limit the secondary damage seen in traumatic CNS injuries.

I have undertaken experiments to develop a novel approach for studying axonal degeneration *in vivo*. Novel antibodies were raised against components of degenerating sciatic nerves and characterised for immunocytochemistry and Western blotting of injured CNS tissues.

Our objectives were as follows:

1. to generate antibodies against antigens expressed in axons undergoing Wallerian degeneration.
2. characterisation of immunostaining on naïve and injured CNS and peripheral tissues.
3. analysis of target antigens recognised by the novel antibodies using a proteomics approach.

We sought to identify specific, novel changes in the portion of axon undergoing Wallerian degeneration. We will look to identify any changes in intact proteins entering the degenerating axon, breakdown products of proteins already there and/or any upregulation of any proteins that may be involved in the process of Wallerian degeneration.

1.11 CHAPTER SYNOPSES

Chapter 2

General methodologies are given in this chapter. Protocols for specialised methodologies will be described in the relevant chapters.

Chapter 3

This chapter describes the production of polyclonal antisera raised against antigens in degenerating axons. Staining of injured and naïve CNS and peripheral tissues was characterised by immunocytochemistry.

The experiments in Chapter 3 clearly demonstrate that I have polyclonal antisera that detect changes in CNS tissues post injury.

Chapter 4

This chapter describes experiments carried out to identify antigens recognised by antisera raised in chapter three. An approach with Western blotting combined with proteomics lead to the identification of a number of proteins, the expression of which may change following axonal injury. The identified proteins were then investigated using immunocytochemistry and Western blotting to determine whether they were involved in Wallerian degeneration.

By using a proteomic approach I have identified three proteins that may be involved in axonal degeneration, albumin, kid-1 and Focal Adhesion Kinase (FAK). Preliminary experiments indicated that FAK may be the most interesting to continue to investigate.

Chapter 5

This chapter describes the results of experiments designed to characterise the expression of one of the proteins identified in chapter 4, focal adhesion kinase (FAK), following injury. The temporal and spatial profile of FAK in a range of CNS tissues, following injury, was investigated using a combined approach of immunocytochemistry and Western blotting.

In this chapter I have shown that FAK is upregulated in glia surrounding the portion of axon distal to the site of nerve injury. In particular, FAK is upregulated in oligodendrocytes from as early as 6hrs post injury.

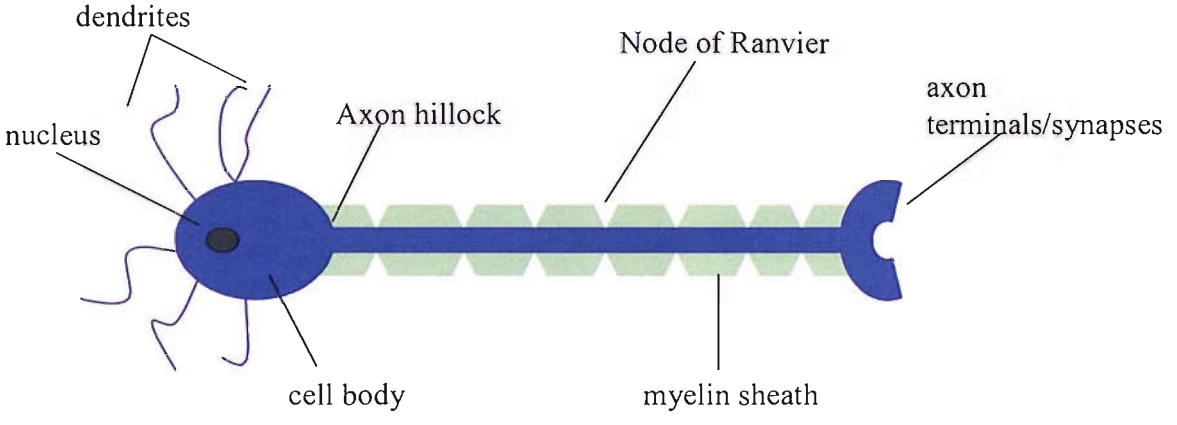

Fig. 1.1 Schematic representation of a neurone. The cell body of the neurone receives information through its associated dendrites. This information is summated in the axon hillock, a specialised structure that attaches the axon to the cell body. If the appropriate threshold is reached, an action potential is generated that then travels along the axon, via the nodes of Ranvier, to the axon terminals/synapses. The synapses then transmit the information to the target cell or tissue. The axon also contains structures that transport signals from the axon terminal to the cell body. These signals are such molecules as neurotrophins that are secreted from the target cell or tissue; they are taken up via the axon terminal/synapse and transported to the cell body.

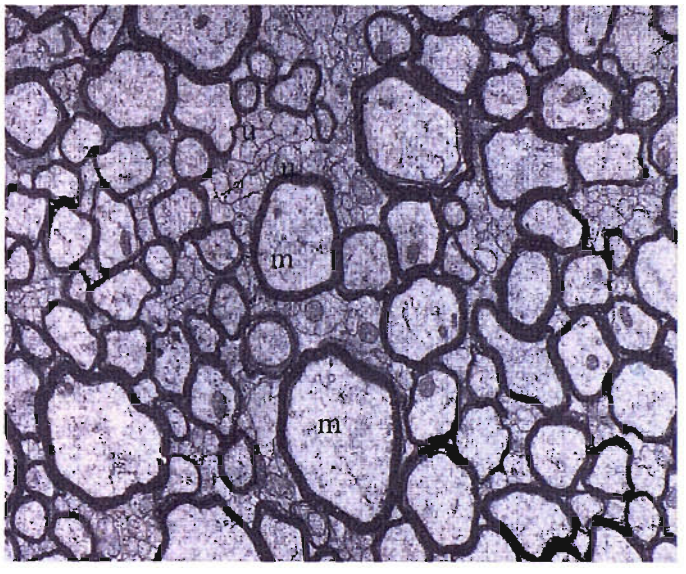

Fig. 1.2. Electron micrograph showing compactly arranged myelinated (m) and unmyelinated (u) axons in rat cerebral white matter (x7000). From Waxman et al., 1995.

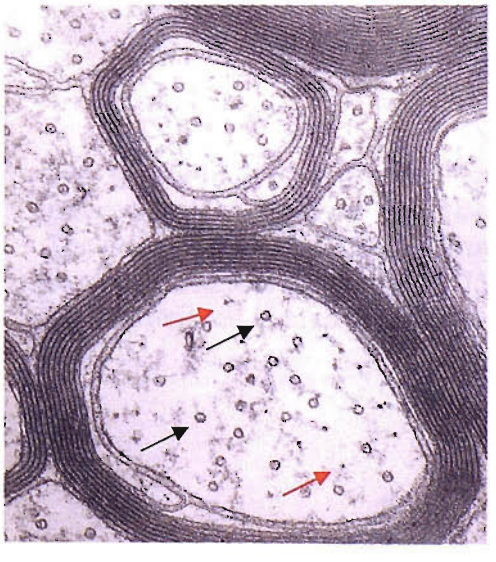

Fig. 1.3. Cross section of myelinated axons. Electron microscope section from normal adult white matter showing neurofilaments (red arrows) and microtubules (black arrows). From Waxman et al., 1995.

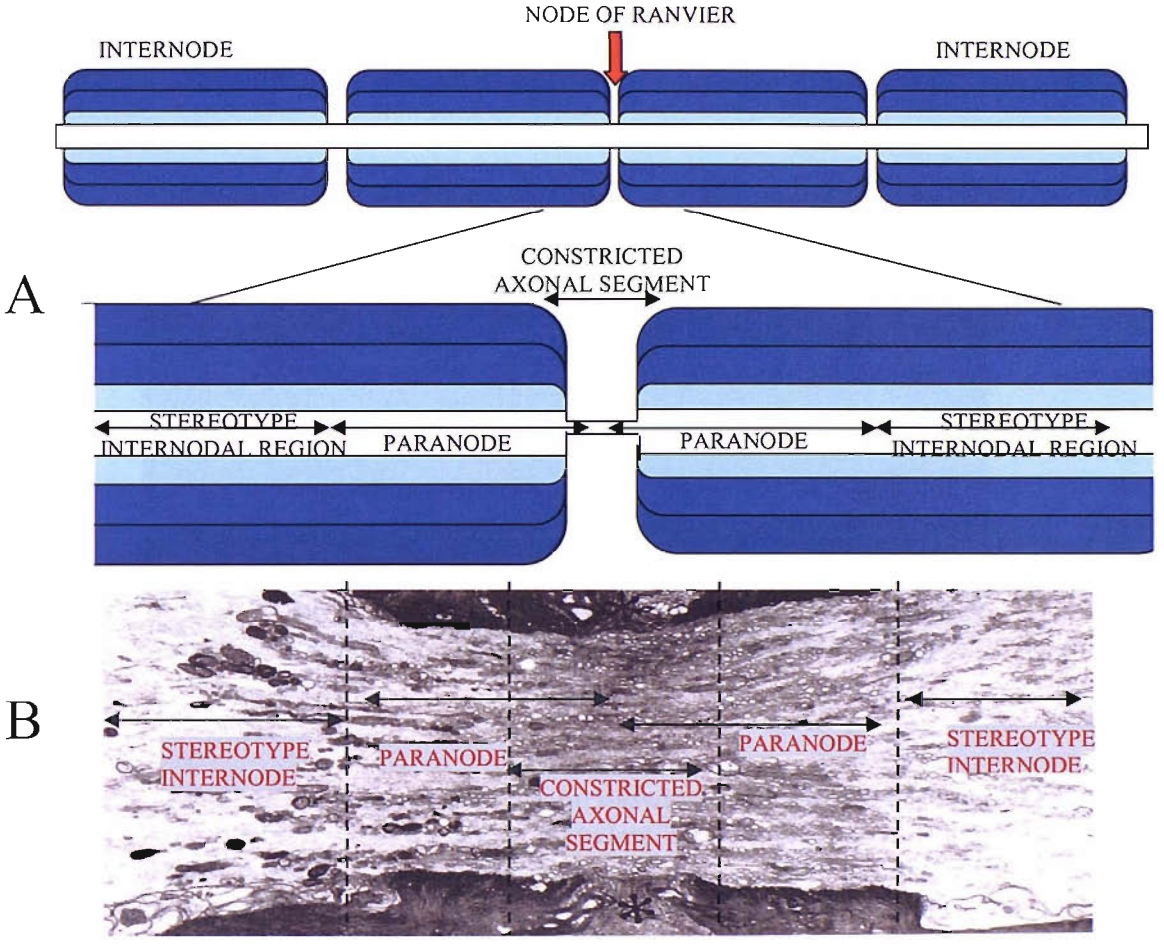

Fig. 1.4 Schematic representation of a typical node of Ranvier (A) and an electron micrograph of the same area (B). (Electron micrograph from Waxman et al., 1995). The node of Ranvier is a small unmyelinated region of the axon that has a cross-sectional area that is reduced by 75-90% compared to the adjacent internode. The portion reduced in area in called the constricted axonal segment.

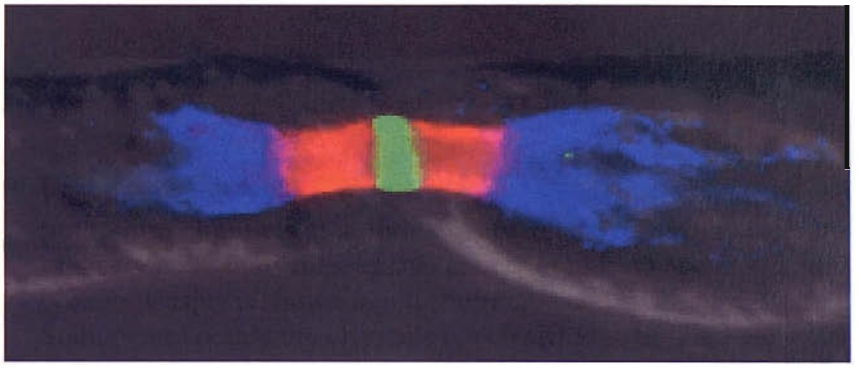

Fig. 1.5 Confocal microscopy image showing clustering of sodium and potassium channels at a node of Ranvier. Sodium channels are shown in green, potassium channels are shown in blue and contactin associated protein (Caspr) is shown in red (from Rasband and Trimmer, 2001). Sodium and potassium channels are clustered to appropriate areas of the node of Ranvier through interactions between the axon and myelin.

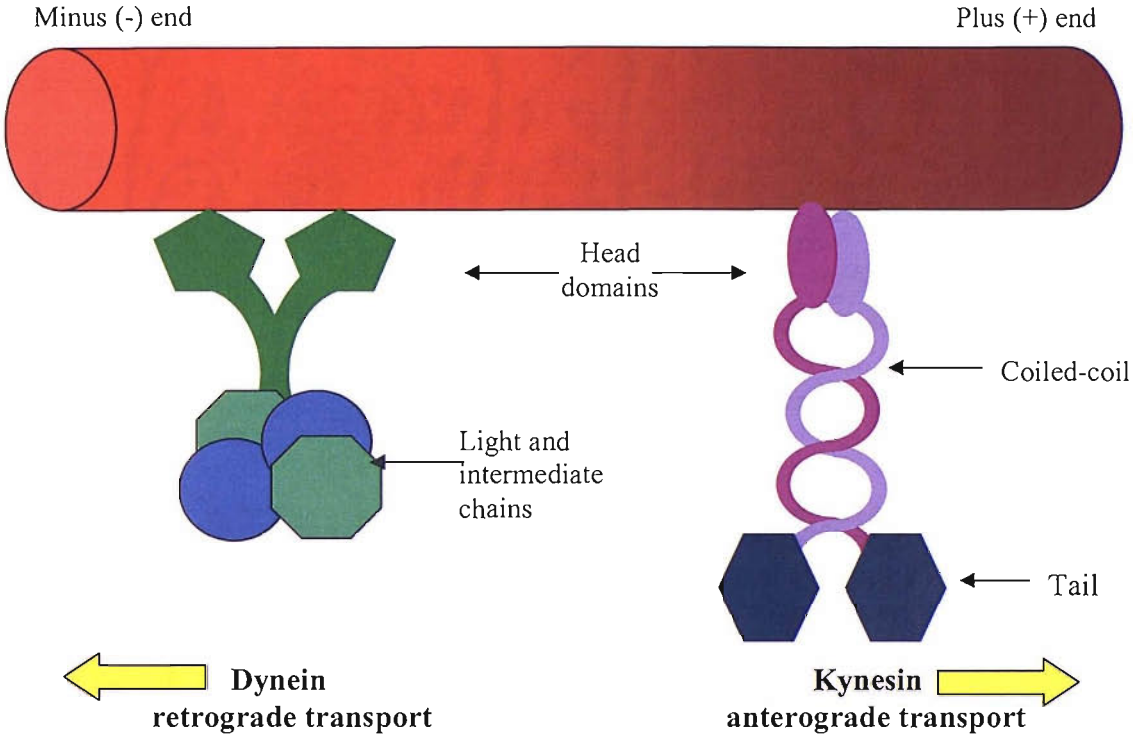

Fig. 1.6 Schematic representation of the proteins involved in anterograde and retrograde axonal transport. Molecular 'motors' termed kynesins and dyneins transport their cargo either away from the cell body (anterograde transport) or towards the cell body (retrograde transport) respectively. The head domains of both kinesins and dyneins are made up of heavy chains that contain the motor domains. The "bodies" of these motors differ. Kynesins have an α-helical coiled-coil domain and a tail domain, whereas dyneins have between one and three heavy chains and a varying number of intermediate and light chains. The complex array of combinations of chains may play an important role in the diversity of proteins that these transport proteins carry.

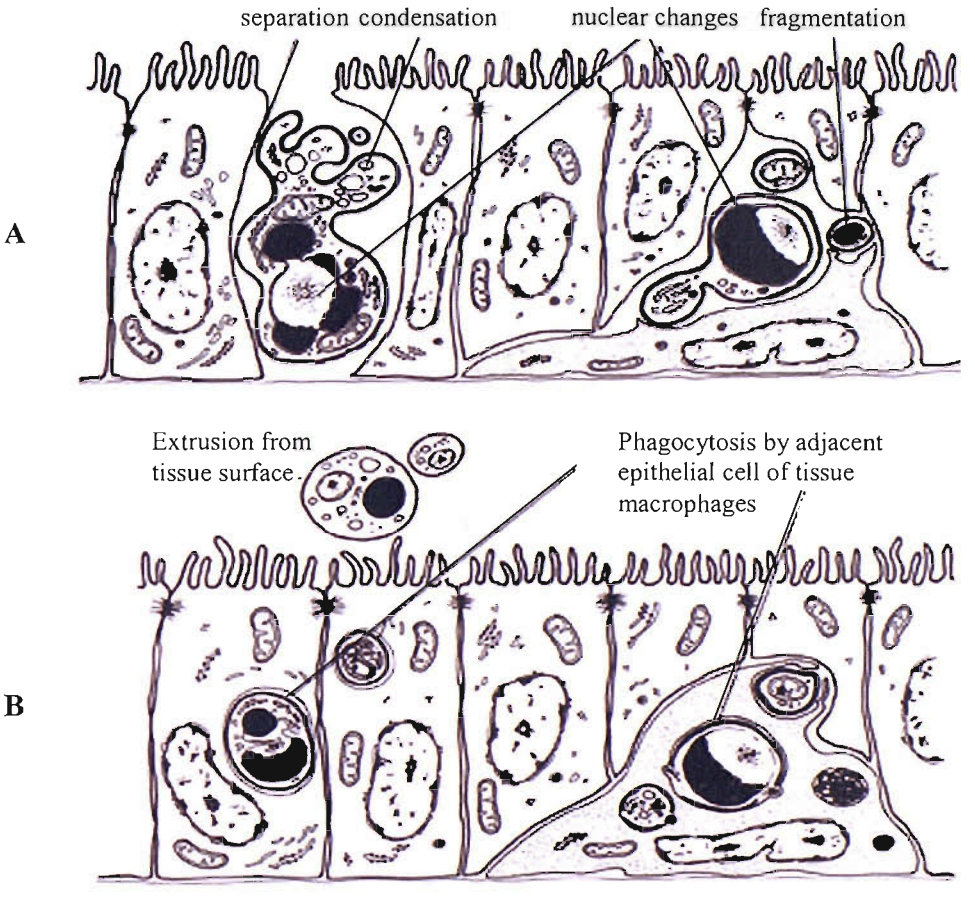

Fig. 1.7. Schematic representation summarising the major morphological changes that occur during apoptosis. (A) Formation of apoptotic cells; (B) Summary of the fate of apoptotic cells. Diagram from Cell Death in Biology and Pathology (1981), Bowen ID and Lockshin R.

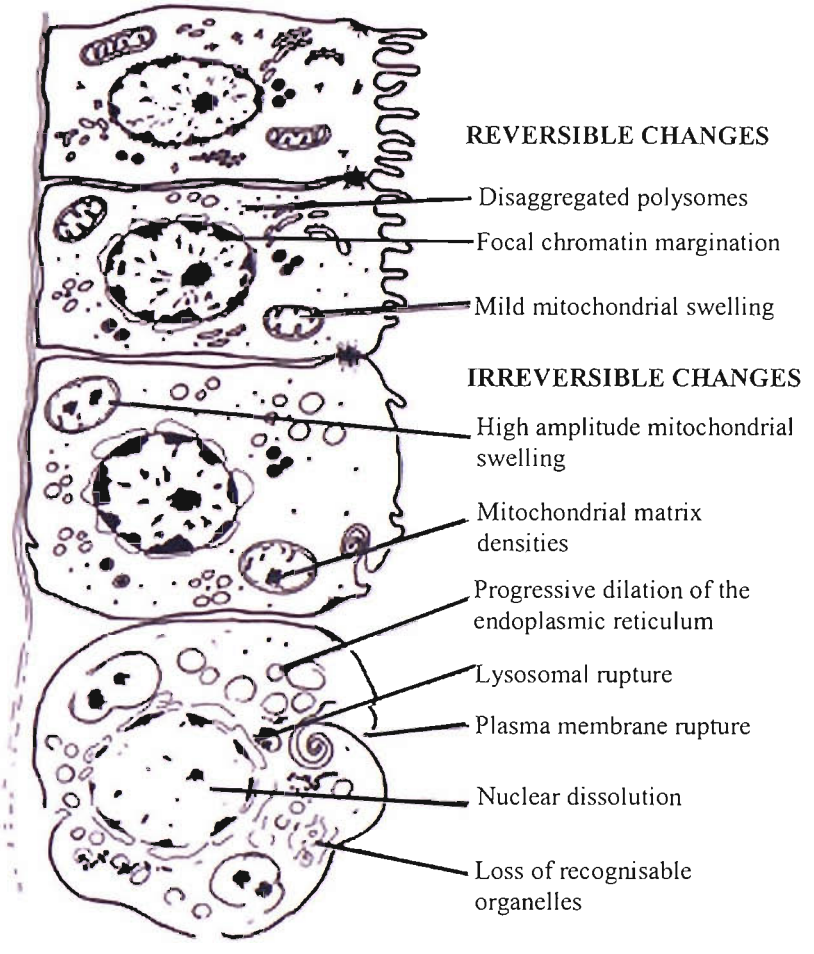

Fig. 1.8. Schematic representation of the key morphological changes that occur in necrosis. Early changes that occur during necrosis can be considered as reversible. However, these changes are followed by irreversible changes. Once the cell has entered these irreversible changes that result in cell death. Diagram from Cell Death in Biology and Pathology (1981), Bowen ID and Lockshin R.

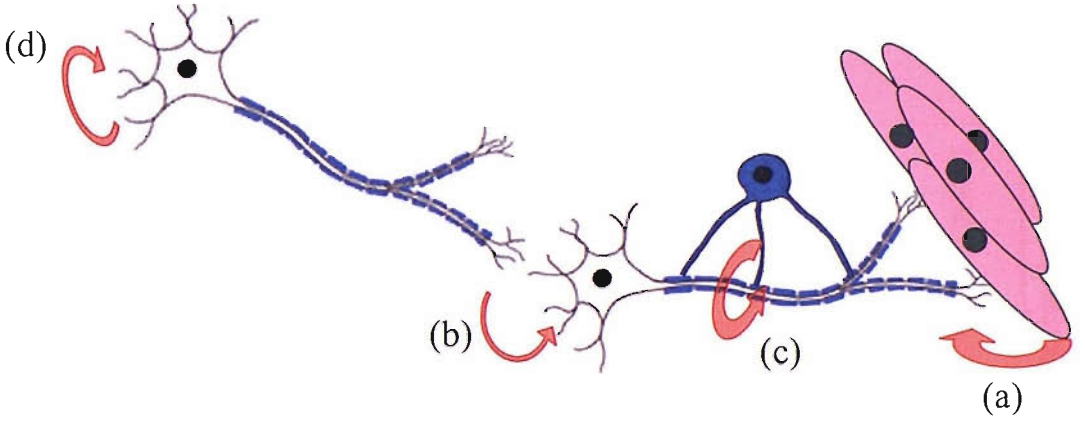

Fig. 1.9. Neurotrophic support of neurones. Neurotrophic factors (NFs) can be obtained (a) from the target cell/tissue, (b) from afferent input, (c) from local interactions with glia. Cells can also express NTs to which they respond in an autocrine fashion (d).

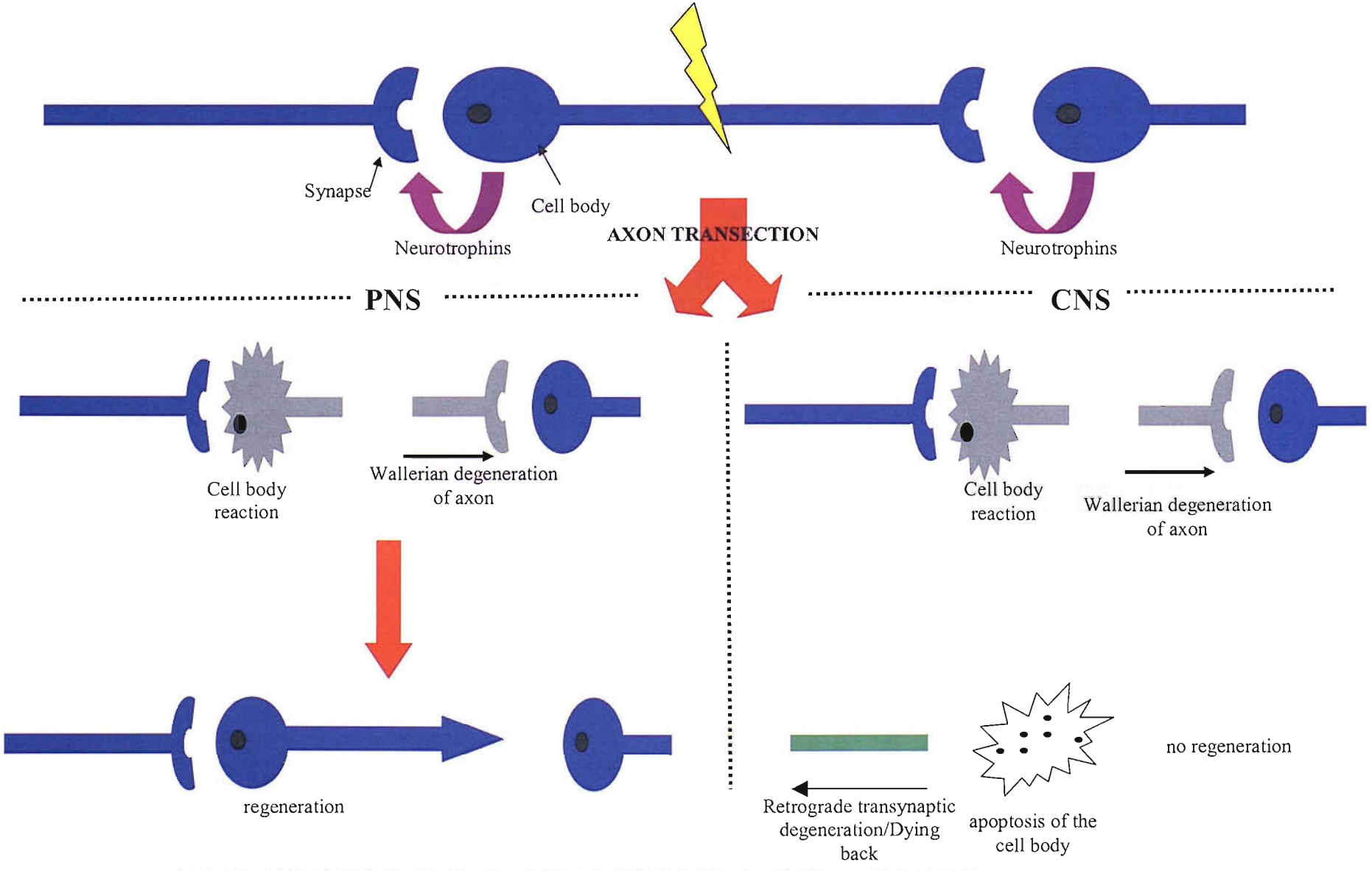

Fig. 1.10 Mechanisms of axonal degeneration. Following axonal transection, in both the PNS and CNS, the segment distal to the site of injury undergoes Wallerian degeneration. The cell body undergoes chromatolysis or the 'cell body reaction', followed by either regeneration (in the PNS) or eventual apoptosis, in the CNS or PNS (depending on the proximity of injury to the cell body). If the cell body dies, axons terminating onto it undergo a process called retrograde transynaptic degeneration, due to a loss of neurotrophic factors.

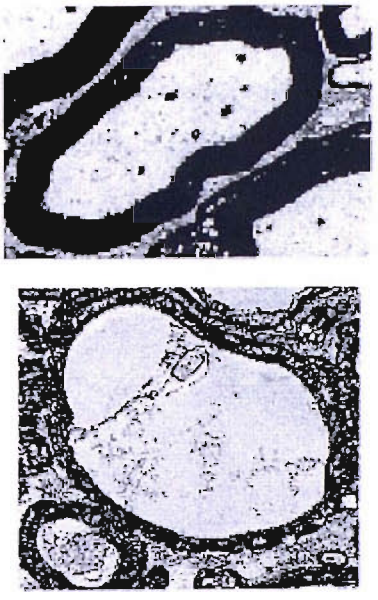

Fig. 1.11 Electron Microscopy photomicrographs comparing a naïve axon and one undergoing degeneration. The EM of a healthy axon (top) shows a clear difference from the axon undergoing degeneration (bottom). There are also changes in the myelin sheath.

EM pictures from Dr D Corkill

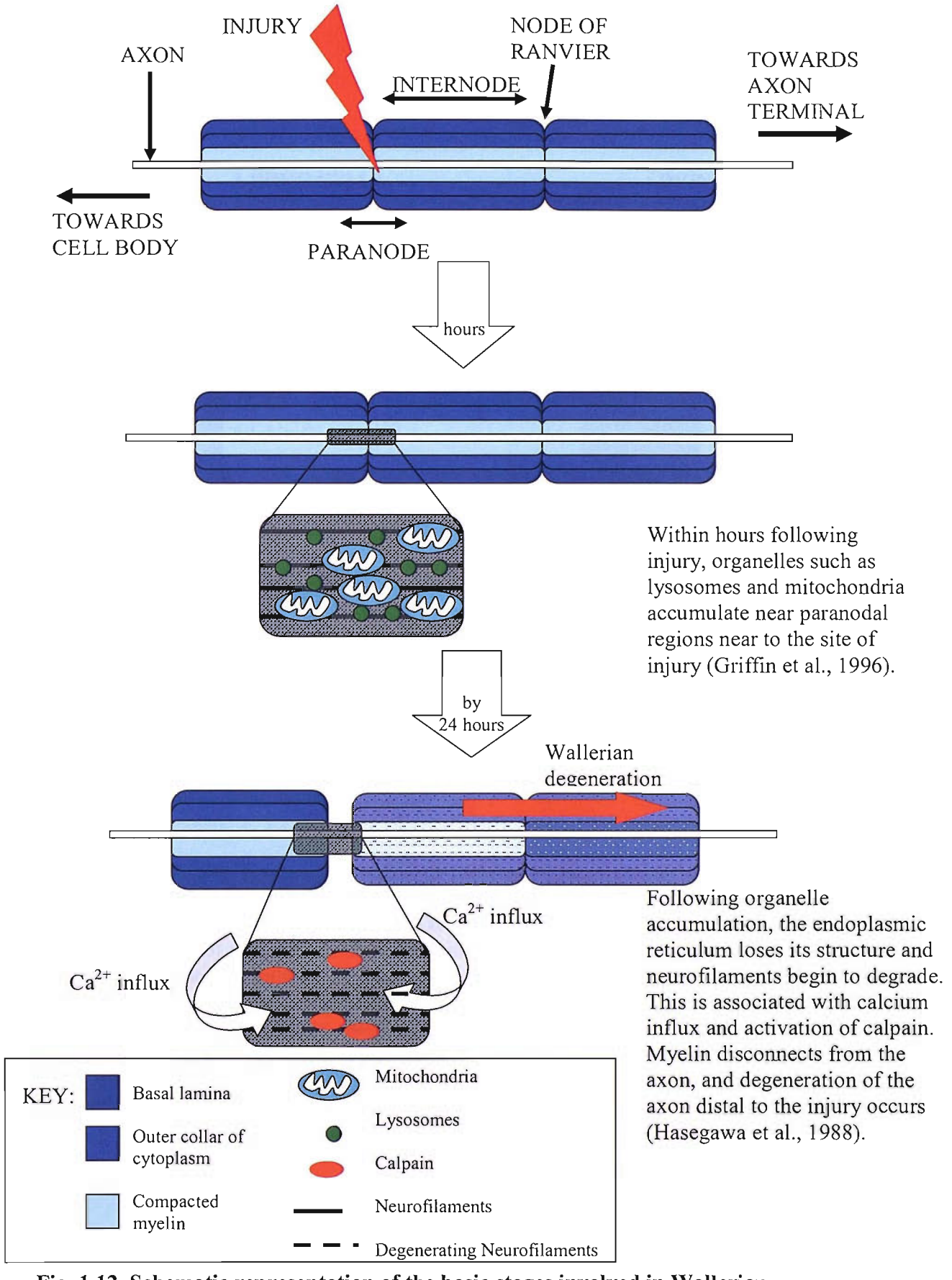

Fig. 1.12 Schematic representation of the basic stages involved in Wallerian degeneration. Following injury to the axon a series of molecular events occur distal to the site of injury. These are the first stages of Wallerian degeneration.

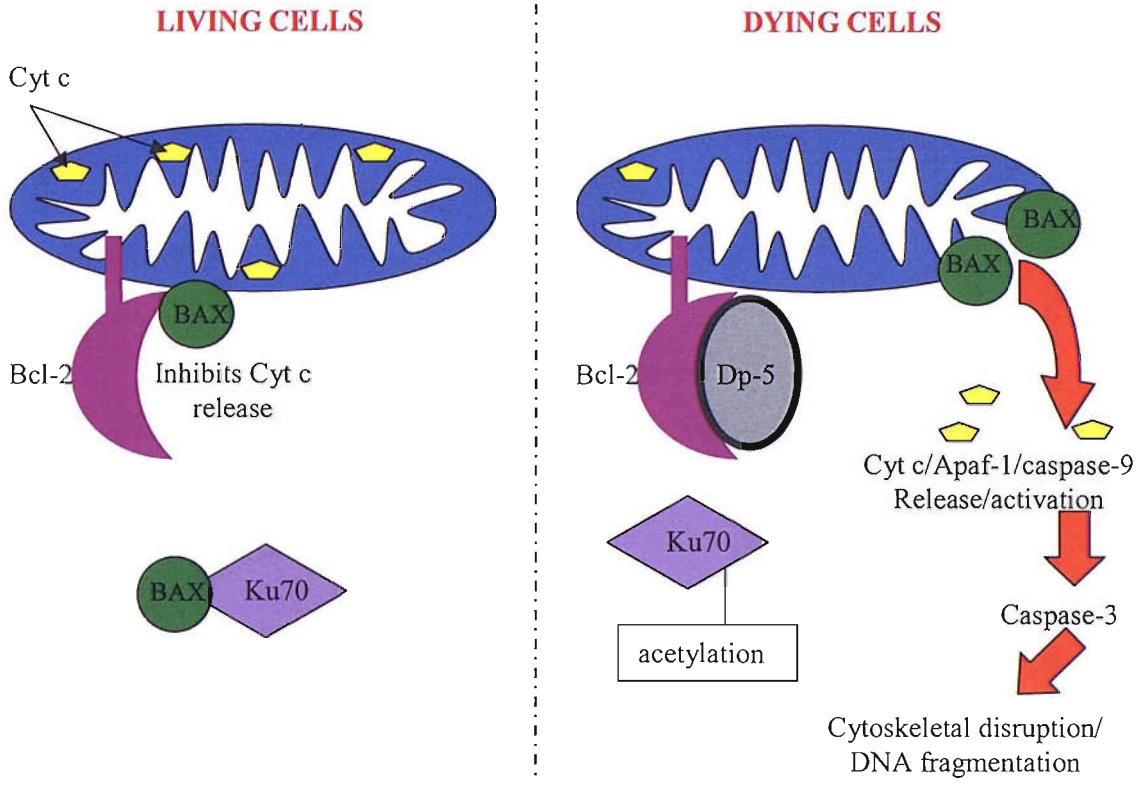

Fig. 1.13. Schematic representation showing some of the actions of Bcl-2 and Bax in living and dying cells. In living cells, Bcl-2 acts at the mitochondrial membrane to inhibit mitochondrial-associated Bax pores from releasing cytochrome c (Cyt c). A DNA repair factor (Ku70) also inhibits 'free' Bax, in the cytoplasm, preventing Bax binding with the mitochondrial membrane. When a cell is programmed to die, Bcl-2 is inhibited from binding Bax by Dp-5, and Ku70 becomes acetylated. This changes its conformation so that it can no longer bind Bax. As a result, free Bax can associate with the mitochondrial membrane, form pores and enable Cyt c release. Released Cyt c activates caspase 3, leading eventually to cell death.

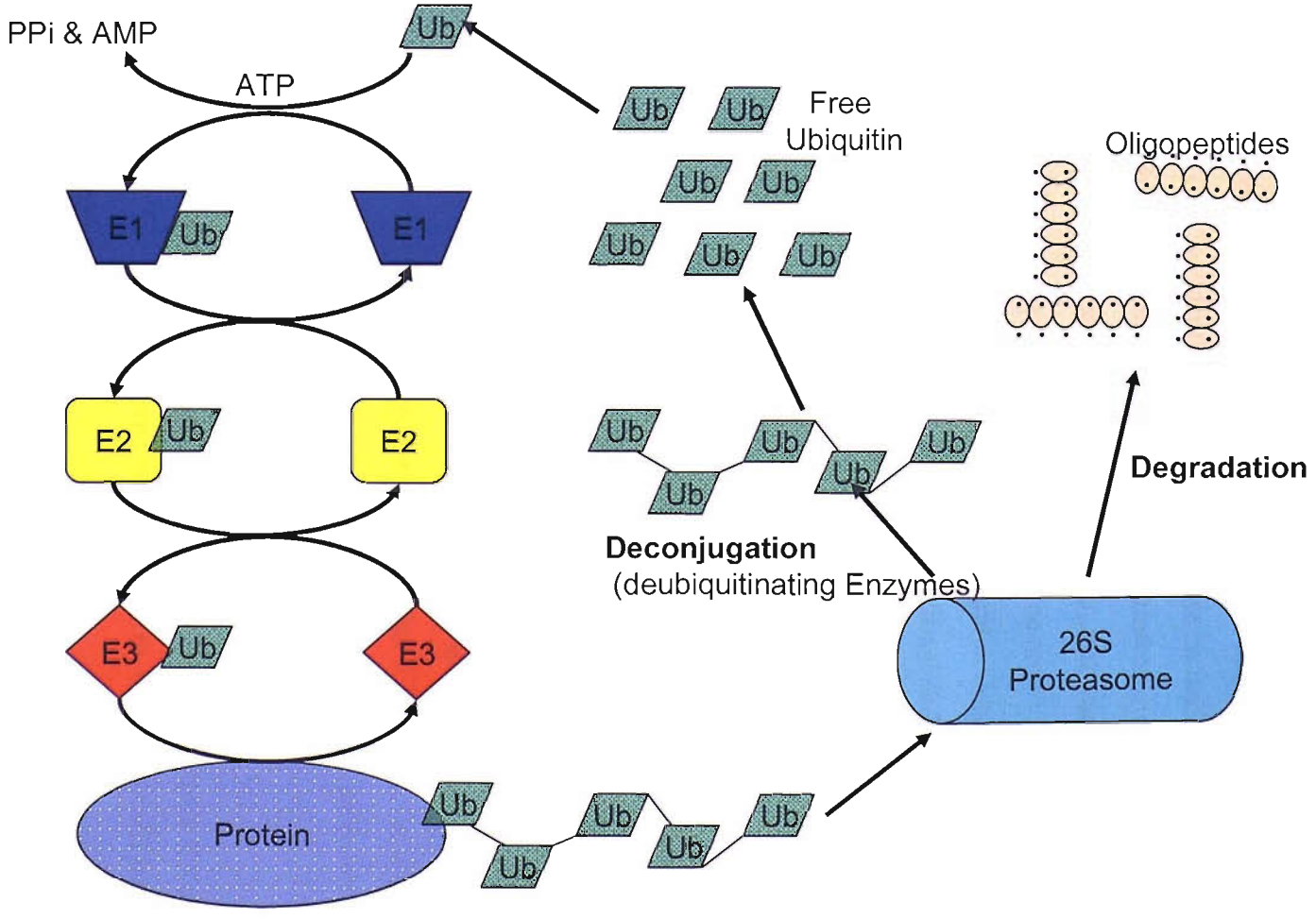

Fig, 1.14 Schematic representation of the Ubiquitin Proteasome Pathway. Ubiquitin becomes covalently linked to itself and/or other proteins wither as a single molecule or as poly-ubiquitin chains. The attachment of ubiquitin to the target protein requires a series of ATP-dependent enzymatic steps by E1 (ubiquitin activating), E2 (ubiquitin conjugating) and E3 (ubiquitin ligating) enzymes. These covalent ubiquitin bonds can be reversed by specific deubiquitinating enzymes.

CHAPTER 2 General Methodologies

2.1 Animals

Experimental rodents (male Wistar rats, typically over 200g) were housed in groups of three or more at an ambient temperature of 21±2°C and on a standard 12h:12h light-dark cycle. Food [standard laboratory chow (RM-1., SDS, UK)] and water were provided *ad libitum*.

Two New Zealand White Rabbits were obtained from Harlan Ltd (UK) and named ELR1 and ELR2 for identification. Rabbits were housed individually, and in order to provide environmental enrichment, they were allowed out every other day into a large area. Dry food (standard laboratory chow), fresh food, and water were provided *ad libitum*.

All animal procedures conformed with the requirements of the UK Home Office animal licensing inspectorate and were carried out under licence. All animals were purchased from Harlan Ltd (UK), unless otherwise stated, and were permitted an acclimatisation period of seven days prior to undergoing a Home Office regulated surgical procedure.

2.2 Anaesthesia

2.2.1 Rats

Unless stated otherwise all animals undergoing surgical procedures were male Wistar rats, typically over 200g. Rodents were anaesthetised with Avertin at a dose of 0.1ml per 10g (i.p) (Appendix I-A), analgesia given was Buprenorphine i.p at 0.01mg/kg. The level of consciousness of the animals was assessed by observing their respiratory pattern and paw withdrawl to gentle pressure. For spinal cord surgery, animals were anaesthetised with Hypnorm/Hypnovel (midazolam 3.38mg/kg, fentanyl citrate 0.21mg/kg, fluanisone 6.75 mg/kg). Terminal anaesthesia for transcardial perfusions was induced with sodium pentabarbitone (Sagatal, i.p at 2.5ml/kg)).

2.2.2 Rabbits

Rabbits were anaesthetised with Hypnorm for surgical procegures (0.5 ml/kg i.m). Terminal anaesthesia was achieved with an overdose of Hypnorm/Hypnoval (i.m).

2.3 Surgery

2.3.1 Sciatic nerve transection

The left thigh and upper leg was shaved and topical lignocaine applied to the area to be incised. A small longitudinal incision was made, approximately 1cm in length, just below the thigh bone to expose the muscle underneath. A small opening was made through the muscle layer using blunt dissection to expose the sciatic nerve. The sciatic nerve was then completely transected using a fine pair of spring scissors and the skin wound closed using 4-0 Mersilk non-absorbable sutures.

2.3.2 Intracranial stab lesions

All surgical procedures were performed under an operating microscope (Wild M650, Leitz, UK). Rats were anaesthetised, the head was then shaved and topical lignocaine applied to the scalp and the ears. The animals were then secured in a stereotaxic frame. The stereotaxic co-ordinates for the striatum relative to bregma were +1 (anterior-posterior), ±3 (medial-lateral), and –4.5 (dorsal-ventral) (Paxinos and Watson 1986).

Briefly, a midline sagittal incision was made through the scalp to expose the underlying skull. Using a dental drill, a burr hole approximately 5x1mm was created in the skull at the appropriate co-ordinates. The dura mater was removed using a fine pair of surgical forceps to expose the underlying brain. A stab lesion was created using a number 11 scalpel blade (Swann-Morton, Sheffield, UK) attached to a needle holder. The skin was re-apposed and the incision was closed with 4-0 Mersilk, non-absorbable sutures.

2.3.3 Spinal cord transections

In order to maintain body temperature, during the procedure rats were placed on a homeothermic blanket unit (Harvard Apparatus). A partial laminectomy was performed at T7 to expose the spinal cord. The muscle was dissected away from T6 and T8 to enable immobilisation of the spine in a stereotaxic frame using clamps. A fine pair of spring scissors were then used to partially transect the spinal cord. The muscle layers were re-apposed using 4/0 Vicryl sutures, and the skin incision closed with 12mm Michel clips.

2.3.4 Optic nerve lesions

The optic nerve was approached from the orbita by incision of the conjunctiva under guidance of a surgical microscope. The optic nerve and retinal blood supply were visualised using an operating microscope (Wild M650, Leitz, UK) and the nerve was then either crushed for 10 seconds with a pair of curved forceps or transected completely using a fine pair of spring scissors. Only one optic nerve was crushed/lesioned in each animal.

Following all surgical procedures animals were placed in a heated box and observed for adverse affects; recovery was uneventful. Once fully conscious the animals were returned to their home cages.

2.4 Tissue Harvesting

The tissues were removed at various timepoints post injury, the details of timepoints are indicate in the specific chapter methods.

2.4.1 Perfusion and tissue fixation

Rats were terminally anaesthetised, and the thoracic cavity opened to expose the heart. A butterfly needle (21-gauge, Venisystems, Abbott, Eire) was inserted into the left

ventricle and a small hole created in the right atrium. The rats were then perfused with 0.9% saline containing 5000U/l heparin (Sigma, UK), until the perfusate ran clear. If required, this was then followed by a fixative [periodate lysine paraformaldehyde (PLP) (Appendix I-B), 4% paraformaldehyde (PAF) (Appendix I-C), 10% neutral buffered formalin (Sigma, UK) or Bouin's (Appendix I-D)], until the animal was sufficiently fixed.

2.4.1.1 Brain removal

Brains were carefully removed and immediately frozen in Tissue-Tek OCT on isopentane (Sakura Finetek Europe B.V., Zoeterwoude, Netherlands) suspended over liquid nitrogen, or snap frozen in liquid nitrogen. The tissue was stored at –20°C or -70°C (snap frozen samples) until required.

Tissues fixed in PLP or PAF were post-fixed for 4-6 hours at 4°C before being transferred into 30% sucrose for cryoprotection (usually overnight or until the brains sunk). The tissue was embedded in OCT as above, and stored at -20°C until required. Formalin and Bouin's fixed tissue was post-fixed for at least 5 days at 4°C. The tissue was dehydrated through increasing concentrations of ethanol and immersed in histoclear for 12-15 hours. Brains were then submerged in paraffin wax (Polywax, TCS, UK) at +40°C for 4 hours, mounted in cassettes and allowed to cool.

2.4.1.2 Sciatic nerve removal

Rats were terminally anaesthetised and distal segments of the transected sciatic nerve (measuring approximately 15-20mm in length) were removed, and snap-frozen in liquid nitrogen or frozen in OCT on isopentane over liquid nitrogen. The samples were kept at either –20°C or -80°C (snap frozen samples) until required.

2.4.1.3 Spinal cord harvesting

Rats were terminally anaesthetised, perfused and either fixed with formalin or Bouin's or left unfixed, as described above. The spinal cord was carefully removed, and either post fixed for a minimum of 3 days before undergoing tissue processing and embedding in paraffin wax (section 2.4.1.1), or snap-frozen in liquid nitrogen following removal and kept at -20°C or -80°C until required.

2.4.1.4 Optic nerve and retina removal

Rodents were terminally anaesthetised, perfused and either fixed with formalin or Bouin's or left unfixed. The naïve and injured optic nerves and retinas were removed and were either post-fixed in the appropriate fixative for a minimum of 3 days before tissue processing and embedding in paraffin wax (section 2.4.1.1), or snap-frozen in liquid nitrogen and stored at -20°C or -80°C until required.

2.5 Western Blots

2.5.1 Tissue preparation

Tissue samples were homogenised in 600µl of a homogenisation buffer (Appendix I-E) and then spun down at 14,000rpm for 30 minutes at 4°C. The supernatant was removed and spun down at 100,000rpm for 1 hour at 4°C. Supernatant was taken and assayed to determine the protein concentration using a Bio-Rad Protein Assay (BioRad), before being aliquoted and stored at -20°C until required.

2.5.2 Western Blot protocol

2.5.2.1 SDS-PAGE

Samples were run on 4-20% gradient Tris-SDS (Tris-sodium dodecyl sulphate) gels (BioRad, UK, 161-1159).

2x Laemmli sample buffer (Sigma, S-3401) was added to the homogenates which were then boiled for 2 minutes. Gels were placed in a BioRad tank and submerged in 1x electrode buffer (Appendix I-F). 5-10µg of samples were loaded per well; the first lane was always loaded with 5µl of a molecular weight marker (Kaleidoscope Pre-stained Standards [BioRad, 161-0324]). Gels were run at 30V for 30 minutes. The voltage was then increased to 60V for a further 90 minutes.

2.5.2.2 Sample transfer

The gel underwent transfer at 4°C for 1 hour with nitrocellulose membrane in transfer buffer (Appendix I-G). A voltage of 100V was used to facilitate the transfer.

2.5.2.3 Blotting

Transfer patterns were confirmed by staining the nitrocellulose membrane for 10 minutes with Ponceau Red (BDH, UK). Differentiation in distilled water revealed the staining of the protein bands (membranes used for fluorescent labelling were not stained with Ponceau Red).

The membrane was then placed in blocking buffer (either 5% skimmed milk powder or 3% BSA in TBST [Appendix I-H]) for 1 hour at room temperature. The primary antibody was added at the appropriate concentration (in blocking buffer) and incubated overnight at 4°C on a rotomixer (Appendix I-I).

The following day, the membranes were washed in TBST (3x5 minutes) before addition of the secondary antibody (horse radish peroxidase-conjugated or fluorescent-conjugated secondary antibody [in the dark]) for 1 hour at room temperature. The membrane was then washed in TBST (3x5mins). Bands were revealed either using Enhanced Chemiluminescence (ECL) [Supersignal West Dura Extended Duration Substrate] (Perbio) and Biomax film (Kodak), or the membranes that had the fluorescent-conjugated secondary antibody were scanned in on the Odyssey machine for analysis using

Licor software. One of the great advantages of using fluorescence to measure the intensity of any bands revealed is that the Odyssey machine and licor software produce accurate and reproducible quantification of proteins across a wide linear range, if saturation occurs the image will appear white and require repeating.

ECL was only used for the experiment detailed in section 3.3.2. All subsequent experiments utilised fluorescence.

2.5.3 Colloidal Blue

Visualisation of total protein following SDS-PAGE was achieved by staining the gel with Colloidal Blue (Brilliant Blue G-Concentrate: Sigma, B2025). Following electrophoresis, the gel was incubated for one hour in a solution of 7% glacial acetic acid in 40% methanol. The gel was then transferred to the working dilution of Brilliant Blue G-Concentrate mixed at a ratio of 4:1 with methanol. This was left (covered) overnight at room temperature. The gel was then destained in 10% acetic acid in 25% methanol for 30 seconds, and rinsed in 25% methanol. The gel was then allowed to destain slowly in 25% methanol for up to 24 hours and scanned using the Odyssey machine at 600nm; once scanned the gel was dried.

2.6 Immunocytochemistry

10μm sections of fresh frozen tissue were cut on a cryostat (Leitz Lauda, 1720 Digital) and mounted on 3-aminopropytriethoxysilane-coated slides. Sections were fixed in ice-cold absolute ethanol or ice-cold acetone for 10-30mins prior to staining. Endogenous peroxidase was inactivated by incubation with absolute methanol containing 0.3% hydrogen peroxide for 20mins at room temperature, this is known as quenching. Sections were then washed in PBS. Non-specific binding was blocked with normal serum obtained from the species in which the secondary biotinylated antibody was raised. Excess blocking serum was removed by gentle tapping and 60μl of primary antibody was added (Appendix I-J). Slides were then incubated at room temperature for 90 minutes. For spinal cord immunocytochemistry, the primary antibody was diluted in blocking buffer to minimise non-specific staining.

Biotinylated secondary antibodies (Vector laboratories, Peterborough, UK) were applied to the sections for 45min (Appendix I-J). Avidin-biotin-peroxidase complex (ABC Elite detection kit, Vector laboratories, Peterborough, UK) was added to each section for 30-45mins. Bound antibodies were revealed by a colorimetric reaction using 3,3'-diaminobenzidine (DAB) as a substrate for the peroxidase enzyme. Slides were washed in PBS to stop the reaction, counterstained with cresyl violet (0.5%, Sigma, UK) and

permanently mounted under coverslips in DePeX (BDH, Merck). Sections were viewed by light microscopy.

Tissues fixed in PLP or PAF were cut as above and mounted on gelatinised slides. The above protocol was followed, but without the alcohol/acetone fixing step.

Tissues fixed in formalin or Bouin's and embedded in paraffin were cut to 10μm on a microtome and floated onto superfrost plus microscope slides (BHD, Merck). Prior to immunocytochemistry, as described above, sections were first heated in a 60°C incubator for 30 minutes to soften the wax. Sections were then dewaxed by submerging them in xylene for 30 minutes, followed by 3 minutes in decreasing concentrations of alcohol solutions (absolute down to 70%). Finally, sections were pre-treated in citric acid (2x3minutes in the microwave) prior to standard immunocytochemistry protocol above. Following the DAB reaction, sections were counterstained with Harris heamotoxylin (BDH, UK) and mounted under coverslips in DePeX (BDH, Merck).

2.7 Double Immunofluorescence

For tissue requiring double immuno-labelling, the same protocol was followed as described in section 2.6. The first primary antibody was applied as described in section 2.6 (Appendix K). A fluorescent secondary antibody was applied for 30 minutes at room temperature, in the dark. Secondary antibodies used were Alexa Fluor conjugated (Molecular Probes, UK), and typically used at a dilution of 1 in 200. All subsequent stages were carried out in the dark.

A second quench is performed to inactivate any peroxidase left unreacted from the first reaction. Sections were then washed in PBS. Non-specific binding was blocked with normal serum obtained from the species in which the secondary fluorescent antibody was raised. Excess blocking serum was removed by gentle tapping and 60μl of the second primary antibody was added (Appendix I-J). Slides were then incubated at room temperature for 90 minutes. For spinal cord immunocytochemistry, the primary antibodies were diluted in blocking buffer to minimise non-specific background staining. The second fluorescent secondary was then applied, and incubated for 30 minutes at room temperature. Sections were then washed in PBS. Finally, sections were mounted with Mowiol aqueous mounting medium to prevent fading, cover slipped and sealed with clear nail varnish. Sections were viewed using the Zeiss Confocal microscope. Images were taken using the LSM510 MetaMorph Version 3.2 package. Secondary antibodies for double immunofluorescence were chosen that had different absorption spectra. The majority of images produced were taken as single optical slices, only Fig. 5.16 was a z series, all images were taken using a setting on 1 airy disc.

2.8 Sciatic nerve tissue preparation

Sciatic nerves were homogenised in a protease inhibitor cocktail solution (Sigma P-2714) using a motorised micro-homogeniser. Samples were then spun down at 14,000rpm for 30 minutes at 4°C, the supernatant was discarded. Pellets were resolubilised in 2% Triton-X-100 (1 hour on a rotometer at 4°C), and spun down at 100,000g for 1 hour at 4°C. The supernatant was removed and the pellet was solubilised using 5% SDS. Samples from all pellets and supernatants were collected and stored at -20°C until analysis.

2.9 Peptide mass fingerprinting

Tris-SDS gels (BioRad, UK) were run, as described in section 2.5, and stained using Commassie Blue solution. The gels were stained with 0.2% Coomassie brilliant blue (BioRad, R-250) in 20% methanol, 0.5% acetic acid for 20 minutes (thus without fixing) and destained using 30% methanol until the protein bands become visable. Once identified, the bands of interest were excised using a clean scalpel blade (Swann-Morton, Sheffield, UK) cutting as close to the edge of the band as possible, before being cubed and stored in Analar water until required.

The following protocol was done in collaboration with Paul Skipp at the Centre for Proteomic Research, University of Southampton, UK.

Reduction and Alkylation

Gel cubes were washed with 100-150µl Analar water (5 mins). This was then spun down to remove excess liquid. Acetonitrile (3-4 times the volume of gel cubes) was added and left for 10-15 minutes until the gel pieces had shrunk. This was then spun down and the liquid removed. The gel cubes were then dried down in a vacuum centrifuge. Once dry 10mM dithiothreitol/0.1M Ammonium Bicarbonate was added (enough to cover the gel) and incubated for 30 minutes at 56°C to reduce the protein (i.e this is in-gel reduction). The gel was spun down and excess liquid was removed. The gel was shrunk again using acetonitrile. Acetonitrile was then replaced with 55mM iodoacetamide/0.1M NH_4HCO_3 and left for 20 minutes at room temperature in the dark. The solution was then removed and the gel washed in 150-200µl 0.1M NH_4HCO_3 for 15 minutes. The gel was then spun down and liquid removed. Once again then gel was shrunk using acetonitrile. The acetonitrile was then removed and the gel dried in a vacuum centrifuge.

In-gel digestion with trypsin

Gels were rehydrated in digestion buffer containing 50mM NH_4HCO_3, 5mM $CaCl_2$ and 12.5ng/µl of trypsin at 4°C for 30-45 minutes. Any remaining supernatant was removed. 5-25µl of the digestion buffer – without trypsin – was added, enough to cover

the gel and to keep the gel wet during enzyme cleavage. The gel was left overnight at 37°C.

Extraction of peptides

10-15µl of NH_4HCO_3 was added and incubated at 37°C for 15 minutes with shaking. The gel was spun down and acetonitrile added (1-2 times the gel volume) and incubated at 37°C for 15 minutes with shaking. The mixture was spun down, and the supernatant collected. 40-45µl of 5% formic acid was added, vortexed for 15 minutes at 37°C, spun down and acetonitrile added (1-2 times gel volume). The mixture was incubated at 37°C for 15 minutes with shaking. The mixture was spun down and the extracts pooled. The extracts were then dried in a vacuum centrifuge.

Peptide desalting using C_{18} reverse phase micro columns

The tryptic peptides were resuspended in 1µl of 80% formic acid and 7µl of water. Stock R2 porous resin (Perkin Elmer) was diluted 10 fold. 1.2mm O.D. x 0.69 mm I.D borosilicate tubes were pulled (5µm tip) and 2µl of the R2 porous resin was added and spun for 5 seconds. The resin level in the tip was then checked. The column was equilibrated with 2 x 4µl water. 4µl of the peptide mixture was added to the column and spun. This was repeated until all of the sample was used. 3 x 4µl washes with water were then carried out. The sample was then eluted using 0.3µl of 50% methanol in 5% formic acid/water into a borosilicate nanovial. The sample was then ready for matrix-assisted laser desorption/ionisation-time of flight mass spectrometry (MALDI-TOF MS) analysis (this was carried out by Paul Skipp).

NB. All of the above experiments, with the exception of the part detailed above in section 2.8 were carried out by myself, Emma Rankine, this includes all of the animal surgery, tissue collection, tissue preparation, tissue processing, immunocytochemistry, western blotting, immunofluorescence and image capturing.

CHAPTER 3 Antisera Production and Characterisation

3.1 Introduction

The current methods, such as silver staining and Amyloid precursor protein immunocytochemistry, for studying axonal degeneration and the information one can deduce from the techniques is limited. Furthermore, these methods are capricious and time consuming; and whilst revealing damaged axons, they are not useful for investigating the mechanisms underlying axonal injury. The antisera I have raised is far less capricious, the staining method can be transferred between different tissues without a need to change the staining protocol.

This chapter describes a strategy I have utilised with a view to developing novel reagents to study axonal degeneration; in particular, Wallerian degeneration. These reagents would enable visualisation of axonal damage by immunocytochemistry, and enable us to identify proteins that are involved in the molecular mechanisms underlying Wallerian degeneration. In addition to describing the production of an antisera raised against degenerating axons, the results in this chapter describe the pattern of staining observed from immunostaining and Western blotting with the antisera produced, in a number of different tissues, both naïve and following injury.

Antisera production

Cells that myelinate the peripheral nerve, Schwann cells, differ from cells that myelinate axons in the CNS, oligodendrocytes. Our strategy was therefore to select for antigens primarily located within the axoplasm. I used a degenerating peripheral nerve as the source of antigen. By doing so I hope to limit any reactivity of the antisera raised to central antigens that are only contained within the axon, excluding for example CNS myelin, astrocytes and microglial antigens.

The typical strategy for raising antisera begins with the protein of interest, and using a pure sample of the peptide as the antigen to raise antisera against. I have utilised an alternative approach. Proteins involved in axonal degeneration are currently unidentified. Thus our antigen will be a homogenate containing a plethora of molecules within damaged axons undergoing Wallerian degeneration with the idea that antisera will be raised against as yet unidentified proteins that are involved in Wallerian degeneration.

Sciatic nerve extracts were prepared as described in section 2.8. In order to enrich for antigens located within the axoplasm, different fractions of sciatic nerve extract were screened with a commercial antibody raised against a common axonal protein, neurofilament (NF-H, the heavy chain of the neurofilament), the antibody I used is specific for axonal NH-H. In order to demonstrate the purity of fractions identified as axoplasmic

(positive for NF-H), these fractions were screened further for contaminants from other cell types (Schwann cells; glial fibrillary acidic protein [GFAP]). Fractions containing principally axoplasmic components were then used as our antigens to raise polyclonal antisera against.

Once generated, the antisera raised against degenerating sciatic nerves were tested on a range of naïve and injured tissues. Optimal dilutions of antisera for immunocytochemistry were determined on different tissue types and using a range of different fixatives. A range of timepoints were investigated to determine any changes in the profile of staining with time. Longitudinal spinal cords, after a dorsal hemi-transection, were used for visualisation of axonal tracts. Other tissues, such as optic nerve and peripheral tissues, were also investigated. Two antisera were raised and termed ELR1 and ELR2, named so as these are my initials.

This chapter describes the production of polyclonal antisera raised against antigens in degenerating axons, and also describes the staining of injured and naïve CNS and peripheral tissues by immunocytochemistry. At this stage I am looking for anything that is involved in axonal degeneration; this may include breakdown products exposing novel epitopes in axons, proteins synthesised de novo in axons or even proteins transferred to degenerating axons from glia.

3.2 Objectives

- to enrich for proteins present within the axoplasm of degenerating sciatic nerves
- to raise polyclonal antisera against these proteins
- to optimise protocols for immunocytochemistry

3.3 Methods

3.3.1 Antigen preparation

Sciatic nerves were prepared as described in section 2.8; the fractions obtained were:

fraction 1: the resolubilised first pellet,

fraction 2: a triton soluble fraction, and

fraction 3: a triton insoluble fraction (i.e. the final pellet dissolved in SDS).

3.3.2 Western blot

SDS-PAGE was carried out (section 2.5) on all fractions collected from sciatic nerves. Nitrocellulose membranes were stained with NF-H (1 in 200) and GFAP (1 in 500), bands were revealed using enhanced chemiluminescence (ECL).

3.3.3 Rabbit immunisation for generation of antibodies

150μg of antigen protein (fraction 3 from a sciatic nerve preparation selected in section 3.3.2) was suspended in 0.25ml complete Freund's adjuvant (Sigma, UK). Once anaesthetised the rabbit's left flank was shaved, and the antigen-adjuvant mix was injected subcutaneously. Rabbits were observed for half an hour following injection to monitor for systemic reactions, none were observed.

Booster inoculations were given at 3-4 week intervals, consisting of 150μg of the same antigen in incomplete Freund's adjuvant (Sigma, UK). Booster inoculations were preceded by a small test bleed to check antibody titres and determine whether additional inoculations were necessary. 1ml test bleeds were taken from the central ear artery or marginal ear vein. Blood was allowed to clot at room temperature for 3-4 hours, and then spun at 14,000rpm for 20 minutes. Serum was collected, aliquoted and frozen at -20°C until use.

3.3.4 Screening of test bleeds by immunocytochemistry (section 2.6)

Serum was screened against rat brain with an intracranial stab lesion (section 2.3.2) at various dilutions (neat to 1:20,000).

3.3.5 Antibody collection

Once the titre of antibody in the serum was deemed high enough, the rabbits were terminally anaesthetised and a needle was inserted into the central ear artery. Blood was collected in a clean glass beaker. Exsanguination was carried out by cardiac puncture. Blood was allowed to clot overnight at room temperature and the serum collected, aliquoted and frozen at -20°C until required.

3.3.6 Antibody dilution and sample fixation

Immunocytochemistry was carried out on fresh frozen brain tissue 7 days following an intracranial stab lesion (section 2.3.2). Serum from the rabbits was used at a range of concentrations (neat to 1 in 20,000). Immunocytochemistry was also carried out on brains fixed in PLP, PAF, formalin, or Bouin's (section 2.6) in order to optimise the staining protocol.

A number of non-nervous system tissues were also collected and stained with the antisera raised (section 2.6).

3.3.7 Timecourse of injury

In order to characterise ELR1 and 2 immunostaining tissues were taken at:

- 24hrs, 3 days, 7 days, 21 days and 28 days following brain injury,
- 6hr, 24hr, 3days and 7 days after spinal cord injury,
- 3days, 7 days and 14 days following optic nerve transection (optic nerves proximal and distal to the injury were removed).

Tissues were fixed in either formalin or Bouin's (determined to be the best fixatives from section 3.3.6).

3.4 Results

3.4.1 Antigen preparation and screening

Three fractions were produced from sciatic nerve homogenates (see methods section 2.8) and were screened against a number of commercial antibodies to determine which fraction contained the highest proportion of axonal enriched peptides. Fraction 3, the final pellet, contained the highest proportion of the heavy chain of neurofilament (NF-H) staining (Fig. 3.1A), a neurofilament located only within neurones. Glial fibrillary acidic protein (GFAP) staining, an intermediate filament expressed in astrocytes, was greatest in the second fraction (Fig. 3.1B). Both NFH and GFAP were highly expressed in F1 (i.e. the fraction before any separtion was carried out (Fig. 3.1 A and B F1)). Consequently fraction 3 was chosen as our antigen for immunisation.

3.4.2 Screening test bleeds against intracranial stab lesions

Serum from test bleeds was screened at a range of dilutions (neat, 1:100, 1:1000, 1:5000, 1:10,000 and 1:20,000) on sections of rat brain injured with an intracranial stab lesion. Initial test bleeds did not reveal any specific staining when compared to a control pre-bleed (data not shown). Booster inoculations were given at monthly intervals, with test bleeds being taken two weeks later. Approximately 3 months following the initial inoculation, staining was observed by immunocytochemistry on lesioned brain sections. The same regime of inoculations and test bleeds continued, until at 6 months when the staining obtained on test tissue was very pronounced (data not shown). At this point animals were exsanguinated for complete serum collection.

3.4.3 Antibody dilution and tissue fixation

Using brain tissue subjected to a cortical stab lesion the optimal dilution for ELR1 and 2 for immunocytochemistry was determined to be 1:10,000. Staining at this concentration was clear with very little non-specific background staining. At lower dilutions background staining became more intense (data not shown).

Clear staining was observed in the white matter bundles near the stab lesion, and in the cortical white matter (data not shown). The staining was not as robust in freshly fixed tissue and there was a high degree of background staining in the tissues fixed in PLP and PAF (data not shown). The most differentiated staining was observed in Bouin's fixed tissue. Unless stated otherwise, all tissues used in subsequent results have been fixed in Bouin's.

3.4.4 Tissues

3.4.4.1 Spinal Cord

Tissue sections following spinal cord transection (day 7 post injury) showed similar staining with both ELR1 and 2 (Fig. 3.2A, ELR2 staining shown only). No staining was observed in a control spinal cord section (data not shown). Staining appeared to be localised to damaged axonal tracts as well as dying cells and cell debris. Staining patterns with ELR1 and 2 were compared to the staining produced by a commercially available antibody raised against amyloid precursor protein (APP; Fig. 3.2B). APP is a protein expressed by all neurones and normally undergoes fast axonal transport. When naïve CNS tissue is fixed with formalin or Bouin's, APP is undetectable. However, following axonal injury, APP builds up in end-bulb like structures in the proximal stump, and is then detectable by immunocytochemistry. APP can therefore be used as a marker of disruption of axonal transport. Staining with the APP antibody revealed typical end-bulb staining (Fig.3.2B). This was very different in appearance to staining with ELR1 and 2. APP staining was only located close to the injury area and was restricted to end-bulbs. However, ELR1 and 2 staining was widespread, finer in appearance to APP staining, and possibly located in damaged axons and cells.

3.4.4.2 Sciatic nerves

Naïve and degenerating (day 2 post injury) sciatic nerve tissue was stained with ELR1 and 2. High levels of staining in naïve tissue led to a significant background effect (Fig. 3.3A). However, in damaged sciatic nerve sections, staining was more intense, suggesting that the background affect may be specific and the antigens recognised may increase following injury (Fig. 3.3B).

3.4.4.3 Optic nerve tissue

Optic nerve tissue (formalin fixed) was taken 28 days following a crush injury was stained with ELR1 and 2. Coronal sections revealed clean, punctate staining with both antisera (Fig. 3.4 A, ELR2 staining shown). In the intact optic nerve no staining was observed with either antibody (Fig.3.4B).

3.4.4.4 Peripheral non-nervous system tissues

A wide range of peripheral non-nervous system tissues were stained with both ELR antibodies; the staining with each antibody was comparable. Surprisingly, staining was observed in the majority of peripheral tissues investigated (Fig. 3.5), being localised to fibrous extracellular layers. However, this was not as robust as the staining observed in the injured CNS tissues (Fig. 3.2, 3.4 and 3.6).

3.4.5 Injury timecourse

3.4.5.1 Intracranial stab lesion

Staining after an intracranial stab lesion was always similar with both ELR1 and ELR2 and was localised to the injured hemispheres only (Fig. 3.6). At 24 hours (Fig. 3.6A) staining was diffuse and localised to the injured hemisphere. Staining was particularly evident in the corpus collosum and white matter bundles in the injured striatum. By 3 days (Fig. 3.6B), staining was punctate in appearance and associated with debris from dying cells and damaged axons. It is also possible that this staining was associated with dying axons visualised in cross section. Punctate staining increased in abundance by 7-21 days post injury (Fig. 3.6C and 3.6D respectively), and although still evident by 28 days post injury (Fig. 3.6E), was decreased in quantity. In the injured hemisphere, cellular staining in both the striatum and the overlying cortex was also observed. There was also some cellular staining in the non-injured cortex.

3.4.5.2 Spinal cord transection

Staining with ELR1 and 2 was similar to each other in appearance but differed from staining for APP. At 6 hrs staining with ELR antisera was diffuse and stained the white matter lightly (Fig. 3.7C), by 24 hours, staining with ELR antisera revealed cells resembling glial cells and possibly other injured cells (Fig. 3.7E). By 3 days staining with ELR antisera revealed endbulb structures and other particulate staining (Fig. 3.7G). 7 days post injury ELR staining was abundant and evident throughout the tissue section (Fig. 3.7I). Staining was associated with axons as well as granular particles. Staining with antibodies raised against APP differed markedly from ELR staining. 6hrs post injury the staining observed with APP was restricted to end-bulb structures (Fig. 3.7D), by 24hrs APP staining was similar to that observed at 6hrs (Fig. 3.7F). By 3 days post injury APP staining peaked and revealed abundant end-bulb staining (Fig. 3.7H), the APP staining at 7 days was sparse (Fig. 3.7J).

3.4.5.3 Optic nerve transection

Optic nerve tissue was removed both distal (Fig. 3.8) and proximal (Fig. 3.9) to the site of injury. Staining with ELR1 and 2 was similar in appearance. Compared to naïve (Fig. 3.8A), which showed no specific staining, tissue distal to the injury at 3 days (Fig. 3.8B) revealed possible axonal staining. By 7 days post injury (Fig. 3.8C) there was abundant staining distal to the injury, possibly associated with glial cells within the optic nerve. There was little staining by 14 days (Fig. 3.8 D).

In comparison to the staining observed in the distal segments of transected optic nerve, there was little immunostaining in the proximal portion of the injured nerve until 14 days post injury (Fig. 3.9B). The staining observed at 14 days was dramatically different

to that seen in Fig. 3.8. Staining in the distal optic nerve 14days following injury revealed cellular staining, however, in the proximal optic nerve, 14days following optic nerve transcetion, the staining appeared more widespread and could not be localised to specific cells.

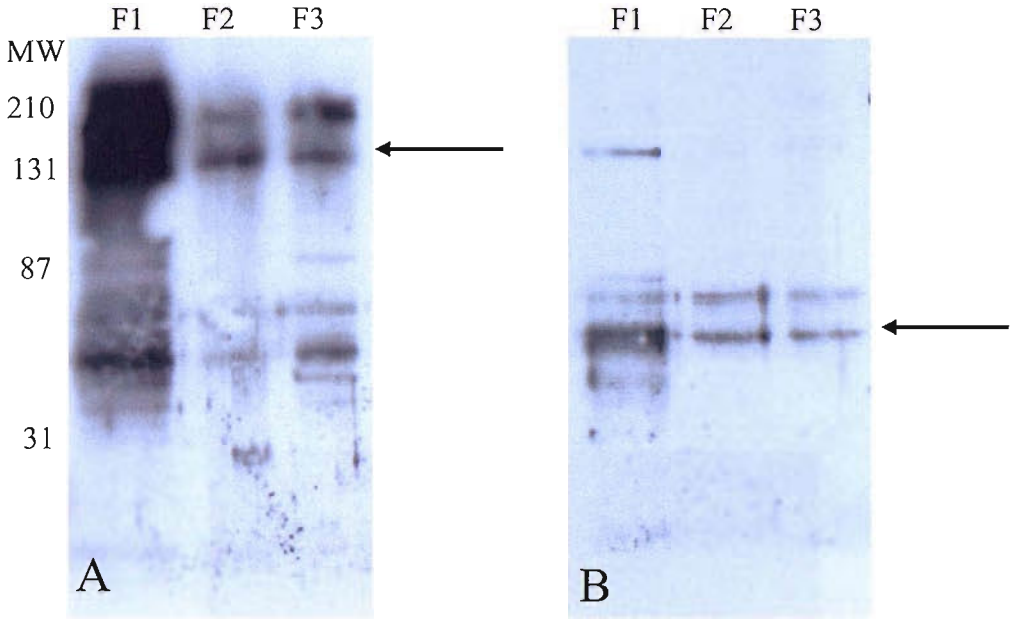

Fig. 3.1 Western Blots to identify sciatic nerve fractions for immunisation. Sciatic nerves undergoing Wallerian degeneration were fractionated (see section 2.8). These were screened with commercial antibodies, to identify which contained proteins principally located within the axoplasm. Fraction 1 (F1) (the primary supernatant), was shown to contain the greatest concentration of the heavy chain of neurofilaments (NF-H; blot A arrow) and Schwann cell-derived proteins (glial-fibrillary acidic protein (GFAP); blot B arrow). Further separation of F1 gave rise to two further fractions (F2 and F3). Within these fractions, NF-H staining was strongest in fraction 3, and GFAP staining was strongest in F2. As a result F3 was identified as containing proteins principally located within the axoplasm and was used as the antigen for immunisation.

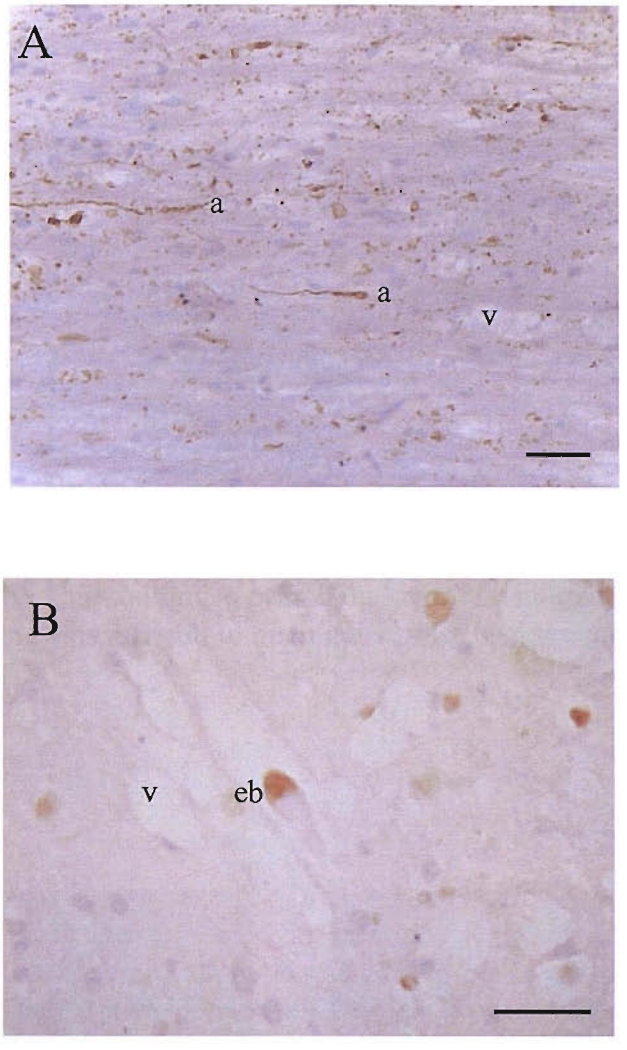

Fig. 3.2 ELR2 staining compared to amyloid precursor protein staining in spinal cord transection injury. Spinal cord (7 days post transection), was stained with ELR2 (A), and antibodies raised to amyloid precursor protein (APP; B). Positive staining with ELR was localised to axons (a) and dying cells and debris (A). Vacuoles (v) were present in the area of damage (A and B). APP staining had a different anatomical pattern. Staining clearly labels end-bulbs (eb) but little else at 7 days.

Scale bar= 30μm

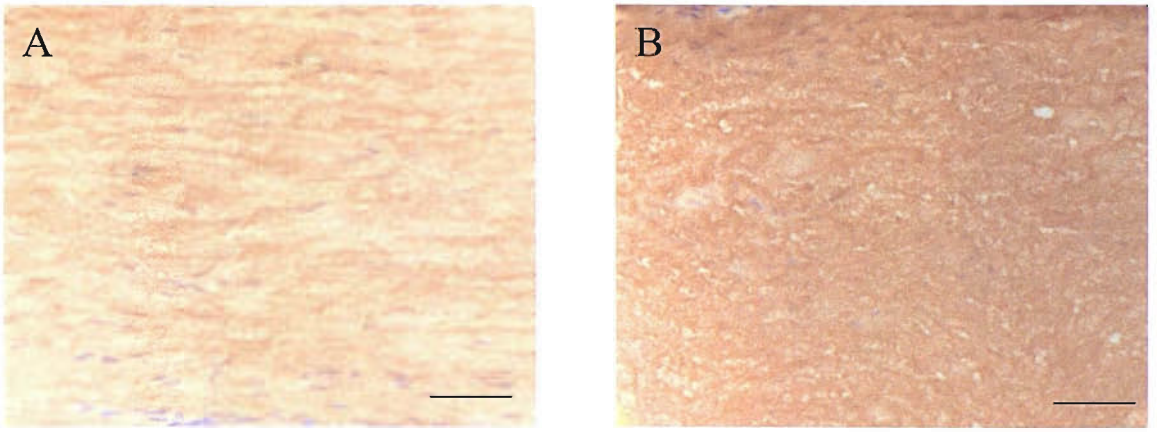

Fig. 3.3 ELR2 staining of naïve and injured sciatic nerves. Positive background staining was seen with ELR2 in both naïve (A) and injured sciatic nerve (B). The staining appeared darker in the injured sciatic nerves, however staining was difficult to distinguish from background staining.

Scale bar = 50μm

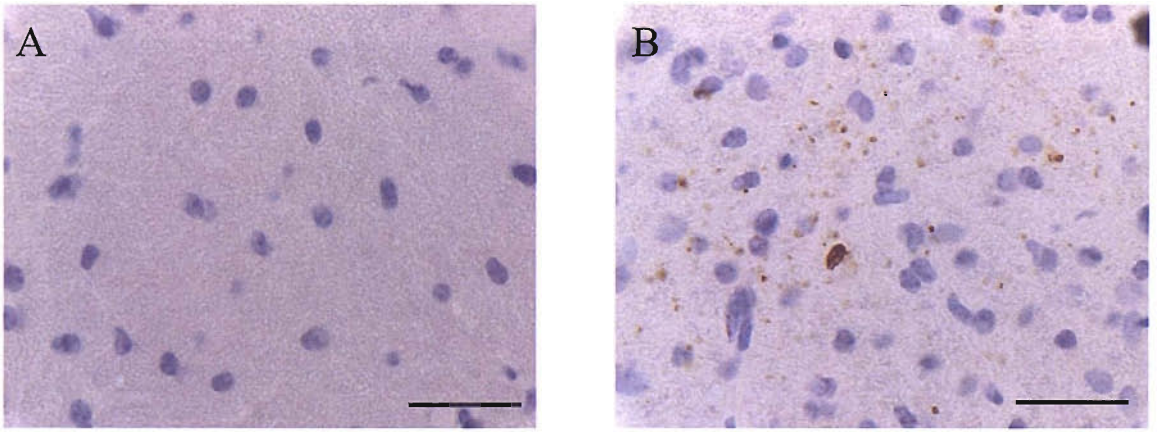

Fig. 3.4 ELR2 staining of injured optic nerve. No staining was observed in naïve optic nerve tissue (A). However, 28 days following crush injury punctate staining was revealed (B). Similar results were obtained for both ELR1 and ELR2 (data shown is from staining with ELR2).

Scale= 30μm

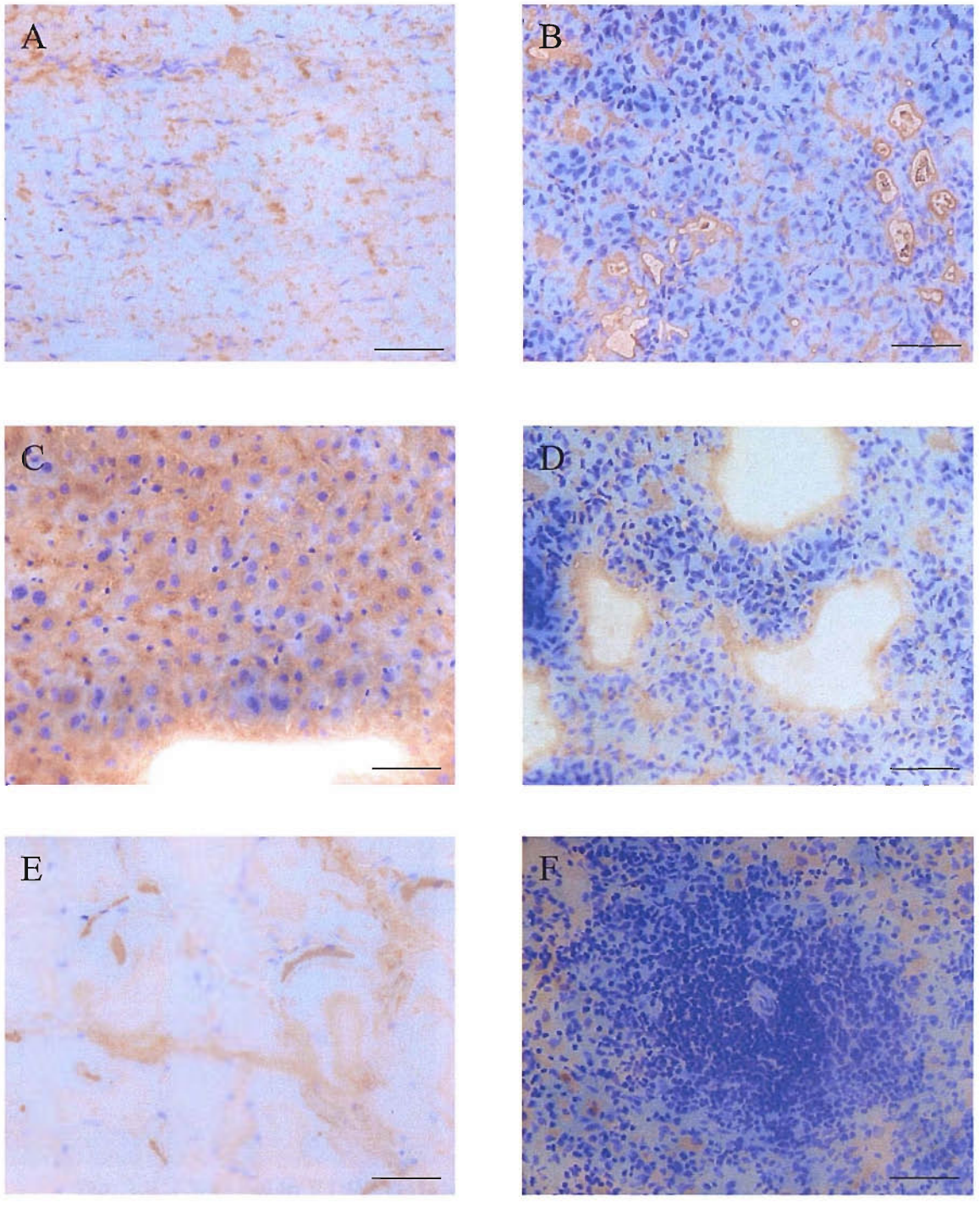

Fig. 3.5 ELR2 staining of naïve peripheral tissues. All staining of peripheral tissues was diffuse in appearance. Staining of heart (A), kidney (B), liver (· C), lung (D), skeletal muscle (E) and spleen (F) does not appear to be as robust as the staining observed following central nervous system injury.

Scale= 50um

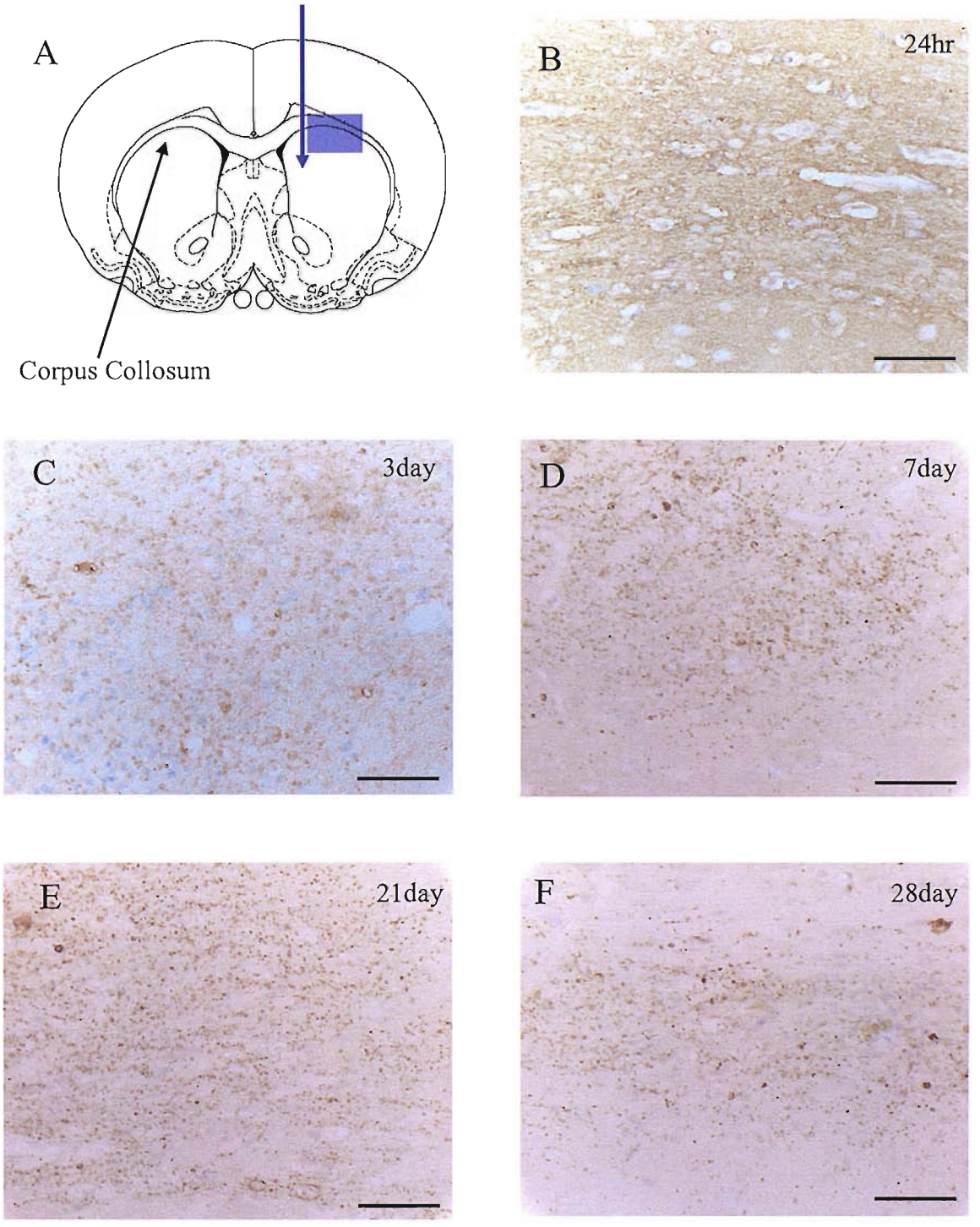

Fig. 3.6 Changes in ELR2 staining following intracranial stab injury. A schematic representation of the site of injury is shown in A. The injury transects the cortical white matter (corpus collosum), resulting in axonal injury. The shaded area demonstrates the region from which photomicrographs are taken.

By 24hours post injury (B) staining was diffuse with some granular staining. By 3 days (C), specific granular staining was observed close to the lesion boundary. Staining along the corpus collosum was more evident by day 7 (D), becoming finer and more pronounced by day 21 (E). Dark granular staining, in the corpus collosum was clear and abundant by 28 day (F). No staining was observed in the non-injured hemisphere at any timepoint.

Scale= 50μm

Fig. 3.7 Comparison of staining by ELR2 and antibodies to amyloid precursor protein (APP). ELR2 and a commercial antibody raised against APP were used to stain spinal cord tissue. Naïve spinal cord stained with ELR2 (A) revealed a low level of non-specific background staining. By 6hrs post injury, ELR2 staining (C) was evident in the white matter, although it was disuse in nature. By 24hrs post injury (E), staining with ELR2 was different to that observed at 6hrs, detecting glial cells (g). 3days post injury (G), ELR2 staining revealed a few end bulb-like structures (eb) as well as glial staining (g), possibly indicating a glial response to injury. ELR2 staining by 7days post injury changed dramatically when compared to the staining at the other timepoints (I), being much more specific and focal. There appeared to be axonal staining (a) as well as cellular debris (d).

The staining observed with the antibody raised against APP differed dramatically from staining with ELR2, described above. Naïve tissue (B) as with ELR2 revealed no specific staining. From as early as 6hrs post injury end-bulbs were present within the tissue (D). The number of end-bulbs stained increased by 24hrs (F) reaching its peak by 3days post injury (H). Staining for APP by 7days (J) revealed few end-bulbs, and they were much less abundant than at 3days.

Scale = 50μm

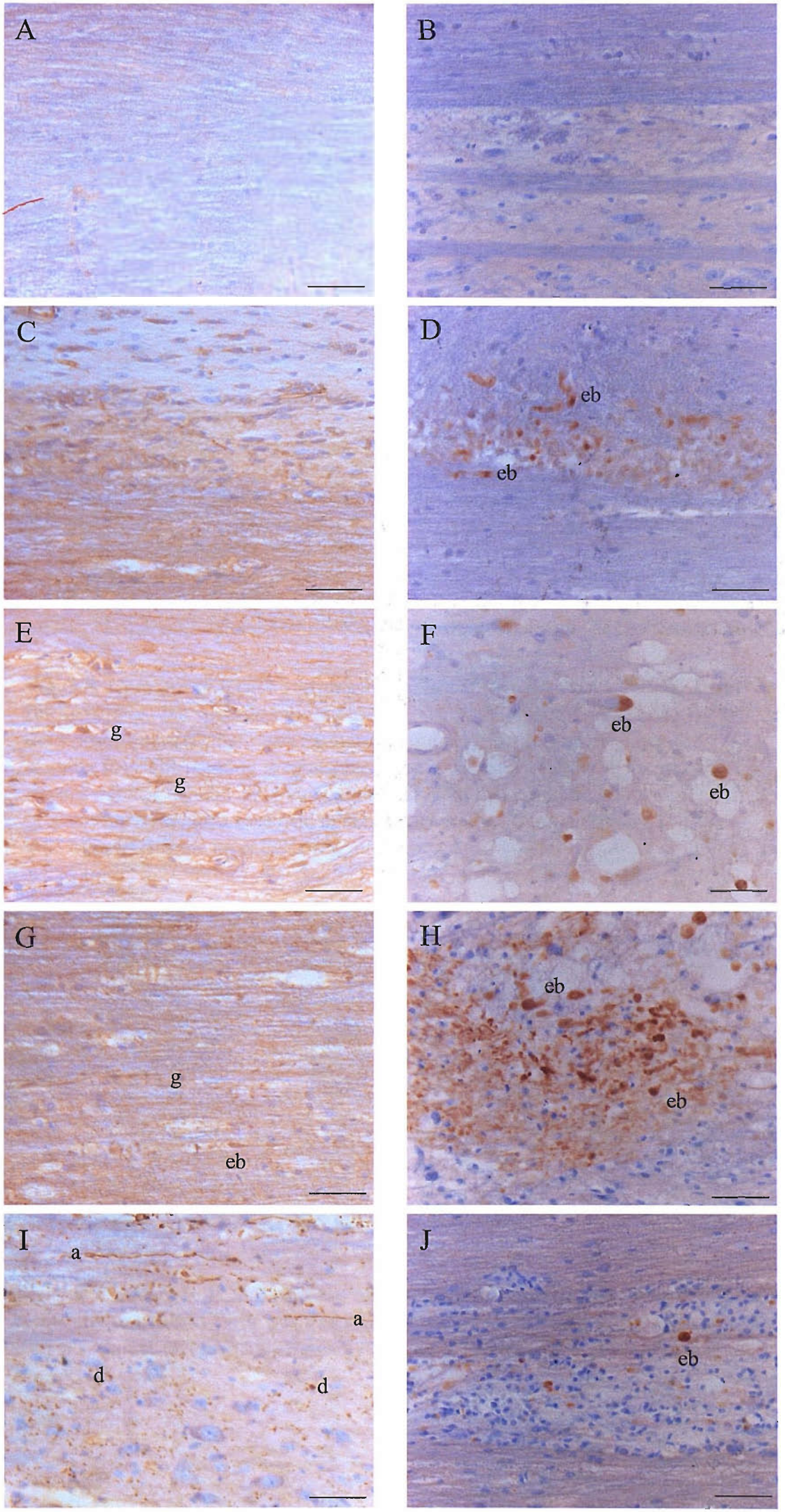
A
B
C
D
eb
eb
E
g
g
F
eb
eb
G
g
eb
H
eb
eb
I
a
a
d
d
J
eb

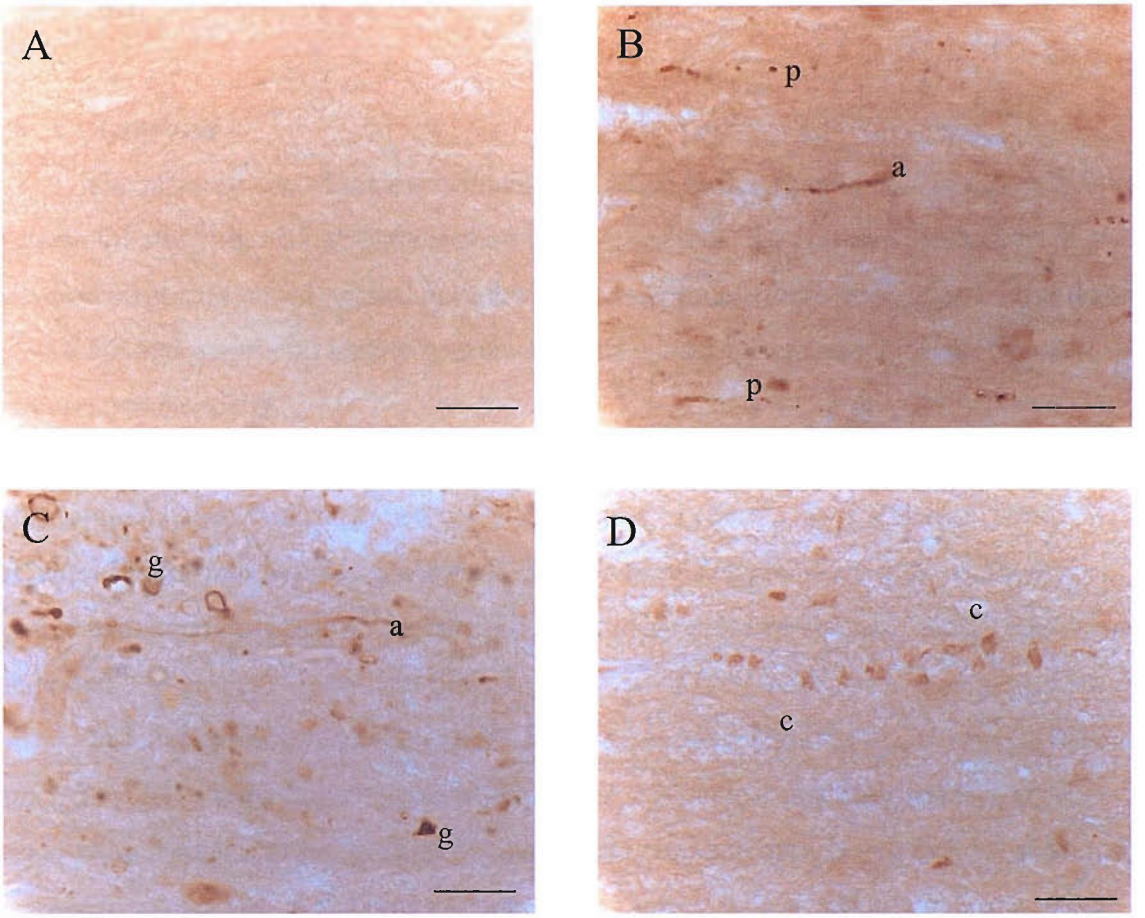

Fig. 3.8 Changes in ELR2 staining following optic nerve transection, distal to the injury. No specific staining is observed in naïve optic nerve (A). By 3 days post injury (B) there was axonal staining (a) aswell as other punctate staining (p). The staining is robust by 7 days post injury (C), with the possible axonal staining (a) and abundant cellular staining that could be glial cells (g), this glial staining may be a response of the glia to injury. The staining by 14 days post injury(D) appears cellular (c).

Scale = 20μm

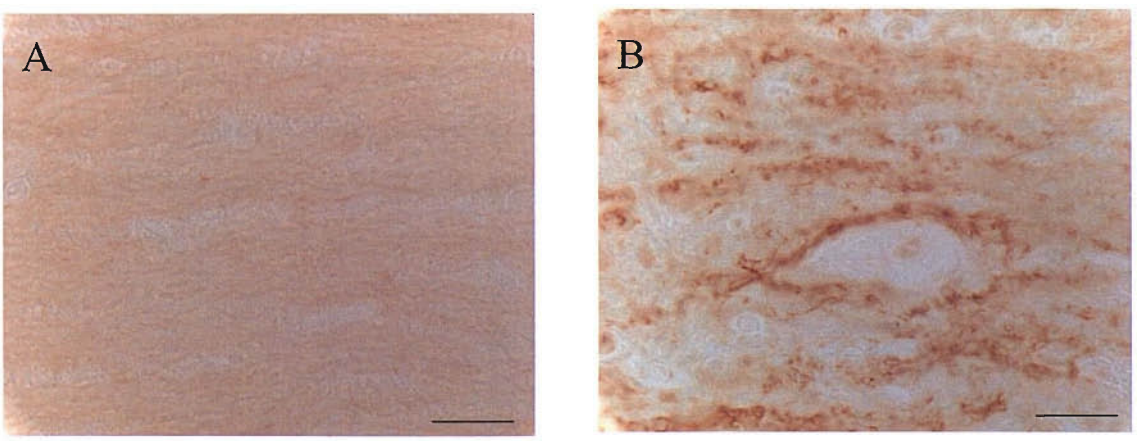

Fig. 3.9 Changes in ELR2 staining following optic nerve transection, proximal to the site to injury. Little positive staining was observed with ELR2 staining by7 days post injury (A). Abundant positive staining was revealed by 14 days post transection (B).

Scale = 20μm

3.5 Conclusions

The primary aim of the experiments described in this chapter was to develop novel antisera for studying axonal degeneration within the CNS. To do this I produced polyclonal antisera raised against antigens in degenerating axons. Staining of injured and naïve CNS and peripheral tissues was characterised, using the antisera raised, by immunocytochemistry.

I have adapted established protocols for enrichment of axoplasmic components from injured sciatic nerves (Zetusky, Calabrese et al. 1979; Carlin, Grab et al. 1980). The enriched axoplasmic fraction generated was used to raise antibodies. Two antibodies, against axonal components of degenerating sciatic nerve (termed ELR1 and ELR2), were generated.

The staining achieved with ELR1 and 2 on various CNS tissues, at various times post injury, have been characterised in the chapter. It is clear that both antisera are recognising antigens within damaged brain, spinal cord and optic nerve that are absent in non-lesioned controls. All staining produced was robust with relatively little non-specific background. Of particular interest was staining following spinal cord injury, which revealed cells and damaged axons. The staining revealed by ELR1 and 2 was in complete contrast to that observed by APP staining. APP staining is an approach widely used to identify injured axons, however, it is restricted to detecting changes in the axons proximal to the site of injury. I believe that, due to the axonal-like staining observed in the longitudinal optic nerve transection tissue, which was absent in the proximal sections, I have antisera that detect axons undergoing Wallerian degeneration. The antisera also detect other components within the tissue, including cells surrounding the injury. This cellular staining may indicate that the cells are responding to the injury, so I therefore may also have an antibody that can be used to detect cellular responses to injury aswell as an antibody that is a marker of Wallerian degeneration.

CHAPTER 4 Western Blot analysis and Proteomics

4.1 Introduction

In Chapter three I clearly demonstrated the production of antisera (ELR1 and 2) that can be used to detect antigens in damaged axons and cells within the CNS following injury. Although histology is the appropriate technique to deduce the location of these antigens within cells and tissues in order to discover which antigens are being recognised, different techniques must be employed, and I have used a proteomics approach. *"The goal of proteomics is a comprehensive, quantitative description of protein expression and its changes under the influence of biological perturbations such as disease or drug treatment"* (Anderson and Anderson 1998).

The principle of the method used in this Chapter was to identify the antigens from damaged CNS tissue that are detected by ELR1 and 2. To do this protein homogenate from damaged CNS tissue was separated by gel electrophoresis, and the proteins detected by ELR1 and 2 were screened using Western blotting. The bands of interest were matched on an acrylamide gel stained using Coomassie Blue to visualise proteins. The identity of the protein in the bands of interest was determined by mass spectroscopy of the excised band.

4.2 Objectives

The aims of the work described in this Chapter were:

- to isolate antigens recognised by ELR1 and ELR2 using Western blot analysis
- to characterise these antigens by peptide mass fingerprinting
- to evaluate the information gathered from peptide mass fingerprinting

4.3 Methods

Proteins from homogenates of naïve and injured brain samples were separated by sodium dodecyl sulphate polyacrylamide gel electrophoresis (SDS PAGE) and either transferred for Western blot analysis using ELR1 and 2 or total protein was visualised in the gel using Coomassie blue. Differences between naïve and injured samples were identified by looking for changes in the band intensities between the naïve and injured samples. The bands of interest were then excised from the gel for further analysis by matrix assisted laser desporption/ionisation-time of flight mass spectroscopy (MALDI-TOF MS). The principles of, and a brief background to MALDI-TOF MS can be found in Appendix II.

4.3.1 Tissue preparation

Samples of naïve and injured brain, spinal cord, optic nerve, retina and peripheral tissues were collected as in section 2.4.

4.3.2 Optimisation of protein loading

In order to quantify any changes I observed in proteins under investigation by Western blot analysis I needed to be certain that protein loading onto the acryalmide gels was equal. I devised a new method to check protein loading. Usually, protein loading is typically standardised using a protein assay first and then checked at the Western blotting stage by staining for a loading control such as actin. Due to the model of injury used the usual method to check for protein loading is unsuitable as there are changes in the expression of actin (the typical protein used) following injury. This was demonstrated by immunocytochemistry on both naïve and injured spinal cord and brain sections using a commercially available antibody raised against actin (A2066, Sigma, UK). For the same reason as with actin, it was decided not to look for another house-keeping protein due to the abundant changes in cellular morphology, cell proliferation (such as microglia) and cell death following injury.

In the new method a Bio-Rad protein assay was used, as in the above method, to determine the protein concentrations in our samples. I then loaded 10μg of each sample on a polyacrylamide gel which then underwent SDS PAGE. The gel was stained with Colloidal Blue stain (Sigma, B2025), which stains total protein within the sample. In order to determine the amount of protein loaded in each lane, the gel was scanned on the Odyssey Scanner. The associated LiCor software was used to determine the intensity of every band in the entire lane of each sample; the program then added together these intensities to give a 'total intensity' value for total protein in each lane. In order to compare any changes between naïve and injured samples these 'total intensities' were corrected to be relative to the appropriate naïve sample and the ratio between naïve and injured sample were determined. The samples were then aliquoted and stored as appropriate. This procedure was followed each time new samples were generated.

4.3.3 Western Blotting

10μg protein were run on acrylamide gels by SDS PAGE. ELR1 and 2 were used at various dilutions (1:1000, 1:5000, 1:10,000 and 1:20,000) to detect proteins in samples from naïve and injured brain. Once an optimal dilution had been determined (1:10,000) the novel antisera were used against samples derived from a range of peripheral tissues that included heart, liver kidney, lung, muscle, skin and spleen. Proteins from tissue homogenates of naïve and injured brain, spinal cord, optic nerve and retina, were then separated on polyacrylamide gels and blotted for ELR1 and 2. All membranes were

scanned on the Odyssey Scanner and the band intensities measured using the LiCor software. The intensities were all divided by the intensity of the naive sample to produce a relative intensity and the 'relative' intensity was corrected for protein loading using the ratio values obtained in Figs. 4.2 and 4.3. A separate gel was run for Coomassie staining for identification of protein bands for subsequent excision and analysis.

4.3.4 Proteomics

In order to characterise proteins recognised by ELR1 and 2 the bands that were revealed by Western blotting were correlated to the protein bands observed on a gel stained with Coomassie blue. The identified bands were excised using a scalpel, cut into small cubes and stored in Analar (filtered) water. They were then taken to the proteomics department (Southampton University) for sequencing by peptide mass fingerprinting. Automated elution of proteins from the 1 or 2D gel (1D in the case of western blots) was carried out. The proteins were then reduced, alkylated and digested in trypsin. The resulting peptide fragments were then analysed by a Time Of Flight Mass Spectrometer (TOF-MS). The mass obtained were entered into a database and a list of possible proteins was revealed. This method of protein identification relies on whether or not the protein of interest have been sequenced – the rat genome had recently been fully sequenced and a protein translation produced [http://rgd.mcw.edu; (Twigger, Lu et al. 2002)] which means that this was an ideal method to use for identification of proteins in the samples (for full method see section 2.9).

4.3.5 Confirmation of proteins detected by MALDI-TOF MS

Proteins detected by MALDI-TOF MS were investigated individually, to determine whether or not they are involved in the injury response in the CNS. Western blot and immunocytochemical analysis was employed to determine whether or not the proteins are present within the CNS tissue, and then used to investigate any changes in expression patterns following injury. Double immunofluorescence was used to determine precisely which cells are expressing the proteins detected by TOF-MS.

Kid-1 antibody, a kind gift from Ralph Witzgall, University of Heidelberg, was used at a dilution of 1 in 300 for immunostaining and 1 in 500 for Western blotting. FAK2 (Sigma, F2918) was used at a dilution of 1 in 2000 for both immunocytochemical and Western blot analysis.

4.3.6 Antibody purification to remove albumin antibody from ELR1 and 2

2ml of Reacti-Gel 6X beads (Pierce, 20259) were taken from the stock and spun down in order to remove excess acetone. Acetone was removed using a 27G x1.25 needle (Becton Dickinson, Z192376) and syringe. 10ml of 0.1M NaBorate buffer (pH 9.0)/0.4M NaCl was added to the beads followed by 1mg of rat albumin (Sigma, A6272). The

mixture was incubated on a rotometer for 40-48hours at 4°C. This time allows for the activated beads to cross-link with the primary amines in albumin. Following incubation, the beads were washed three times with 10ml 1M Tris/HCl buffer (pH 8.8), to neutralise free amines, and then incubated in 10ml Tris buffer for 4 hours at 4°C. The beads were washed again. 0.5ml of the beads were then added to 100µl polyclonal antibody serum and the samples rotated overnight at 4°C to remove the albumin antibody. The serum was then used immediately for Western blotting or for immunocytochemical analysis, or aliquoted and frozen until required. The beads could be cleaned (i.e. the albumin antibody could be unlinked from the beads) and reused. To unlink the antibody, the beads were incubated with 0.1M glycine/HCl (pH 2.5) at room temperature for 30 minutes on a rotometer. This was repeated four times to remove all of the antibody. The glycine/HCl/albumin antibody mixture must be neutralised with 100µl Tris/HCl (pH 8.0) immediately. Albumin antibody could be used, for immunostaining or Western blotting, once removed from the beads. The beads can then be resuspended in 5ml PBS/0.1% Tween/0.02% Sodium Azide and kept in the fridge until desired.

N.B. In between each stage the beads in solution were spun down at 2500rpm for 2 minutes to collect the beads at the bottom of the conical tube.

4.4 Results

4.4.1 Protein loading control

The differences in actin staining between naïve and following injury of both spinal cord and brain samples can be seen in Fig. 4.1. Naïve spinal cord and brain (Fig. 4.1A and B respectively) show a basal level of actin staining that one would expect in any tissue. However, following injury the pattern of staining is dramatically different from as early as 6hrs post injury (Fig. 4.1C-spinal cord and D- brain). The staining, from the morphology appears to be mainly located within microglial cells. Actin staining at 3d (Fig. 4.1E and F, spinal cord and brain respectively) and 7d (Fig. 4.1G and H, spinal cord and brain respectively) post injury show similar staining to that of 6hrs although the possible microglial staining has changed from a ramified morphology to one of activated microglia. This clearly demonstrates why I cannot use actin as our loading control for Western blot analysis.

An example of an acrylamide gel, stained with Colloidal blue, along with the Odyssey scan of the brain samples used can be seen in Fig. 4.2A and B respectively. The 'total intensities' of the entire lanes were determined using the Licor Odyssey software. The 'total intensity' of the test samples (i.e. sample of injured tissue) was divided by the 'total intensity' of the control sample (i.e. the naïve band) to calculate a relative intensity for all samples (Fig.4.2 C show this data expressed graphically). The ratios between the

samples of control and injured tissue are shown in Fig.4.2D, is the data that the subsequent Western blot data is corrected by. The same procedure was carried out for spinal cord (Fig. 4.3), optic nerve (Fig. 4.4) and retina (Fig. 4.5) homogenate prior to their use for Western blotting.

4.4.2 Western Blot Analysis

4.4.2.1 Optimisation of antibody dilution to be used for Western Blotting

Western blotting with the ELR1 and 2 antisera revealed that a 1 in 10,000 dilution of produced the clearest signal (Fig. 4.6). A dominant band of approximately 70kDa was seen with all antibody dilutions. Bands of lower molecular weights were present in all dilutions when ELR2 was used; the bands were at approximately 40kDa and 30kDa (Fig. 4.6B).

4.4.2.2 Peripheral tissues

Western blot analysis of a random selection of peripheral tissues all produced similar staining the peripheral tissues stained were kidney, spleen, liver, lung, heart, skin and skeletal muscle (Fig. 4.7). A band at approximately 70kDa was clearly evident in all samples. Extra bands at approximately 40kDa were also seen in skeletal muscle, skin and spleen.

4.4.2.3 CNS tissue

Staining with ELR1 and 2 produced similar results, although ELR2 was more sensitive. For the remainder of the Western blots ELR2 was used as the antibody of choice for further analysis. ELR2 revealed multiple bands across the timecourse of brain injury investigated and the intensity of the bands made it difficult to identify differences between naïve and injured samples (Fig. 4.8). Once the major antigens that ELR1 and 2 detect have been identified they can be removed to purify the polyclonal antibodies. This will remove some of the staining observed and produce a cleaner picture for further analysis.

4.4.3 Proteomics

4.4.3.1 Isolation of proteins

Protein bands that appeared to have different levels of expression, between samples of naïve and injured brain, by Western blot analysis using ELR2, were correlated with bands on a Colloidal gel. The identified bands were then excised from the gel for analysis using MALDI-TOF MS. Five protein bands were sequenced in total.

4.4.3.2 MALDI-TOF MS

MALDI-TOF MS generated a number of possibilities for each band sequenced. This may be due to there being more than one protein within the band sequenced (i.e. when a band is excised from the gel there may be more than one protein within that piece of gel) or sequence similarity between proteins. The proteins identified from the bands sequenced

are as follows, also shown are the percentages of the protein represented by the whole or partial peptide sequenced (coverage):

Band 1: Albumin (coverage 21%)

Band 2: P0 myelin (coverage 13.7%) and/or Kid-1 (a zinc finger protein) [coverage 6.2%]

Band 3: P0 myelin (coverage 17.3%) and/or Kid-1 (coverage 8.2%) and/or FAK2 (focal adhesion kinase 2) [coverage 8.4%]

Band 4: P0 myelin (coverage 13.7%) and/or secretogranin II precursor (coverage 8.9%)

Band 5: Tubulin (coverage 14.2%)

The proteins analysed by MALDI-TOF MS generated a mass that equates to a sequence of amino acids. The sequence was matched against peptide sequences in the rat protein database. The results generated result in a list of proteins that contain either the whole, or part of the sequence generated by MALDI-TOF MS. This unfortunately means that the results obtained may not be the protein that was detected by Western blotting and will therefore need to be investigated to identify whether the proteins are important in our injury models.

4.4.4 Confirmation of peptide mass fingerprinting results

4.4.4.1 Band 1; rat albumin

To determine whether ELR1 and 2 recognise rat albumin, an acrylamide gel was run with a serial dilution of rat albumin (1µg down to 15ng), using naïve brain as a positive control. The staining produced with both ELR1 and 2 was almost identical (Fig. 4.9A, ELR2) and demonstrated a dose-dependent pattern, determined by measuring the intensities of the bands using the Odyssey-LiCor system (Fig. 4.9B). This indicated that ELR1 and 2 contain antibodies to rat albumin. Staining was determined to be specific for rat albumin over chicken ovalbumin as Western blots of chicken ovalbumin revealed no staining (Fig. 4.9C). Preincubation of rat albumin in ELR1 and 2, prior to use in a Western blot, blocked all staining (data not shown), however, no staining was blocked when ELR1 and 2 were preincubated with ovalbumin (data not shown). However, other ovalbumins have not been tested and it can't be ruled out that ELR1 and 2 may cross react with ovalbumins of other species.

4.4.4.2 Bands 2 and 3; Kid-1

Kid-1 is a zinc finger protein, named Kid-1 as it was predominantly found in the **k**idney, is suppressed after renal **i**schemia and appears late in renal **d**evelopment (Witzgall, Obermuller et al. 1998). Kid-1 was used for Western blotting and immunocytochemistry on naïve and injured brain tissue/tissue homogenate (Fig. 4.10). There was no significant

change in Kid-1 expression by Western blot analysis as determined using the Odyssey machine (Fig. 4.10A and B). Immunocytochemistry using the anti-Kid-1 antibody revealed staining in the cell bodies of neurones throughout the brain, there was no staining of glia, this was particularly evident as there was no staining of the oligodendrocytes in the cortical white matter (Fig. 4.10). The staining was identical in naïve and injured brain (Fig. 4.10C and D respectively).

4.4.4.3 Band 3; FAK

Focal adhesion kinase (FAK) is a protein tyrosine kinase that co-localizes with integrins in cellular focal adhesions; it is highly expressed in the CNS as well as other tissues. In non-neuronal cells FAK2 is thought to control the turnover of focal adhesions and thereby control cell spreading and motility (Girault, Costa et al. 1999). At present the functions of FAK2 in the adult CNS are not clear but it may play a role in synaptic plasticity and neuronal survival (Zalewska, Ziemka-Nalecz et al. 2003).

Brain homogenate at various times post intracranial stab injury were run on an acrylamide gel and blotted with an anti-FAK polyclonal antibody following transfer of the proteins to a nitrocellulose membrane. There are changes in the level of expression of FAK, 125kDa (Fig. 4.11A). Immunocytochemical analysis revealed changes between naïve and injured brain samples (Fig. 4.11B and C respectively), there was a change in the pattern of staining when comparing naïve tissue to injured tissue, the injured tissue had decreased staining adjacent to the injury. The changes in protein levels of FAK expression detected by Western blotting and immunocytochemistry will be investigated further (see Chapter 5).

4.4.5 Antibody purification

Because albumin is detected after electrophoresis of all samples, and was very intense, it may be masking other bands. I decided to try to eliminate the antibody that was recognising albumin from the polyclonal antibody ELR2. This was achieved as set out in section 4.3.6. The purified antibody was then used on a Western blots of brain, spinal cord, optic nerve and retina, naïve and at a number of timepoints post injury. Although the 70kDa band was still clearly stained the intensity was decreased and changes in other band intensities became apparent throughout the injury timecourse. The fact that the bands at 70kDa are still very dominant may be indicate that not all the albumin antibodies have been removed from ELR 2, or that ELR2 recognises another protein of 70kDa, not just albumin. The band intensities were analysed on the Odyssey-LiCor system and divided by the naïve intensity, to obtain a relative intensity, and corrected for protein loading using the ratios from Figs. 4.2-4.5., the results are displayed graphically.

Brain injury

The purified novel antibody ELR2 showed differences in intensities of at least three bands when used against brain homogenate at a number of timepoints post injury (Fig. 4.12A). The three bands revealed by the purified ELR2 antibody had molecular weights of approximately 70kDa, 55kDa and 30kDa. Injured brain samples at a number of timepoints post injury showed significant differences from naïve levels (see Fig. 4.12, table C).

Band 1 (approx. 70-80kDa) shows an increase by 24hrs with an approximate two fold increase in expression. By 3days post injury the increase in expression had increased further, however, by 7days post injury the level of expression was significantly lower than that of naïve.

Band 2 (approx. 50-55kDa) is increased when compared to naïve by 6hrs post injury showing a 2fold increase. By 24hrs the increase is close to six times that of naïve, increasing further by 3 days to around 9 times that of naïve. The level of band 2 expression by 7 days post injury is significantly lower than naïve.

Band 3 (approx. 25-30kDa) shows the same pattern of expression as bands 1 and 2 by increasing over the first three days post injury and then decreasing to below naïve levels by 7 days.

Spinal Cord

In total, six bands were observed to change their pattern of expression when ELR2 was blotted against spinal cord tissue at a range of timepoints following partial cord transection (Fig. 4.12B).

Band 1 had a molecular weight of approximately 70kDa, band 2: 65kDa, band 3: 55-60kDa, band 4: 50kDa, band 5: 41kDa and band 6: 31kDa. All bands showed the same general pattern of increasing in expression over the first three days and then decreasing by 7days post injury. A number of the differences were significantly different from that of naïve (Fig. 4.12C).

Optic nerve

There was only one band that could be visualised with ELR2 on optic nerve tissue pre and post-injury (Fig. 4.13A). The band (approximately 70kDa) showed a significant increase by 24hrs, which was the only timepoint to show any significant difference from naïve (Fig. 4.13C).

Retina

Two main bands were observed in the retina samples when blotted with ELR2 (Fig. 4.13B). Band 1 had a molecular weight of approximately 70kDa, and showed an increase in expression over the seven day timecourse and was significantly increased at 24hr and 7

days post-injury. Band 2 (around 55-60kDa) also showed an increase in intensity over the seven days, although this was only significant at day 7 (Fig. 4.13C).

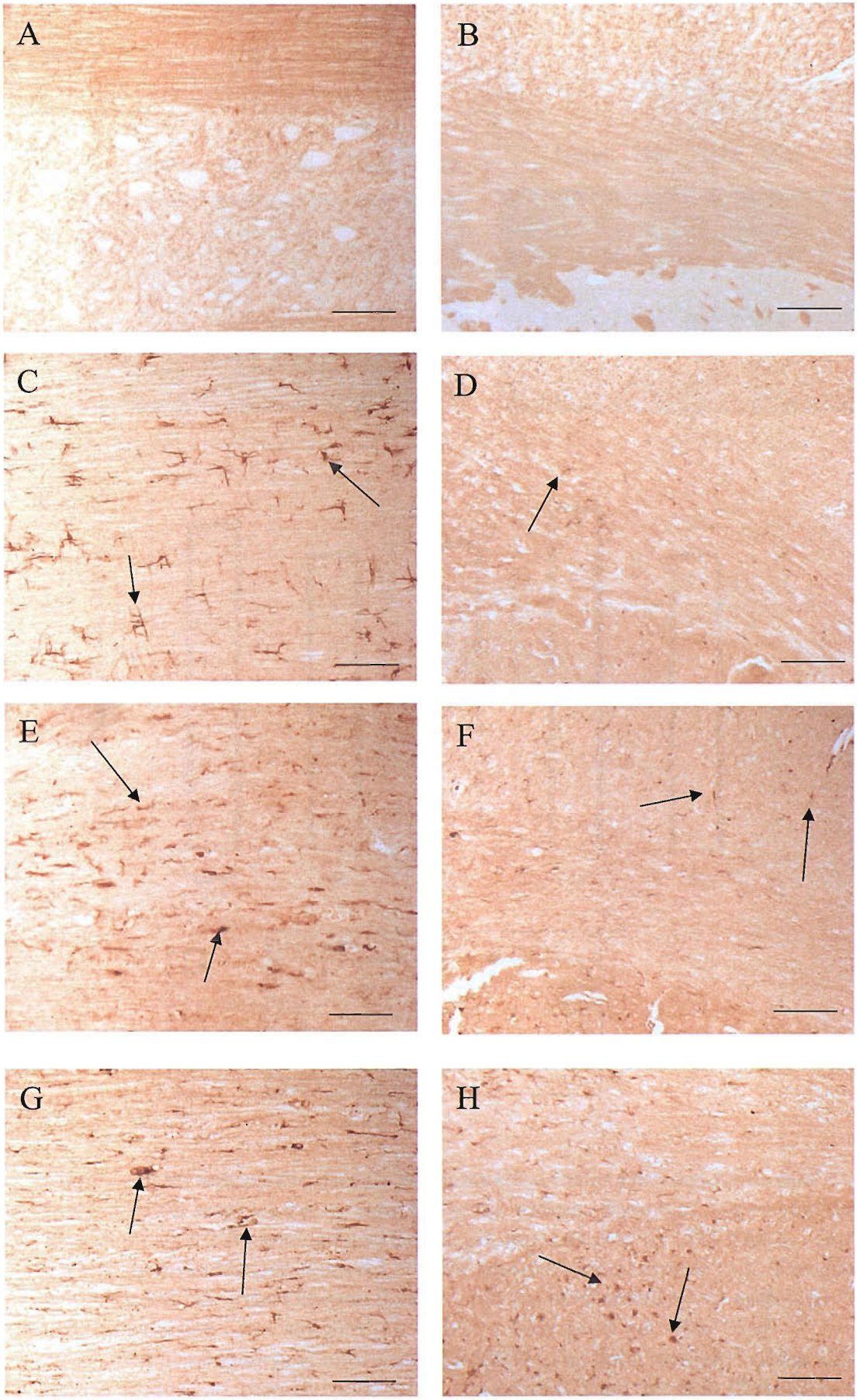

Fig. 4.1 Immunocytochemistry demonstrating the changes in actin staining following injury in the spinal cord and brain. Actin immunostaining, following both partial transection injury in the spinal cord and intracranial stab lesion in the brain, change dramatically over time. In naïve sections, both spinal cord (A) and brain (B) show a background staining of actin. However, the pattern of immunostaining of actin changed following injury, due to remodelling of cells and cell migration. This can be observed in both the spinal cord and brain at 6hr (C and D respectively), 3d (E and F respectively) and at 7 d (G and H respectively) where actin signal can be observed in both the gray and white matter. Arrows indicate cellular staining.

Scale bar = 100μm

A

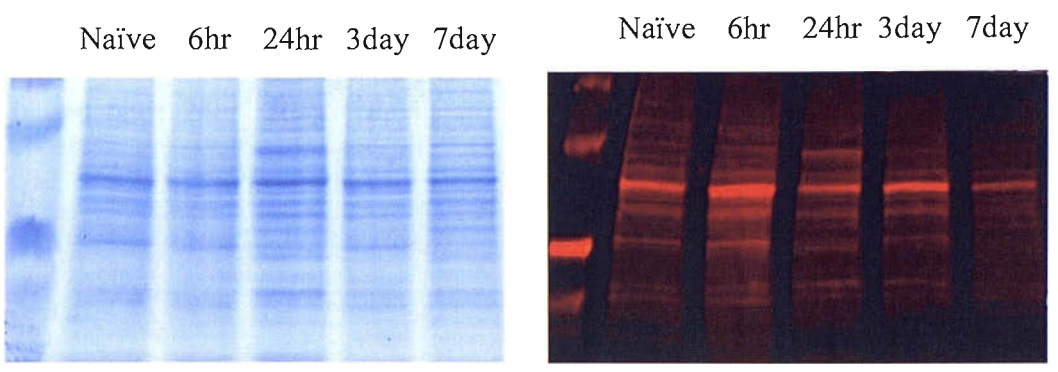

C

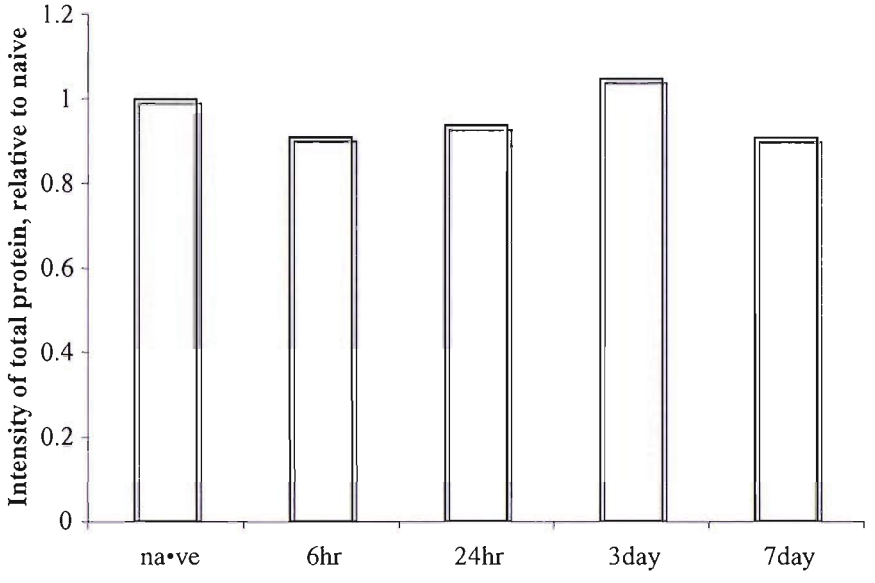

D

sample	ratio to naïve
naïve	1
6hr	0.909
24hr	0.936
3day	1.047
7day	0.908

Fig. 4.2 Determining the protein concentration ratios between naïve and injured brain samples using 'total intensity' values. Sample (10µg protein) was loaded onto a 4-20% gradient acrylamide gel and separated by SDS PAGE. The gel was then stained (see section 2.5.4) for analysis of total protein (A). The gels were scanned using the Odyssey Scanner, and the 'total intensity' of each lane determined using Licor software, (B) shows a fluorescent gel. The 'total intensities' of samples post injury were divided by the 'total intensity' of the naive lane to produce an intensity value relative to naïve (C) and the ratio (D) used as the correction factor for any future Western blots using these samples.

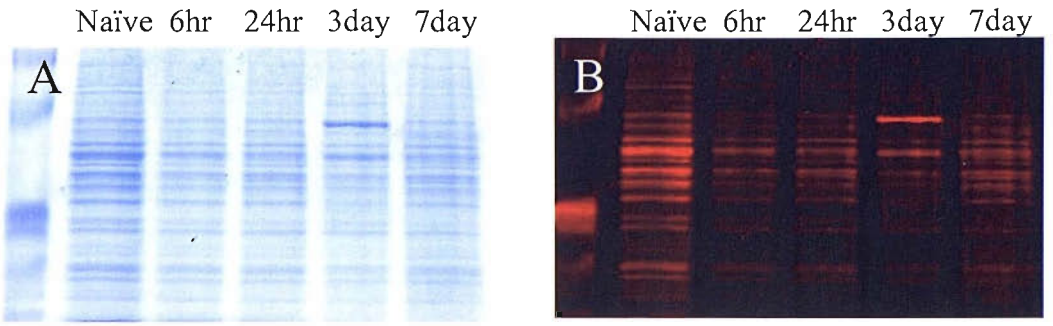

C

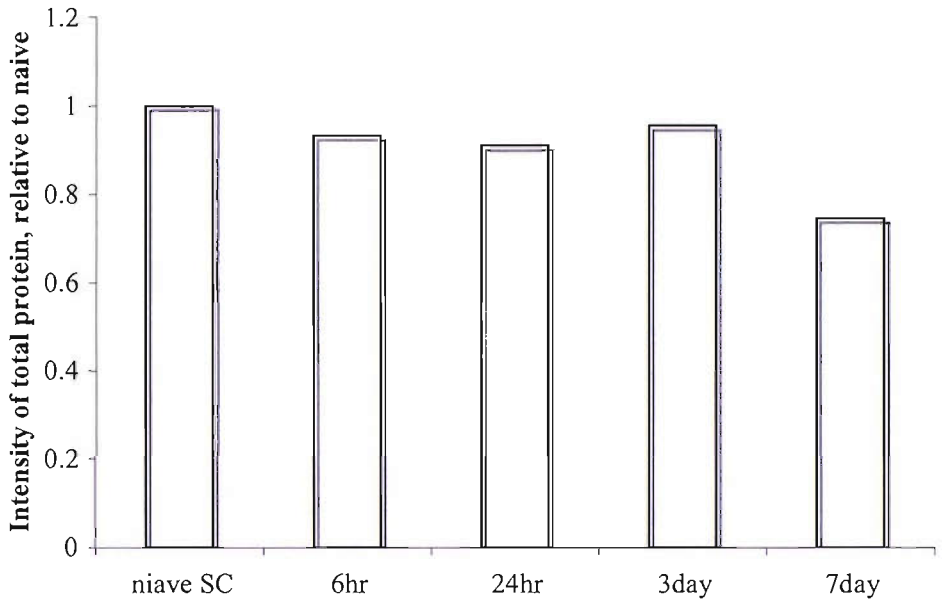

D

sample	ratio to naïve
naive SC	1
6hr	0.933
24hr	0.911
3day	0.956
7day	0.746

Fig. 4.3 Determining the protein concentration ratios between naïve and injured spinal cord samples using 'total intensity' values. Sample (10µg protein) was loaded onto a 4-20% gradient acrylamide gel and separated by SDS PAGE. The gel was then stained (see section 2.5.4) for analysis of total protein (A). The gels were scanned using the Odyssey Scanner, and the 'total intensity' of samples post injury were divided by the 'total intensity' of the naive lane to produce an intensity value relative to naïve (C) and the ratio (D) used as the correction factor for any future Western blots using these samples.

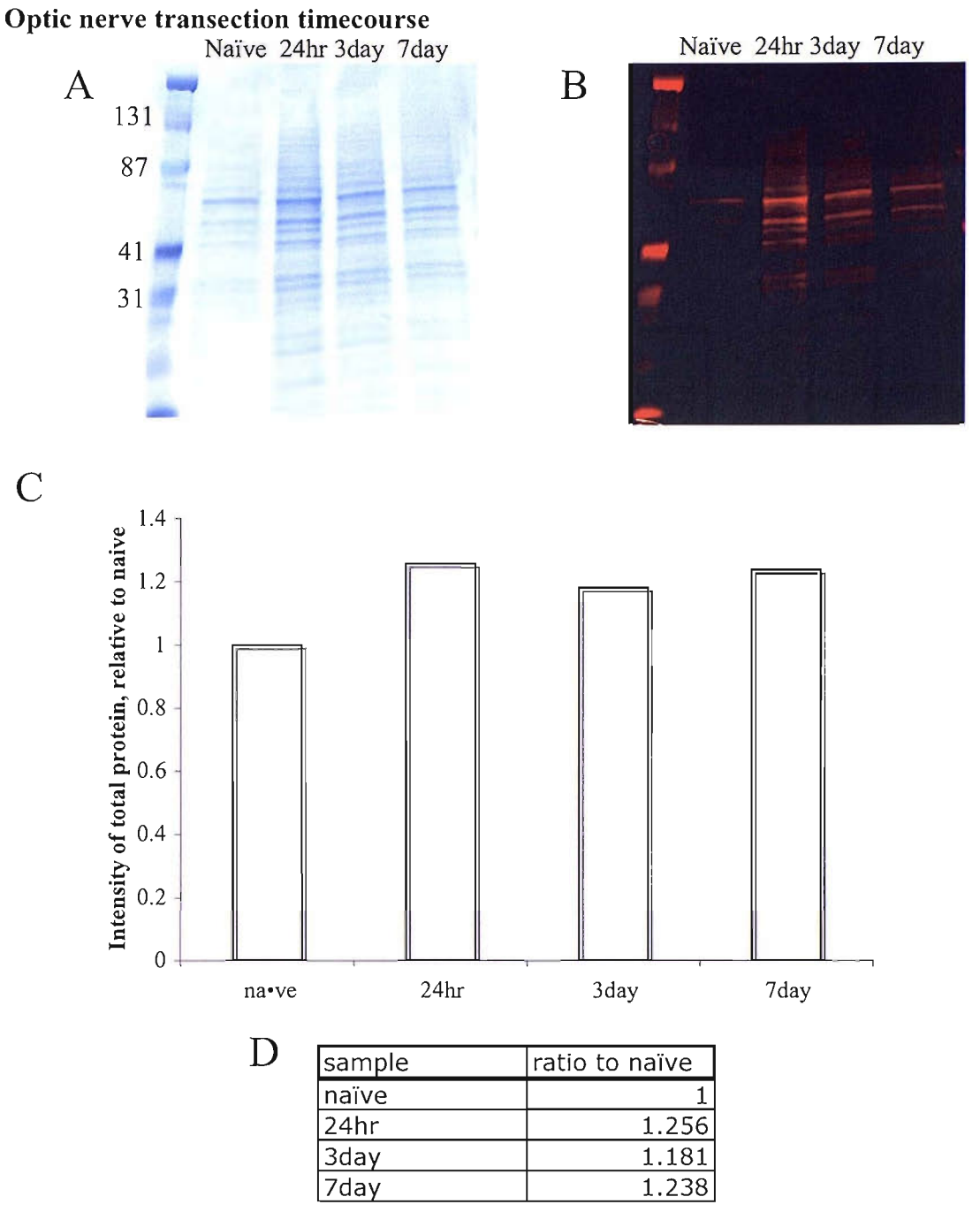

D

sample	ratio to naïve
naïve	1
24hr	1.256
3day	1.181
7day	1.238

Fig. 4.4 Determining the protein concentration ratios between naïve and injured optic nerve samples using 'total intensity' values. Sample (10µg protein) was loaded onto a 4-20% gradient acrylamide gel and separated by SDS PAGE. The gel was then stained (see section 2.5.4) for analysis of total protein (A). The gels were scanned using the Odyssey Scanner, and the 'total intensity' of samples post injury were divided by the 'total intensity' of the naive lane to produce an intensity value relative to naïve (C) and the ratio (D) used as the correction factor for any future Western blots using these samples.

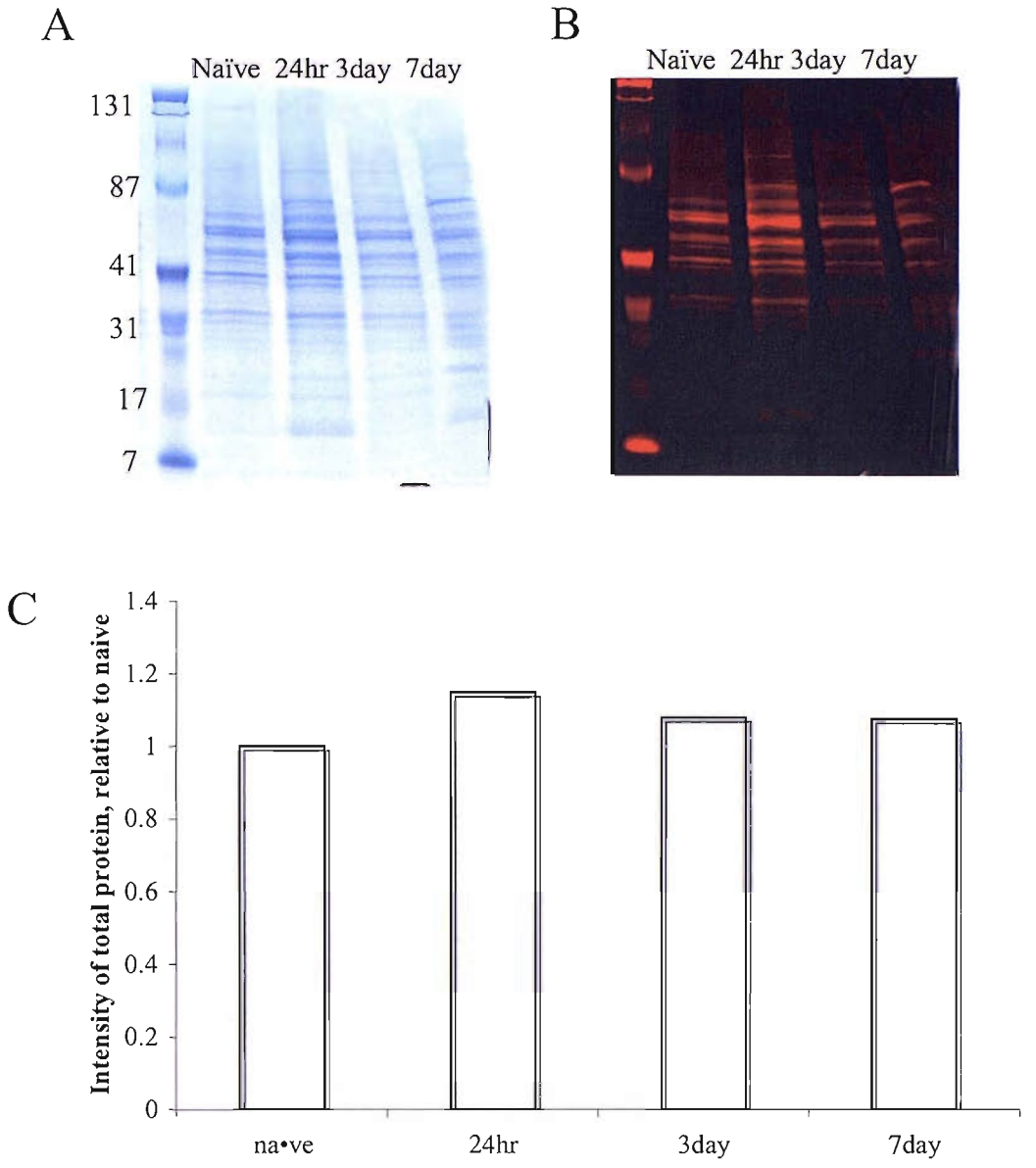

D

sample	ratio to naïve
naïve	1
24hr	1.149
3day	1.081
7day	1.077

Fig. 4.5 Determining the protein concentration ratios between naïve and injured retina samples using 'total intensity' values. Sample (10µg protein) was loaded onto a 4-20% gradient acrylamide gel and separated by SDS PAGE. The gel was then stained (see section 2.5.4) for analysis of total protein (A). The gels were scanned using the Odyssey Scanner, and the 'total intensity' of samples post injury were divided by the 'total intensity' of the naive lane to produce an intensity value relative to naïve (C) and the ratio (D) used as the correction factor for any future Western blots using these samples.

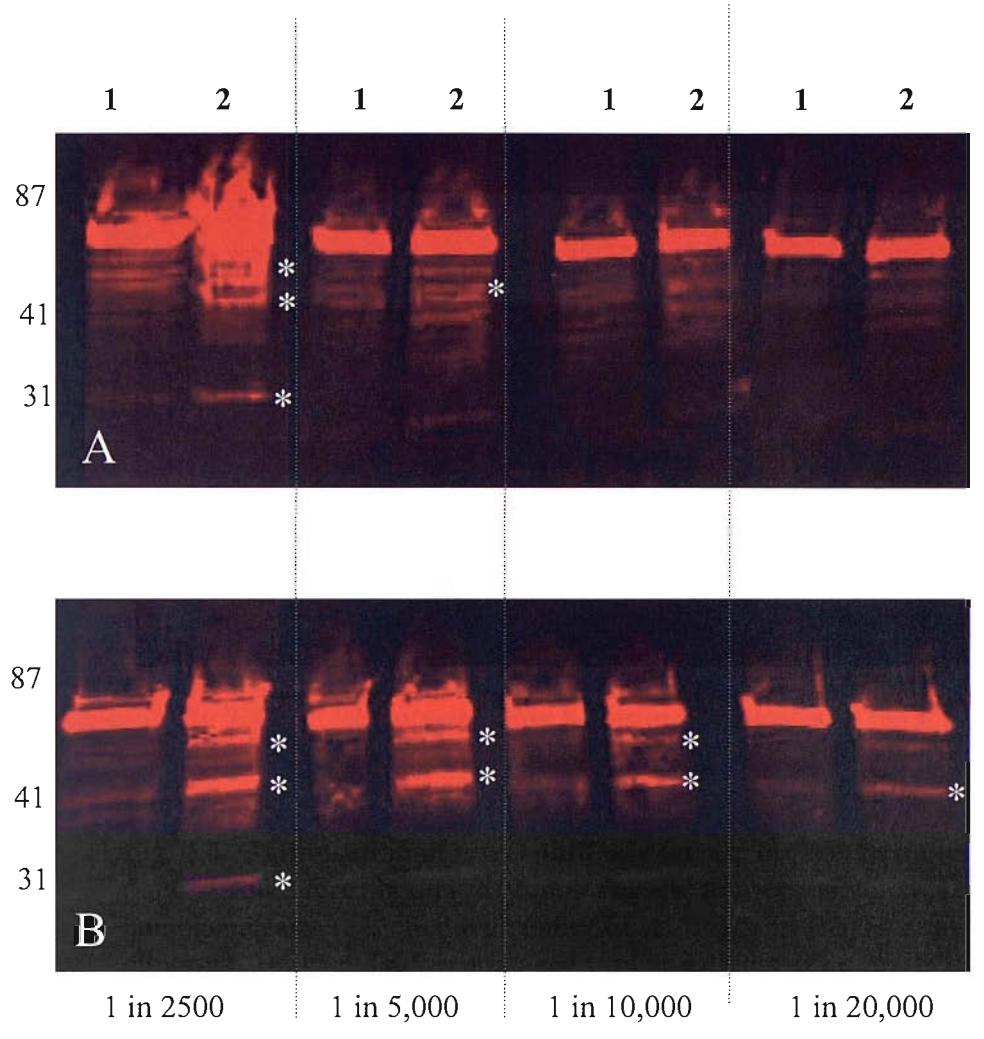

Fig. 4.6 Optimisation of novel antibody for use on Western blots. Naïve (lane 1) and injured brain (7days post cortical transection injury; lane 2) tissue homogenates were blotted with either ELR1 (A) or ELR2 (B) at a range of dilutions. Both antibodies produced similar patterns of reactivity showing a major band at approximately 70kDa. There are a number of bands that appear at lower molecular weights when the antibody dilution was lower. A band around 31kDa can be seen in lane 2 when stained with both ELR1 and ELR2 at 1 in 2500; a band of approximately 40-45kDa appeared in all injured samples (lane 2) stained with ELR2 (B). By eye, it can be observed that there are differences between the banding patterns in the naïve brain samples (lanes 1) compared to the injured brain samples (lane 2) see *.

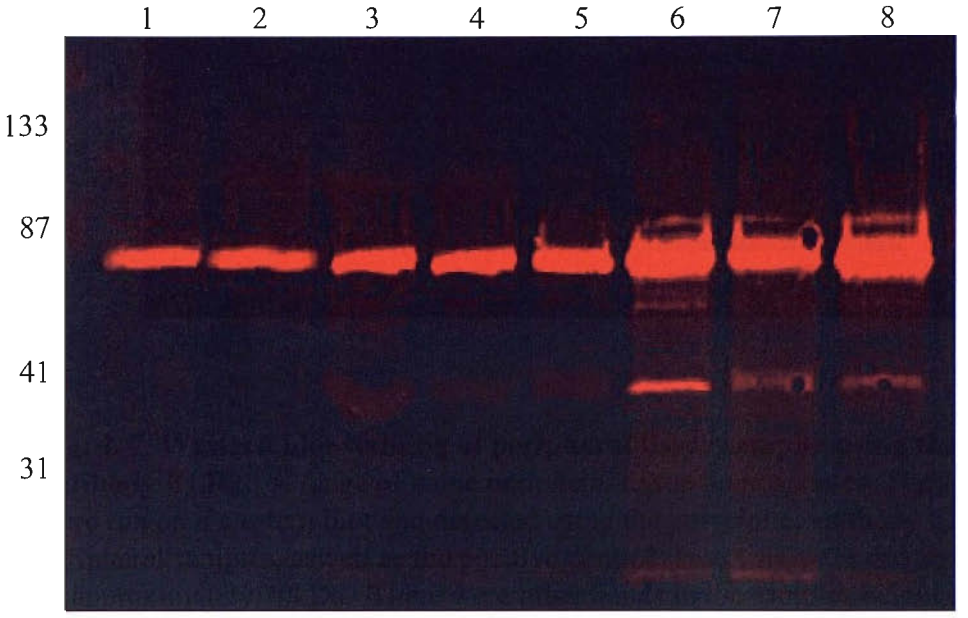

Fig. 4. 7 Western blot staining of peripheral tissue samples using the polyclonal antibody ELR2. A range of naïve peripheral tissue homogenates (10μg per lane) were run on a western blot and detected using the polyclonal antibody ELR2. All the peripheral samples, aswell as the positive control (lane 1 naïve brain) showed a band of approximately 70kDa. There were other bands in the samples in lanes 6, 7 and 8 which were skeletal muscle, skin and spleen respectively.

Key: lane 1, naïve brain; lane 2, heart; lane 3, live;, lane 4, kidney; lane 5, lung; lane 6, skeletal muscle; lane 7, skin; lane 8, spleen.

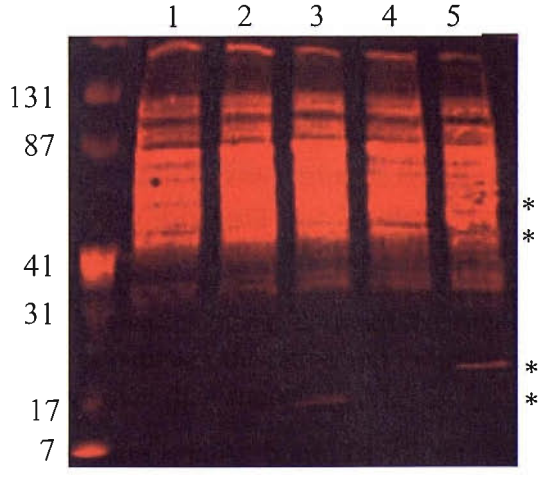

Fig. 4.8 Western blot using ELR2 on samples of naïve and injured brain. Samples of naïve and injured brain, at a number of timepoints post injury, were blotted with ELR2. The result was multiple bands being detected across all samples, the intensities of which make it difficult to conclude whether there are any differences between the naïve and injured samples. A few bands can be seen to change over the timecourse (*).

Key: lane 1, naïve brain; lane 2, 6hr post injury (p.i); lane 3, 24hr p.i; lane 4, 3days p.i; lane 5, 7days p.i.

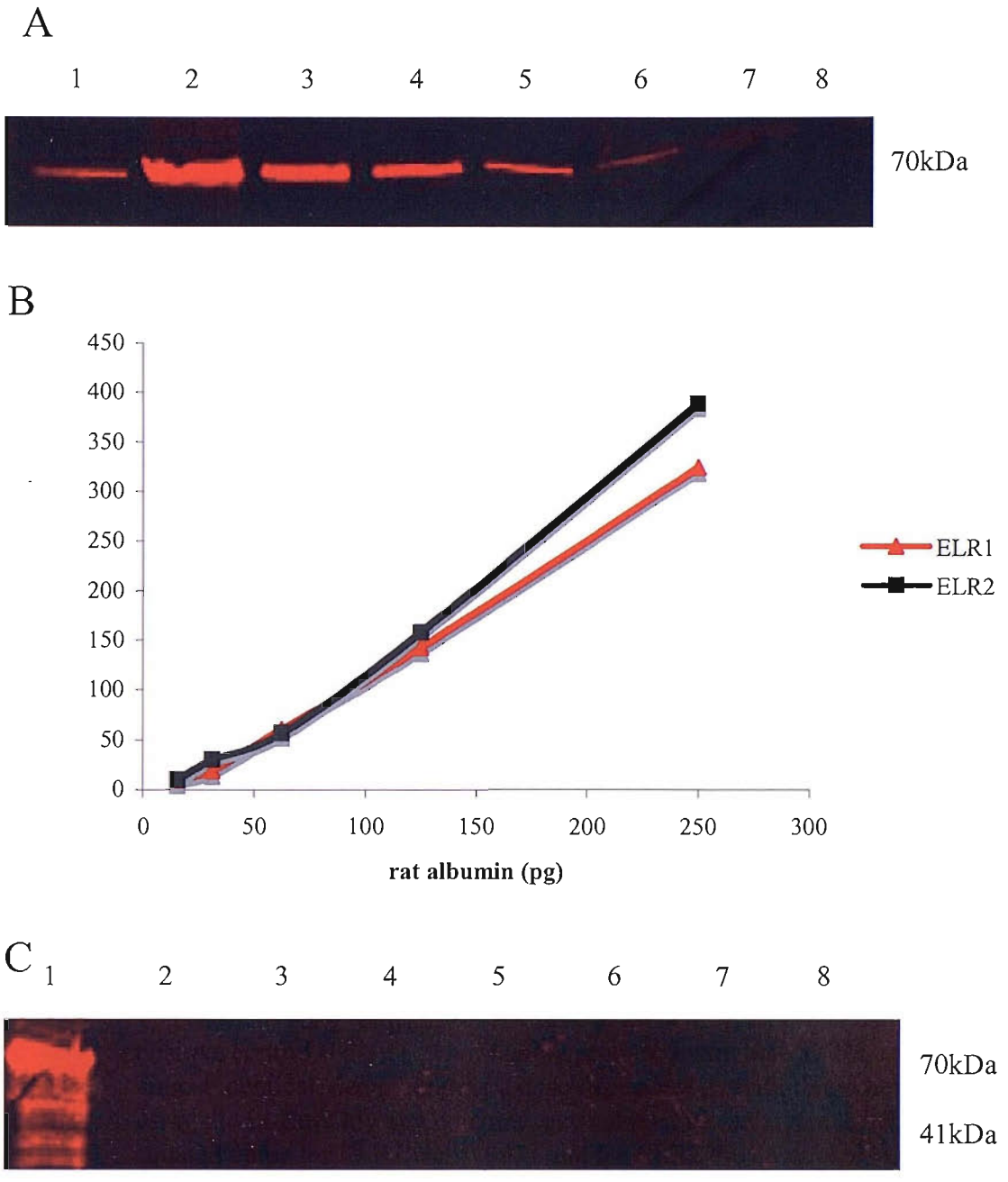

Fig. 4.9 Characterisation of rat albumin staining with the antibodies ELR1 and 2. (A) Rat albumin was used on a Western blot in a serial dilution from 1µg down to 15ng (lanes 2 to 7). Naïve brain homogenate was used as a positive control (lane 1). The staining produced with both ELR1 and ELR2 was almost identical, demonstrating a dose-dependent pattern, that when quantified using the Li-Cor Odyssey machine, gave almost identical results (B) The R-squared value for ELR1 was 0.9971 and for ELR2 the R-squared value was 0.9905, which indicates a positive correlation between albumin and antibody used. Chicken ovalbumin was used as a negative control and run on a Western blot at the sample protein concentrations as in A (i.e. 1µg down to 15ng) (C). No staining, (chicken ovalbumin has a molecular weight of 45kDa) except for the positive control in lane 1, was observed, indicating that ELR1 and 2 detect rat albumin over chicken ovalbumin. Ovalbumin from other species would need to be tested in order to discover the specificity of ELR1 and 2 for rat albumin.

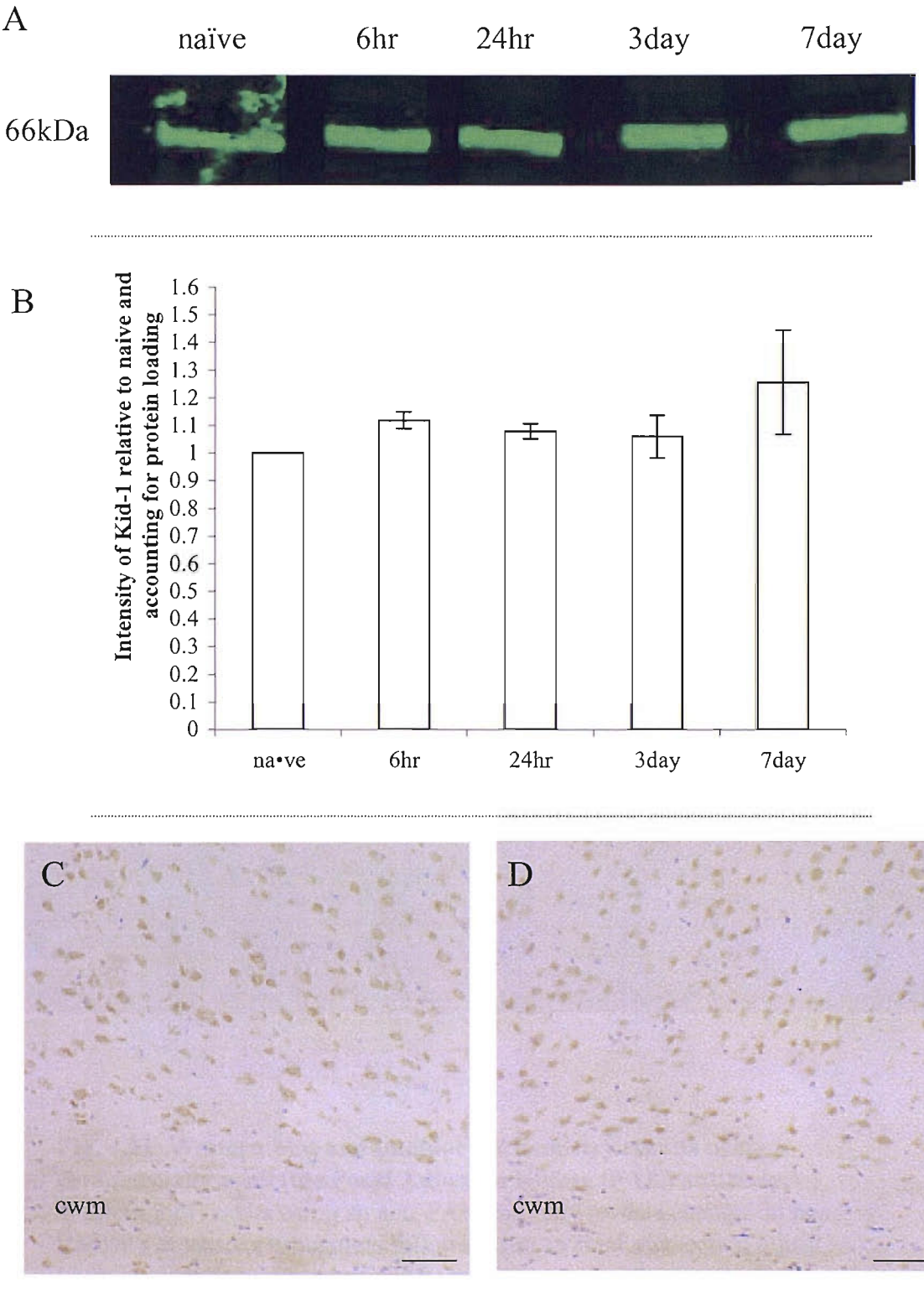

Fig. 4.10 Western blot and immunocytochemical staining with Kid-1. Western blot, with an anti-Kid-1 antibody, on intracranial lesioned brain tissue post injury (A) showed no differences in intensity values at any timepoint post injury when compared to the naïve intensity level (B). Immunocytochemistry results showed no differences in staining between naïve (C) and injured brain (D, d7 post injury). The staining appears to be located in the cell bodies of the neurones and not within glial cells. There is no staining in the cortical white matter (cwm).

Scale = 50μm

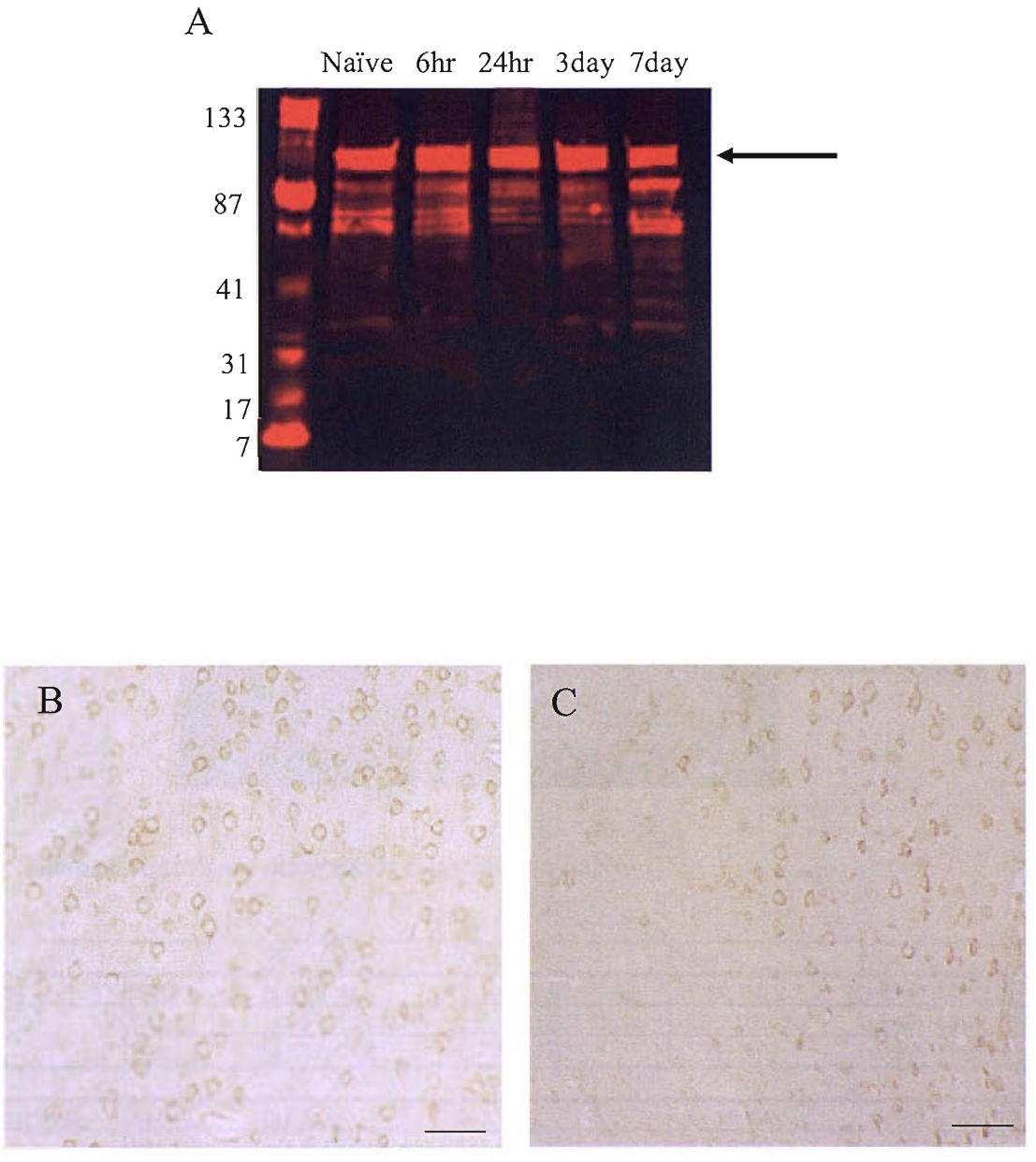

Fig. 4.11 Western blot and immuocytochemistry results using a commercially available Focal Adhesion Kinase (FAK) antibody. Western blot results using an anti-FAK antibody reveals changes in band intensity at various timepoints following intracranial transection injury (A). Immunocytochemistry on naïve (B) and injured (C, 3days post injury) brain revealed a loss of staining around the injury, and a change in pattern of the staining.

Scale = 50μm

A - Brain

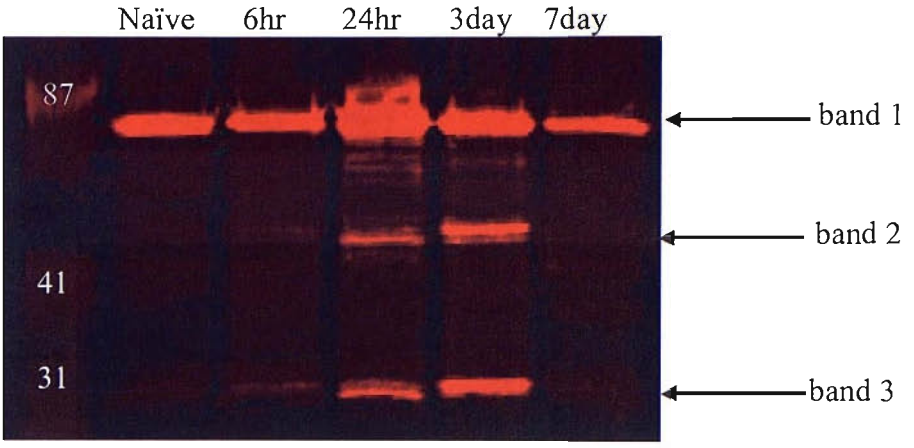

B - Spinal cord

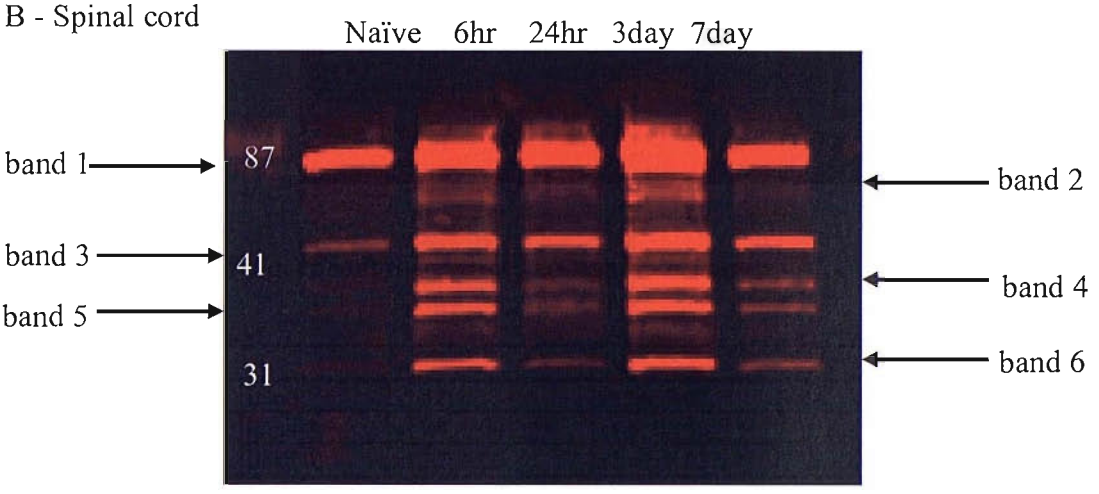

C - Table of significant differences compared to naive

		6hr	24hr	3day	7day
Brain	Band 1	x1.11; ns	x1.66; 0.02; *	x1.38; 0.03; *	x0.64; 0.007; *
	Band 2	x1.89; 0.003; **	x5.6; 0.005; **	x8.7; 0.01; *	x0.42; 0.003; **
	Band 3	x1.27; 0.06	x2.69; 0.027; *	x5.39; 0.03; *	x0.50; 0.026; *
Spinal cord	Band 1	x1.5; ns	x1.3; ns	x1.6; 0.026; *	x0.78; 0.003; **
	Band 2	x3.9; 0.05; *	x3.3; 0.07	x5.5; 0.02; *	x1.27; 0.02; *
	Band 3	x3.4; 0.05; *	x2.4; 0.05; *	x4.95; 0.02; *	x1.76; 0.04; *
	Band 4	x6.8; ns	x3.7; ns	x12; 0.06	x2.7; 0.07
	Band 5	x5.9; ns	x3.9; ns	x11.7; ns	x3.1; ns
	Band 6	x5.7; 0.08	x3.2; ns	x9.8; ns	x2.7; 0.08

Fig. 4.12 Western blot staining using ELR2 on samples of naïve and injured brain (A) and naïve and injured spinal cord (B). An example of a Western blots with ELR2 on samples of brain before and following an intracranial stab lesion can be viewed in (A). An example of a Western blot with ELR2 on samples of naïve and injured spinal cord (following a partial spinal cord transection) can be viewed in (B). The bands revealed, when scanned using the Odyssey Scanner, in both the brain and spinal cord Western blots were measured using the associated Li-Cor software. The intensities of the samples that had been injured were divided by the intensity of the naïve band to produce a 'relative intensity'. The intensities were corrected for protein loading (see method section 4.3.2). Statistical significance from naïve was determined using a non parametric anova test with Dunnetts Multiple comparison and the results can be viewed in table (C). The fold increase/decrease and the p-values are displayed in the table; ns indicates where the data was not significantly different from naive. Significance is achieved where $p<0.05$ (*) and $p<0.005$(**).

A - Optic nerve

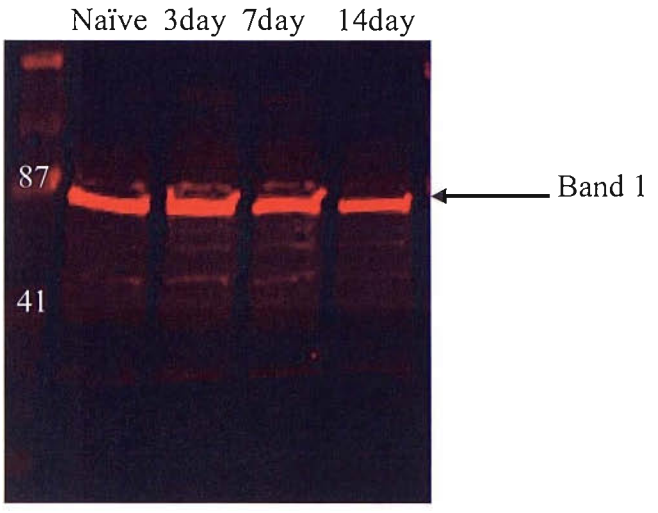

B - Retina

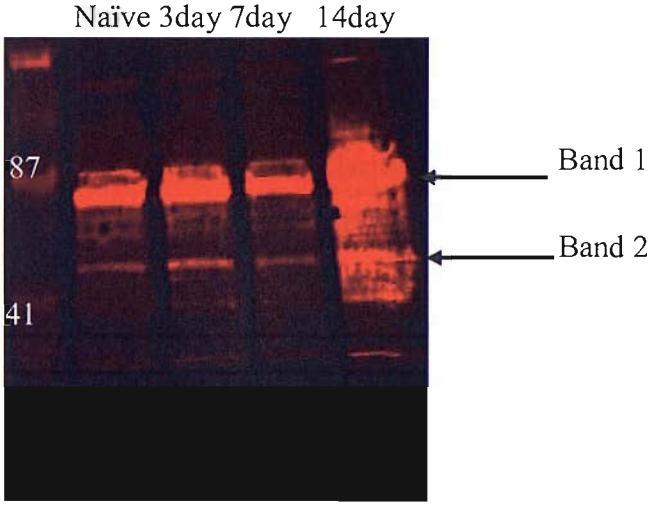

		3day	7day	14day
Optic nerve	Band 1	x1.3; 0.0003; ***	x1.08; ns	x1.04; ns
Retina	Band 1	x1.3; 0.0062; *	x1.3; ns	x1.9; 0.0018; **
	Band 2	x1.23; ns	x1.43; ns	x3.53; 0.002; **

Fig. 4.13 Western blot analysis with ELR2 on samples of naïve and injured optic nerve and retina. Samples of naïve and injured optic nerve (A) and retina (B), following optic nerve transection, were analysed by Western blot with ELR2. The intensity of the bands revealed were measured using the Odyssey-LiCor system. The intensities of the samples injured by optic nerve transection were divided by the intensity of the naïve bands to produce a relative intensity value. To determine whether the data was statistically different the data was analysed by Anova tests with Dunnetts Multiple comparisons and the P-values are shown in the table above (C).

4.5 Conclusion

The aim of this chapter was to use a proteomics approach in order to identify antigens recognised by ELR1 and 2 in damaged CNS tissue. By using a mixture of 1D gel electrophoresis, Western blotting and MALDI-TOF MS a number of proteins have been identified. Their possible role in Wallerian degeneration is discussed below.

4.5.1 Albumin

Western blot analysis revealed the presence of a 70kDa antigen, recognised by ELR1 and 2 in all tissues studied. The band on the gel was sequenced and shown to be rat albumin. ELR1 and 2 recognised recombinant rat albumin, reacting in a concentration-dependent manner. In order to determine if albumin was present in injured nervous tissue a commercial antibody was used to stain tissue following intracranial stab lesion and spinal cord transection. This antibody had never been tested previously by immunohistochemistry and the results were disappointingly inconclusive due to very high background staining (data not shown).

An important question that requires clarification is why immunisation of rabbits with the antigens that were present in the axoplasm of transected rat sciatic nerve resulted in the production of antibodies that were able to recognise *rat albumin*. Following sciatic nerve injury the blood-nerve barrier has been shown to break down within the first day of injury (de la Motte and Allt 1976; Seitz, Reiners et al. 1989). Albumin has also been shown to penetrate into damaged sciatic fibres during the first two days following injury (Hirakawa, Okajima et al. 2003). Therefore, it is likely that albumin originating from the blood has penetrated into the axoplasm of damaged sciatic nerves prior to their removal for immunisation.

Release of blood proteins into the brain following BBB breakdown triggers proliferation of astrocytes and other glial cells which leads to formation of glial scars (Skoff 1975). It is known that albumin and its associated lipids have effects on astrocytes (Nadal, Fuentes et al. 1995). Albumin causes a reduction in intracellular calcium whereas a lipid factor, associated with the native form of albumin, induces repetitive calcium spiking and DNA synthesis (Nadal, Fuentes et al. 1995). By stimulating focal long lasting opening of BBB tight junctions, by application of bile salts, Seiffert and colleagues (2004) have shown extravasation of serum proteins into the brain extracellular space. These serum proteins caused activation of astrocytes, followed by a lasting hypersynchrony of neuronal cells limited to the treated area, which the authors equated to focal epileptic activity (Seiffert, Dreier et al. 2004). This information implies a role for serum proteins, including albumin, in contributing to disease processes.

A 70kDa peptide (suggestive of albumin) was also identified in all naïve and injured nervous tissue. It is widely accepted that albumin is incapable of penetrating naïve sciatic nerves (Hirakawa, Okajima et al. 2003). Furthermore, in contrast to sciatic nerve transection, crush injury to the optic nerve results in no breakdown of the blood-brain barrier (BBB) (Perry, Brown et al. 1993). This raises the questions of why albumin was shown to be present in all tissues studied and what is its role. This question can be answered by the fact that there is a small concentration of albumin in CNS tissues. In the normal brain there is 30-50μg/mL of albumin whereas the normal blood albumin concentration is typically 35-30mg/mL, one thousand times greater (Nadal, Fuentes et al. 2001) and the normal CSF albumin concentration is 0.2mg/mL (Seyfert, Faulstich et al. 2004). The concentration gradients set up due to these differences highly influence the movement of albumin following a breakdown in the blood brain barrier, i.e. following injury there would be a tendency for albumin to move down its concentration gradient from the blood into the brain. Indeed it is also important to also consider the fact that there might be another protein of 70kDa that is also being recognised by ELR1 and 2.

The spinal cord staining observed, particularly at day 7 post injury, indicates that albumin may be entering the axons following injury. Injured axons have been shown to take up proteins via their injured end and it is this phenomenon that researchers have taken advantage of to study axonal degeneration. Tracers, such as HPR and Lucifer Yellow have been used as dyes to detect axonal damage or axonal resealing (Howard, David et al. 1999); addition of these dyes close to the injury site results in uptake into the axons and axonal transport along the axon. If I am detecting albumin in axons using the antibodies produced this would demonstrate that axonal damage has occurred, and may prove to be a useful tool. This is different to using APP immunocytochemistry as APP becomes concentrated in the end bulbs of injured proximal axons, whereas albumin may be taken up into the distal portion of transected axons, i.e. the portion undergoing Wallerian degeneration. This would show us that a transection injury has occurred, APP immunocytochemistry alone cannot be used to deduce this.

The work using the albumin specific antibodies was not continued due to time constraints. It may be an interesting area to continue to investigate as follow on work from this thesis. It is difficult to conclude that the staining I am seeing using ELR1 and 2 in the axons is albumin, due to the complexity of the polyclonal antibody. I therefore thought it would be more interesting at this stage to continue work on the other proteins identified.

Purification of the ELR antisera (i.e. removal of some of the antibody that is recognising albumin) revealed bands, other than those already detected, by Western blot

analysis. This indicates that other proteins are recognised, by ELR1 and ELR2, which may be involved in the mechanisms of axonal degeneration.

4.5.2 Kid-1

The second protein identified as possibly being recognised by ELR1 and 2 was Kid-1. Kid-1 is a zinc finger protein believed to function as a transcription factor. It was named Kid-1 as it is predominantly found in the **k**idney, is suppressed after renal **i**schemia and appears late in renal **d**evelopment (Witzgall, Obermuller et al. 1998). Witzgall et al, have raised antibodies against the Kid-1 protein (Witzgall, Obermuller et al. 1998). These antibodies were used to investigate the expression of Kid-1 in naïve and injured brain samples. Immunocytochemistry revealed Kid-1 signal in the cell bodies of neuronal cells throughout the entire sections. The level of expression as detected by both Western blot and immunocytochemistry did not change when naïve brain was compared to a number of timepoints post injury.

4.5.3 FAK

Focal adhesion kinase 2 (FAK2) is a 125kDa, non-receptor tyrosine kinase which when activated is phosphorylated, resulting in the recruitment of a number of cell signalling proteins (Schaller, Borgman et al. 1992). In neuronal cells FAK2 is phosphorylated in response to depolarisation and/or neurotransmitter release (Siciliano, Toutant et al. 1996). The role of FAK2 in neurones is unclear; however, in non-neuronal cells it appears to control turnover of focal adhesions (Calalb, Polte et al. 1995).

FAK expression, detected by Western blotting, has revealed some interesting findings that warrant further investigation. There are changes in the expression at the protein level throughout a timecourse of intracranial stab injury. Preliminary investigations by immunocytochemistry also revealed changes in expression of FAK following CNS injury. Chapter 5 will investigate fully the pattern of FAK expression in a timecourse of brain, spinal cord, optic nerve and retinal injury, both by immunocytochemistry and Western blotting.

CHAPTER 5 Focal Adhesion Kinase

5.1 Introduction

This chapter describes the results of experiments designed to characterise the expression of focal adhesion kinase (FAK), following injury. The temporal and spatial profile of FAK after injury was investigated in different CNS compartments using a combined approach of immunohistochemistry and Western blotting. A brief description of what is currently known about the role of FAK in the CNS follows.

Focal adhesions are sites of contact between a cell and the surrounding extracellular matrix (ECM). These contacts function as connections between the cytoskeleton and the ECM to confer structural integrity and to act as signalling organelles that enable cells to sense their environment. Actions at focal adhesions not only modulate cell adhesion and shape but also influence gene expression (Calalb, Polte et al. 1995). These points of contact are enriched in integrins (transmembrane proteins) and in cytoskeletal and signalling proteins. These proteins include talin, actinin, vinculin, paxillin and of particular interest, focal adhesion kinase (FAK). FAK is an important element in the signal transduction pathways underly integrin-mediated changes in cell behaviour and growth, and was first isolated as a novel protein tyrosine kinase by Schaller and colleagues (Schaller, Borgman et al. 1992). Rous sarcoma virus (RSV) affects cell growth, regulation and structure. RSV infected cells were investigated using monoclonal antibodies targeted to phosphotyrosine-containing proteins. A 125kDa protein that localised to focal adhesions was identified and named focal adhesion kinase (FAK).

Following integrin engagement, i.e. when integrins bind to their extracellular ligands, FAK is recruited to the cell membrane where it undergoes autophosphorylation on tyrosine 397; this in turn increases FAKs enzymatic activity. As well as integrin engagement, a number of growth factors and hormones can induce FAK activation (Zachary, Sinnett-Smith et al. 1992; Rankin and Rozengurt 1994; Seufferlein and Rozengurt 1994). Activation (i.e. phosphorylation) of FAK results in the recruitment of cell signalling proteins to the cell membrane (Girault, Costa et al. 1999). FAK phosphorylation is dependent on an intact cytoskeleton as treatment with cytochalasin D, which selectively disrupts actin filament networks, blocks the recruitment and hence phosphorylation of FAK (Zachary, Sinnett-Smith et al. 1992; Rankin and Rozengurt 1994; Seufferlein and Rozengurt 1994).

FAK Structure

As mentioned above, FAK is a 125kDa protein, the catalytic domain of which shows the same structural characteristics as other protein tyrosine kinases. However, the catalytic domain is located between two non-catalytic domains, which are unique to FAK.

The amino-terminus of FAK can directly associate with the cytoplasmic domain of the integrin molecules that have been stimulated. The carboxyl-terminus is responsible for targeting FAK to the focal adhesion and has been designated the focal adhesion targeting domain (FAT) (Fig. 5.1). This domain is believed to interact with a cytoskeletal anchoring protein, such as paxillin (Turner, Glenney et al. 1990). FAK has been identified in most of the cell lines and tissues examined, and is highly expressed in both neurones in culture and adult brain. In some cells the carboxyl terminal is expressed without the catalytic or amino terminal portions of FAK, this constitutively expressed protein is known as FAK related non-kinase (FRNK) and is a 41,000 Mr protein. FRNK, which lacks the site of autophosphorylation and catalytic domains, can also be recruited to focal adhesions. The role of FRNK has not been fully investigated, but it may act as a down-regulator of FAK.

The site of autophosphorylation of FAK, tyrosine 397, is also a high affinity-binding site for Src and Fyn (cytoplasmic proteins with tyrosine specific protein kinase activity). By activating Src or Fyn, FAK transduces the information from the integrin's extracellular signal into cytoplasmic signals (Fig. 5.2). In unactivated cells Src and Fyn are quiescent as their enzymatic activity is repressed through the action of negative regulatory phosphorylation at the C terminus, their phosphorylated tyrosine intramolecularly binds to their own Src homology 2 (SH2) domain (regions which recognise 3-6 residues C-terminal to a phosphorylated tyrosine). When FAK undergoes autophosphorylation a high affinity Src/Fyn SH2 binding domain is created causing displacement of the Src/Fyn intramolecular binding, thus activating Src or Fyn. FAK's interaction with Src leads to further phosphorylation of FAK and hence activation, at multiple tyrosine residues.

The role of FAK

The role of FAK is to act as a signalling protein to transduce signals from the cell surface, i.e. the focal adhesions, to the inside of the cell to elicit a response.

The formation of focal adhesions is under the control of a GTPase, Rho. Regulation of Rho activity and focal adhesions is critical in cell migration. Rho activity decreases when cells are migrating, and increases when focal adhesions are being formed (Ren, Kiosses et al. 2000). Close regulation of Rho is very important as activating or inactivating Rho diminishes migration. Fibroblasts from FAK deficient mice show an increase in focal adhesions and consequently a decrease in cell migration (Ilic, Furuta et al. 1995). Conversely, FAK overexpression leads to an increase in migration rate. Focal adhesions are unstable in rapidly spreading FAK overexpressing cells; their stability is improved when Rho activity is increased. In FAK deficient cells Rho activity is always high, thus focal adhesions are stable. FAK is needed to decrease Rho activity to promote

focal adhesion turnover and cell migration (Ren, Kiosses et al. 2000). The involvement of FAK in migration may therefore have implications within the CNS for neuronal growth cone migration.

As mentioned above, FAK has important functions in signalling initiated via integrin stimulation (Fig. 5.2). It is now recognised that FAK is also important in growth factor stimulated cell migration, e.g. FAK can become activated by the interactions of such growth factors as platelet derived growth factor (PDGF) and epidermal growth factor (EGF) with their appropriate receptors (Sieg, Hauck et al. 2000). FAK interacts with the growth factor receptors via its amino-terminal region, through an as yet unknown protein X (Fig. 5.2) (Sieg, Hauck et al. 2000).

It has been proposed that FRNK may regulate proliferation and migration by acting as an endogenous inhibitor of FAK (Taylor, Mack et al. 2001). FRNK was investigated in vascular smooth muscle cells, where FRNK has been reported to be selectively expressed (Taylor, Mack et al. 2001). Increasing FRNK expression can modulate smooth muscle cell growth and migration. FRNK expression is highest in developing vessels and is increased in later times (day 14) post vessel injury. This suggests that FRNK contributes to the regulation of proliferative and/or migratory signals. FAK needs to be well regulated as alterations in smooth muscle cell growth and migration are implicated in the pathogenesis of atherosclerosis, hypertension and restenosis.

An important role for FAK that has emerged over the last 10 years is its role in apoptosis. During apoptosis, FAK is cleaved in a caspase-dependent manner, resulting in a fragment similar to FRNK, i.e. the FAT domain without the catalytic domain, the 'new' fragment is capable of blocking FAK (van de Water, Houtepen et al. 2001), this may be a mechanism to prevent FAKs potential anti-apoptotic characteristics. Anoikis is the onset of apoptosis caused by loss of cell contact. Anoikis is physiologically important in controlling cell number; the expression of activated FAK has been shown to confer resistance to apoptosis by anoikis (Frisch, Vuori et al. 1996). 2A7, an antibody raised against FAK results in apoptosis by binding FAK and inhibiting its recruitment to focal adhesions (Hungerford, Compton et al. 1996). How apoptosis arises as a consequence of FAK inhibition is unclear. Inhibition of FAK may initiate an apoptotic program or lead to cessation of cell spreading which in turn leads to apoptosis. As well as a role in anoikis, FAK also has an important role in chemically induced apoptosis. Toxic chemical application typically induces both necrosis and apoptosis of cells in vitro. By using renal proximal tubule epithelial cells and a well characterised nephrotoxicant [S-(1,2-dichlororovinyl)-L-cysteine (DVCV)], which depending on treatment conditions causes either necrosis or apoptosis, FAK has a role in apoptosis but not necrosis (van de Water,

Houtepen et al. 2001) as overexpression of FRNK or FAT increases the rate of onset of chemically induced apoptosis, but has no effect on necrosis.

FAK in the CNS

It is essential that cells within the CNS, and in particular – neurones, are closely and precisely guided in their growth and spreading. Axon growth/navigation relies on the fine-tuning of the interactions between cell adhesion molecules and the cytoskeleton of the growth cone. FAK is highly expressed in neurones in culture and in the adult brain, although FAK^+, an isoform of FAK is selectively enriched in neuronal cells (Derkinderen, Siciliano et al. 1998).

FAK is distributed throughout the neuron. In vitro, high levels of FAK expression are seen in perikaryon and distal tips of growing processes of hippocampal cultures harvested from E18 rat embryos. The strongest signals are in the growth cones (Contestabile, Bonanomi et al. 2003). Using GFP-tagged FAK and FAK^+ both FAK proteins exhibit similar distribution, although the reason for the two different isoforms is unclear (Contestabile, Bonanomi et al. 2003). FAK is localised most intensely in growth cones suggesting that it may have an important role in neurite growth and migration, as occurs in peripheral cells. Integrins and growth factors are important in FAK activation and regulation in the periphery. In the nervous system integrins and growth factors play an important role activating FAK to regulate neurite growth (Ivankovic-Dikic, Gronroos et al. 2000). FAK has been identified in cultured oligodendrocytes, with high levels during development, followed by downregulation of FAK in fully differentiated oligodendrocytes. FAK's presence in oligodendrocytes suggests a role in regulating the motility of these cells (Kilpatrick, Ortuno et al. 2000). FAK is seen in astrocytes, with FAK and FAK^+ selectively targeted to focal adhesions along the cell membranes (Contestabile, Bonanomi et al. 2003).

FAK cannot be investigated using knockout mice due to the early embryonic lethality of FAK knockout embryos. FAK has been studied in the developing dorsal forebrain of rats using targeted deletion of the FAK gene (Beggs, Schahin-Reed et al. 2003). A conditional FAK knockout mouse has been generated, the fax-flox mouse, which enables tissue specific deletion of FAK. Deletion from neuronal and glial precursors of the dorsal telencephalon results in severe dysplasia (Beggs, Schahin-Reed et al. 2003). The disruption of FAK expression in the developing dorsal forebrain resulted in mice with overmigrating cells through the marginal zone and occasionally into the subarachnoid space, i.e. they have neuronal ectopias. This indicates that FAK is required for the formation of normal connections between cells contributing to the basal lamina.

FAK in CNS disease

Synaptic plasticity, as studied in long-term potentiation or depression (LTP/LTD), requires tyrosine phosphorylation. Alterations in the FAK signalling pathways may lead to diseases such as epilepsy, hypoxia and possibly Alzheimer's disease, to mention a few, it is therefore important to understand tyrosine phosphorylation in the nervous system. FAK is an important tyrosine kinase in the nervous system, as it translocates the signals mediated by neurotransmitter release or depolarisation into neurones to relay information and produce intracellular responses (Siciliano, Toutant et al. 1996).

FAK in CNS injury

As mentioned above FAK has an important role in apoptosis. Following an injury such as ischemia in the CNS there is a delay after which neurons undergo an apoptosis-like programmed cell death. Following transient forebrain ischemia in gerbils, cell death in the CA1 region occurs three to four days following the injury (Zalewska, Ziemka-Nalecz et al. 2003). The delay preceding death suggests cellular and extracellular reactions that result in apoptosis. Inactivation of FAK due to a loss of contact with the ECM results in apoptosis; anoikis (Frisch, Vuori et al. 1996). Following ischemia there is an increase in proteolytic activity that leads to ECM degradation (Giannelli, Falk-Marzillier et al. 1997). This degradation may result in FAK inactivation and hence anoikis. In a model of ischemia, FAK phosphorylation was shown to increase to 200% of control levels at 6hrs. However, by 72hrs the FAK phosphorylation had decreased to 50% of the control. This decrease in FAK co-incided with neuronal death (Zalewska, Ziemka-Nalecz et al. 2003). The authors hypothesise that this may implicate FAK in the role of delaying apoptosis following an ischemic insult, however, they also hypothesise that FAK may be acting in a neuroprotective manner; the exact mechanisms are not clear at this time.

FAK is implicated in is Alzheimer's disease (AD). Aβ is a 4kDa peptide, 39-43 amino acids in length, which accumulates as extracellular deposits in AD brain. Contact between Aβ and neurones is neurotoxic in vitro, although the mechanisms of action are unclear. Aβ peptide can stimulate phosphorylation of FAK (not an increase in FAK protein), an increase of 25% at 6 hours rises to 266% at 4 days (longest timepoint observed) (Zhang, Lambert et al. 1994). When FAK is stimulated by Aβ it interacts with Fyn (a member if the Src-family of tyrosine kinases that is neuronally enriched) and, its activity is repressed through intramolecular binding. However, following autophosphorylation of FAK, Fyn interacts with FAK via an SH2 domain (Zhang, Qiu et al. 1996). Following FAK-Fyn interaction Fyn becomes activated leading to a diverse

range of cellular functions including apoptosis. Some of the diverse actions that FAK can influence are summarised in Fig. 5.3.

Hypothesis

The role of FAK in following axonal injury has not been investigated. The literature to date indicates a role for FAK in apoptosis and although axonal degeneration is a process distinct from apoptosis, FAK may have relevance to axons undergoing degeneration following injury. Loss of contact between the axon and myelin may lead to cell death of the associated glial cell, i.e. the Schwann cell in the PNS and the oligodendrocyte in the CNS.

I hypothesise that FAK expression may be either increased in axons or glia in response to injury or possibly both. In order to determine where FAK is expressed in naïve CNS tissues and following injury I will induce an injury to axonal tracts that initiates Wallerian degeneration. I investigated FAK expression in intracranial stab lesion, optic nerve crush injury and spinal cord partial transection models both by Western blot analysis and by immunocytochemistry. The response will be investigated at a range of timepoints post injury.

I have shown that FAK is upregulated in glia surrounding the portion of axon distal to the site of nerve injury. In particular, FAK is upregulated in oligodendrocytes from as early as 6hrs post injury.

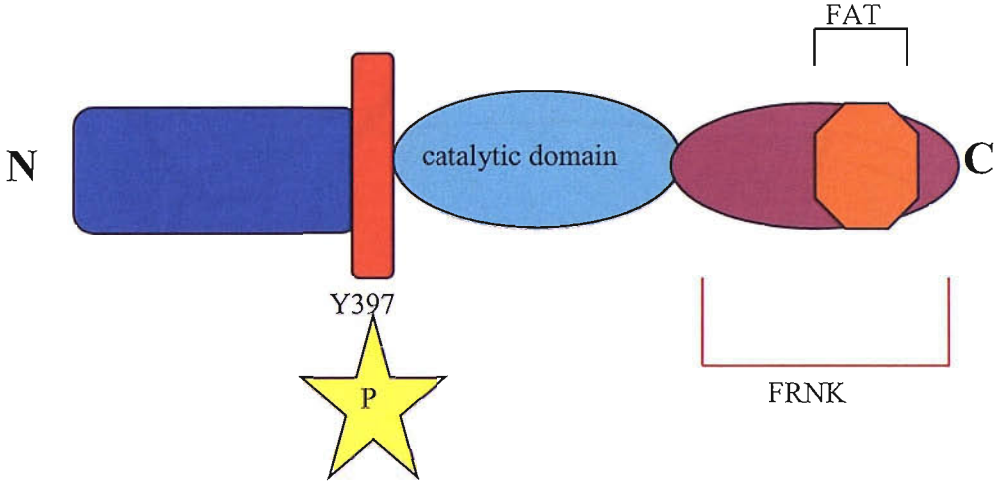

Fig. 5.1 Schematic diagram of the functional domains of focal adhesion kinase. FAK is targeted to focal adhesion by the focal adhesion targeting (FAT) domain within the C-terminal region. Once FAK has been recruited, to the focal adhesion, tyrosine 397 undergoes autophosphorylation. The site of autophosphorylation is also a high affinity-binding site for Src and Fyn, upon binding Src and Fyn can then initiate a whole cascade of cellular events. Diagram modified from Parsons et al., 1994.

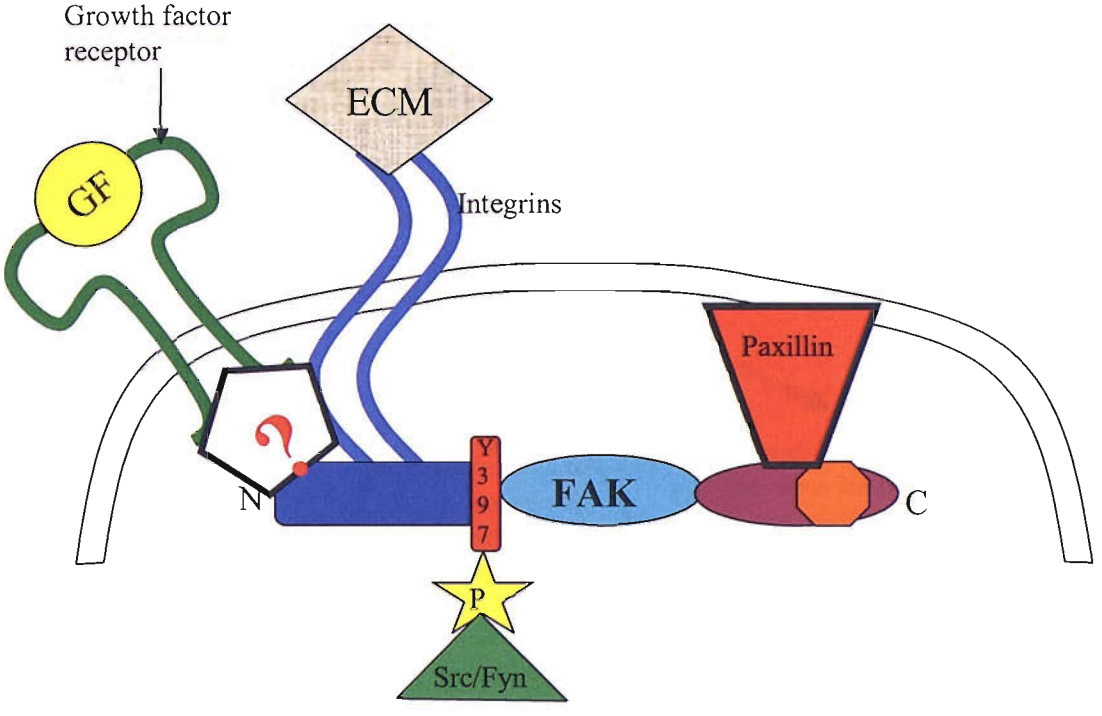

Fig. 5.2 Schematic representation of focal adhesion kinases interactions with activated growth factor receptors and integrins. Following FAK recruitment to the cell membrane, tyrosine 397 (Y397) on FAK undergoes autophosphorylation, as indicated by P. This phosphorylation in turn can lead to cellular changes such a cell migration, growth or apoptosis via activation of one of a number of intracellular proteins, for example Src or Fyn. FAK has important functions in signaling initiated via both integrin and growth factor stimulation. FAK interacts with integrins through the amino (N)-terminal integrin binding domain and growth factors have also been shown to interact via FAKs N-terminal region, possibly through an as yet unknown protein X (?) (Adapted from Sieg el al., 2000).

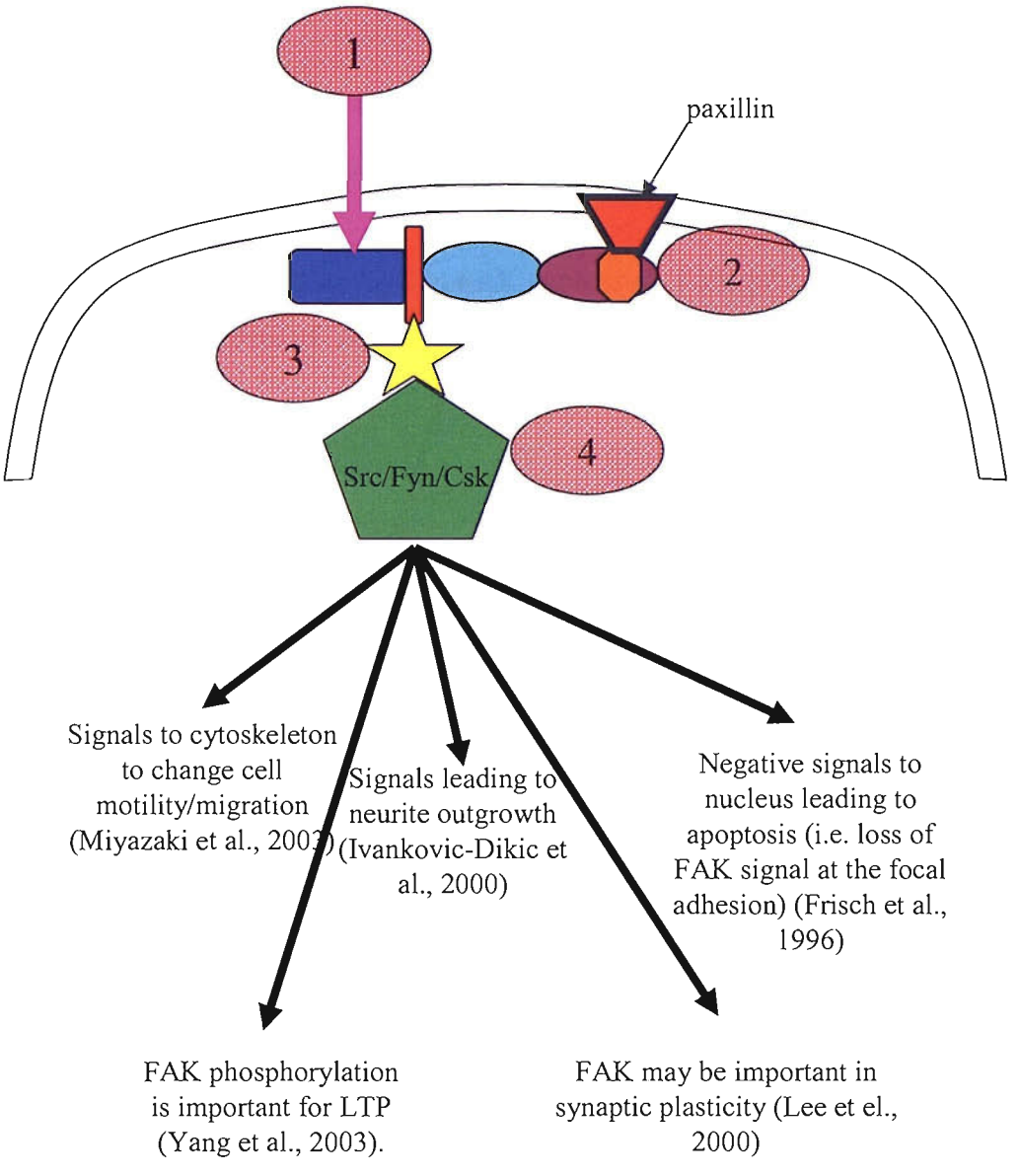

Fig. 5.3 Summary of some of the consequences of FAK activation.
Following integrin engagement and/or growth factor receptor (GFR) activation (1) FAK is recruited to the Focal Adhesions (FAs) at the cell membrane. FAK interacts with the intracellular portion of the integrin/GFR at the amino-terminal and also with other cytoskeletal proteins, such as paxillin (2) at the carboxyl-terminal. Following this interaction FAK undergoes autophosphorylation (3; star) which increases FAKs catalytic activity. This phosphorylation can activate a number of Src-like proteins (4) which, depending on the stimulus, causes a range of cellular reactions, summarised in the diagram (see text for more details).

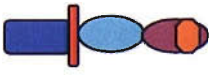 = FAK

5.2 Objectives

- To characterise the expression patterns of FAK following injury in different CNS compartments.
- To characterise any changes in FAK expression at the protein level following CNS injury in different of CNS tissues.

5.3 Methods

5.3.1 Antibody trials

Two antibodies raised against the c-terminal of FAK were used in order to determine which antibody had the higher affinity for FAK within tissue homogenate. A Sigma antibody (F2918, Sigma, UK) and a Santa Cruz antibody (sc-558) were used to assay naïve and injured brain tissue by Western blot. To ensure specific binding, the peptide sequence to which the antibodies were raised was used to conduct a blocking experiment (sc-558, Santa Cruz). The antibodies were used alone by standard Western blotting protocol at a dilution of 1 in 1000. In parallel, the antibodies were preincubated with excess peptide, overnight at 4°C before use for Western blotting.

5.3.2 Western blot analysis

Anti-FAK antibody (sc-558, Santa Cruz, UK) was used to analyse FAK expression in different CNS tissue homogenates (10µg protein loaded per well) by Western blot in both naïve and injured tissue, see the table below for details of those tissues studied.

The intensity of the bands detected was determined using the Odyssey machine, Licor software. This was carried out as detailed in Section 4.3.3. The membranes were scanned using the Odyssey machine, then the resulting bands can be drawn around using the Licor software. The intensity value given is the pixel intensity. In order to detect any changes compared to naïve, all the intensities were divided by the intensity of the naïve sample produced from the same membrane. This 'relative' intensity was then corrected for protein loading using the ratio values obtained in Figs. 4.2 and 4.3.

5.3.3 Immunocytochemical analysis

Naïve and injured CNS tissues were investigated for FAK immunoreactivity. See the table below for details of timepoints and tissues studied.

	Brain Stab lesion ICC/WB	spinal cord partial transection ICC/WB	optic nerve transection (distal) ICC/WB	retina -following optic nerve transection ICC/WB
naïve	X	X	X	X
6hr	X	X		
24hr	X	X		
3day	X	X	X	X
7day	X	X	X	X
14day			X	X

Anti-FAK antibody (Santa Cruz) was used at a dilution of 1 in 100 for optimal staining (section 2.6).

5.3.4 Co-expression of FAK

In order to determine the identity of the cells expressing FAK in our models I used double immunofluorescence microscopy. Anti-FAK antibody was used in combination with the following antibodies on naïve and injured brain, spinal cord, optic nerve, both proximal and distal to the injury, and retina:

1) CC1, to detect oligodendrocytes,
2) GFAP, to detect astrocytes and Muller cells (in the retina),
3) Neurofilament-H (NF-H) to stain the axons,
4) Neu n, a neuronal marker,
5) Tomato lectin, to detect blood vessels.

The details of each antibody can be seen in Appendix K.

The idea behind these experiments was to determine which cells FAK was expressed in following CNS injury. I looked for co-expression of FAK, as at this time I only wanted to determine which cells FAK was located in, not what FAK co-localised with. I used single slice images to determine this information. I used a Zeiss Confocal microscope and images were taken using the LSM510 MetaMorph Version 3.2 package.

The protocol for double immunohistochemistry was followed from section 2.7. Alexa Fluor 555; red signal, (Molecular probes) was always used to amplify the FAK signal, and Alexa Fluor 488, green signal, (Molecular probes) was used to detect the second antibody, i.e. to determine the cell-type. Typically, where the two antibodies co-localise, the red and green fluorescence results in a yellow signal.

Confocal microscopy was used to further investigate the co-expression of FAK within particular cell populations. The selected tissue was scanned through the entire

section to produce a 3D z-stack image. This image was then be used to determine whether the two proteins being identified are within the same cell.

5.4 Results

5.4.1 FAK blocking experiment

Anti-FAK antibodies, from Sigma and Santa Cruz, were used to probe naïve and injured brain samples using Western blotting. They were used alone or following blocking by preincubation with the peptide sequence to which the antibodies were raised. Whilst both antibodies showed specificity for FAK, by detecting a band at 125kDa, the Santa Cruz antibody showed less 'non-specific' binding (Fig. 5.4). Multiple bands were observed that were not blocked by preincubation of the Sigma antibody with the peptide sequence to which it was raised (Fig. 5.4A). However, using the Santa Cruz antibody almost all the antibody binding was blocked following pre-incubation with the peptide to which the antibody was raised against (Fig. 5.4B). As a consequence of these results all further experiments with an anti-FAK antibody were conducted using the Santa Cruz antibody.

5.4.2 FAK expression following brain injury

Western Blotting

Western blot analysis comparing levels of FAK expression in naïve brain tissue to injured brain tissue can be seen in Fig. 5.5. The data is summarised below (data was analysed using a non parametric Anova with Dunnetts Multiple comparison test).

	percentage, compared to naïve	p =
Naïve	100	n/a
6hr	101	>0.05
24hr	60	<0.01; *
3day	80	>0.05
7day	49	<0.001; **

The data show a decline in FAK expression over the 7day timecourse.

Immunocytochemistry

Formalin fixed brain tissue showed signal in neurones throughout the brain (Fig. 5.6). There is a loss of FAK signal following injury when compared to naïve brain (Fig. 5.6A); at all time points studied FAK signal decreases around the lesion (Fig. 5.6B, C and D). Some positive signal was observed in glial cells around the injury, this was particularly evident 24hrs post injury (Fig. 5.6B).

Bouin's fixed naïve brain tissue showed different expression to that seen after formalin fixation. Neuronal FAK expression was not seen, however, signal was observed in vessels in naïve tissue (Fig. 5.7A), this was also evident throughout the timecourse of

injury investigated. However, FAK signal increases over the timecourse including possible glial cell expression in close proximity to the injury area (Fig. 5.7).

5.4.3 FAK expression following spinal cord injury

Western Blotting

The pattern of FAK expression in spinal cord following injury was similar to the expression seen after brain injury (Fig. 5.5). The changes observed in the Western blot can be viewed in Fig. 5.8, and are summarised in the table below (data was analysed using a non parametric Anova with Dunnetts Multiple comparison test).

	percentage, compared to naïve	p =
Naïve	100	-n/a
6hr	107	>0.05
24hr	92	<0.05; **
3day	99	>0.05
7day	75	<0.05; **

Immunocytochemistry

Low power (Fig. 5.9) and high power (Fig. 5.10) figures have been constructed to show the diverse changes that occurred at different timepoints following partial spinal cord transection. The low power figure (Fig. 5.9) clearly shows that compared to naïve spinal cord, where there is minimal FAK signal, by 6hrs (Fig. 5.9B) post injury there was abundant signal throughout the tissue. This continues to increase throughout the timecourse.

In order to study the morphology of the cells, higher power photomicrographs were taken (Fig. 5.10). Naïve tissue (Fig. 5.10A and B) exhibits minimal FAK expression. Background staining was seen throughout the sections with a few possible blood vessels. By 6 hours post injury (Fig. 5.10C and D) there was signal in glial cells as well as in vessels. 24hrs post injury (Fig. 5.10E and F) also revealed glia and vessel signal. A similar pattern was observed at 3days post injury (Fig. 5.10G and H). FAK appears more abundant by 7 days post injury (Fig. 5.10I and J), with some signal in microglia and oligodendrocytes (determined by morphology). This has not been quantified for this thesis as I am looking at this qualitatively.

Double immunofluorescence

CC1 – oligodendrocytes

The co-expression of FAK with an oligodendrocyte marker, CC1, throughout the spinal cord timecourse can be seen in Fig. 5.11. The figure clearly shows that in naïve tissue, FAK does not co-express with CC1 (Fig. 5.11A-C). However, following injury there is an increase of FAK within oligodendrocytes and clear co-expression is observed at

all of the timepoints investigated (Fig. 5.11D-O). However, not all of the FAK is co-expressed with CC1 as can be seen in Fig. 5.11 D-F, and J-L.

GFAP – astrocytes

GFAP and FAK co-expression was limited. The co-expression of FAK with GFAP was apparent 3days post injury (Fig. 5.12J-L) and persisted in the 7day timepoint (Fig. 5.12M-O); however, the co-expression was limited. At earlier times after injury FAK signal was often surrounded by GFAP staining (Fig. 5.12G-I) which may indicate that FAK is expressed in cells that are in contact with astrocytes, possibly blood vessels.

Neurofilament (NF-H) – axons

There was no co-expression of NF-H with FAK staining at any timepoint studied (Fig. 5.13).

Neu N – neurones

FAK did not appear in neurons in detectable levels until 3days post injury (Fig. 5.14J-L). FAK expression remained elevated at 7days post injury (Fig. 5.14M-O). NeuN is a transcription factor and has a different pattern of expression than FAK; the expression observed at 3days and 7days does not appear to be in the same cellular sub-compartment, however, it is clear from the spatial distribution that both FAK and NeuN are within the same cell (NeuN is mainly nuclear with some cytoplasmic expression, whereas FAK is cytoplasmic and is also located at focal adhesions at the cell membrane).

Tomato lectin – blood vessels/microglia

The low level of FAK signal in naïve tissue follows a similar distribution to that seen when the tissue is stained for tomato lectin (Fig. 5.15A-C). Tomato lectin in naïve sections revealed mainly blood vessels. The FAK staining in the naïve tissue, whilst direct co-expression is not observed, mirrors the tomato lectin staining. By 6hrs post injury there is clear co-expression of FAK with tomato lectin (Fig. 5.15D-F). Co-expression is apparent through the 7day timecourse (Fig. 5.15G-O show representative images of FAK-tomato lectin double staining). The staining observed at 24hrs (Fig. 5.15G-I) shows FAK and tomato lectin in close proximity. Whilst they are not showing direct co-expression, i.e. the colours do not overlap, they still may be within the blood vessels, but expressed in different cellular areas.

SUMMARY OF SPINAL CORD FAK EXPRESSION

	oligodendrocytes	astrocytes	Axons	neurones	Blood vessels
Naïve	-	-	-	-	+/-
6hr	+++	-	-	-	++
24hr	+++	-	-	-	++
3day	+++	+/-	-	+/-	++
7day	+++	+/-	-	+/-	++

Key: - = no double signal; +/- = limited double signal; ++ = double signal; +++ = abundant double signal.

Co-expression Conclusion

The most striking double immunofluorescence, and possible co-expression of FAK within a cell type was with CC1, the oligodendrocyte marker. On further analysis of a typical cell that appeared to have FAK and CC1 within the same cell I can conclude that FAK was detected in oligodendrocytes (Fig. 5.16).

5.4.4 FAK expression following optic nerve crush injury

Due to the complexity of the models of injury studied so far (i.e. the spinal cord has both ascending and descending axons), in order to separate out the proximal and distal injuries from one another and to isolate the cell body I have used optic nerve transection as a model of injury. This model allows us to visualise each compartment in isolation form the others in order to determine which cells are responding to the injury.

Western blotting

The Western blot analysis of FAK expression in the optic nerve distal to the site of injury (i.e. that part disconnected from the cell body) can be seen in Fig. 5.17. The changes observed did not show significant differences from naïve, however, there was a trend of FAK to increase over the first 3 days post injury and then decrease (from that seen at 3day, but still higher than naïve) by 7days post injury.

	percentage, compared to naïve	Significance
Naïve	100	n/a
3day	126	>0.05
7day	187	>0.05
14day	140	>0.05

Immunocytochemistry

a. Distal optic nerve

Immunocytochemical analysis of FAK expression in optic nerve distal from the site of injury revealed changes in FAK from 3days onwards (Fig. 5.18). Naïve optic nerve revealed a low level of background staining (Fig. 5.18A). 3days post injury FAK signal was seen throughout the optic nerve (Fig. 5.18B). By 7days the signal had a similar distribution to that seen at 3days, however, there was also some fine thread-like staining, this may be within axons (Fig. 5.18C). 14days post injury the cellular signal was more abundant than that observed at earlier timepoints (Fig. 5.18D). Some signal was also detected in the vasculature, this was seen at all times after injury.

b. Proximal optic nerve

FAK immunoreactivity of the proximal optic nerve differed quite considerably from that of the distal optic nerve. The first signs of differences in FAK expression were seen at 14days post injury (Fig. 5.19D). At this time FAK expression was seen within cells and some of the vasculature. There were no obvious differences in expression at either 3day (Fig. 5.19B) or 7days after injury (Fig. 5.19C) when compared to naïve (Fig. 5.19A).

Double Immunofluorescence

FAK expression was visualised in red in all images, the second antibody used was visualised in green.

a. Distal optic nerve

CC1 – oligodendrocytes

Naïve optic nerve showed no co-expression of FAK with CC1 (Fig. 5.20A-C). Co-expression was still absent 3days after injury (Fig. 5.20D-F), this is strikingly different from the results for spinal cord where co-expression was observed as early as 6hrs post injury. However, by 7days post injury there was abundant co-expression of FAK with CC1 (Fig. 5.20G-I), which was also observed at 14days post injury (Fig. 5.20J-L).

GFAP – astrocytes

There was no co-expression of FAK with GFAP at any timepoint (Fig. 5.21). There is some 'yellow' signal in Fig. 5.21I and L; however, from the morphology it is clear that this is where the staining is in close proximity.

Neurofilament (NF-H) – axons

There was no co-expression observed when the distal optic nerve was double stained for FAK and NF-H (Fig. 5.22).

Tomato lectin – blood vessels and microglia

There was no obvious co-expression between FAK and tomato lectin until 14days post injury (Fig. 5.23J-L). At 14days post injury the co-expression appears to be within microglia cells (from morphology).

SUMMARY OF FAK EXPRESSION IN OPTIC NERVE, DISTAL TO AN INJURY

	oligodendrocytes	Astrocytes	Axons	neurones	blood vessels
Naïve	-	-	-	-	+/-
3day	+++	-	-	-	++
7day	+++	-	-	-	++
14day	+++	+/-	-	+/-	++

Key: - = no double signal; +/- = limited double signal; ++ = double signal; +++ = abundant double signal.

b. Proximal optic nerve

CC1 – oligodendrocytes

There is no co-expression of FAK with CC1 at any timepoint studied in the proximal optic nerve (Fig. 5.24).

GFAP – astrocytes

There is no co-expression of FAK and GFAP in the naïve optic or proximal optic nerve at any timepoint post injury (Fig. 5.25).

Neurofilament (NF-H) – axons

No co-expression was observed when optic nerve, proximal to the injury was stained for both FAK and NF-H (Fig. 5.26).

Tomato lectin – blood vessels and microglia

Co-expression of FAK and tomato lectin was observed in proximal optic nerve 14days post injury (FIG. 5.27J-L). Earlier timepoints (Fig. 5.27 A-I) did not reveal any co-expression.

SUMMARY OF FAK EXPRESSION IN OPTIC NERVE, PROXIMAL TO AN INJURY

	oligodendrocytes	Astrocytes	Axons	neurones	blood vessels
Naïve	-	-	-	-	+/-
3day	-	-	-	-	+
7day	-	-	-	-	+
14day	-	+/-	-	+/-	+

Key: - = no double signal; +/- = limited double signal; ++ = double signal; +++ = abundant double signal.

5.4.5 FAK expression in the retina following optic nerve transection

Following optic nerve transection the retina was removed in order to study whether the injury resulted in any changes in FAK expression within the retina. This allows isolation of those cell bodies that have had their axon transacted.

Western blotting

There appears to be a biphasic change of FAK expression, at different timepoints, in the retina following optic nerve transection (Fig. 5.28). The changes observed are not significantly different from naïve. 3days post injury the levels of FAK expression increases compared to naive, followed by a decrease, to below that of naïve by 7days, increasing again (to similar levels to that of 3days) by 14days post injury.

	percentage, compared to naïve	Significance
Naïve	100	n/a
3day	123	>0.05; ns
7day	76	>0.05; ns
14day	120	>0.05; ns

ns= not significantly different from naïve

Immunocytochemistry

There appears to be little change in FAK expression in the retina over the timecourse studied (Fig. 5.29). There may be an increase in the blood vessel staining, by 7-14days-post injury (Fig. 5.29E-H) (determined by morphology), although the differences from naïve are not striking.

Double immunofluorescence

GFAP – Muller cells

There was some co-expression with FAK and GFAP from 3days post injury (Fig. 5.30D-F) although the majority of GFAP was not co-localised with FAK (Fig. 5.30H-L).

Neurofilament (NF-H) – axons

There was no co-expression between FAK and NF-H at any timepoint studied (Fig. 5.31).

NeuN – neuronal cell bodies

There was some co-expression of FAK with NeuN at 3days and 7days post injury (Fig. 5.32D-J). The coexpression was not widespread, the majority of NeuN staining did not co-localise with FAK.

Tomato lectin – blood vessels and microglia

There was abundant co-expression of FAK and tomato lectin from 3days through to 14days post injury (Fig. 5.33D-L). From the morphology it appears that the co-expression is limited to the blood vessels.

SUMMARY OF FAK EXPRESSION IN THE RETINA, FOLLOWING OPTIC NERVE TRANSECTION

	oligodendrocytes	Astrocytes	Axons	neurones	blood vessels
Naïve	-	-	-	-	+/-
3day	+++	-	-	-	+
7day	+++	-	-	-	+
14day	+++	+/-	-	+/-	++

Key: - = no double signal; +/- = limited double signal; ++ = double signal; +++ = abundant double signal.

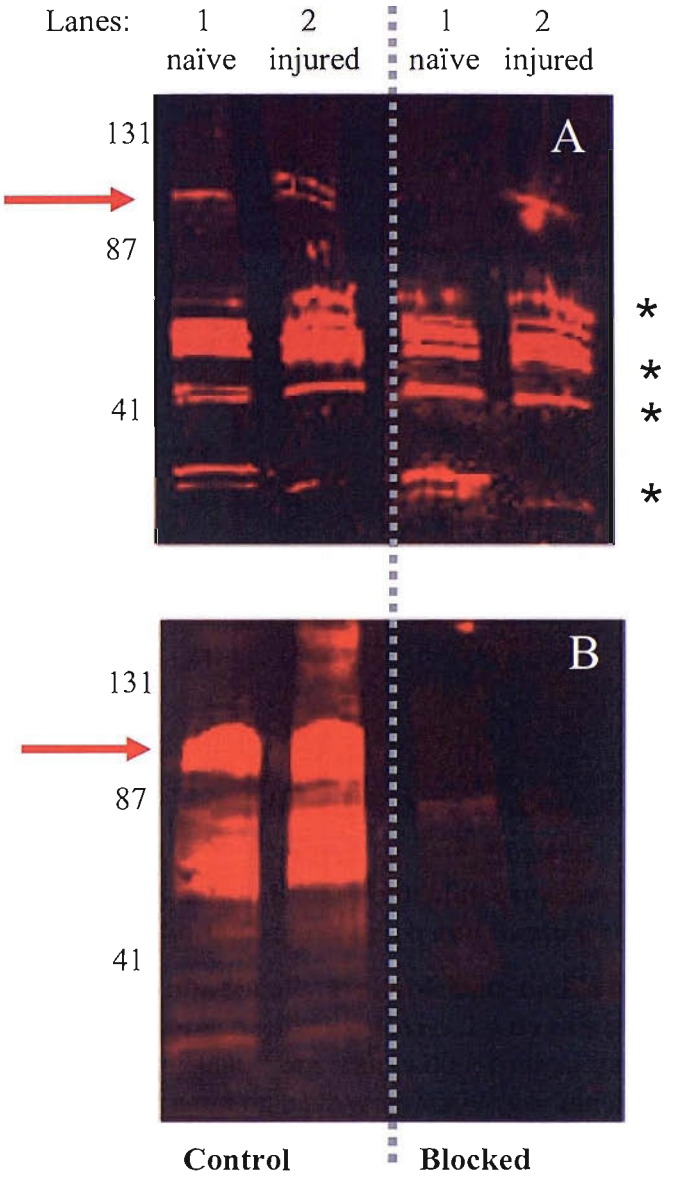

Fig. 5.4 Focal Adhesion Kinase blocking experiment with antibodies purchased from both Sigma Aldrich and Santa Cruz.

We tested two commerically available anti-FAK antibodies to determine which one was more specific for FAK. To do this naïve brain homogenate (lane 1) and homogenate from brain with a cortical transection injury (3day post injury, lane 2) were run on a polyacrylamide gel and transferred to nitrocellulose membrane for blotting with an anti-FAK antibody obtained from either Sigma Aldrich (A) or Santa Cruz Biotechnology (B). The antibodies were either alone **(control)**, or **blocked** by preincubation with the peptide sequence to which the antibodies were raised against (see text). Preincubation with the FAK peptide abolished the FAK band (arrow) in both blots whether stained with the Sigma Aldrich or Santa Cruz antibodies. The antibody from Sigma Aldrich, as well as detecting FAK, bound a number of lower molecular weight bands in a non-specific manner. These bands were determined to be non-specific as the staining was not blocked in the blocking experiment (see *). The antibody from Santa Cruz also detects bands at a lower molecular weights, these were determined to be specific as the staining was abolished in the blocking experiment. These bands may be breakdown products of FAK or possibly the phosphorylated non-related kinase of FAK (FRNK) that is autonomously expressed in cells.

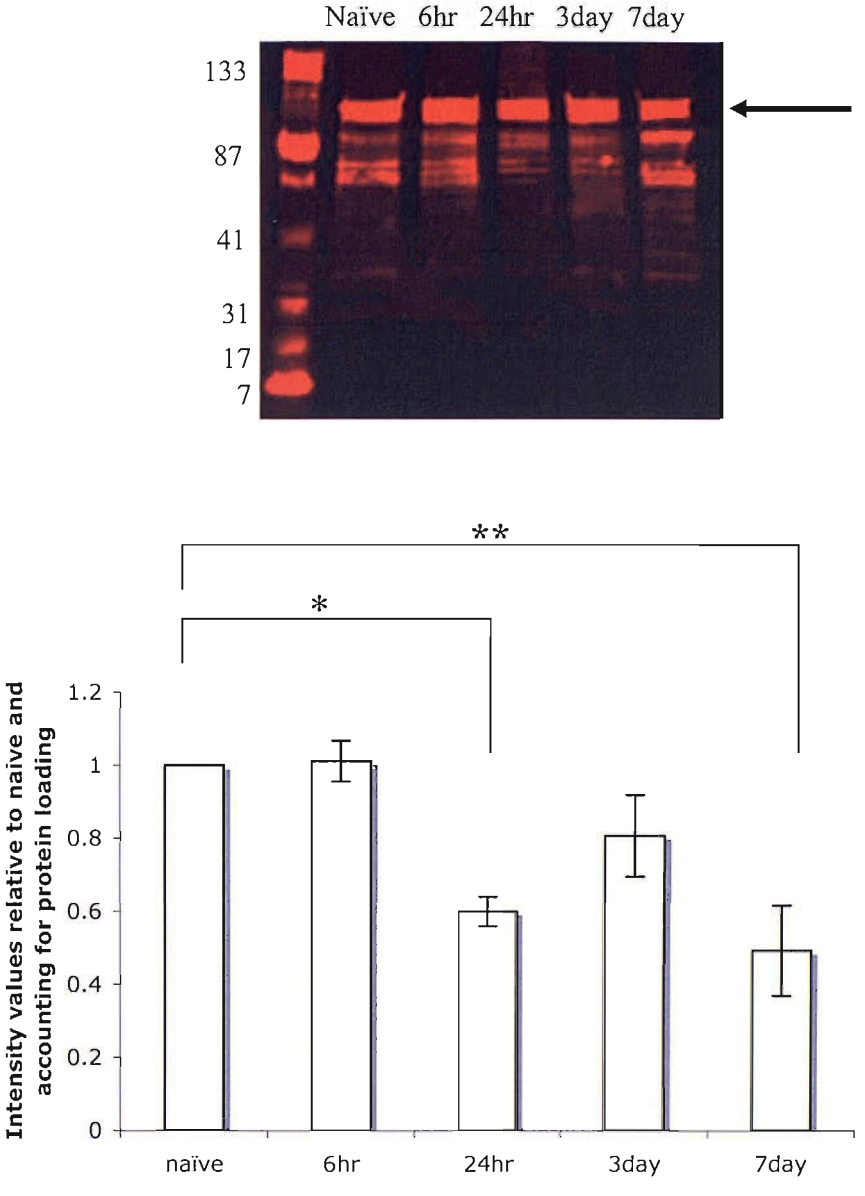

Fig. 5.5 Quantification of the changes in the relative levels of Focal Adhesion Kinase protein levels at a range of timepoints following an intracranial transection injury. The intensity values for the FAK bands, 125kDa (arrow), at the various timepoints were measured using the Odyssey scanner and corrected to account for any differences in protein loading (see Chapter 4).

Following intracranial stab injury, through the cortical white matter, FAK levels decline significantly by 24 hours with a decrease of 40 percent (P=0.01, *). By 3 days the levels had increased slightly from 24 hours, however, the level is 20 percent lower than naïve, although this is not significantly different. FAK levels then significantly decrease again at 7 days, showing a 46 percent decline compared to naïve (P=0.001, *).

N=3 animals per lane and n=5 western blots for each gel

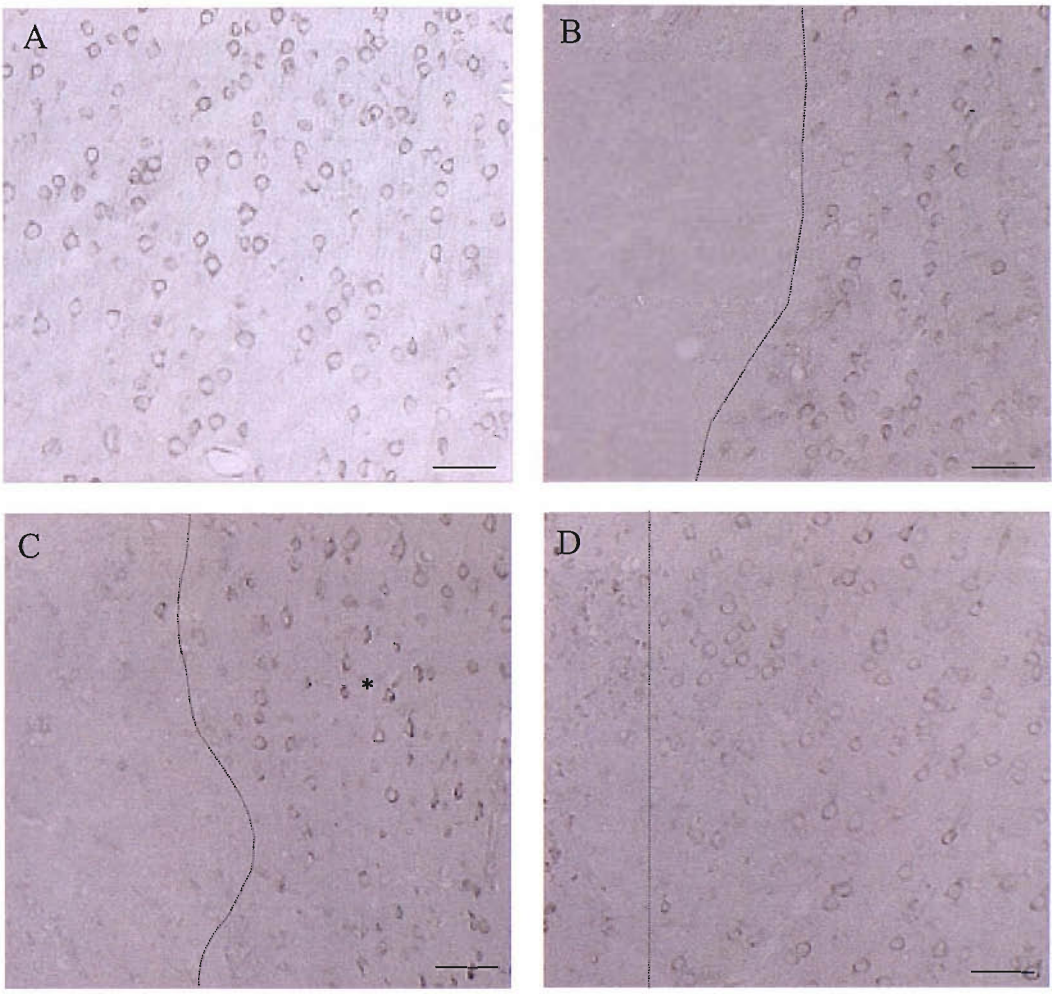

Fig. 5.6 FAK immunostaining of naïve and injured brain fixed in formalin.

Neurons throughout the naïve section (A) show FAK signal. Following injury there is a marked decrease in signal surrounding the injury border at 24hr (B), 3days (C) and 7days (D) post injury. On the basis of cellular morphology it appears that glial cells adjacent to the injury are positive for FAK signal, this is particularly evident at 3days (C;*).

Scale = 50μm

..... = injury border

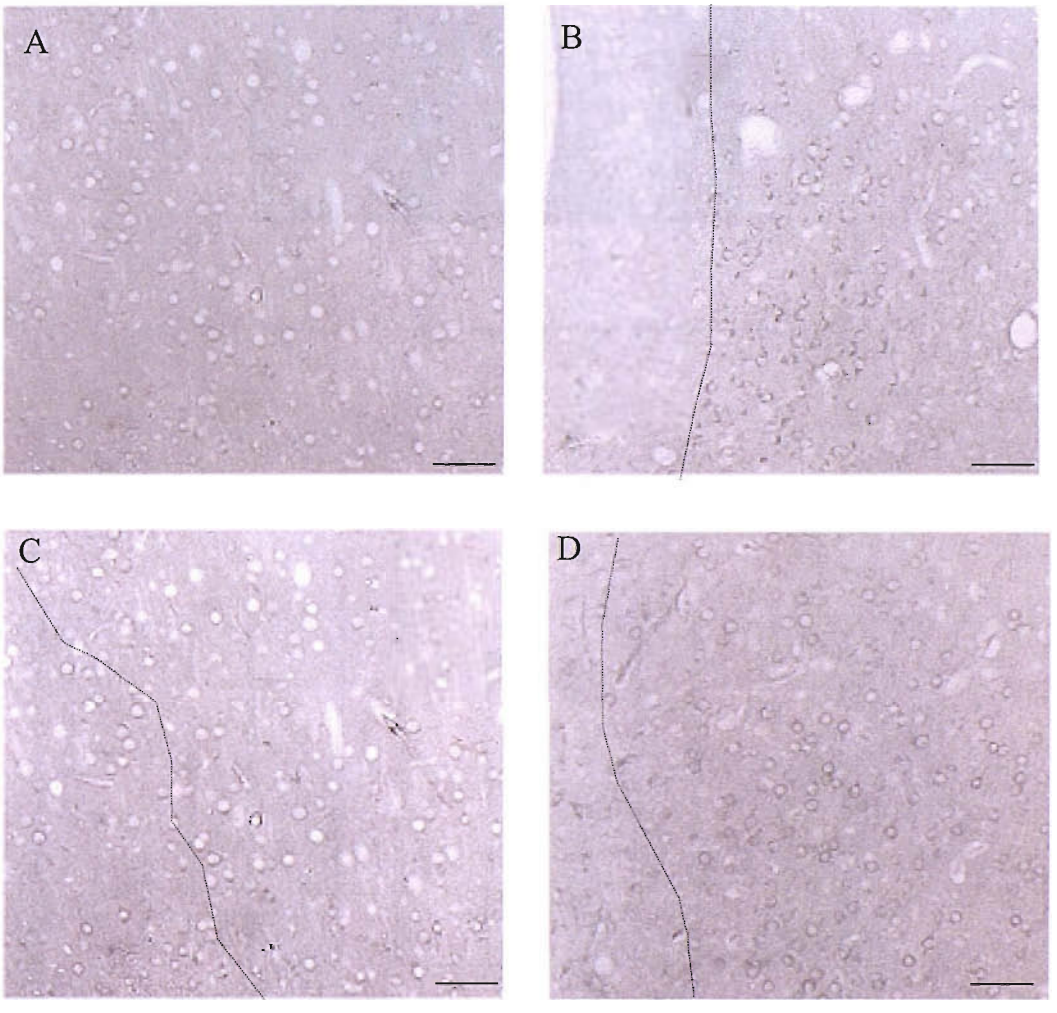

Fig. 5.7 FAK immunostaining of naïve and injured brain fixed in Bouin's. There is little FAK signal in naïve brain (A). 24hrs post intracranial stab lesion (B) there is an increase in FAK positive staining close to the injury boarder. Positive staining is also revealed in tissue 3days (C) and 7days (D) post injury. On the basis of cellular morphology it appears that the cellular signal observd close to the injury border is glial aswell as neuronal.

Scale = 50μm

= injury border

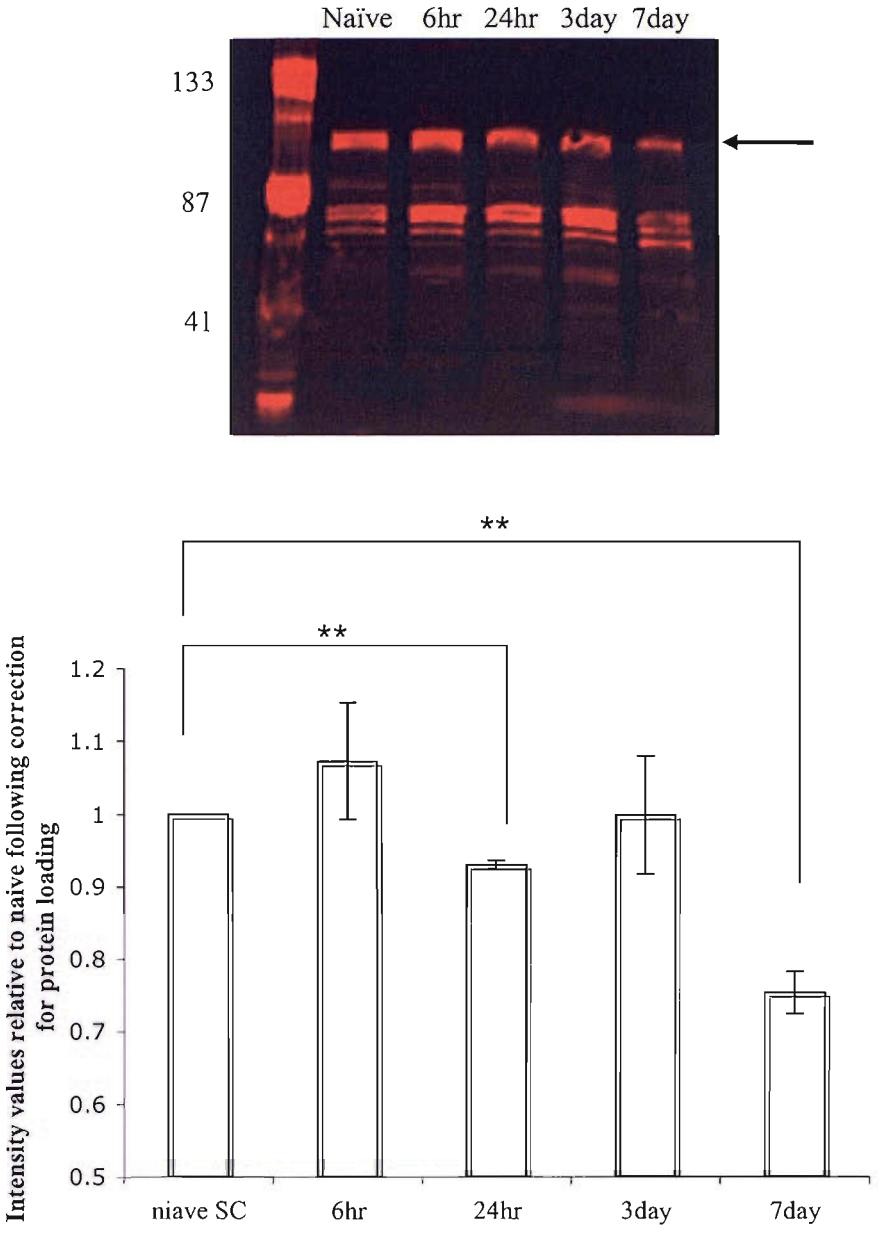

Fig. 5.8 Quantification of the changes in the relative levels of Focal Adhesion Kinase protein expression at a range of timepoints following spinal cord partial transection injury. • • The intensity values, for the FAK bands at 125kDa (arrow), were measured using the Odyssey scanner at the various timepoints post injury and the levels were made relative to naive FAK. These values were then corrected to account for any differences in protein loading (see Chapter 4) and plotted on the graph above.

By 24 hours post injury the levels of FAK expression decreased significantly from naïve by almost 10 percent ($P<0.05$, **). The levels then returned to naïve levels by 3 days post injury. By 7 days post injury the FAK levels declined significantly to around 20 percent of naïve ($P<.0.05$, **).

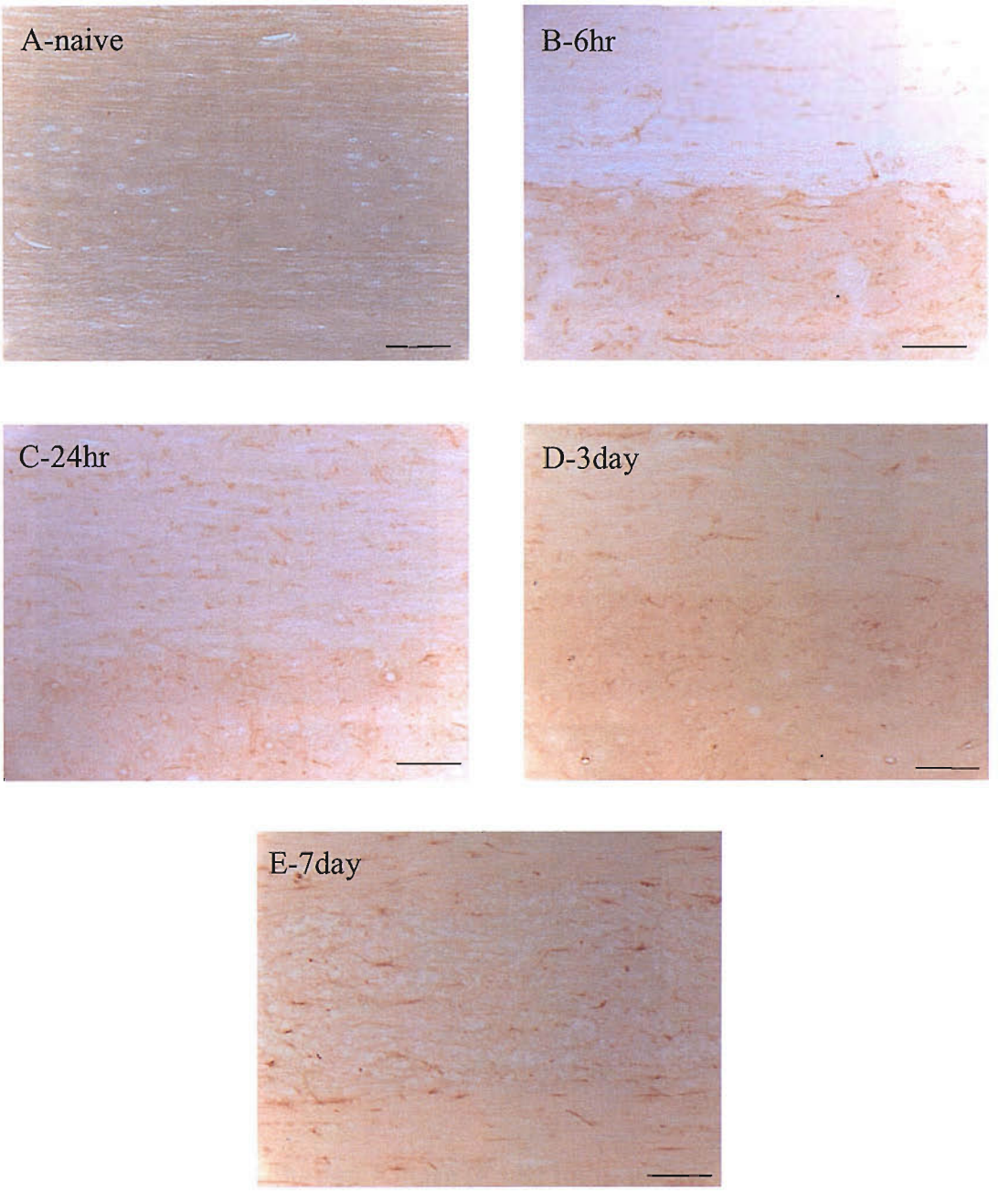

Fig. 5.9 Low power photomicrographs of Focal Adhesion Kinase (FAK) staining following partial spinal cord transection. Following partial spinal cord transection the spinal cord was removed at a number of times post injury and fixed in Bouin's fixative. 10μm thick sections were then stained in order to detect FAK protein within the tissue. By 6hrs post injury (B) there is abundant staining of glia and blood vessels that continues to intensify over the 7day timecourse. Higher power photomicrographs can be viewed in Fig 5.9.

Scale bar = 100μm

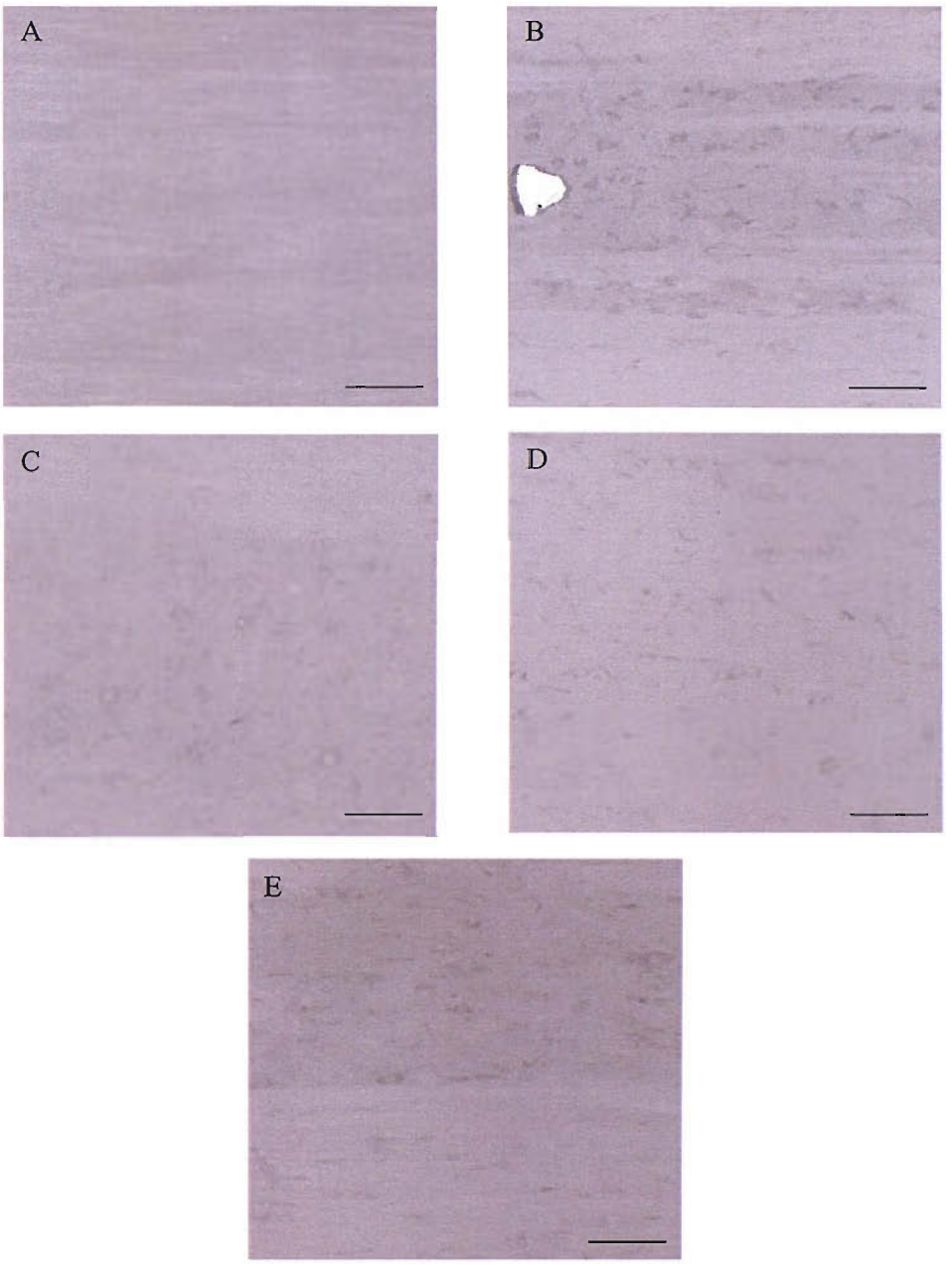

Fig. 5.10 Focal Adhesion Kinase (FAK) immunocytochemistry of naïve and injured spinal cord. Naïve and injured spinal cords, at a number of time points following partial spinal cord transection, were removed and fixed in Bouin's fixative. It is clear from Fig. 5.8 that there was a dramatic change in FAK expression over the 7 day time course. Here we have taken two representative sections at a higher magnification to show the morphology of those cells that become FAK positive.

Naïve tissue (A) show low signal for FAK in some blood vessels with low background signal. By 6hrs (B) post injury, there is abundant signal, which on the basis of morphology appears to be expressed in glial cells and blood vessels. A similar signal was observed throughout the time course (24hr: C; 3day: D), although the staining became most intense by 7days post injury (E).

Scale = 50μm

Fig. 5.11 Co-expression of FAK and CC1, an oligodendrocyte marker, at different timepoints following partial spinal cord transection. Naïve and injured spinal cord tissue was stained by immunofluorescence to visualise both FAK (red) and CC1 (green) to determine whether FAK is expressed in oligodendrocytes following injury.

Naïve spinal cord showed no co-expression of FAK in oligodendrocytes (A-C). However, following injury there was clear co-expression at all timepoints studied (D-O).

D-F: 6hr post injury (p.i), G-I: 24hr p.i, J-L: 3day p.i and M-O: 7day p.i.

Scale bar = 10um

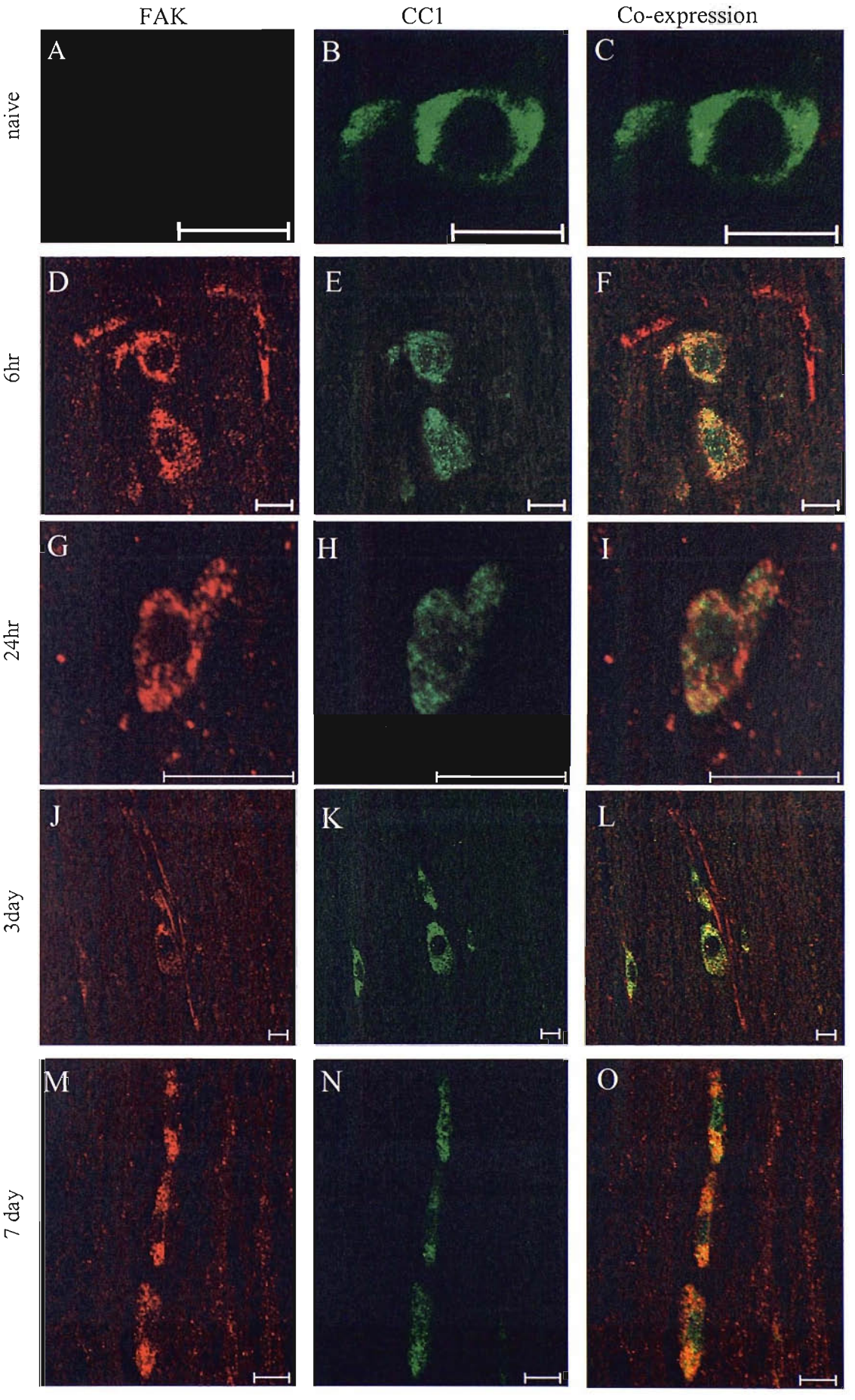

Fig. 5.11 FAK (red) and CC1, oligodendrocyte (green) co-expression

Fig. 5.12 Co-expression of FAK and GFAP, an astrocyte marker, at different timepoints following partial spinal cord transection. Anti-GFAP antibody (green), which is an intermediate filament located in astrocytes, was used in a double immunofluorescence experiment with an anti-FAK antibody (red) to determine whether FAK is present in naïve and/or injured astrocytes.

Naïve spinal cord (A-C) and spinal cord 6hr (D-F) and 24hr (G-I) post injury did not show any co-expression of FAK with GFAP. Co-expression was observed in the tissue taken both 3days (J-L) and 7days (M-O) post injury.

Scale = 50μm

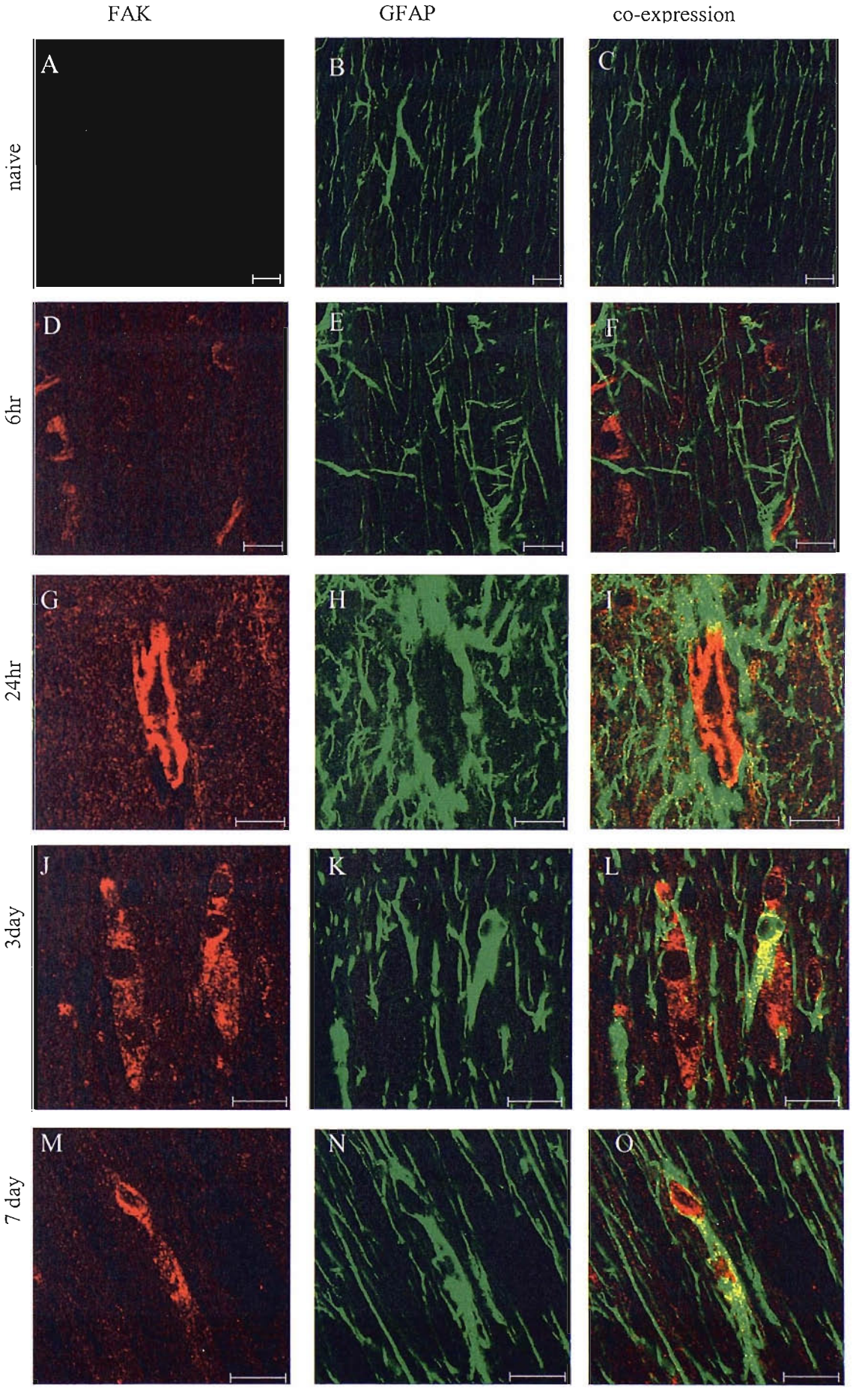

Fig. 5.12 FAK and GFAP Co-expression in naïve and injured spinal cord.

Fig. 5.13 FAK and Neurofilament co-expression in spinal cord tissue. NF-H (green), an anti-neurofilament antibody that is used to detect axons, was used in conjunction with an anti-FAK antibody (red) to determine if FAK is expressed in axons in naïve and/or injured spinal cord.

Co-expression was not observed in naïve spinal cord or at any timepoint post injury.

A-C: naïve, D-F: 6hr post injury (p.i), G-I: 24hr p.i, J-L: 3day p.i and M-O: 7day p.i.

Scale = 50μm

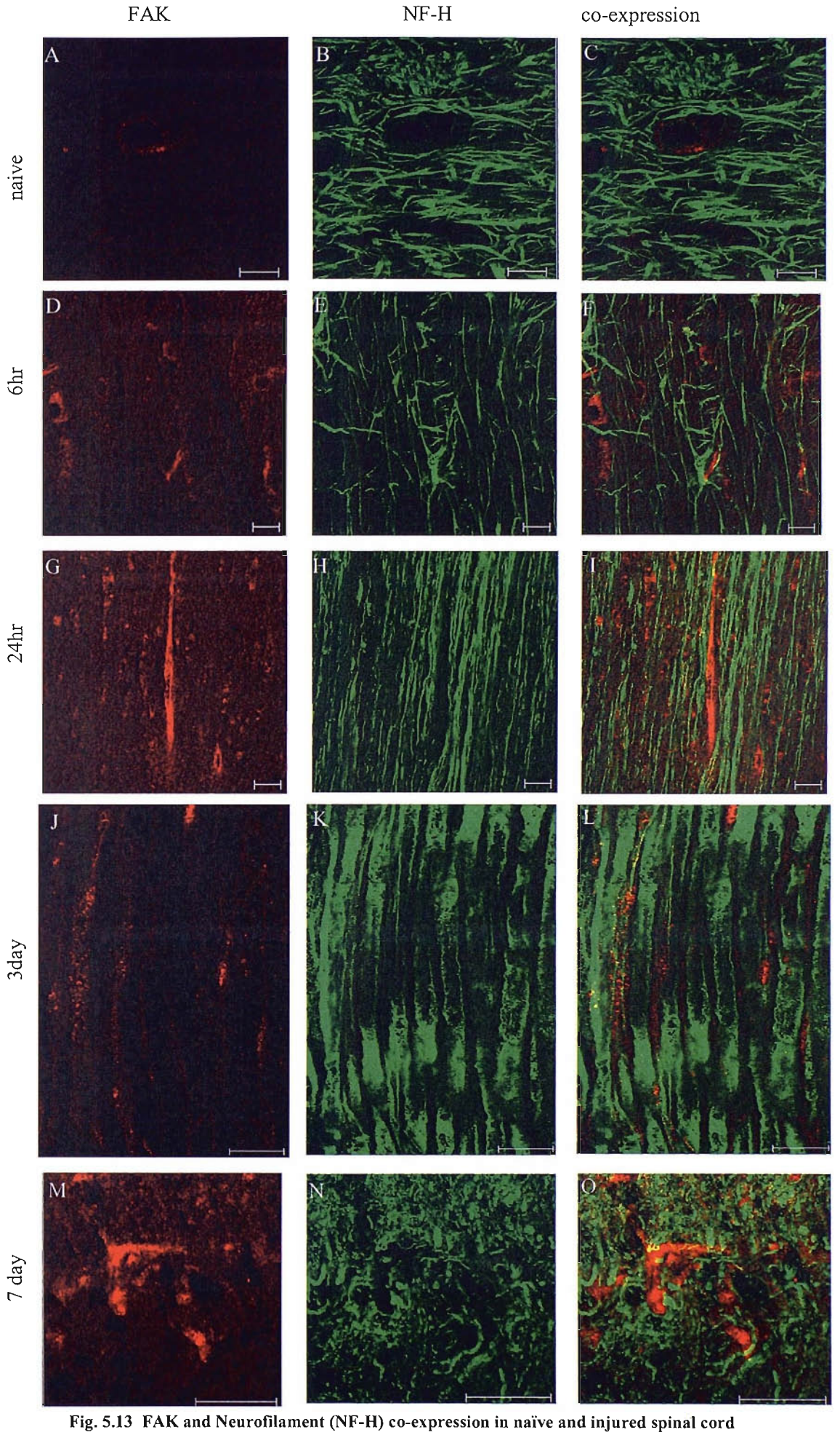

Fig. 5.13 FAK and Neurofilament (NF-H) co-expression in naïve and injured spinal cord

Fig. 5.14 FAK and NeuN co-expression in spinal cord tissue. To determine if FAK is located in neuronal cell bodies an anti-NeuN antibody was used together with an anti-FAK antibody to identify any co-expression.

Limited co-expression was observed at 3days (J-L) and 7days (M-O) post spinal cord injury. No co-expression was observed in naïve (A-C), 6hr (D-F) or 24hr (G-I) tissue.

Scale = 20μm

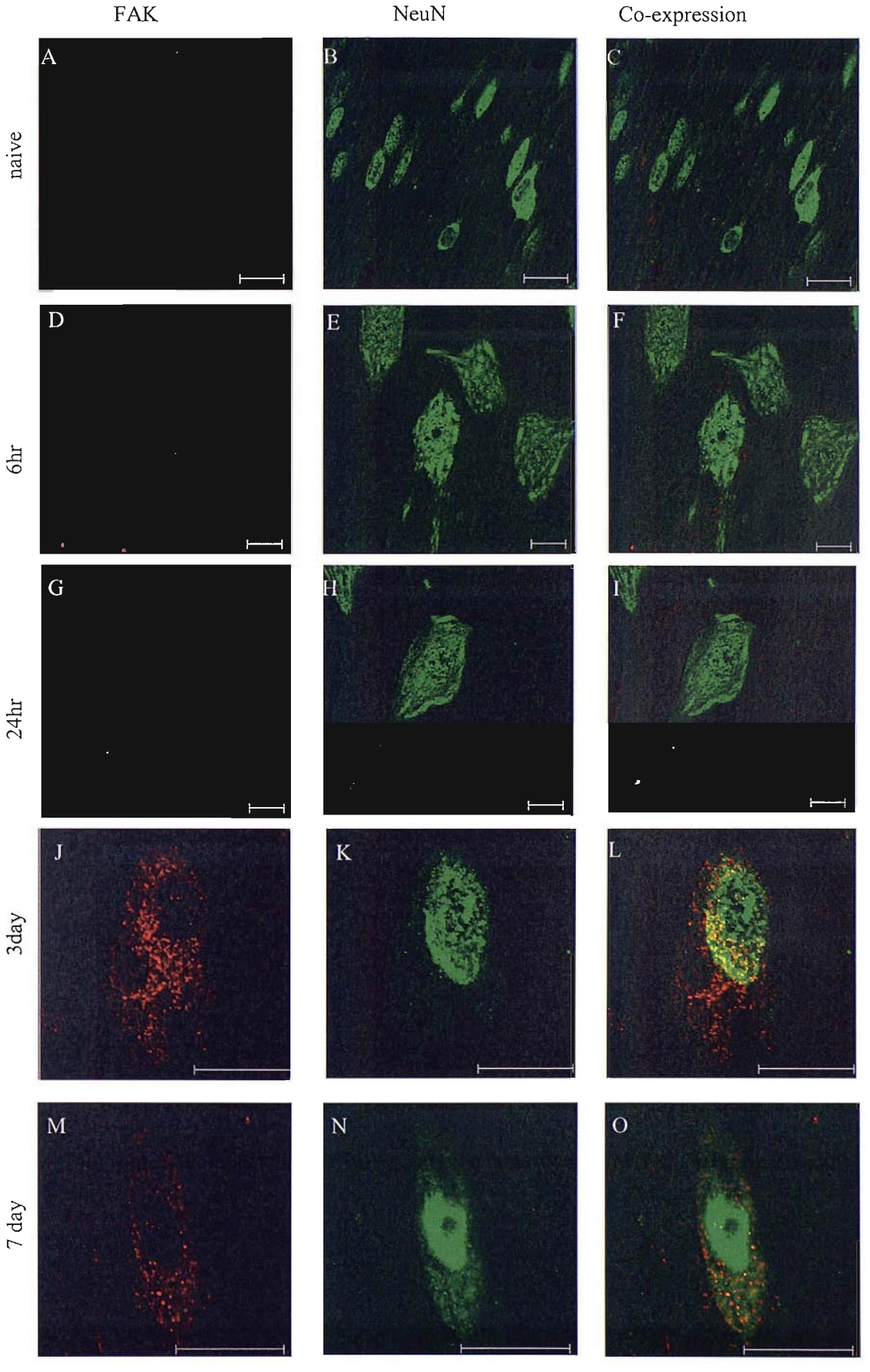

Fig. 5.14 FAK and NeuN co-expression in naïve and injured spinal cord tissue

Fig. 5.15 FAK and tomato lectin co-expression in spinal cord tissue. Tomato lectin (green) was used with an anti-FAK antibody (red) to determine whether FAK is expressed in blood vessels in spinal cord tissue, both naïve and following injury.

Co-expression was observed in naïve and injured spinal cord tissue in all sections studied.

A-C: naïve, D-F: 6hr post injury (p.i), G-I: 24hr p.i, J-L: 3day p.i and M-O: 7day p.i.

Scale = 10μm

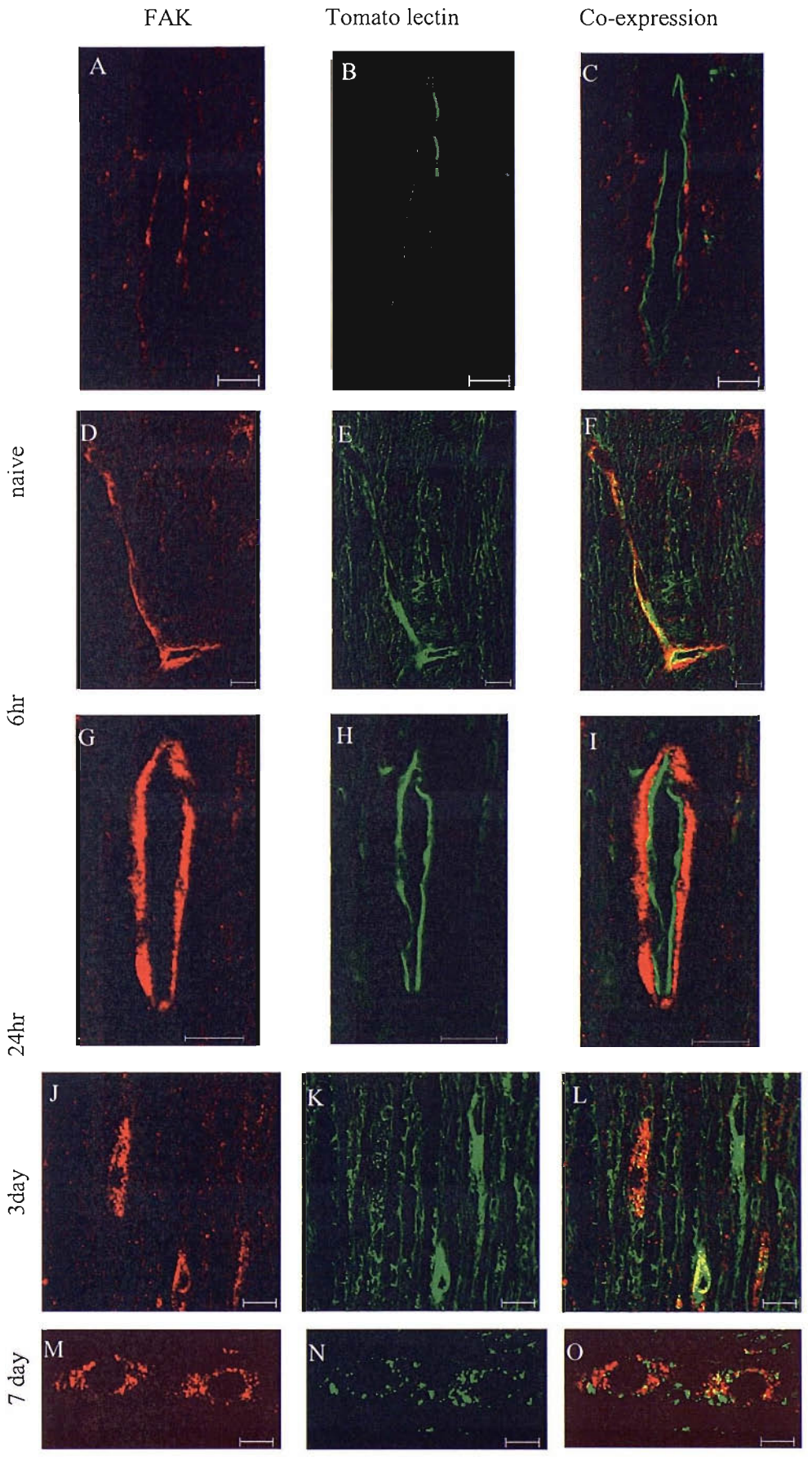

Fig. 5.15 Co-expression of FAK and tomato lectin in spinal cord tissue, naïve and following injury.

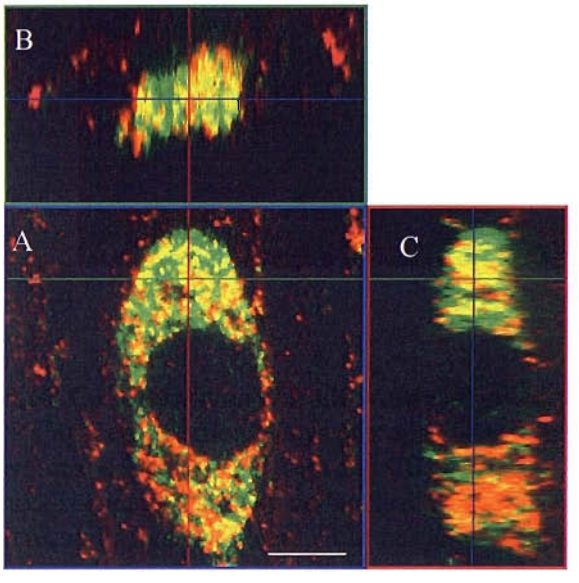

Fig. 5.16 Co-localisation of FAK within oligodendrocytes. Confocal image from a spinal cord section, 3days post spinal cord partial transection, double stained for the FAK protein (red) and CC1, a marker of oligodendrocytes (green). The image A shows co-localisation of the red and green signals some of which result in a yellow colour. The image was studied using the Zeiss LSM V Image Examiner software, which shows that the FAK signal and the CC1 signal are within the same structure, i.e. in the oligodendrocyte. B and C show orthogonal view of the staining at the levels of the red (B) and green (C) lines.

Scale = 5μm

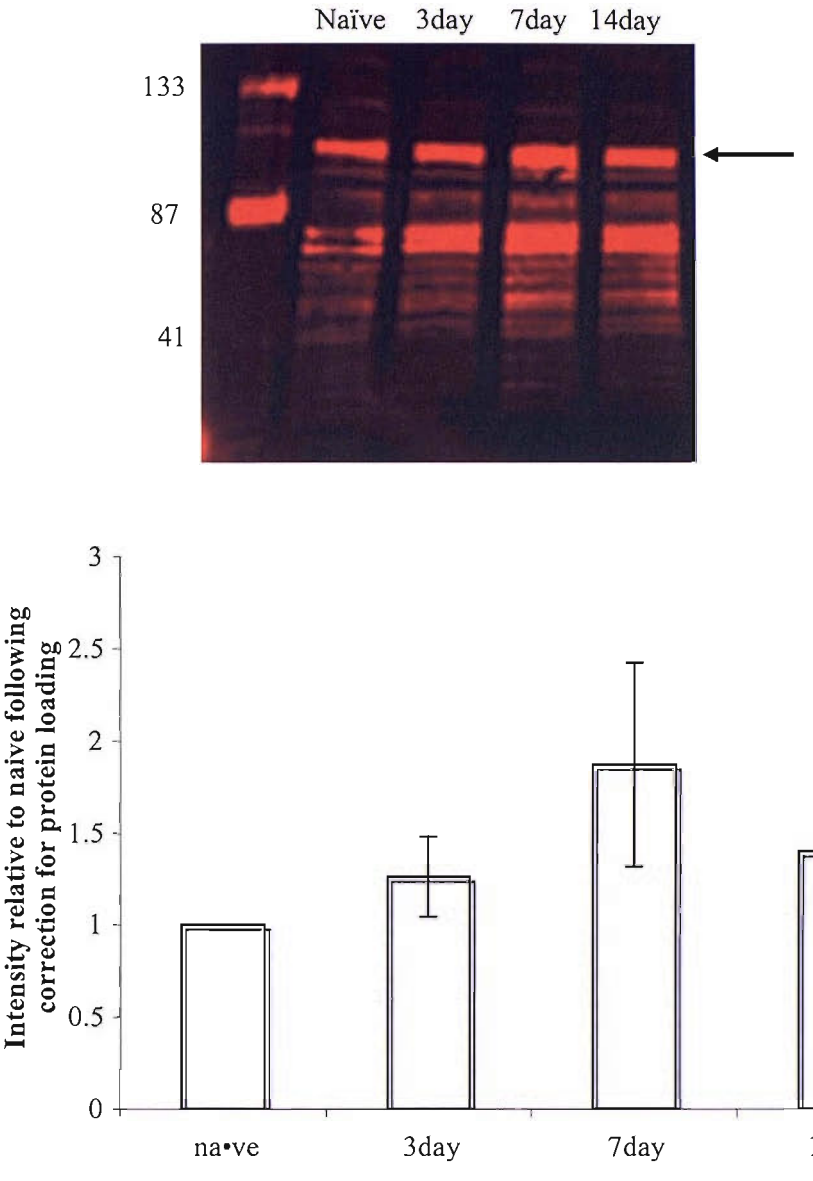

Fig. 5.17 Changes in Focal Adhesion Kinase expression in the distal portion of the optic nerve following optic nerve transection. Changes in expression of FAK (arrow) were measured at a number of timepoints post optic nerve transection in the distal portion of the optic nerve, i.e the portion containing axons disconnected from the cell body. The intensity values relative to naïve and corrected for protein loading (see Chapter 4) have been plotted on the above graph.

Following optic nerve transection the levels of FAK appear to increase over the first three days followed by a decrease tending towards naïve levels by day 7 post injury, however, none of these values are significant.

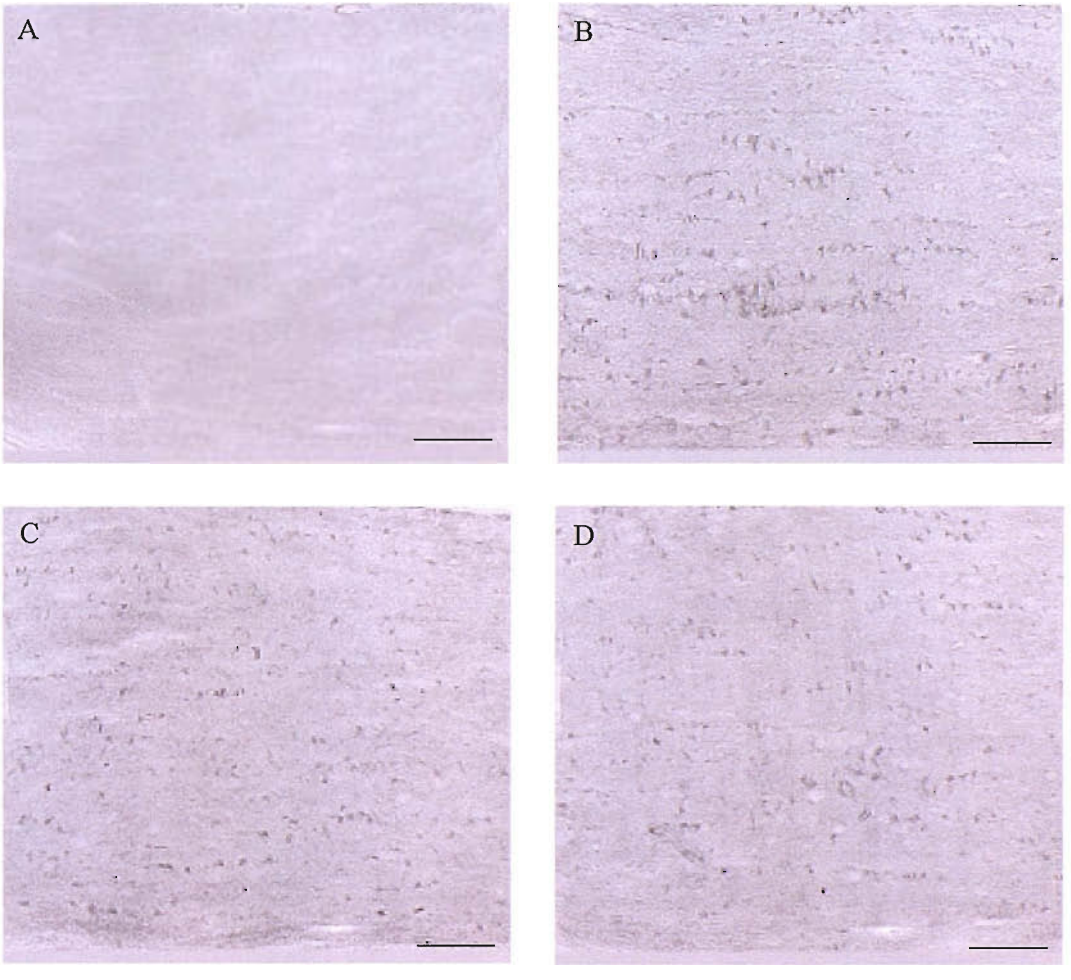

Fig. 5.18 FAK immunoreactivity in optic nerve distal to a transection injury. The optic nerve was transected 2mm behind the eye, tissue was removed either 3, 7 or 14days post injury. Immunocytochemistry was then used to identify FAK protein in the distal portion of the optic nerve.

Naïve optic nerve (A) revealed a low level of background signal. Following injury cellular signal was revealed throughout the distal optic nerve, i.e the portion of optic nerve disconnected from the cell body. FAK signal was observed at 3day (B), 7day (C) and 14days (D) post injury.

Scale = 50μm

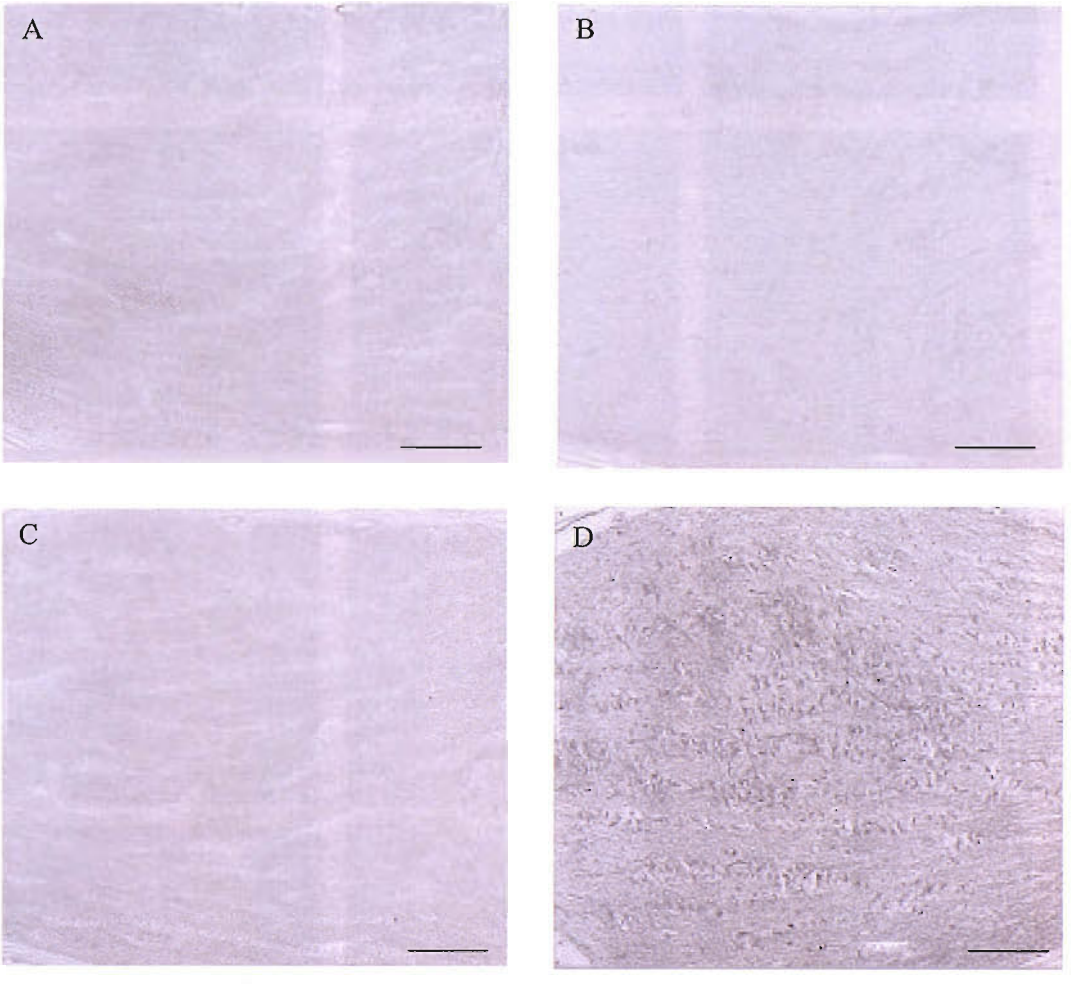

Fig. 5.19 FAK immunoreactivity in the proximal optic nerve following transection injury. Optic nerve was transected 2mm behind the eye and tissue was taken 3, 7 or 14days post injury. The proximal segments were then stained for the FAK protein to identify whether there are any changes in expression of FAK post injury.

Naïve optic nerve (A) revealed a low level of background staining. Following injury little change, compared to naïve, was observed by 3day (B) or 7days (C). However, by 14days post injury (D) cellular staining was revealed.

Scale = 50μm

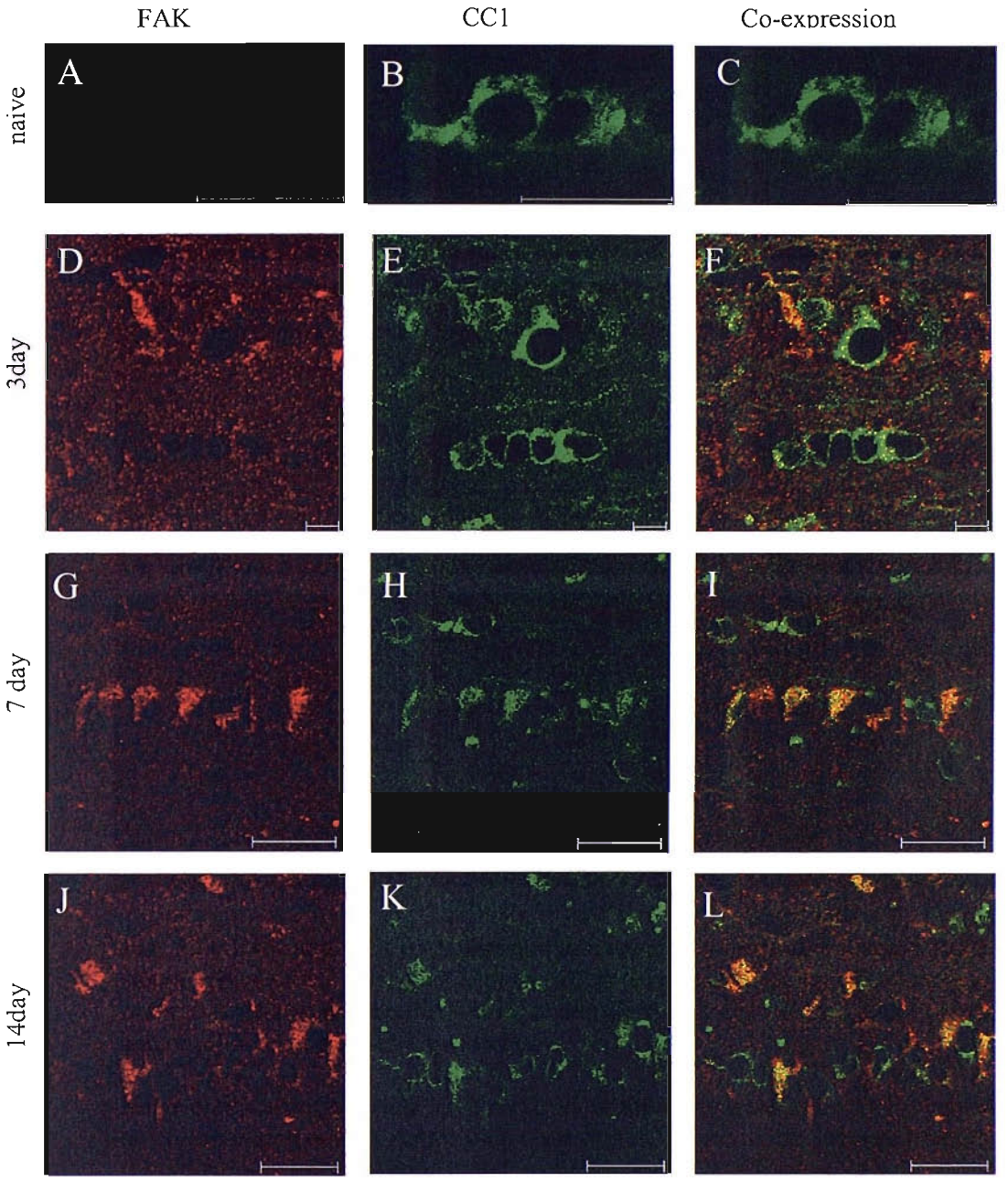

Fig. 5.20 FAK and CC1 co-expression in transected optic nerve distal from the site of injury. FAK (red) and CC1 (green), an oligodendrocyte marker, were used in order to determine whether FAK is located in oligodendrocytes in naïve optic nerve and/or following optic nerve transection.

Naïve optic nerve (A-C) and optic nerve 3days following transection (D-F) showed no co-expression of FAK within oligodendrocytes. However, by 7days post injury (G-I) there was abundant co-expression of FAK and CC1 indicating a FAK expression within oligodendrocytes following injury. Co-expression was also evident in tissue 14 days post injury (J-L).
Scale = 20um

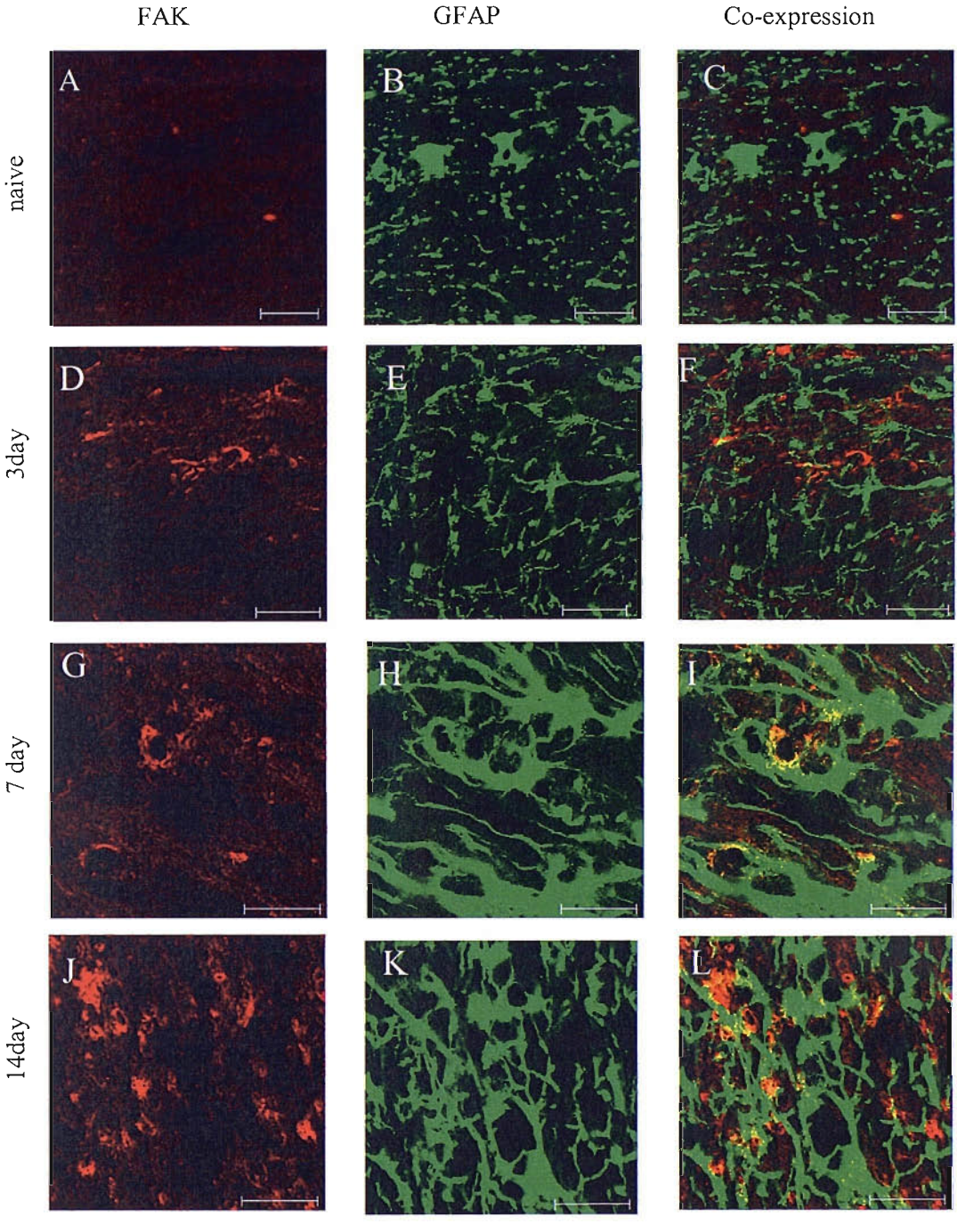

Fig. 5.21 FAK and GFAP co-expression in optic nerve distal to a transected injury. FAK (shown in red) and GFAP (shown in green), an astrocytic marker, were used to determine whether FAK is expressed in astrocytes before and/or after optic nerve transection.

There was no co-expression of FAK with GFAP in naïve or injured optic nerve.

A-C: naïve, D-F: 6hr post injury (p.i), G-I: 24hr p.i, J-L: 3day p.i and M-O: 7day p.i.

Scale 20um

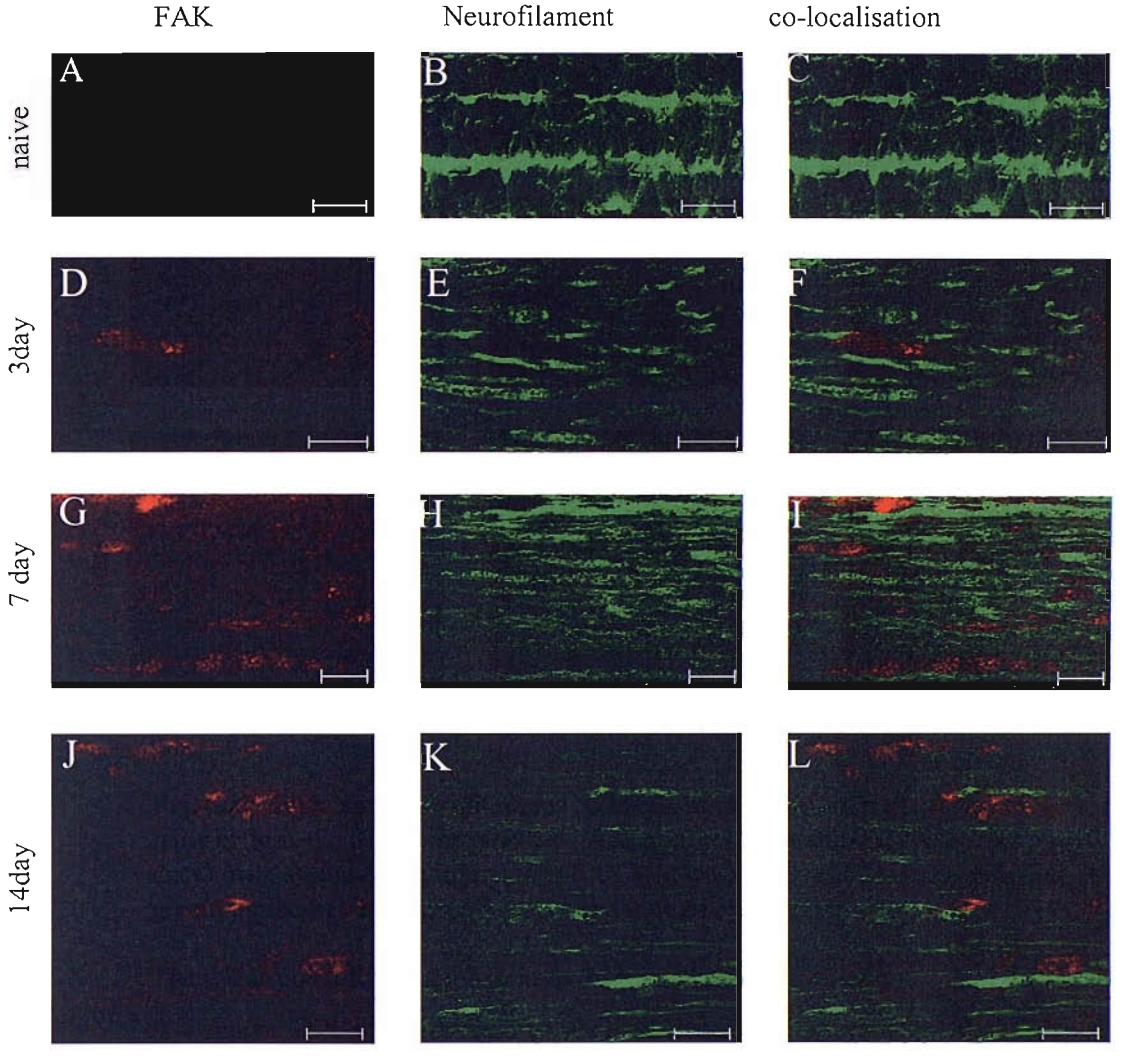

Fig. 5.22 FAK and neurofilament co-localisation in optic nerve distal to optic nerve transection. To determine whether FAK is expressed within axons, in optic nerve tissue distal from a transection injury, anti-FAK (shown in red) and anti-neurofilament (shown in green) antibodies were used in naïve and injured optic nerve.

There was no co-localisation in naïve or injured samples studied.

A-C: naïve, D-F: 6hr post injury (p.i), G-I: 24hr p.i, J-L: 3day p.i and M-O: 7day p.i.

Scale = 20um

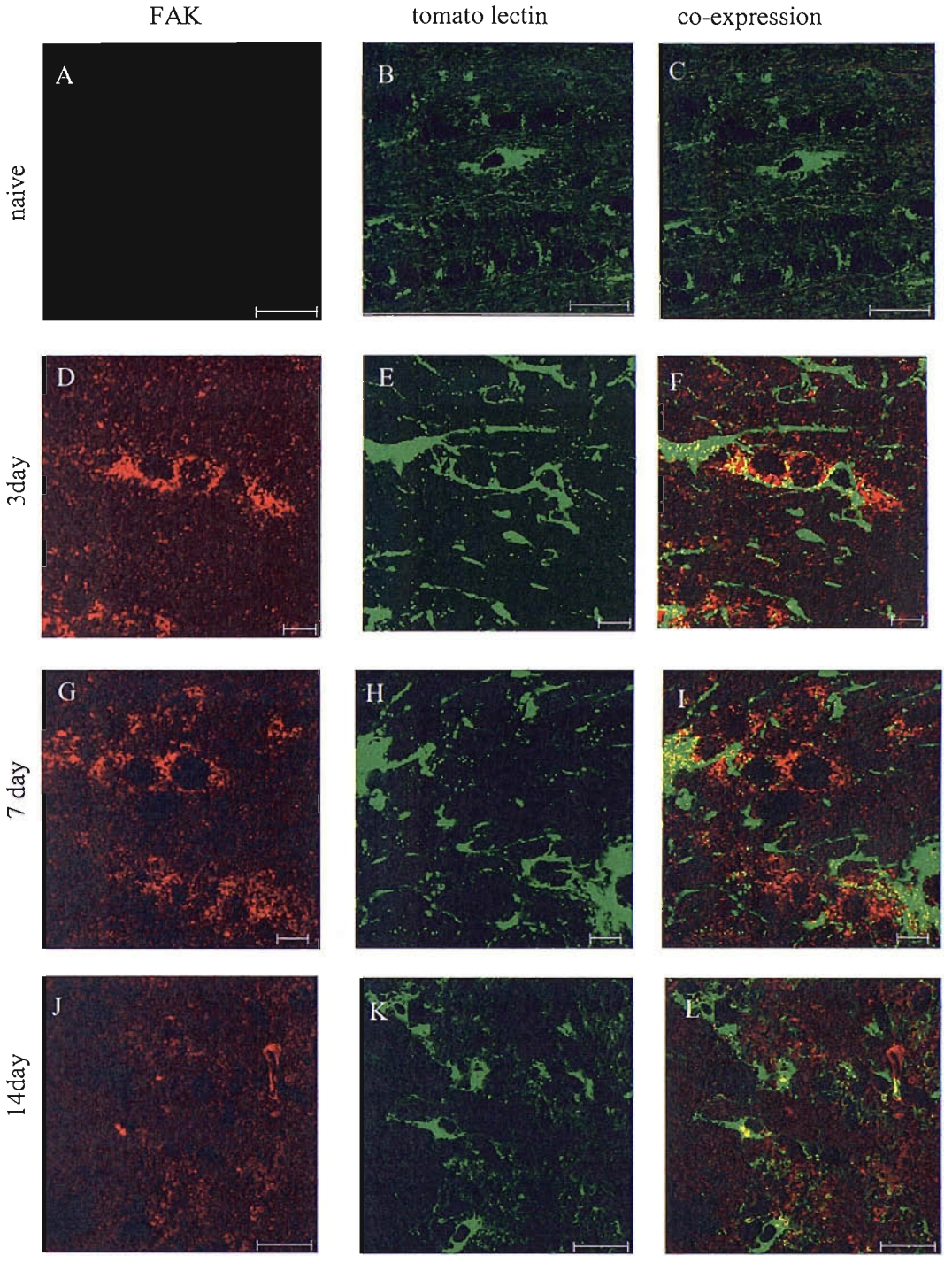

Fig. 5.23 Co-expression of FAK and tomato lectin in optic nerve distal from a transection injury. Naïve and injured optic nerve were stained for FAK (shown in red) and tomato letin (shown in green) to determine whether FAK is expressed in microglia and/or blood vessels following optic nerve transection.

There was no co-expression until 14days post injury (J-L) where, from the morphology, it appears that FAK is within microglia.

A-C: naïve, D-F: 3day post injury (p.i), G-I: 7day p.i, J-L: 14day p.i

Scale 20um

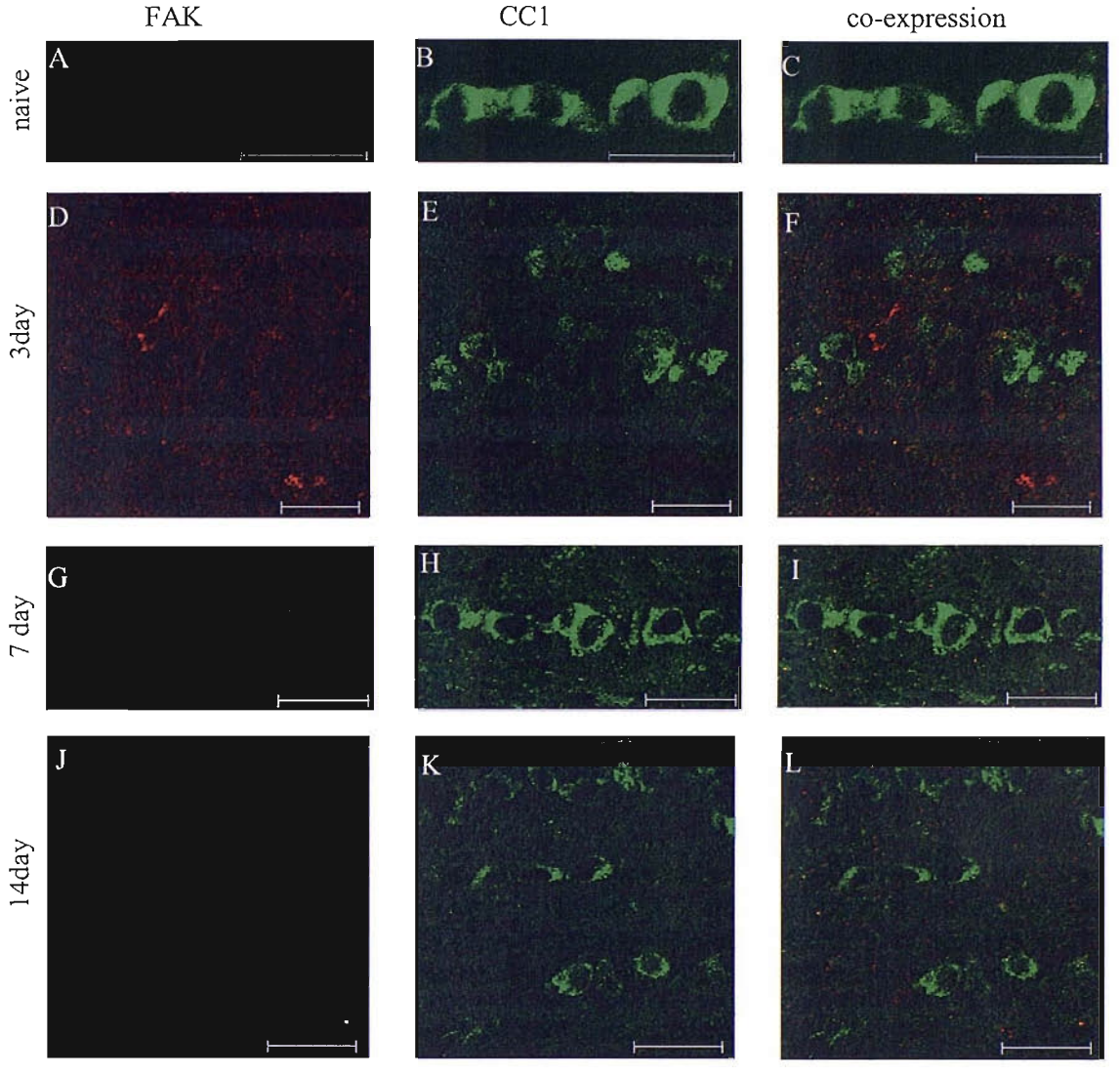

Fig. 5.24 FAK and CC1 (an oligodendrocyte marker) co-expression in optic nerve, proximal to a transection injury. An anti-CC1 antibody (shown in green) was used with an anti-FAK antibody (shown in red) to determine whether FAK was expressed in oligodendrocytes, in the proximal optic nerve, following optic nerve transection.

No co-expression was observed in any tissue studied.

A-C: naïve, D-F: 3day post injury (p.i), G-I: 7day p.i, J-L: 14day p.i.

Scale 20um

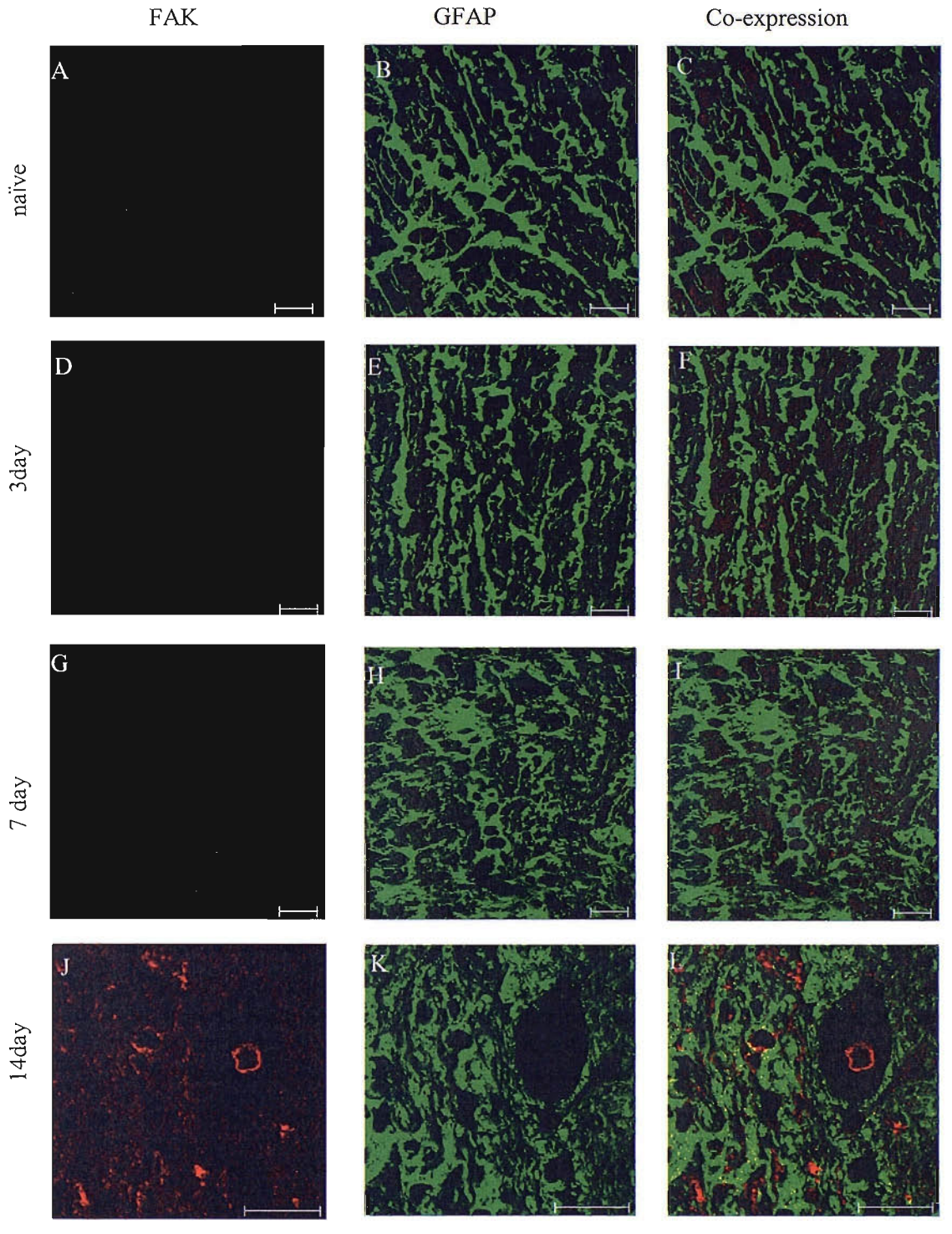

Fig. 5.25 Co-expression of FAK and GFAP in optic nerve, proximal to the site of injury. An anti-GFAP antibody (shown in green) was used together with an anti-FAK antibody to determine whether FAK is expressed in astrocytes in naïve and injured optic nerve (proximal to the site of optic nerve transection).

There was no co-expression of GFAP and FAK at any timepoint studied.

A-C: naïve, D-F: 3day post injury (p.i), G-I: 7day p.i, J-L: 14day p.i.

Scale = 20um

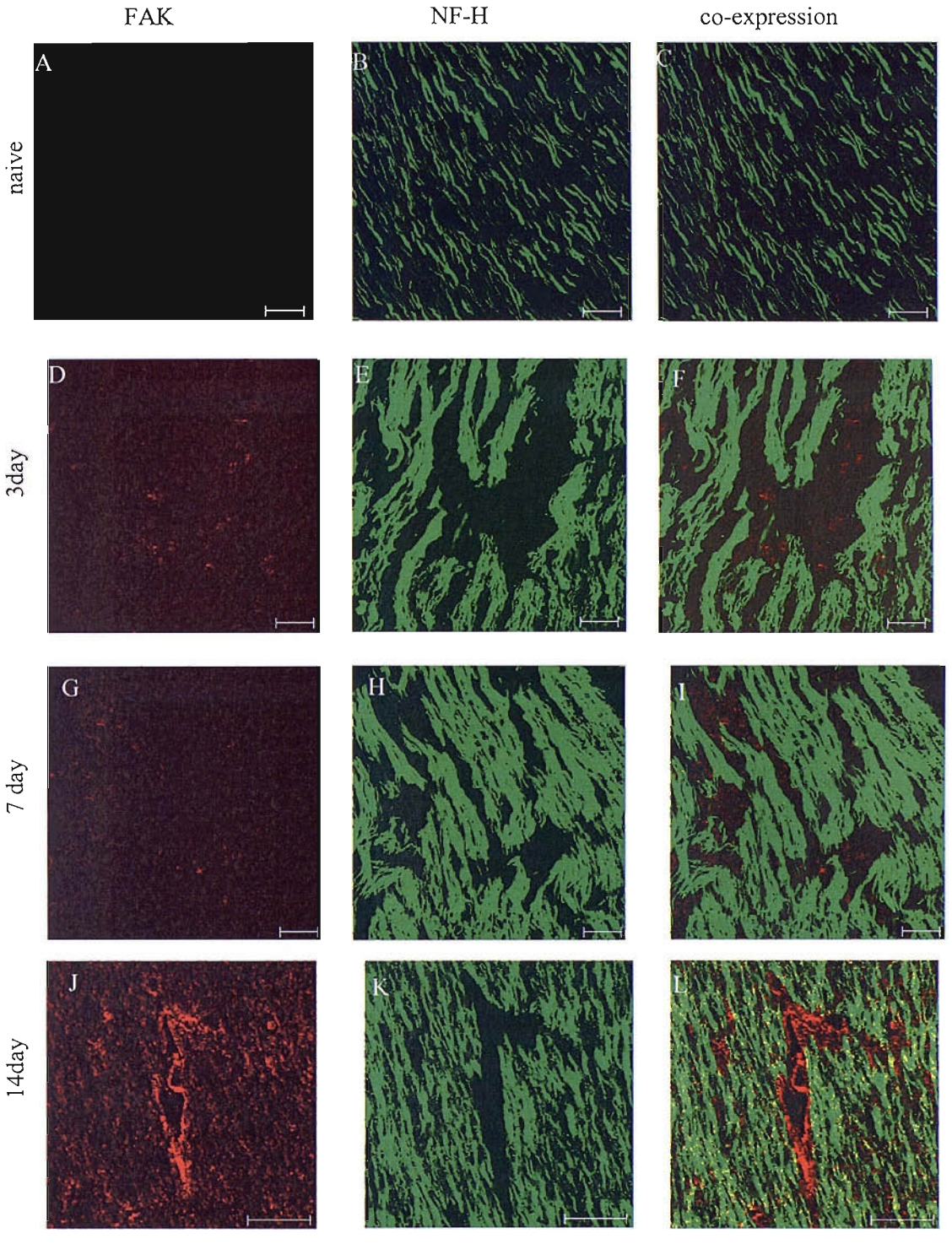

Fig. 5.26 FAK and neurofilament (NF-H) co-expression in optic nerve proximal to the site of optic nerve transection. To determine whether FAK (shown in red) was expressed in axons in naïve and/or injured optic nerve (proximal to a transection injury) an anti-neurofilament antibody (shown in green) was used to reveal axons.

No co-expression was observed in naïve or at any timepoint following optic nerve injury.

A-C: naïve, D-F: 3day post injury (p.i), G-I: 7day p.i, J-L: 14day p.i.

Scale 20um

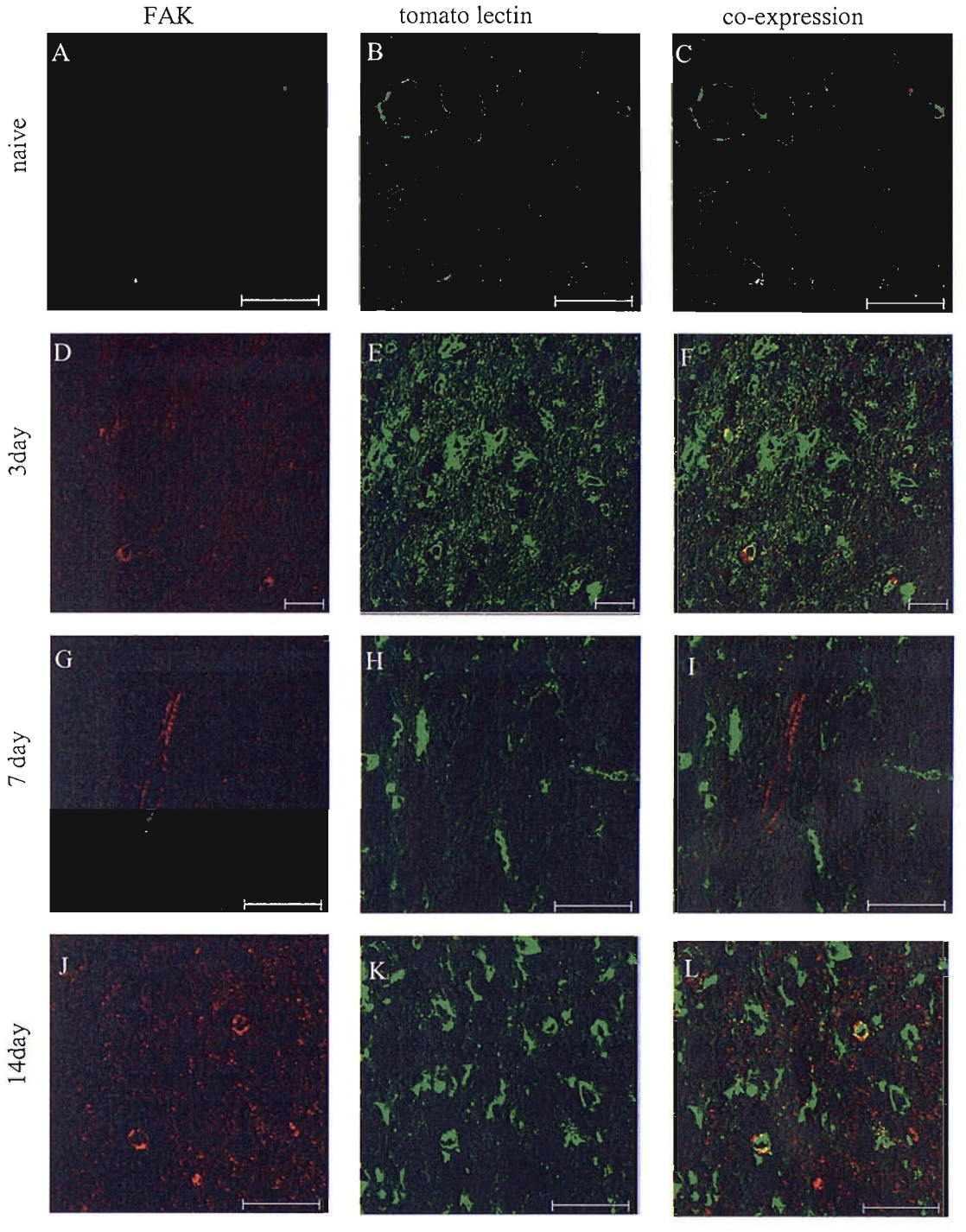

Fig. 5.27 Co-expression of FAK and tomato lectin in optic nerve proximal from the site of injury. Naïve and transected optic nerve, proximal from the site of injury (i.e. still connected to the cell body), were immunostained for FAK (shown in red) and tomato lectin (shown in green). This was to determine whether FAK expression changes in blood vessels and/or microglia following optic nerve transection.

Co-expression was not observed until 14days post injury (J-L).

A-C: naïve, D-F: 3day post injury (p.i), G-I: 7day p.i, J-L: 14day p.i.

Scale 20um

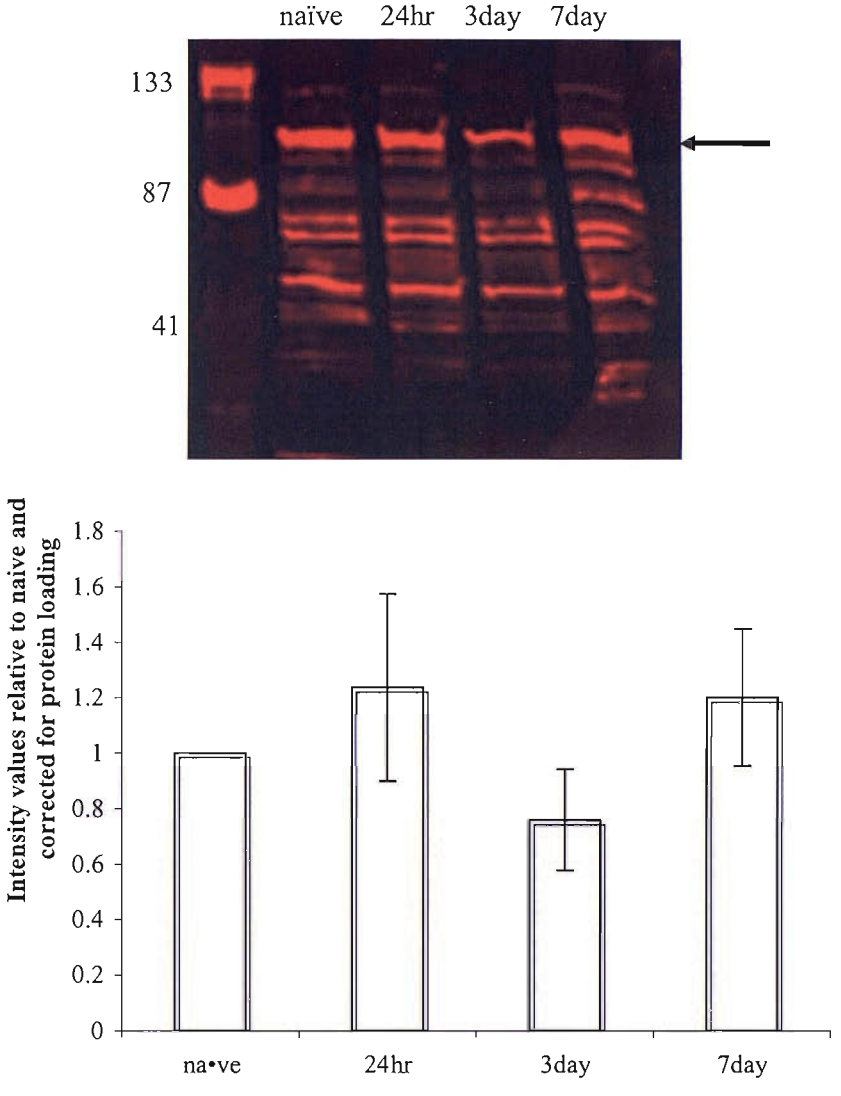

Fig. 5.28 Quantification of changes in Focal Adhesion Kinase levels in the retina following optic nerve transection. Following optic nerve transection, at a range of timepoints post injury, the retina was removed for analysis of FAK protein levels by Western blotting. The intensity values relative to naïve and corrected for protein loading have been plotted against the timecourse in the above graph.

There appears to be a biphasic change in FAK expression levels (arrow), following optic nerve transection, in the retina. By 24 hours post injury FAK expression increases by 24 percent compared to naïve, levels then decrease by 24 percent compared to naïve at 3 days post injury. The levels of FAK then increase again by 20 percent (compared to naïve) by day 7. These changes are not significantly different from naïve.

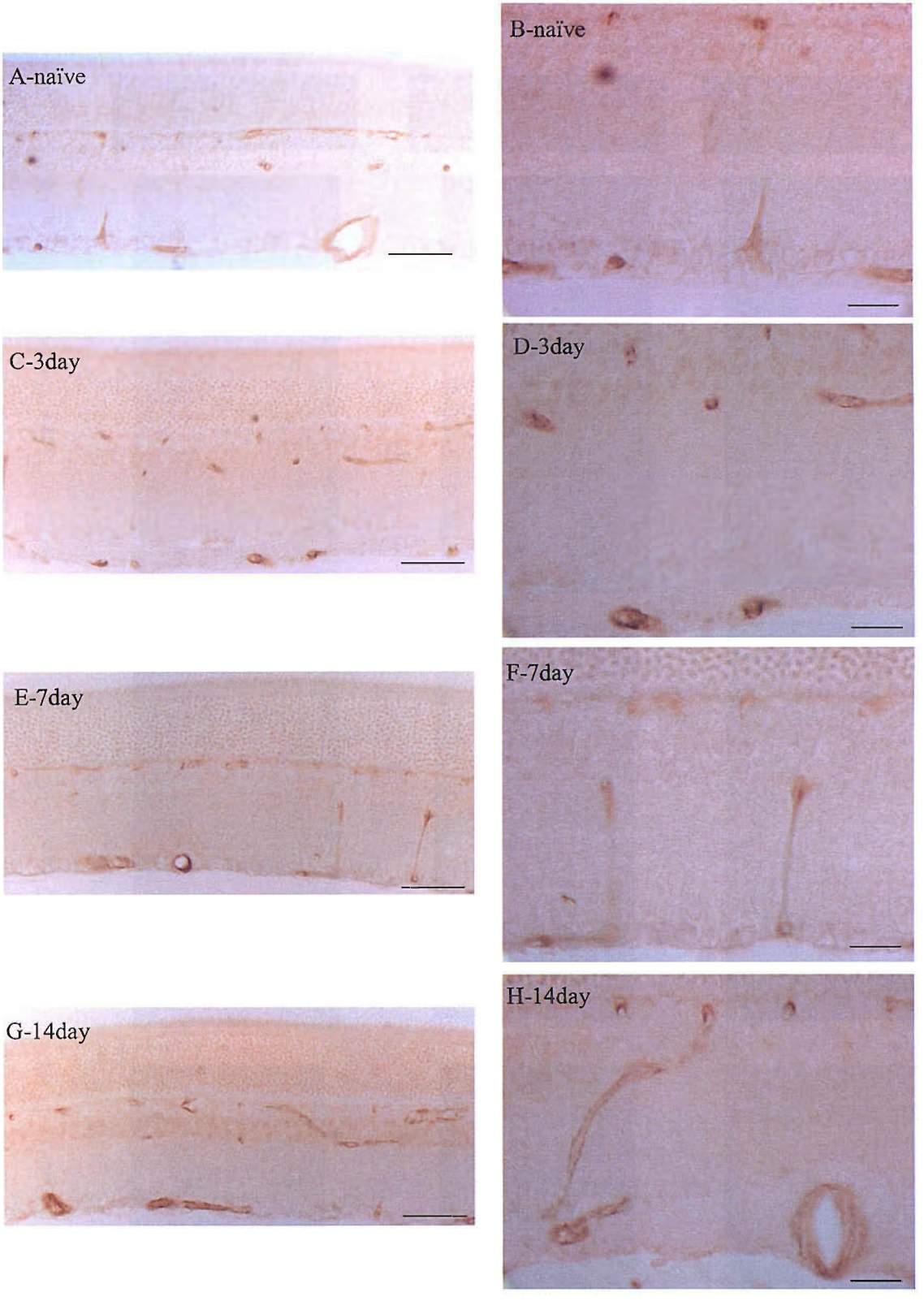

Fig. 5.29 FAK immunostaining in retinal tissue, naïve and following optic nerve transection. Naïve retina and retina from rats that had undegone an optic nerve transection injury were stained to reveal the expression patterns of FAK.

The main differences observed between naïve and injured retina was the increase in blood vessel staining following optic nerve injury in sections from 7day (E and F) and 14days (G and H) post injury.

A and B: naïve; C and D: 3day post injury (p.i.); E and F: 7day p.i.; G and H: 14day p.i.

Scale = 10um

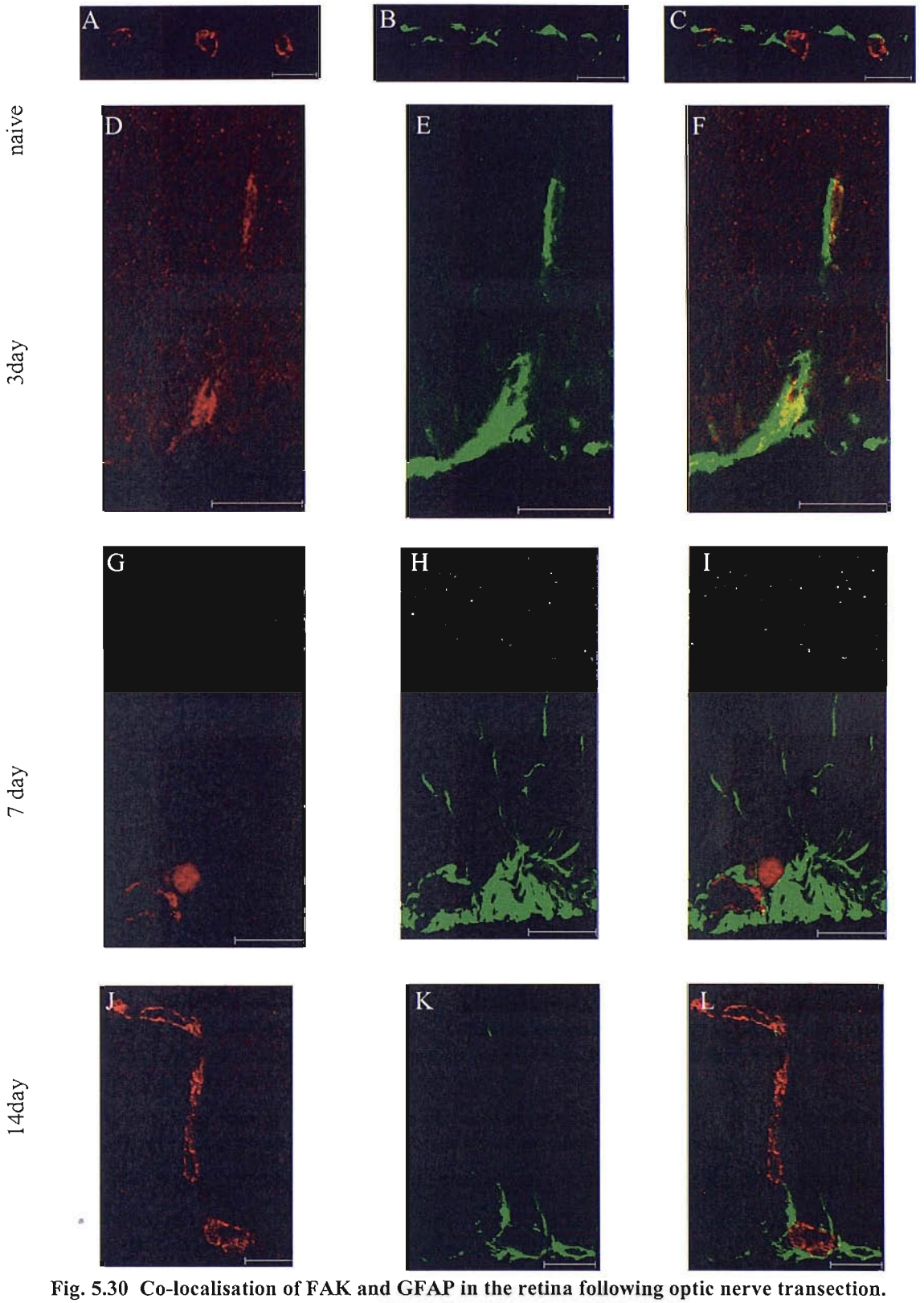

Fig. 5.30 Co-localisation of FAK and GFAP in the retina following optic nerve transection. An anti-GFAP antibody was used together with FAK to determine whether FAK is present within Muller cells in both naïve and injured retina.

Limited co-localisation (yellow) was observed in retina 3days following optic nerve transection (D-F). There was no other co-localisation observed in naïve or injured retina.

A-C: naïve, D-F: 3day post optic nerve transection, G-I: 7days post injury, J-L: 14days post-injury.

Scale = 20um

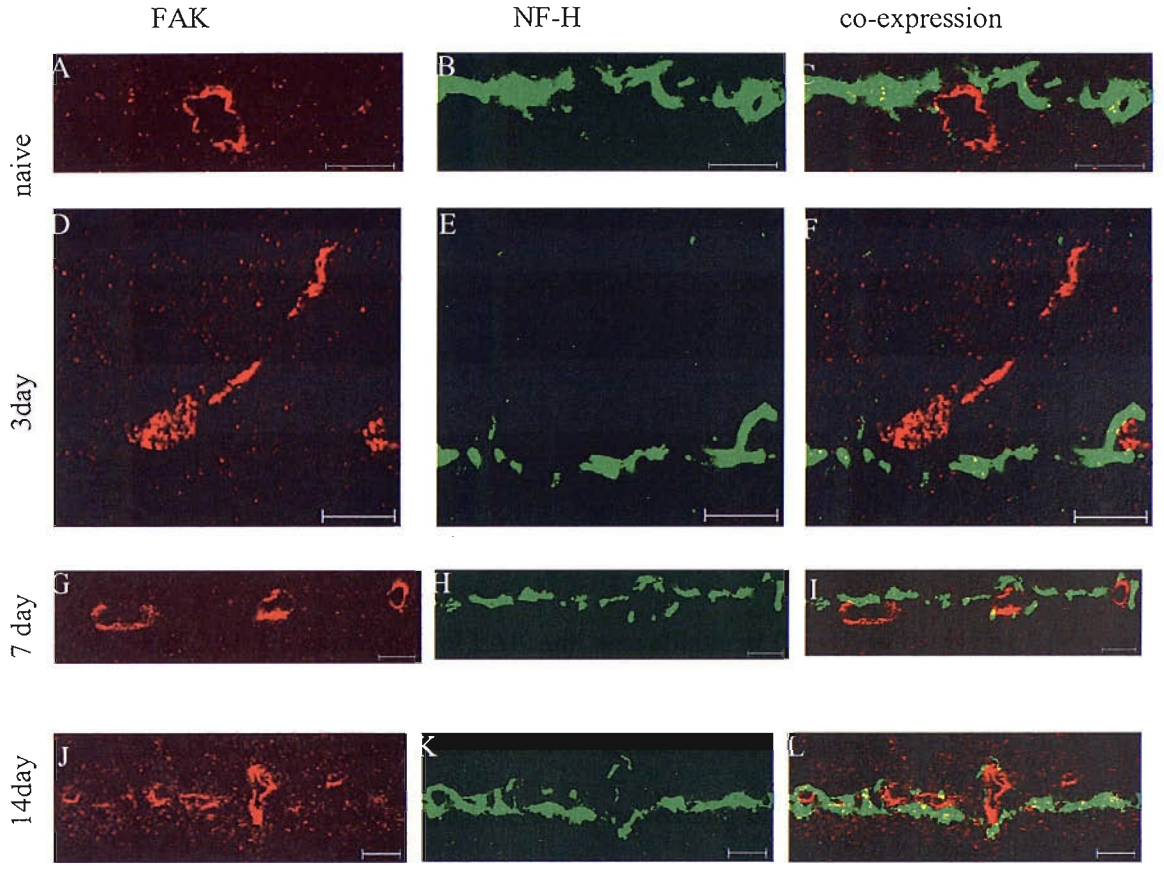

Fig. 5.31 Co-expression of FAK and neurofilament (NF-H) in the retina following optic nerve transection. To determine whether FAK was expressed in axons, either in naïve retina or retina following an optic nerve transection injury, FAK (shown in red) and NF-H (shown in green) were used to look for any co-expression.

There was no co-expression observed in naïve retina or at any timepoint post injury.

A-C: naïve, D-F: 3day post injury (p.i), G-I: 7day p.i, J-L: 14day p.i

Scale 10um

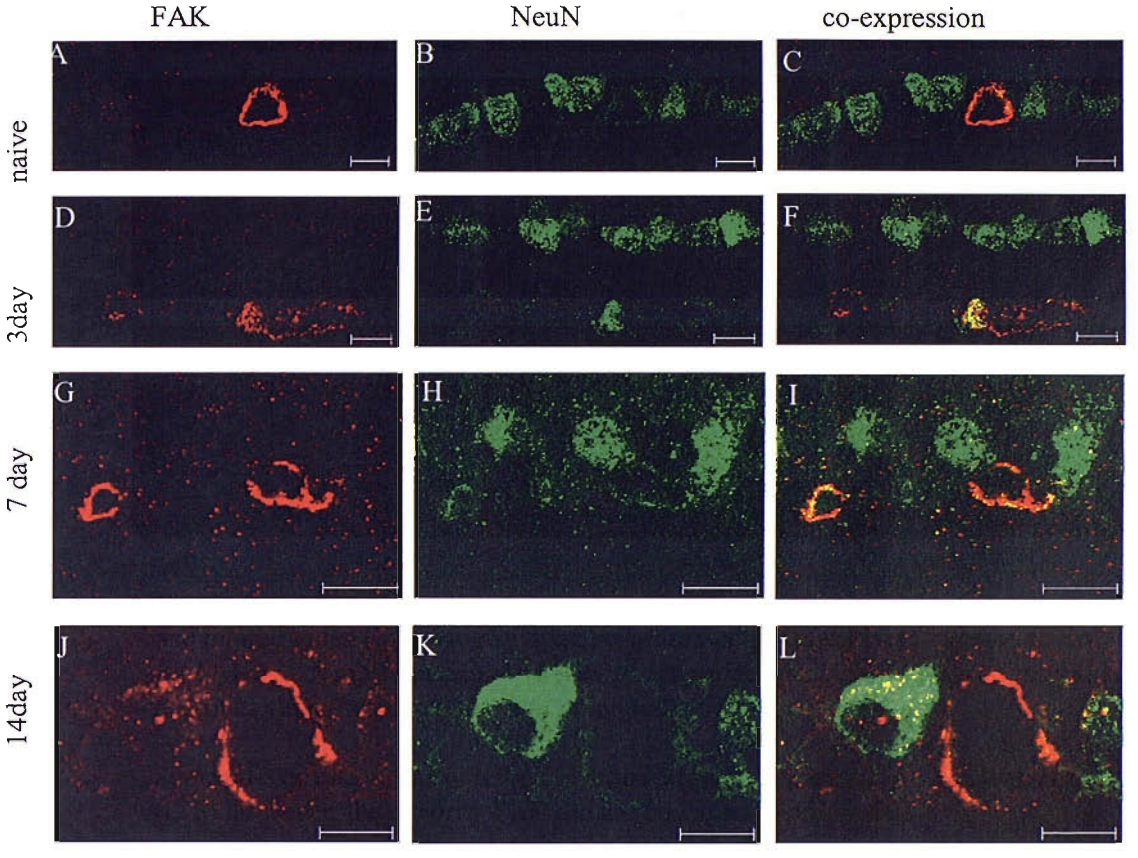

Fig. 5.32 FAK and NeuN co-expression in the naïve and injured retina. Naïve and injured retina (following an optic nerve transection injur) were immunostained for FAK and NeuN, a neuronal marker, to determine whether FAK was expressed in neurones either in naïve retina and/or injured retina.

Some co-expression was observed in retina 3days following optic nerve transection (D-F), however, the majority FAK did not co-express with NeuN.

A-C: naïve, D-F: 3day post injury (p.i), G-I: 7day p.i, J-L: 14day p.i

Scale = 10μm

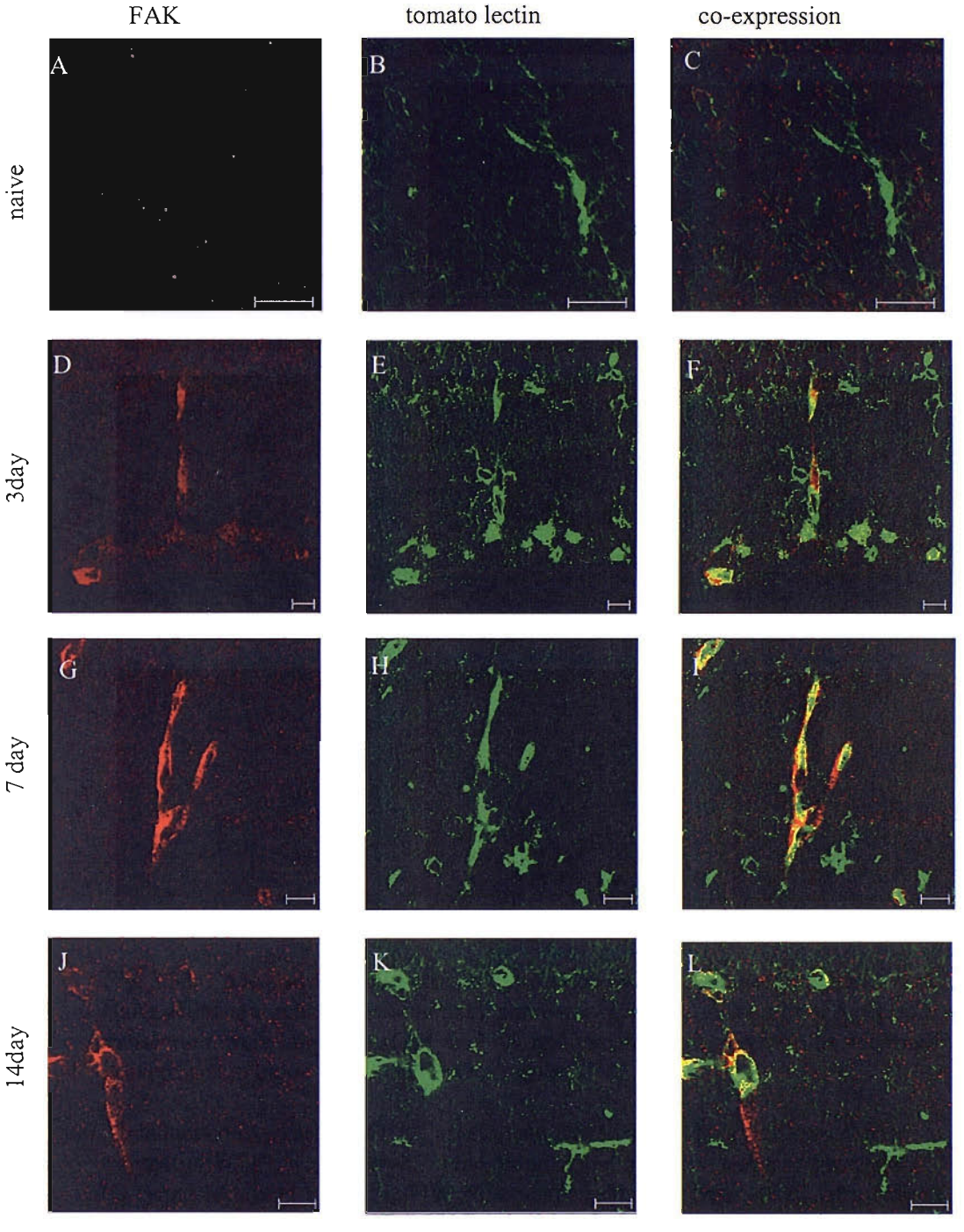

Fig. 5.33 FAK and tomato lectin co-expression in the naïve and injured retina. Naïve retina and retina following optic nerve transection, at a number of timepoints post transection, were immunostained for FAK and tomato lectin to determine whether FAK is expressed in blood vessels and/or microglia.

Abundant co-expression of FAK and tomato lectin, from 3days post optic nerve transection (D-F), was observed in the retina. Co-expression was also observed at 7day (G-I) and 14days (J-L) post injury. No co-expression was observed in naïve retina (A-C).

Scale 10um

5.5 Conclusions

This chapter describes the results of experiments designed to characterise the expression of one of the proteins identified in chapter 4, focal adhesion kinase (FAK), following injury. I investigated the temporal and spatial profile of FAK in a range of CNS tissues, following injury, using a combined approach of immunocytochemistry and Western blotting. The area of tissue taken for analysis by Western blot and immunocytochemistry and the CNS injury is important to consider when thinking about the possible roles FAK may be playing in the injuries studied. The models of brain and spinal cord injuries and the tissue taken can be considered as similar. Both injuries were transection injuries and the tissue taken for Western blot analysis encompassed the trauma area and the tissue completely surrounding the injury. On the other hand, the optic nerve tissue taken for study was distal or remote from the site of injury. The retina is different again, here I looked at the cell bodies of the injured optic nerve axons, and the tissue taken is not in direct contact with the injury. When studying the tissues by immunocytochemistry I can look at a larger area and study the temporal and spatial aspects of FAK expression adjacent to and distal to the lesion.

Brain and spinal cord

Following an intracranial stab injury or spinal cord partial transection, tissue was collected at a number of timepoint post injury. Western blot analysis revealed a change of FAK expression over the 7day timecourse that showed a similar pattern in both the brain and spinal cord tissue analysed. An overall decrease in FAK expression, over the 7days, was observed when compare to naïve. As mentioned above it is important to consider which portion of tissue was removed for analysis when thinking about what these results may show. For the brain injuries I excised the tissue immediately surrounding the injury site, approximately 4mmx4mm cube through the entire cross-section of the brain. For the spinal cord injury I collected 3-4cm of spinal cord tissue, the site of injury was in the centre of the tissue taken. The decrease in FAK is likely to be due to the death of cells surrounding the injury. This was supported by the brain immunocytochemical results that show a clear loss of FAK expression in the tissue adjacent to the injury when the tissue was fixed in formalin.

When brain tissue was fixed in Bouin's fixative the pattern of signal was different to that observed when the tissue was fixed in formalin. It appears as if the Bouin's fixative suppressed the normal levels of FAK signal, and only detects FAK that has either increased in expression or possibly changed in cellular location. Tissue fixed in Bouin's showed an increase in signal in glia surrounding the injury. This increase may be associated with an injury response of the adjacent glial cells. The glia that are positive for

FAK may be involved in proliferation and migration following injury. FAK activation and recruitment to the cell membrane may be occurring in these cells. FAK may be one mechanism by which these cells, in response to the changes in the surrounding environment, are initiating these responses. Three days following injury there is an influx of macrophages, which take on microglia morphology when they enter the CNS tissue. Although the double immunofluorescence was not ideal to show FAK signal within microglia, imaging by conventional immunocytochemistry revealed cellular morphology indicative of microglial staining. Some of the possible microglial signal, at 3 and 7days post injury, is likely to be due to the infiltrating macrophages, although this cannot be definitively concluded from this study. FAK is an important protein involved in migration of cells, so it therefore follows that I may be observing an increase in FAK staining at this time due to migrating microglial/macrophages.

Inactivation of, and a decrease of FAK at focal adhesions due to the loss of contact with the ECM results in apoptosis (anoikis) (Frisch, Vuori et al. 1996), it may follow therefore that one mechanism by which the damage to the brain tissue leads to cell death is via cellular pathways activated by the inactivation/ downregulation of FAK. This is supported by the immunocytochemistry, fixed in formalin (Fig. 5.6) that showed a loss of FAK signal in neuronal and glial cells surrounding the injury area.

Immunocytochemical analysis of FAK over the 7days following spinal cord injury revealed striking changes when compared to naïve tissue. Naïve tissue revealed little signal, other than background staining and some signal in the vasculature. However, as early as 6hrs after injury cellular expression of FAK and signal in the vasculature was seen throughout the tissue section. The pattern of expression was complicated and it was difficult to identify which cells were expressing signal. Therefore, double fluorescence was used to identify which cells following injury showed altered FAK expression.

Double immunofluorescence revealed that in the spinal cord FAK expression changes in oligodendrocytes, astrocytes, blood vessels and also some neuronal cell bodies. The most striking co-expression observed was that of FAK and CC1, the oligodendrocyte marker. Co-expression between FAK and CC1 was not detected in naïve spinal cord. However, by 6hrs following injury dramatic co-expression was observed. Co-expression was confirmed using confocal microscopy. This is an interesting observation and will be discussed later.

FAK expression was also detected, to a lesser extent, in astrocytes 3days and 7days post injury. Astrocytes become activated in response to injury (Dunn-Meynell and Levin 1997) and communicate with the ECM in order to co-ordinate their response; an increase in FAK may be one such mechanism by which they do this. Staining of blood vessels is

observed throughout the injury timecourse, including some in naïve spinal cord. Following injury there is an increase in FAK expression in vessels, although not all of the double immunofluorescence appeared to co-localise, the expression pattern mirrored that of tomato lectin, which was used to identify vessels. This may indicate that the two target antigens are expressed in different cellular locations within the vasculature. Tomato lectin is also often used to detect microglia within the rat CNS , however, in our sections the tomato lectin stained very few microglia, and it is therefore hard to ascertain whether FAK expression is also increased in these glia. However, the morphology of the cells revealed by immunocytochemistry and by a process of elimination (as I have stained for all other glia) it is probable that many microglia are also FAK positive. This would not be a surprise as microglia are highly responsive cells that change their morphology as well as migrating and proliferating following injury, so require a greater level of communication with the ECM, which may be in part mediated by FAK.

There was no expression of FAK within axons at any of the time points studied. From the images in Figs. 5.13, 22, 26 and 31 there was no co-expression of neurofilament-H and FAK. This, on one hand may be surprising due to the method by which we identified FAK as an interesting protein, i.e. through work with ELR1 and 2 antisera, however, the staining produced by ELR1 and 2 was not only axonal, but also glial in nature. It is therefore not surprising that one of the proteins we identified turned out to be glial in origin.

Optic nerve - a. Distal optic nerve

Western blot analysis of FAK expression in optic nerve, distal to the injury, revealed a different pattern of expression than that seen in both the brain and spinal cord following injury. Although levels of expression were not significantly different from that in naïve tissue, there was a trend for increased expression over the first 7 days post injury followed by a slight decrease by day 14. The area of tissue taken for Western blot analysis was the entire optic nerve from the site of injury to the optic chiasm; this region was also investigated using immunocytochemistry. Immunocytochemistry revealed little staining in naïve optic nerve, however, from 3days after injury cellular expression was observed which increased in quantity up to the latest timepoint studied. I employed double immunofluorescence to determine which cells were expressing FAK.

FAK signal increased abundantly within oligodendrocytes. Oligodendrocytes in naïve optic nerve were negative for FAK signal, however 7days following injury there was abundant co-expression of FAK with CC1, the oligodendrocyte marker. No co-expression of FAK with astrocytes or axons and very little with tomato lectin was seen until 14 days after injury. There was limited co-expression of FAK and tomato lectin that appeared to

be within microglia, however, as mentioned earlier the tomato lectin antibody used appeared to preferentially stain the blood vessels and was not ideal for detecting microglia. Double immunofluorescence did not show any co-expression with those cells observed at 3days. By conventional immunocytochemistry, by a process of elimination and by their morphology I may conclude that there is FAK signal within microglia. As with the spinal cord this would be compatible with microglia remodelling, proliferating and migrating following injury, also with the fact that there would be an influx of macrophages into the tissue beginning at 3days post injury.

b. Proximal optic nerve

There was little change in FAK immunoreactivity in the proximal optic nerve until 14days post injury. Co-expression studies only revealed that there was some double staining of FAK with tomato lectin at 14days post injury. From the morphology of the staining it appears that the co-expression was within blood vessels.

Retina

Western blot analysis did not reveal any significant changes in FAK expression following optic nerve transection and the immunocytochemistry results revealed little if any changes through the timecourse studied; there appears to be more vessel staining by 14days post injury, however this has not been qualntified. Co-expression studies revealed some Muller cell staining from 3days post injury, although the majority of Muller cells were not double stained with FAK. The most striking co-expression observed was of FAK with tomato lectin. There was some co-expression in naïve tissue, however, post injury there was abundant co-expression at all timepoints studied.

FAK expression has been shown to confer resistance to apoptosis in anoikis (Frisch, Vuori et al. 1996); it therefore follows that the increased expression in the glial cells observed by immunocytochemistry, aswell as being involved in migratory and proliferation actions, may be a protective mechanism by the cells which have lost some degree of cell-cell/matrix contact, caused by the injury.

FAK and the Oligodendrocyte

The most striking observation from this chapter is the co-expression of FAK with the oligodendrocyte marker, CC1, following injury. FAK was not detected in oligodendrocytes in the naïve tissues studied. The changes were observed at the earliest timepoint studied in spinal cord, 6hr post injury, and at the earliest timepoint studied in the optic nerve, 3days post injury. The co-expression is observed throughout the timecourse.

FAK is highly expressed in cultured oligodendrocytes during development but is then downregulated in fully differentiated oligodendrocytes (Kilpatrick, Ortuno et al.

2000) which supports our negative findings in the naïve CNS tissues. It has been suggested that this indicates a role for FAK in regulating the motility of these cells. The fact that I have detected FAK expression in oligodendrocytes following injury may implicate FAK in the injury response of oligodendrocytes.

Our findings indicate that the oligodendrocytes are 'detecting' or 'recognising' that the axon has been injured. I have found that the oligodendrocyte is responding to the injury as early as 6hrs post injury, which precedes axonal disintegration, which typically begins at 3days post injury in the CNS. FAK may therefore be involved in the early signalling events that inform the oligodendrocyte that its associated axon is in trouble. However, what the oligodendrocyte actually does in response to this information is as yet unknown.

CHAPTER 6 General Summary and Discussion

Axonal injury occurs in a wide variety of injuries and disease processes in the CNS and PNS. Information travels to muscles of the body from the brain, down the spinal cord, to control and initiate movements. Sensory information travels in the reverse direction, from the sensory organs up the spinal cord to the brain. Following injury, either traumatic injury or injury due to a disease process, information can no longer pass to or from the appropriate sites which can in turn lead to a wide variety of disabilities. Such disabilities may include a lack or loss of sensation, such as touch, hearing and sight, loss of motor movements (i.e. resulting in paralysis, loss of organ control, such as bowel, bladder and lung function) and, depending on the site of injury, death. Axonal injury occurs following traumatic brain and spinal cord injuries, and occurs as part of the disease processes in such diseases as Multiple Sclerosis, Motor Neuron disease and Alzheimer's disease to mention but a few. Within the CNS axonal regeneration does not occur, as discussed in the Introduction. If I can deduce the mechanisms involved in the early stages of axonal degeneration it is possible, in the future, that I may be able to prevent the processes from occurring and prevent the devastating consequences that occur.

The tools currently available to investigate axons can be used to study their anatomical pathways, to investigate axonal transport and can also be used as an indicator that an injury has occurred, however, they do not help in furthering our knowledge of the mechanisms involved in axonal degeneration.

The original aim of this project was to develop a new tool to enable investigation of the molecular mechanisms involved in axonal degeneration, more specifically Wallerian degeneration. Wallerian degeneration is the process of axon and myelin breakdown following an event that has caused the axon to become disconnected from its associated cell body, and therefore is cut off from its primary source of protein synthesis and nutritional support. Wallerian degeneration was believed to be a passive process whereby the axon simply withered away due to the loss of support from the cell body, however it is now known, thanks to the serendipitous discovery and much work on the *Wld*^{s} mutant mouse to be an active process akin to programmed cell death. The mechanisms involved in Wallerian degeneration are as yet unknown, although the genetics has been determined. It was the aim at the beginning of this project to unravel some of the mechanisms involved, however, by embarking along this line of investigation I have uncovered what may be one of the earliest responses in the oligodendrocytes following axonal injury.

I began my project by raising antibodies against a plethora of molecules, enriched in the axoplasm, extracted from sciatic nerves undergoing Wallerian degeneration. The antisera raised were used on a range of CNS tissue, both naïve and following injury. The

antibodies within the antisera detected many structures in CNS tissue following injury only. I investigated brain, spinal cord and optic nerve at a number of timepoints following transection injuries. The results were striking and clearly demonstrated that the antibodies within the antisera I raised detect differences between naïve and injured tissue. Differences, following brain injury, were observed from 6hrs through to our latest timepoint studied, 28days post injury. This in itself is in contrast to such techniques as APP immunocytochemistry where axonal injury and the associated end-bulbs can only be observed until 3-5 days following injury, after this time APP is cleared and can no longer be visualised.

In order to determine the antigens detected by the antibodies in the antisera, I used a proteomics approach. Firstly, I determined whether the antiera could be used on Western blots to detect changes in proteins between naïve and CNS tissues following injury. The results clearly revealed a number of bands upregulated in brain following injury. I located the bands that changed on a colloidal protein gel in order to excise the bands of interest for sequence analysis by MALDI-TOF MS. This technique resulted in the identification of rat albumin, Kid-1, a transcription factor, and Focal Adhesion Kinase (FAK), a non-receptor protein kinase that is targeted to focal adhesions when activated. On reflection this may not have been the best technique to use due to the difficulty in locating the correct band from the western blot on a corresponding gel for excision.

On reflection it was perhaps not surprising that our polyclonal antisera contained antibodies against rat albumin. The injury induced in the sciatic nerve results in breakdown of the blood-nerve barrier within the first day of injury. Therefore it follows that albumin from the blood, which is at a higher concentration than in the sciatic nerve, penetrates into the nerve prior to removal for immunisation. It would have been wise to attempt to remove the albumin from the fraction to be used before immunisation. This may have allowed a greater immune response against another immunogenic protein within the fraction used for immunisation.

The second protein identified as possibly increasing in concentration following injury was Kid-1. However, both immunocytochemistry and Western blot analysis revealed no difference in Kid-1 between naïve and injured brain. Previous descriptions of Kid-1 have been somewhat restricted to the kidney as this is the site of its original discovery (Witzgall, O'Leary et al. 1993). Kid-1 has previously been detected in the brain and is obviously not simply a kidney transcription factor, however, it appears to not have a role in axonal degeneration.

The third and final protein identified for further investigation, FAK, turned out to be extremely interesting.

Focal Adhesion Kinase

Preliminary investigations into FAK expression, in naïve and injured brain, revealed changes both by immunocytochemistry and Western blot analysis. These changes were further investigated through a number of different timepoints post injury in the brain, spinal cord, optic nerve and retina.

Western blot analysis of both brain and spinal cord revealed a similar picture. Protein levels remained similar to that of naïve levels when tissue was removed at 6hrs post injury. However, FAK protein levels decreased significantly by 24hr, followed by a slight increase by 3days, which was not significantly different from naïve, and then significantly decreasing again, to similar levels observed at 24hrs, by 7days post injury.

The immunocytochemical analysis revealed a strikingly different picture when compared to what you may expect to observe given the Western blot data. Focusing on the spinal cord results I observe very little staining in the naïve spinal cord. However, following injury, as early as 6hrs post injury, I observe abundant FAK signal that continues throughout the timecourse investigated. Glia and blood vessels were found to become FAK positive following injury. The most striking glial cell to demonstrate FAK signal throughout the timecourse was the oligodendrocyte. The differences between the Western blot data and the immunocytochemistry may be due to the fixation used for the immunocytochemistry or the area of tissue taken, this was discussed in detail in an earlier chapter.

In order to determine whether FAK reactive cells are responding to damage occurring around axons undergoing Wallerian degeneration or retrograde degeneration I changed our animal model from spinal cord injury to optic nerve injury. By transecting the optic nerve behind the eye, the axons within the optic nerve disconnected from the eye would undergo Wallerian degeneration, and the axons proximal to the lesion and still connected to the eye would undergo retrograde degeneration. This model also allows us to visualise the cell bodies of the damaged axons, i.e. the retinal ganglion cells within the retina can be investigated.

The FAK Western blot data from optic nerve distal from injury and the retina following injury revealed similar patterns. The changes were not significantly different, however there was a trend of FAK expression to increase over the first 7days post injury and then begin to decline at 14days. The immunocytochemical images from optic nerve containing axons undergoing Wallerian degeneration, show an increase in FAK signal from the earliest timepoint investigated, 3days post injury. Naïve optic nerve showed no specific FAK signal. There was abundant glial cell reactivity throughout the distal nerve throughout the timecourse investigated. The oligodendrocyte was the primary glial cell to

be shown to be FAK positive by double immunofluorescence. However, from the morphology of the cells by standard immunocytochemistry, I believe that microglial are also positive for FAK following injury. The proximal optic nerve showed no increase in FAK signal until 14days post injury. Immunocytochemistry of FAK revealed little change in FAK signal between naïve retina and retina following optic nerve transection.

As discussed earlier, FAK is highly expressed in cultured oligodendrocytes during development but is then downregulated in fully differentiated oligodendrocytes (Kilpatrick, Ortuno et al. 2000). The fact that I did not find FAK in oligodendrocytes in naïve tissues follows the findings of Kilpatrick at al. It has been suggested that this indicates a role for FAK in regulating the motility of these cells. The fact that I have detected FAK expression in oligodendrocytes following injury may implicate FAK in the injury response of oligodendrocytes. This work shows that FAK signal within oligodendrocytes can be detected as early as 6hrs post spinal cord injury, which is days earlier than the physical changes observed in the axon following injury. The above findings have been summarised in Fig. 6.1.

A valuable lesson to take from this work is that it is important to use a multidiseplinary approach when investigating results obtained from a proteomics approach. The data I obtained from our Western blot approach may have given us a completely different picture of the role FAK may play in the injury response had I not also used immunocytochemistry to investigate FAK expression. I feel that it is important for any future work using proteomics that the proteins identified should be investigated both by Western blot and immunocytochemistry. By using both approaches it is possible to obtain a much fuller picture of what is happening to the protein under investigation both at the level of protein expression and also in respect to its location and distribution within the tissue under investigation.

Future Work

There is an abundance of work that could be continued from the work begun in this thesis. I raised antibodies that detect damage within the CNS following injury. Identification of the antigens recognised by the antibodies may help to unravel some of the mechanisms that are occurring during Wallerian degeneration. A proteomics approach may be the ideal technique to do this. The use of 2D gel electrophoresis where proteins can be separated not only by weight but also charge would enable isolation of single proteins detected by our antibodies. These isolated proteins could then be sequenced by MALDI-TOF MS. Following identification these proteins would then need to be investigated both by Western blotting and immunocytochemistry to determine their role in Wallerian degeneration.

Another approach in order to try to achieve the original aim of this thesis, to determine the molecular mechanisms of axonal degeneration, would be use a new technique that has recently been used in our laboratory, in conjunction with the Proteomics Department at Southampton University. iTRAQ (is a stable isotope method for relative protein quantification using mass spectrometry. iTRAQ labels primary amines within the proteins, up to four samples can be compared in one run which would allow an injury timecourse to be investigated. The data obtained would show changes in proteins levels between the samples investigated. Axoplasm from naïve and injured axons, either from peripheral (sciatic nerve) or central (optic nerve) axons could be studied.

There is also much work that could be done to further our understanding of the role that FAK may be playing in the injury response in the CNS. It would be interesting to investigate what the signals are that are causing FAK activation. Indeed, the first thing to be done would be to determine whether it is activation of FAK that is occurring or simply an increase in the protein itself. Due to the early response of FAK it is more likely to activation rather than production. This could be investigated using an antibody against phosphorylated FAK that has been activated by phosphorylation at tyr397. I did begin to study this aspect, however, the antibodies used were not ideal and required abundant optimisation experiments, given more time this would have been an interesting avenue to embark down.

One method that could be used to further study the role of FAK in degeneration would be to utilise RNA interference, or RNAi as it is commonly abbreviated to. RNAi does not interfer with the DNA, instead it silences the expression of some the RNA genes to which it is targeted to. By using this technique it would be possible to silence the expression of the FAK protein in targeted cells in order to investigate it's role following injury.

The FAK signal I have detected is an early event. The injury, which disconnects the axon from its associated cell body, not only cuts the axon off from its source of proteins and nutrients, but also stops any action potentials (APs) from being transmitted. It is possible that the oligodendrocytes are 'sensing' that the axon is longer transmitting APs and this in itself is a signal that the axon may be beginning to undergo degeneration.

To further our understanding of the role that FAK is playing in the response to injury in the CNS, the downstream events that FAK is known to activate could also be investigated. FAK is known to activate other protein tyrosine kinases such as Src and Fyn. The expression of these proteins could be investigated to identify which pathways FAK is turning on following activation.

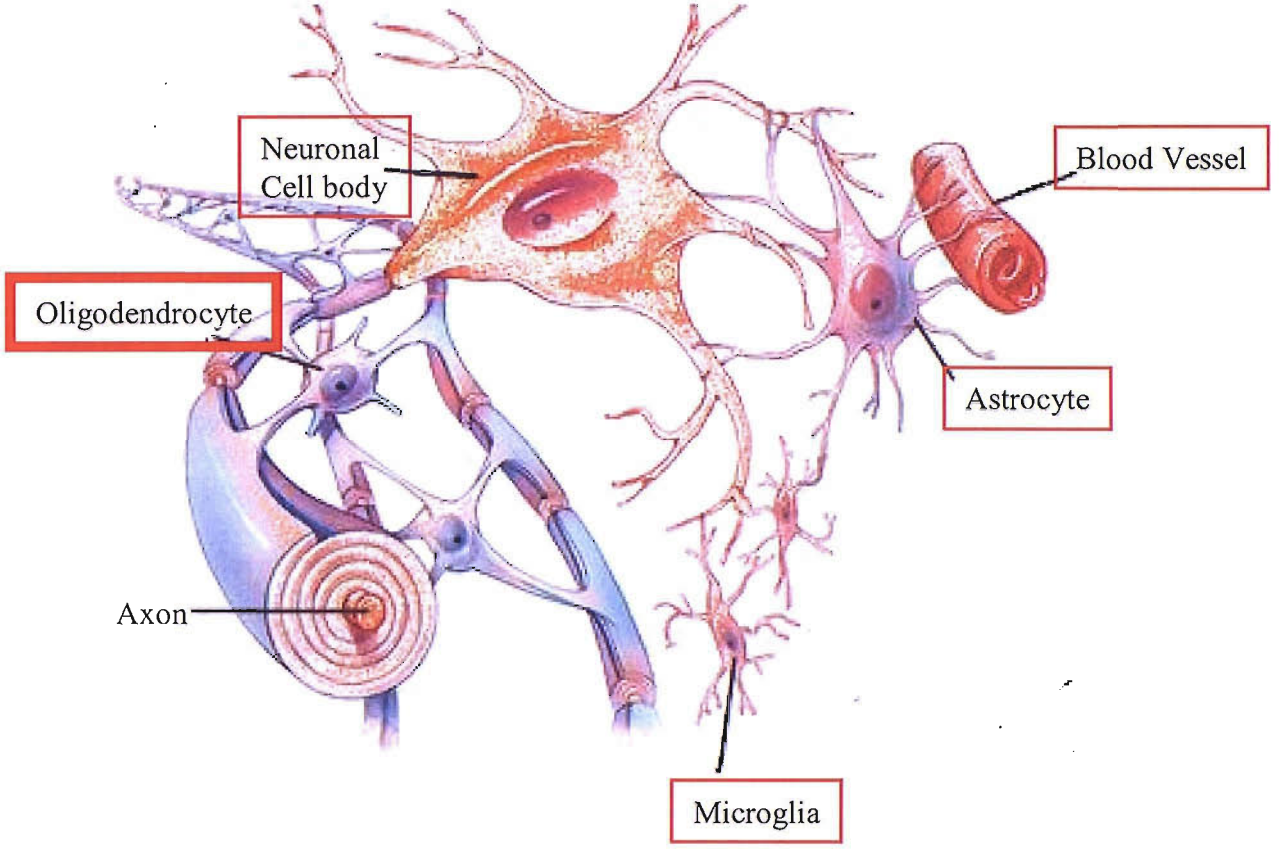

Fig. 6.1 Schematic diagram to summarise the locations of FAK following injury. The findings of this thesis have indicated that FAK is highly upregulated in the Oligodendrocyte as early as 6hrs post injury, distal from the injury. FAK was also shown to be expressed in neurones, blood vessels and to some extent in astrocytes and microglia.

This work did not indicate that FAK is expressed in axons.

Diagram form the Student Online Learning Centre; www.mhhe.com .

APPENDIX I

A Avertin Preparation

2.5g 2,2,2, tri bromo ethanol crystals
15.5ml tertiary amyl alcohol

Method:
Add the alcohol to the whole 25g bottle of tri bromo ethanol. Mix well by shaking, label as rat avertin concentrate and store in the dark, in the chemical cupboard.

Anaesthetic solution:
250ml 0.9% saline (autoclaved)
20ml Analar absolute alcohol
5ml of rat concentrate

Method:
Mix in a dark bottle, covered with foil, stirring overnight (it takes at least 6 hours to dissolve). Filter and store in the fridge. DO NOT USE IF CRYSTALS ARE PRESENT.

DOSE: 10ml/kg given i.p

B Periodate Lysine Paraformaldehyde (PLP) preparation

To make 1l:

1. Dissolve 13.7g lysine HCl in 375ml distilled water
2. Dissolve 1.8g di-Sodium hydrogen orthophoshate dihydrate (Sorenson's salt) in 100ml distilled water.
3. Add this to lysine solution till pH=7.4
4. Discard any remaining phosphate solution
5. Dissolve the required amount of paraformaldehyde in 200ml distilled water (i.e. for 1.5% PLP use 15g paraformaldehyde)
6. USE FUME CUPBOARD
7. Add paraformaldehyde, add few drops 1M NaOH with stirring to clear solution. Leave to cool.
8. Weigh 2.14g sodium periodate
9. To make the final solution, mix the lysine HCl solution, the paraformaldehyde solution and the sodium periodate together. Make up to 1l with 0.1M phosphate buffer.

C 4% Paraformaldehyde (PAF) preparation

1. Mix 4g paraformaldehyde with 40ml distilled water.
2. Heat up to about 60°C
3. Clear the solution with NaOH
4. Make the solution up to 50ml with distilled water.
5. Make up to 100ml with 0.2M phosphate buffer.

D Bouins preparation

To make 105mls:

75mls Saturated picric acid
25mls 40% Formaldehyde solution
5mls Glacial acetic acid

E Homogenisation Buffer

10mM Amino-n-caproic acid (ICN Biomedicals, UK),
1mM disodium EDTA (Sigma, UK),
0.5mM Benzamidine HCL.H20 (Sigma, UK)
and 0.02mM ABESF.HCl (Calbiochem, UK)
dissolved in 0.5M NaCl (Sigma, UK),
2.5mM $NaH_2PO_4.{}_2H_2O$
and 7.5mM $Na_2HPO_4.{}_2H_2O$,
final pH 7.3.

F Electrode buffer

0.25M TRIS,
1.92M glycine,
10%w/v SDS

G Transfer buffer

1×Laemlli buffer
20% methanol

H TBST

10mM Tris,
140mM NaCl,
0.2% Tween-20

I Antibody Table for Western Blot

Antibody	Antigen	Target Cell	Species raised in	Blocker	Dilution	Secondary/dilution
FAK	Focal adhesion kinase	All cells expressing FAK	Rabbit polyclonal	Goat serum (10%)	1:1000	Goat anti-rabbit HRP or fluorescence/1:200
GFAP	Cow Glial fibrillary acidic protein	Astrocytes in the CNS, Schwann cells in the PNS	Rabbit polyclonal	Milk or 3% BSA	1 in 1500	Anti-rabbit HRP or fluorescence/ 1 in 5000
Kid-1	Transcription factor	Primarily kidney cells, but also expressed in CNS	Rabbit polyclonal	Goat serum (10%)	1;200	Goat anti-rabbit HRP or fluorescence /1:200
NFH	Heavy chain of the neurofilament complex	Neurofilaments/ axons	Rabbit polyclonal	Milk or 3% BSA	1 in 1500	Anti-rabbit HRP or fluorescence/ 1 in 5000

J Antibody Table for Immunocytochemistry

Antibody	Antigen	Target Cell	Species raised in	Blocker	Dilution	Secondary/dilution
APP	Amyloid precursor protein	Axon (within all cells)	Mouse monoclonal	Horse serum (10%)	1:1000	Horse anti-mouse peroxidase/1:100
ED1	Single chain glycoprotein	Macrophages	Mouse monoclonal	Horse serum	1:200	Horse anti-mouse peroxidase /1:100
FAK	Focal adhesion kinase	All cells expressing FAK	Rabbit polyclonal	Goat serum (10%)	1:1000	Goat anti-rabbit peroxidase /1:200
Kid-1	Transcription factor	Primarily kidney cells, but also expressed in CNS	Rabbit polyclonal	Goat serum (10%)	1;200	Goat anti-rabbit peroxidase /1:200

K Antibody Table for Immunofluorescence

Antibody	Antigen	Target Cell	Species raised in	Blocker	Dilution	Secondary/dilution
CC1	Adenomatous poluposis	Oligodendrocytes	Mouse monoclonal	Horse serum (10%)	1:1000	Horse anti-mouse peroxidase/1:100
GFAP	Cow Glial fibrillary acidic protein	Astrocytes in the CNS, Schwann cells in the PNS	Mouse monoclonal	Horse serum (10%)	1:1000	Horse anti-mouse peroxidase/1:100
NFH	Heavy chain of the neurofilament complex	Neurofilaments/ axons	Mouse monoclonal	Horse serum (10%)	1:1000	Horse anti-mouse peroxidase/1:100
Neu N	Transcription factor	Neuronal cell bodies	Mouse monoclonal	Horse serum (10%)	1:1000	Horse anti-mouse peroxidase/1:100

APPENDIX II

Peptide Mass Fingerprinting

The aim of peptide mass fingerprinting or peptide sequencing is to convert the protein of interest into peptides using sequence specific proteases, then, using a mass spectrometer measure the molecular weights of the fragments and determine the sequence of the peptides. Using databases the identity of the protein under investigation are deduced.

MALDI, developed in 1987, has increased the upper mass limit for mass spectrometry to over 300kDa and has enabled the analysis of large molecules much more accurately than the methods available previously, such as a technique known as Edman degradation (Mano and Goto 2003; Steen and Mann 2004). Mass spectrometry not only is much more sensitive than previous techniques, but is also much more efficient and can fragment peptides in seconds instead of hours or days. Peptides are generated from the protein of interest for analysis as the whole proteins may be difficult to study. Proteins may be modified or processed in such a way that they will not all be soluble under the same conditions, and many detergents interfere with mass spectrometry. The mass spectrometer is most efficient at obtaining sequences from peptides up to approximately 20 amino acids in length, the whole protein would be to large to analyse whole. Trypsin is generally the protease used to fragment the protein into peptides. Trypsin is stable and extremely specific; cleavage occurs at the carboxy-terminal side of arginine and lysine residues. Using this method only achieves partial sequence retrieval; only a small percentage of the peptides will end up sequenced, which is usually enough to identify the protein with. However, the data produced does not identify other characteristics such as post-translational modifications.

Following peptide generation, the samples must be introduced into the mass spectrometer. This is generally achieved via a microscale capillary high-performance liquid chromatography (HPLC) column. The HPLC column is directly attached to the

mass spectrometer and the peptides are eluted from the column using a solvent gradient so that the peptides enter the mass spectrometer in order of their hydrophobicity. The peptides leave the column and enter the mass spectrometer through a needle, as the peptides are expelled through the needle the liquid is vapourised leading to ionisation of the peptides, this is known as 'electrospray ionisation'; the inventors of this technique John Fenn, Koichi Tanaka and Kurt Wuthrich were jointly awarded the Nobel Prize for chemistry in 2002. In MALDI mass spectrometry however, the peptides are ionised by matrix-assisted laser desorption/ionisation, the samples are deposited on a metal target for ionisation; some MALDI mass spectrometers are capable of fragmenting the peptides aswell as generating the mass data (see Fig. AII.1).

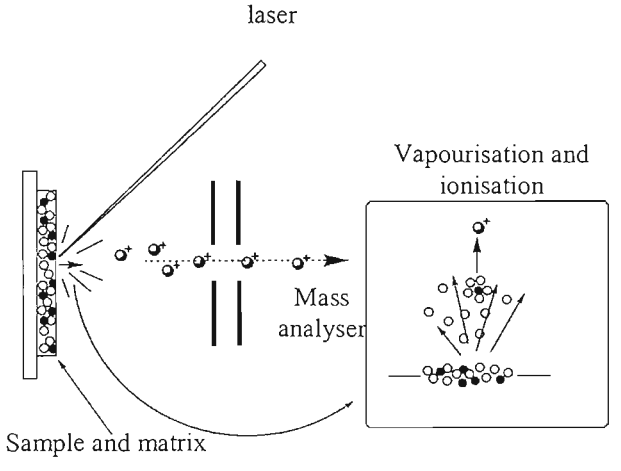

Fig. AII.1 Matrix-assisted laser desorption/ionisation source. The laser beam irradiates the sample on the target plate together with the matrix molecules. The sample and matrix molecules become vapourised. The co-desorption results in proton transfer between the matrix and sample molecules (Figure from (Mano and Goto 2003). MALDI is then commonly coupled with TOF-MS.

The peptide ions generated enter the mass spectrometer through a small hole or transfer capillary. Inside the mass spectrometer the environment is under a vacuum and the ions entering are controlled by electric fields. There are a few varieties of mass spectrometer, however, the type used in this work is a time of flight (TOF) mass spectrometer. The same kinetic energy is applied to the group of ions entering the mass spectrometer, the ions differ in mass/charge (m/z) ratios and the time for each ion to travel

through a known region under control of a constant electric field depends on their m/z ratios. The mass spectrum data obtained (Fig. AII.2) from the peptides are then searched against protein databases using a specific database-searching programme. These techniques and others used in biomedical and biological spectrometry are reviewed by (Mano and Goto 2003).

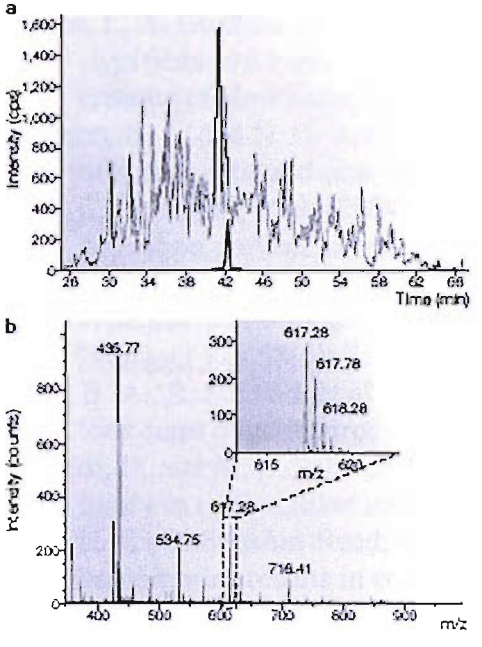

Fig. AII.2 Example of a Mass-spectrometry spectra. The total ion intensity from the entire MS run is shown in **a**. The trace shows the total ion current. (**b**) shows the mass spectrum of the peptides eluted 0.1 minute prior to the bold trace in (**a**). The insert shows the mass-to-charge values of the fragments of peptide around the protein of interest. This 'fingerprint' of the fragments can then be used to search the database for protein matches. Diagram from (Steen and Mann 2004)

Using this technique, peptide sequences can be deduced and possible proteins identified. The results obtained from this technique are an indication that the identified protein may be within the samples, the results need to then be confirmed by other means; I shall use immunocytochemistry and Western blot analysis.

Aguayo, A. J., G. M. Bray, et al. (1990). "Regrowth and connectivity of injured central nervous system axons in adult rodents." Acta Neurobiol Exp (Warsz) **50**(4-5): 381-9.

Aguayo, A. J., G. M. Bray, et al. (1990). "Synaptic connections made by axons regenerating in the central nervous system of adult mammals." J Exp Biol **153**: 199-224.

Al-Chalabi, A. and C. C. Miller (2003). "Neurofilaments and neurological disease." Bioessays **25**(4): 346-55.

Aloe, L. (2004). "Rita Levi-Montalcini: the discovery of nerve growth factor and modern neurobiology." Trends Cell Biol **14**(7): 395-9.

Alvarez, J., A. Giuditta, et al. (2000). "Protein synthesis in axons and terminals: significance for maintenance, plasticity and regulation of phenotype. With a critique of slow transport theory." Prog Neurobiol **62**(1): 1-62.

Anderson, N. L. and N. G. Anderson (1998). "Proteome and proteomics: new technologies, new concepts, and new words." Electrophoresis **19**(11): 1853-61.

Araki, T., Y. Sasaki, et al. (2004). "Increased nuclear NAD biosynthesis and SIRT1 activation prevent axonal degeneration." Science **305**(5686): 1010-3.

Baba, H., H. Akita, et al. (1999). "Completion of myelin compaction, but not the attachment of oligodendroglial processes triggers K(+) channel clustering." J Neurosci Res **58**(6): 752-64.

Barres, B. A., R. Schmid, et al. (1993). "Multiple extracellular signals are required for long-term oligodendrocyte survival." Development **118**(1): 283-95.

Bartholdi, D. and M. E. Schwab (1998). "Oligodendroglial reaction following spinal cord injury in rat; transient upregulation of MBP mRNA." Glia **23**(3): 278-84.

Beggs, H. E., D. Schahin-Reed, et al. (2003). "FAK deficiency in cells contributing to the basal lamina results in cortical abnormalities resembling congenital muscular dystrophies." Neuron **40**(3): 501-14.

Berger, F., M. H. Ramirez-Hernandez, et al. (2004). "The new life of a centenarian: signalling functions of NAD(P)." Trends Biochem Sci **29**(3): 111-8.

Bignami, A., D. Dahl, et al. (1981). "The fate of axonal debris in Wallerian degeneration of rat optic and sciatic nerves. Electron microscopy and immunofluorescence studies with neurofilament antisera." J Neuropathol Exp Neurol **40**(5): 537-50.

Bisby, M. A. and P. Keen (1985). "The effect of a conditioning lesion on the regeneration rate of peripheral nerve axons containing substance P." Brain Res **336**(2): 201-6.

Bradbury, E. J., L. D. Moon, et al. (2002). "Chondroitinase ABC promotes functional recovery after spinal cord injury." Nature **416**(6881): 636-40.

Brittis, P. A., Q. Lu, et al. (2002). "Axonal protein synthesis provides a mechanism for localized regulation at an intermediate target." Cell **110**(2): 223-35.

Brown, M. C., E. R. Lunn, et al. (1992). "Consequences of slow Wallerian degeneration for regenerating motor and sensory axons." J Neurobiol **23**(5): 521-36.

Brown, M. C., V. H. Perry, et al. (1991). "Macrophage dependence of peripheral sensory nerve regeneration: possible involvement of nerve growth factor." Neuron **6**(3): 359-70.

Burne, J. F., J. K. Staple, et al. (1996). "Glial cells are increased proportionally in transgenic optic nerves with increased numbers of axons." J Neurosci **16**(6): 2064-73.

Calalb, M. B., T. R. Polte, et al. (1995). "Tyrosine phosphorylation of focal adhesion kinase at sites in the catalytic domain regulates kinase activity: a role for Src family kinases." Mol Cell Biol **15**(2): 954-63.

Carlin, R. K., D. J. Grab, et al. (1980). "Isolation and characterization of postsynaptic densities from various brain regions: enrichment of different types of postsynaptic densities." J Cell Biol **86**(3): 831-45.
Chao, D. T. and S. J. Korsmeyer (1998). "BCL-2 family: regulators of cell death." Annu Rev Immunol **16**: 395-419.
Cohen, H. Y., S. Lavu, et al. (2004). "Acetylation of the C terminus of Ku70 by CBP and PCAF controls Bax-mediated apoptosis." Mol Cell **13**(5): 627-38.
Cohen, H. Y., C. Miller, et al. (2004). "Calorie restriction promotes mammalian cell survival by inducing the SIRT1 deacetylase." Science **305**(5682): 390-2.
Coleman, M. and V. Perry (2002). "Axon pathology in neurological disease: a neglected therapeutic target." Trends Neurosci **25**: 532.
Coleman, M. P., L. Conforti, et al. (1998). "An 85-kb tandem triplication in the slow Wallerian degeneration (Wlds) mouse." Proc Natl Acad Sci U S A **95**: 9985-90.
Conforti, L., A. Tarlton, et al. (2000). "A Ufd2/D4Cole1e chimeric protein and overexpression of Rbp7 in the slow Wallerian degeneration (WldS) mouse." Proc Natl Acad Sci U S A **97**: 11377-82.
Contestabile, A., D. Bonanomi, et al. (2003). "Localization of focal adhesion kinase isoforms in cells of the central nervous system." Int J Dev Neurosci **21**(2): 83-93.
Cowan, W. M., J. W. Fawcett, et al. (1984). "Regressive events in neurogenesis." Science **225**(4668): 1258-65.
David, S. and A. J. Aguayo (1981). "Axonal elongation into peripheral nervous system "bridges" after central nervous system injury in adult rats." Science **214**(4523): 931-3.
de la Motte, D. J. and G. Allt (1976). "Crush injury to peripheral nerve. An electron microscope study employing horseradish peroxidase." Acta Neuropathol (Berl) **36**(1): 9-19.
Deckwerth, T. L., J. L. Elliott, et al. (1996). "BAX is required for neuronal death after trophic factor deprivation and during development." Neuron **17**(3): 401-11.
Derkinderen, P., J. Siciliano, et al. (1998). "Differential regulation of FAK+ and PYK2/Cakbeta, two related tyrosine kinases, in rat hippocampal slices: effects of LPA, carbachol, depolarization and hyperosmolarity." Eur J Neurosci **10**(5): 1667-75.
Dong, H., A. Fazzaro, et al. (2003). "Enhanced oligodendrocyte survival after spinal cord injury in Bax-deficient mice and mice with delayed Wallerian degeneration." J Neurosci **23**(25): 8682-91.
Dubois-Dauphin, M., H. Frankowski, et al. (1994). "Neonatal motoneurons overexpressing the bcl-2 protooncogene in transgenic mice are protected from axotomy-induced cell death." Proc Natl Acad Sci U S A **91**(8): 3309-13.
Dunn-Meynell, A. A. and B. E. Levin (1997). "Histological markers of neuronal, axonal and astrocytic changes after lateral rigid impact traumatic brain injury." Brain Res **761**: 25-41.
Dupree, J. L., J. A. Girault, et al. (1999). "Axo-glial interactions regulate the localization of axonal paranodal proteins." J Cell Biol **147**(6): 1145-52.
Enevoldson, T. P., G. Gordon, et al. (1984). "The use of retrograde transport of horseradish peroxidase for studying the dendritic trees and axonal courses of particular groups of tract cells in the spinal cord." Exp Brain Res **54**(3): 529-37.
Eng, H., K. Lund, et al. (1999). "Synthesis of beta-tubulin, actin, and other proteins in axons of sympathetic neurons in compartmented cultures." J Neurosci **19**(1): 1-9.
Fadok, V. A., D. L. Bratton, et al. (2000). "A receptor for phosphatidylserine-specific clearance of apoptotic cells." Nature **405**(6782): 85-90.
Fang, C., M. Bernardes-Silva, et al. (2005). "The cellular distribution of the Wld(s) chimeric protein and its constituent proteins in the CNS." Neuroscience.

Fernando, F. S., L. Conforti, et al. (2002). "Human homologue of a gene mutated in the slow Wallerian degeneration (C57BL/Wld(s)) mouse." Gene **284**: 23-9.
Finn, J. T., M. Weil, et al. (2000). "Evidence that Wallerian degeneration and localized axon degeneration induced by local neurotrophin deprivation do not involve caspases." J Neurosci **20**(4): 1333-41.
Fournier, A. E., T. GrandPre, et al. (2001). "Identification of a receptor mediating Nogo-66 inhibition of axonal regeneration." Nature **409**(6818): 341-6.
Fournier, A. E. and S. M. Strittmatter (2001). "Repulsive factors and axon regeneration in the CNS." Curr Opin Neurobiol **11**(1): 89-94.
Frisch, S. M., K. Vuori, et al. (1996). "Control of adhesion-dependent cell survival by focal adhesion kinase." J Cell Biol **134**(3): 793-9.
Gaete, J., G. Kameid, et al. (1998). "Regenerating axons of the rat require a local source of proteins." Neurosci Lett **251**(3): 197-200.
Galbraith, J. A. and P. E. Gallant (2000). "Axonal transport of tubulin and actin." J Neurocytol **29**(11-12): 889-911.
Gentleman, S. M., M. J. Nash, et al. (1993). "Beta-amyloid precursor protein (beta APP) as a marker for axonal injury after head injury." Neurosci Lett **160**(2): 139-44.
George, R. and J. W. Griffin (1994). "Delayed macrophage responses and myelin clearance during Wallerian degeneration in the central nervous system: the dorsal radiculotomy model." Exp Neurol **129**(2): 225-36.
Giannelli, G., J. Falk-Marzillier, et al. (1997). "Induction of cell migration by matrix metalloprotease-2 cleavage of laminin-5." Science **277**(5323): 225-8.
Gillingwater, T. H., J. E. Haley, et al. (2004). "Neuroprotection after transient global cerebral ischemia in Wld(s) mutant mice." J Cereb Blood Flow Metab **24**(1): 62-6.
Girault, J. A., A. Costa, et al. (1999). "FAK and PYK2/CAKbeta in the nervous system: a link between neuronal activity, plasticity and survival?" Trends Neurosci **22**(6): 257-63.
Giuditta, A., E. Menichini, et al. (1991). "Active polysomes in the axoplasm of the squid giant axon." J Neurosci Res **28**(1): 18-28.
Grant, G., H. Hollander, et al. (2004). "Suppressive silver methods-a tool for identifying axotomy-induced neuron degeneration." Brain Res Bull **62**(4): 261-9.
Griffin, J. W., E. B. George, et al. (1996). "Wallerian degeneration in peripheral nerve disease." Baillieres Clin Neurol **5**(1): 65-75.
Hampton, D. W., K. E. Rhodes, et al. (2004). "The responses of oligodendrocyte precursor cells, astrocytes and microglia to a cortical stab injury, in the brain." Neuroscience **127**(4): 813-20.
Hancock, W. O. and J. Howard (1999). "Kinesin's processivity results from mechanical and chemical coordination between the ATP hydrolysis cycles of the two motor domains." Proc Natl Acad Sci U S A **96**(23): 13147-52.
Hasegawa, M., J. Rosenbluth, et al. (1988). "Nodal and paranodal structural changes in mouse and rat optic nerve during Wallerian degeneration." Brain Res **452**(1-2): 345-57.
Henderson, C. E. (1996). "Programmed cell death in the developing nervous system." Neuron **17**(4): 579-85.
Henderson, C. E. (1996). "Role of neurotrophic factors in neuronal development." Curr Opin Neurobiol **6**(1): 64-70.
Hirakawa, H., S. Okajima, et al. (2003). "Loss and recovery of the blood-nerve barrier in the rat sciatic nerve after crush injury are associated with expression of intercellular junctional proteins." Exp Cell Res **284**(2): 196-210.
Hirokawa, N. (1993). "Axonal transport and the cytoskeleton." Curr Opin Neurobiol **3**(5): 724-31.

Hoffmann, P. R., A. M. deCathelineau, et al. (2001). "Phosphatidylserine (PS) induces PS receptor-mediated macropinocytosis and promotes clearance of apoptotic cells." J Cell Biol **155**(4): 649-59.
Howard, M. J., G. David, et al. (1999). "Resealing of transected myelinated mammalian axons in vivo: evidence for involvement of calpain." Neuroscience **93**(2): 807-15.
Hungerford, J. E., M. T. Compton, et al. (1996). "Inhibition of pp125FAK in cultured fibroblasts results in apoptosis." J Cell Biol **135**(5): 1383-90.
Ilic, D., Y. Furuta, et al. (1995). "Reduced cell motility and enhanced focal adhesion contact formation in cells from FAK-deficient mice." Nature **377**(6549): 539-44.
Ivankovic-Dikic, I., E. Gronroos, et al. (2000). "Pyk2 and FAK regulate neurite outgrowth induced by growth factors and integrins." Nat Cell Biol **2**(9): 574-81.
Jackowski, A. (1995). "Neural injury repair: hope for the future as barriers to effective CNS regeneration become clearer." Br J Neurosurg **9**(3): 303-17.
Kaplan, B. B., Z. S. Lavina, et al. (2004). "Subcellular compartmentation of neuronal protein synthesis: new insights into the biology of the neuron." Ann N Y Acad Sci **1018**: 244-54.
Kasprzak, A. A. and L. Hajdo (2002). "Directionality of kinesin motors." Acta Biochim Pol **49**(4): 813-21.
Kilpatrick, T. J., D. Ortuno, et al. (2000). "Rat oligodendroglia express c-met and focal adhesion kinase, protein tyrosine kinases implicated in regulating epithelial cell motility." Neurosci Lett **279**(1): 5-8.
Korsmeyer, S. J. (1992). "Bcl-2 initiates a new category of oncogenes: regulators of cell death." Blood **80**(4): 879-86.
Kottis, V., P. Thibault, et al. (2002). "Oligodendrocyte-myelin glycoprotein (OMgp) is an inhibitor of neurite outgrowth." J Neurochem **82**(6): 1566-9.
Krajewski, S., J. K. Mai, et al. (1995). "Upregulation of bax protein levels in neurons following cerebral ischemia." J Neurosci **15**(10): 6364-76.
Kull, F. J. (2000). "Motor proteins of the kinesin superfamily: structure and mechanism." Essays Biochem **35**: 61-73.
Kumar, S. and D. L. Vaux (2002). "Apoptosis. A cinderella caspase takes center stage." Science **297**(5585): 1290-1.
Lamb, A. H. (1977). "Retrograde axonal transport of horseradish peroxidase for determining motor projection patterns to the developing limb in Xenopus." Brain Res **134**(2): 197-212.
Lasek, R. J., C. Dabrowski, et al. (1973). "Analysis of axoplasmic RNA from invertebrate giant axons." Nat New Biol **244**(136): 162-5.
Laser, H., T. G. Mack, et al. (2003). "Proteasome inhibition arrests neurite outgrowth and causes "dying-back" degeneration in primary culture." J Neurosci Res **74**(6): 906-16.
Lawson, L. J., L. Frost, et al. (1994). "Quantification of the mononuclear phagocyte response to Wallerian degeneration of the optic nerve." J Neurocytol **23**(12): 729-44.
Lehmann, M., A. Fournier, et al. (1999). "Inactivation of Rho signaling pathway promotes CNS axon regeneration." J Neurosci **19**(17): 7537-47.
Lev, N., Y. Barhum, et al. (2004). "Bax-ablation attenuates experimental autoimmune encephalomyelitis in mice." Neurosci Lett **359**(3): 139-42.
Li, M., A. Shibata, et al. (1996). "Myelin-associated glycoprotein inhibits neurite/axon growth and causes growth cone collapse." J Neurosci Res **46**(4): 404-14.
Lin, S. J. and L. Guarente (2003). "Nicotinamide adenine dinucleotide, a metabolic regulator of transcription, longevity and disease." Curr Opin Cell Biol **15**(2): 241-6.
Lockshin, R. A. and Z. Zakeri (2002). "Caspase-independent cell deaths." Curr Opin Cell Biol **14**(6): 727-33.

Loewy, A. D. (1969). "Ammoniacal silver staining of degenerating axons." Acta Neuropathol (Berl) **14**(3): 226-36.
Longart, M., L. Y, et al. (2004). "Neuregulin-2 is developmentally reulated and targeted to dendrites of central neurons." J Comp Neurol. **472**(2): 156-72.
Lu, J., K. W. Ashwell, et al. (2001). "Fluororuby as a marker for detection of acute axonal injury in rat spinal cord." Brain Res **915**: 118-23.
Lubinska, L. (1977). "Early course of Wallerian degeneration in myelinated fibres of the rat phrenic nerve." Brain Res **130**(1): 47-63.
Ludwin, S. K. (1990). "Oligodendrocyte survival in Wallerian degeneration." Acta Neuropathol (Berl) **80**(2): 184-91.
Ludwin, S. K. (1990). "Phagocytosis in the rat optic nerve following Wallerian degeneration." Acta Neuropathol (Berl) **80**(3): 266-73.
Lunn, E. R., V. H. Perry, et al. (1989). "Absence of Wallerian Degeneration does not Hinder Regeneration in Peripheral Nerve." Eur J Neurosci **1**(1): 27-33.
Luo, L. and D. D. O'Leary (2005). "Axon retraction and degeneration in development and disease." Annu Rev Neurosci **28**: 127-56.
Lyon, M. F., B. W. Ogunkolade, et al. (1993). "A gene affecting Wallerian nerve degeneration maps distally on mouse chromosome 4." Proc Natl Acad Sci U S A **90**: 9717-20.
Mack, T. G., M. Reiner, et al. (2001). "Wallerian degeneration of injured axons and synapses is delayed by a Ube4b/Nmnat chimeric gene." Nat Neurosci **4**: 1199-206.
Mandelkow, E. and E. M. Mandelkow (2002). "Kinesin motors and disease." Trends Cell Biol **12**(12): 585-91.
Mano, N. and J. Goto (2003). "Biomedical and biological mass spectrometry." Anal Sci **19**(1): 3-14.
Mattson, M. P. and W. Duan (1999). ""Apoptotic" biochemical cascades in synaptic compartments: roles in adaptive plasticity and neurodegenerative disorders." J Neurosci Res **58**(1): 152-66.
McKeon, R. J., R. C. Schreiber, et al. (1991). "Reduction of neurite outgrowth in a model of glial scarring following CNS injury is correlated with the expression of inhibitory molecules on reactive astrocytes." J Neurosci **11**(11): 3398-411.
Merry, D. E. and S. J. Korsmeyer (1997). "Bcl-2 gene family in the nervous system." Annu Rev Neurosci **20**: 245-67.
Mi, S., X. Lee, et al. (2004). "LINGO-1 is a component of the Nogo-66 receptor/p75 signaling complex." Nat Neurosci **7**(3): 221-8.
Miledi, R. and C. R. Slater (1970). "On the degeneration of rat neuromuscular junctions after nerve section." J Physiol **207**(2): 507-28.
Mukhopadhyay, G., P. Doherty, et al. (1994). "A novel role for myelin-associated glycoprotein as an inhibitor of axonal regeneration." Neuron **13**(3): 757-67.
Mukoyama, M., K. Yamazaki, et al. (1989). "Neuropathology of gracile axonal dystrophy (GAD) mouse. An animal model of central distal axonopathy in primary sensory neurons." Acta Neuropathol (Berl) **79**: 294-9.
Nadal, A., E. Fuentes, et al. (2001). "Glial cell responses to lipids bound to albumin in serum and plasma." Prog Brain Res **132**: 367-74.
Nadal, A., E. Fuentes, et al. (1995). "Plasma albumin is a potent trigger of calcium signals and DNA synthesis in astrocytes." Proc Natl Acad Sci U S A **92**(5): 1426-30.
Nixon, R. A. (1980). "Protein degradation in the mouse visual system. I. Degradation of axonally transported and retinal proteins." Brain Res **200**(1): 69-83.
Ochs, S. (1975). "Waller's concept of the trophic dependence of the nerve fiber on the cell body in the light of early neuron theory." Clio Med **10**(4): 253-65.
Paxinos, G. and C. Watson (1986). The Rat Brain in Stereotaxic Coordinates, Fourth Edition, Academic Press.

Perry, V. H., M. D. Bell, et al. (1995). "Inflammation in the nervous system." Curr Opin Neurobiol **5**: 636-41.
Perry, V. H., M. C. Brown, et al. (1993). "Macrophage responses to central and peripheral nerve injury." Adv Neurol **59**: 309-14.
Perry, V. H., M. C. Brown, et al. (1987). "The macrophage response to central and peripheral nerve injury. A possible role for macrophages in regeneration." J Exp Med **165**(4): 1218-23.
Perry, V. H., M. C. Brown, et al. (1991). "Very Slow Retrograde and Wallerian Degeneration in the CNS of C57BL/Ola Mice." Eur J Neurosci **3**: 102-105.
Perry, V. H., M. C. Brown, et al. (1990). "Evidence that Very Slow Wallerian Degeneration in C57BL/Ola Mice is an Intrinsic Property of the Peripheral Nerve." Eur J Neurosci **2**: 802-808.
Perry, V. H., J. W. Tsao, et al. (1995). "Radiation-induced reductions in macrophage recruitment have only slight effects on myelin degeneration in sectioned peripheral nerves of mice." Eur J Neurosci **7**(2): 271-80.
Peters, A., S. L. Palay, et al. (1970). The Fine structure of the Nervous System. New York.
Pettmann, B. and C. E. Henderson (1998). "Neuronal cell death." Neuron **20**(4): 633-47.
Properzi, F., R. A. Asher, et al. (2003). "Chondroitin sulphate proteoglycans in the central nervous system: changes and synthesis after injury." Biochem Soc Trans **31**(2): 335-6.
Raff, M. C., A. V. Whitmore, et al. (2002). "Axonal self-destruction and neurodegeneration." Science **296**(5569): 868-71.
Rankin, S. and E. Rozengurt (1994). "Platelet-derived growth factor modulation of focal adhesion kinase (p125FAK) and paxillin tyrosine phosphorylation in Swiss 3T3 cells. Bell-shaped dose response and cross-talk with bombesin." J Biol Chem **269**(1): 704-10.
Rasband, M. N. and J. S. Trimmer (2001). "Developmental clustering of ion channels at and near the node of Ranvier." Dev Biol **236**(1): 5-16.
Ren, X. D., W. B. Kiosses, et al. (2000). "Focal adhesion kinase suppresses Rho activity to promote focal adhesion turnover." J Cell Sci **113 (Pt 20)**: 3673-8.
Ribchester, R. R., J. W. Tsao, et al. (1995). "Persistence of neuromuscular junctions after axotomy in mice with slow Wallerian degeneration (C57BL/WldS)." Eur J Neurosci **7**(7): 1641-50.
Rios, J. C., C. V. Melendez-Vasquez, et al. (2000). "Contactin-associated protein (Caspr) and contactin form a complex that is targeted to the paranodal junctions during myelination." J Neurosci **20**(22): 8354-64.
Sagot, Y., M. Dubois-Dauphin, et al. (1995). "Bcl-2 overexpression prevents motoneuron cell body loss but not axonal degeneration in a mouse model of a neurodegenerative disease." J Neurosci **15**(11): 7727-33.
Sajadi, A., B. L. Schneider, et al. (2004). "Wlds-mediated protection of dopaminergic fibers in an animal model of Parkinson disease." Curr Biol **14**(4): 326-30.
Schaller, M. D., C. A. Borgman, et al. (1992). "pp125FAK a structurally distinctive protein-tyrosine kinase associated with focal adhesions." Proc Natl Acad Sci U S A **89**(11): 5192-6.
Schlaepfer, W. W. and M. B. Hasler (1979). "Characterization of the calcium-induced disruption of neurofilaments in rat peripheral nerve." Brain Res **168**(2): 299-309.
Schnell, L. and M. E. Schwab (1990). "Axonal regeneration in the rat spinal cord produced by an antibody against myelin-associated neurite growth inhibitors." Nature **343**(6255): 269-72.
Schwab, M. E. and P. Caroni (1988). "Oligodendrocytes and CNS myelin are nonpermissive substrates for neurite growth and fibroblast spreading in vitro." J Neurosci **8**(7): 2381-93.

Seiffert, E., J. P. Dreier, et al. (2004). "Lasting blood-brain barrier disruption induces epileptic focus in the rat somatosensory cortex." J Neurosci **24**(36): 7829-36.
Seitz, R. J., K. Reiners, et al. (1989). "The blood-nerve barrier in Wallerian degeneration: a sequential long-term study." Muscle Nerve **12**(8): 627-35.
Seufferlein, T. and E. Rozengurt (1994). "Lysophosphatidic acid stimulates tyrosine phosphorylation of focal adhesion kinase, paxillin, and p130. Signaling pathways and cross-talk with platelet-derived growth factor." J Biol Chem **269**(12): 9345-51.
Seyfert, S., A. Faulstich, et al. (2004). "What determines the CSF concentrations of albumin and plasma-derived IgG?" J Neurol Sci **219**(1-2): 31-3.
Shimura, H., N. Hattori, et al. (2000). "Familial Parkinson disease gene product, parkin, is a ubiquitin-protein ligase." Nat Genet **25**: 302-5.
Siciliano, J. C., M. Toutant, et al. (1996). "Differential regulation of proline-rich tyrosine kinase 2/cell adhesion kinase beta (PYK2/CAKbeta) and pp125(FAK) by glutamate and depolarization in rat hippocampus." J Biol Chem **271**(46): 28942-6.
Sieg, D. J., C. R. Hauck, et al. (2000). "FAK integrates growth-factor and integrin signals to promote cell migration." Nat Cell Biol **2**(5): 249-56.
Skoff, R. P. (1975). "The fine structure of pulse labeled (3-H-thymidine cells) in degenerating rat optic nerve." J Comp Neurol **161**(4): 595-611.
Sorenson, C. M. (2004). "Bcl-2 family members and disease." Biochim Biophys Acta **1644**(2-3): 169-77.
Sotelo, J. R., A. Kun, et al. (1999). "Ribosomes and polyribosomes are present in the squid giant axon: an immunocytochemical study." Neuroscience **90**(2): 705-15.
Steen, H. and M. Mann (2004). "The abc's (and xyz's) of peptide sequencing." Nat Rev Mol Cell Biol **5**(9): 699-711.
Steward, O. (1992). "Signals that induce sprouting in the central nervous system: sprouting is delayed in a strain of mouse exhibiting delayed axonal degeneration." Exp Neurol **118**(3): 340-51.
Stoll, G., J. W. Griffin, et al. (1989). "Wallerian degeneration in the peripheral nervous system: participation of both Schwann cells and macrophages in myelin degradation." J Neurocytol **18**(5): 671-83.
Susalka, S. J., W. O. Hancock, et al. (2000). "Distinct cytoplasmic dynein complexes are transported by different mechanisms in axons." Biochim Biophys Acta **1496**(1): 76-88.
Syntichaki, P. and N. Tavernarakis (2003). "The biochemistry of neuronal necrosis: rogue biology?" Nat Rev Neurosci **4**(8): 672-84.
Tang, S., R. W. Woodhall, et al. (1997). "Soluble Myelin-Associated Glycoprotein (MAG) Found in Vivo Inhibits Axonal Regeneration." Mol Cell Neurosci **9**(5/6): 333-46.
Tanida, I., T. Ueno, et al. (2004). "LC3 conjugation system in mammalian autophagy." Int J Biochem Cell Biol **36**(12): 2503-18.
Tapia, M., N. C. Inestrosa, et al. (1995). "Early axonal regeneration: repression by Schwann cells and a protease?" Exp Neurol **131**(1): 124-32.
Taylor, J. M., C. P. Mack, et al. (2001). "Selective expression of an endogenous inhibitor of FAK regulates proliferation and migration of vascular smooth muscle cells." Mol Cell Biol **21**(5): 1565-72.
Trapp, B. D., P. Hauer, et al. (1988). "Axonal regulation of myelin protein mRNA levels in actively myelinating Schwann cells." J Neurosci **8**(9): 3515-21.
Trapp, B. D., J. Peterson, et al. (1998). "Axonal transection in the lesions of multiple sclerosis." N Engl J Med **338**: 278-85.
Turner, C. E., J. R. Glenney, Jr., et al. (1990). "Paxillin: a new vinculin-binding protein present in focal adhesions." J Cell Biol **111**(3): 1059-68.
Twigger, S., J. Lu, et al. (2002). "Rat Genome Database (RGD): mapping disease onto the genome." Nucleic Acids Res **30**(1): 125-8.

van de Water, B., F. Houtepen, et al. (2001). "Suppression of chemically induced apoptosis but not necrosis of renal proximal tubular epithelial (LLC-PK1) cells by focal adhesion kinase (FAK). Role of FAK in maintaining focal adhesion organization after acute renal cell injury." J Biol Chem **276**(39): 36183-93.

Vila, M., V. Jackson-Lewis, et al. (2001). "Bax ablation prevents dopaminergic neurodegeneration in the 1-methyl- 4-phenyl-1,2,3,6-tetrahydropyridine mouse model of Parkinson's disease." Proc Natl Acad Sci U S A **98**(5): 2837-42.

Waller, A. (1850). "Experiments on the section of glossopharyngeal and hypoglossal nerves of the frog and observations of the alternatives produced thereby in the structure of their primitive fibers." Philos Trans R Soc Lond Biol. **140**: 423.

Waxman, S., P. Stys, et al., Eds. (1995). The Axon.

White, F. A., C. R. Keller-Peck, et al. (1998). "Widespread elimination of naturally occurring neuronal death in Bax-deficient mice." J Neurosci **18**(4): 1428-39.

Whitmore, A. V., T. Lindsten, et al. (2003). "The proapoptotic proteins Bax and Bak are not involved in Wallerian degeneration." Cell Death Differ **10**(2): 260-1.

Witzgall, R., E. O'Leary, et al. (1993). "Kid-1, a putative renal transcription factor: regulation during ontogeny and in response to ischemia and toxic injury." Mol Cell Biol **13**(3): 1933-42.

Witzgall, R., N. Obermuller, et al. (1998). "Kid-1 expression is high in differentiated renal proximal tubule cells and suppressed in cyst epithelia." Am J Physiol **275**(6 Pt 2): F928-37.

Zachary, I., J. Sinnett-Smith, et al. (1992). "Bombesin, vasopressin, and endothelin stimulation of tyrosine phosphorylation in Swiss 3T3 cells. Identification of a novel tyrosine kinase as a major substrate." J Biol Chem **267**(27): 19031-4.

Zalewska, T., M. Ziemka-Nalecz, et al. (2003). "Transient forebrain ischemia modulates signal transduction from extracellular matrix in gerbil hippocampus." Brain Res **977**(1): 62-9.

Zetusky, W. J., V. P. Calabrese, et al. (1979). "Isolation and partial characterization of human CNS axolemma-enriched fractions." J Neurochem **32**(3): 1103-9.

Zhai, Q., J. Wang, et al. (2003). "Involvement of the ubiquitin-proteasome system in the early stages of wallerian degeneration." Neuron **39**(2): 217-25.

Zhang, C., M. P. Lambert, et al. (1994). "Focal adhesion kinase expressed by nerve cell lines shows increased tyrosine phosphorylation in response to Alzheimer's A beta peptide." J Biol Chem **269**(41): 25247-50.

Zhang, C., H. E. Qiu, et al. (1996). "A beta peptide enhances focal adhesion kinase/Fyn association in a rat CNS nerve cell line." Neurosci Lett **211**(3): 187-90.

Zheng, J. Q., T. K. Kelly, et al. (2001). "A functional role for intra-axonal protein synthesis during axonal regeneration from adult sensory neurons." J Neurosci **21**(23): 9291-303.